Hazy 3

a brief introduction to Cloudy

results & computational environment

version 06.02

G.J. Ferland
Department of Physics and Astronomy
University of Kentucky, Lexington
http://www.nublado.org

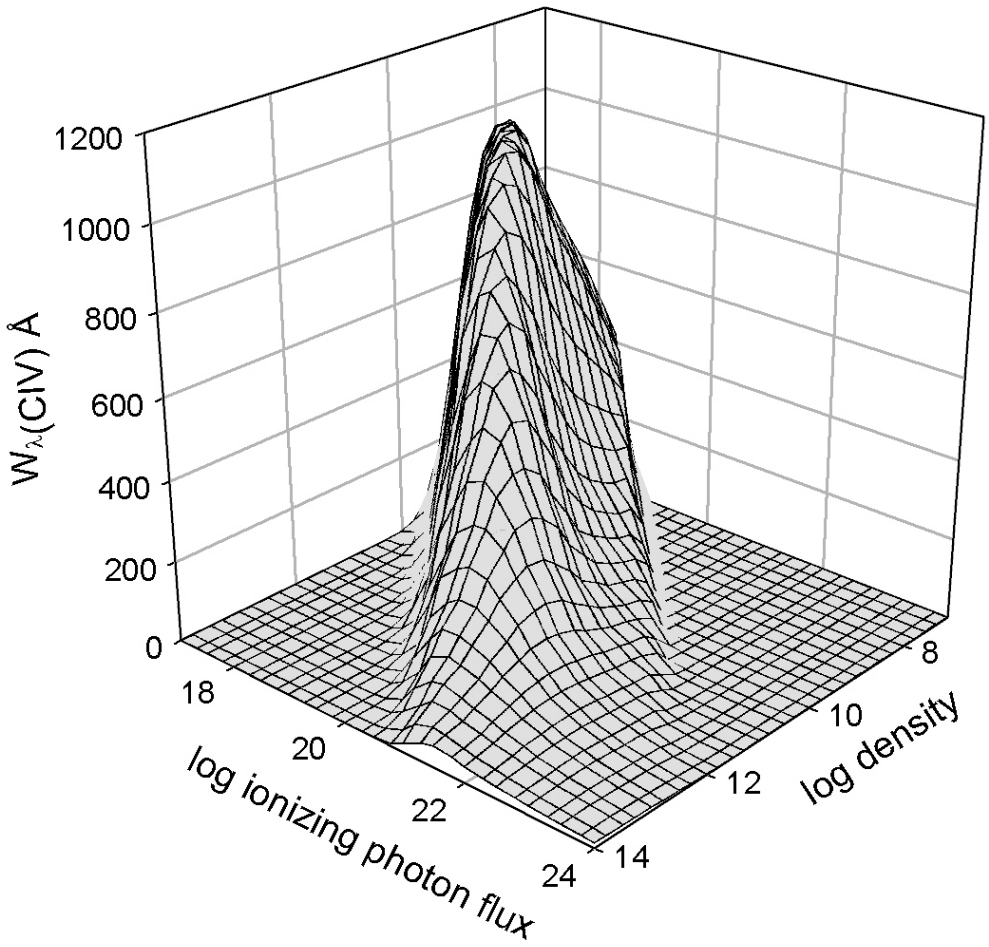

The predicted equivalent width of the C IV λ;1549 doublet for a broad range of cloud densities and distances from the central object for emission-line clouds in active nuclei. This shows the powerful selection effects that occur in any spectroscopic observation.

Use of this program is not restricted provided each use is acknowledged upon publication. The bibliographic reference to this version of Cloudy is "version xx.xx of the code last described by Ferland, G.J., et al 1998, PASP, 110, 761-778." The version number, shown here as "xx.xx", should be given and can be found on the first lines of the code's output.

Cloudy is an evolving code. Updates are made on a roughly quarterly basis. You should confirm that you have the most recent version of the code by checking the web site http://www.nublado.org.

February 28, 2006.

CLOUDY 06.02

G. J. Ferland
Department of Physics and Astronomy
University of Kentucky
Lexington

Table of Contents

List of Figures

List of Tables

1. OTHER DETAILS

1.1. Overview

This section outlines some of the major versions of Cloudy, and gives an indication of the direction development will take in the next few years. Its development began in August of 1978, at the Institute of Astronomy, Cambridge, and has been continued at The University of Kentucky, The Ohio State University, and during extended visits to the Joint Institute for Laboratory Astrophysics, the Royal Greenwich Observatory, IOA Cambridge, Cerro Tolodo Interamerican Observatory, and the Canadian Institute for Theoretical Astrophysics. Figure 1 shows the evolution of the code, as indicated by its size as a function of time[1].

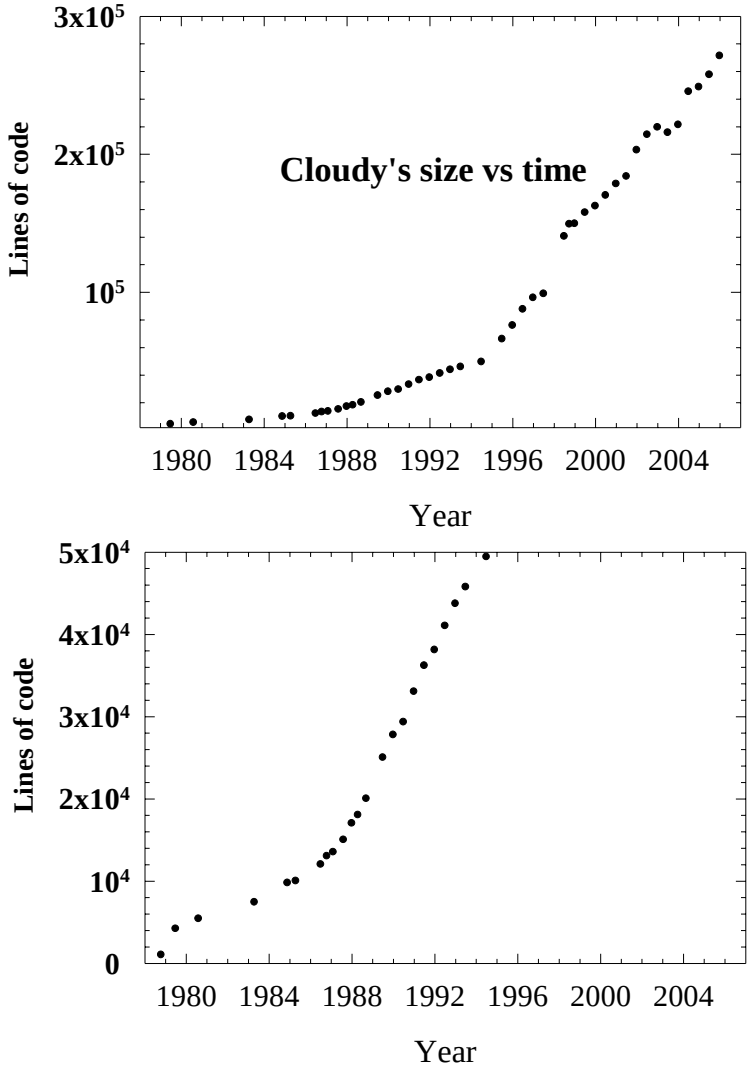

Figure 1 The size of the code as a function of time. The code grows roughly 7% larger per year, with growth spurts and slowdowns at times. There are several changes in slope evident – the year and cause are: 1985 – mainframe to Unix; 1993 – Unix to windows; the jump at 1999 – the Fortran to C conversion. size

1.2. Cloudy and Moore's Law

Moore's Law is due to Gordon Moore, one of the founders of Intel Corporation. He observed that modern CPU's become about twice as powerful every 18 months. This trend has held true for the past twenty years, shows no sign of failing, and seems to be associated with our ability to control complexity.

[1] Before mid-1995 the size was the total number of lines in the distributed source. After 1995 the size only includes the number of lines excluding block datas. When the code was converted to C the block datas were converted to external data files. These external files are now far larger than the code itself.

By this standard the growth of Cloudy has been conservative, in that it is growing slower and complex on the Moore's law timescale. As an example, the Meudon 1985 Meeting planetary nebula test (**pn_paris.in** in the distributed test cases) has always taken about one minute to compute.

1.3. A brief history

Cloudy was born at the Institute of Astronomy, Cambridge, in August of 1978, in the computing environment described in the web document http://www.nublado.org/gary/computing1970s.htm . Its original purpose was to simulate emission-line regions of Active Nuclei, a major research emphasis at the time.

The code is about to enter its third computer language. It was originally written in FORTRAN IV and advanced through several dialects, reaching FORTRAN 77 in 1994 (version 84). Version 90 was written in a mix of FORTRAN 77 and MILSPEC extensions. This is the most advanced Fortran that can be used with open source compilers. It moved to ANSI 89 C in 1999 with the release of version 96 and will move to C++ in the near future.

1.4. Acknowledgments

Comments or suggestions which led to the improvement of Cloudy were made by the many individuals acknowledged on the web site http://www.nublado.org .

Peter G. Martin and Hagai Netzer had special roles during the early development of the code. Peter added several of the commands that deal with ordering of supplemental line lists and the luminosity options on the **blackbody** command, insisted that Cloudy run on a VAX, provided access to the University of Toronto VAX 11/780 during the 1980's, and more recently hosted the group at CITA during a sabbatical. Hagai and I have spent countless hours arguing over methods, assumptions, and just whose code had the bug. These comparisons are the only way to debug codes as large as Cloudy or ION.

Peter van Hoof has gone over the code very carefully, finding many problems, and expanding its capabilities. The current version of the grain physics was developed by Peter, Peter Martin, and Joe Weingartner. Peter is the maintainer.

The expansion of the simulations into the PDR was done by N. Abel and G. Shaw as part of their theses. R. Porter developed the He-like isoelectronic sequence.

Sections of the code are taken from public domain software, as acknowledged in this document and in the source. Portions of the code were written by K. Blagrave, R.F. Carswell, S.A. Cota, J. Ferguson, J. Kingdon, K.T. Korista, P.G. Martin, P. T. O'Brien, P. van Hoof, D. Verner, and K. Volk.

The development of Cloudy would not have been possible without twenty six years of continuous support by The National Science Foundation. This began with AST 80-2522, and has been continued with grants 83-05094, 85-12414, 87-19607, 90-19692, 93-19034, 96-17083, 00-71180, and most recently AST 03-07720. The support of

NASA through its ATP program has been vital. Support from the University of Kentucky Center for Computational Sciences is also gratefully acknowledged.

1.5. Overall Code Structure

This section outlines the flow control in the higher levels of the code.

1.5.1. The main program

When used as a stand-alone program, control passes to program ***main*** contained in **`maincl.c`**, which initializes the code by calling ***cdInit***. It then reads the input stream from standard input and passes the line images to the code by calling ***cdRead***. The main routine calls ***cdDrive*** to compute the model and then checks whether any problems occurred during the calculation by calling ***cdNwcns***. It then prints a brief summary of what happened and stops. The organization is shown in Figure 2.

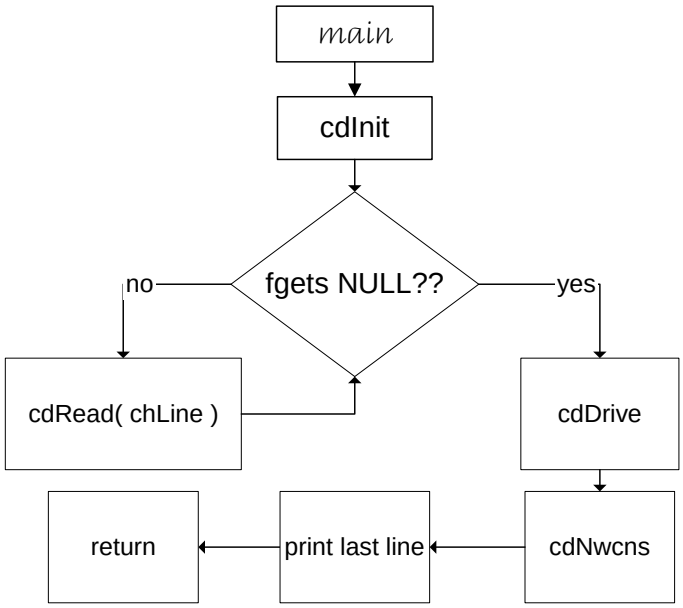

Figure 2 This shows the structure of the main program.

The code can be called by the user as a subprogram of other, larger, code. There is no difference in the way the stand-alone and subroutine versions of the code work – when used as a stand-alone program the main program simply reads standard input and passes the command strings into the code through calls to routine ***cdRead***, and this is done by the calling routine in the subroutine case. The one difference is that the main routine includes logic to identify whether the input stream is the header of a previous calculation.

1.5.2. Routine cdDrive

cdDrive is called to execute the code, both in the stand-alone and subroutine versions. ***cdDrive*** decides whether to compute a single model or an optimization run by checking whether the keyword **`vary`** occurred on any command line. If the keyword does not appear then it simply calls routine ***cloudy*** to compute a single model. If the keyword **`vary`** does occurrs then ***cdDrive*** calls ***DoOptimize***, the routine that varies parameters to match a set of observations.

1.5.3. Routine Cloudy

Most of the actual work performed in the computation of a model is done is subroutine Cloudy (Figure 3). This routine controls the zone and iteration variables ***nzone*** and ***iter***.

At its outermost level the routine controls the number of iterations and stops when the simulation is complete. Within this loop is an inner loop that determines

whether a particular iteration is complete. This inner loop controls the integration over zones and checks stopping criteria to determine whether the structure is complete.

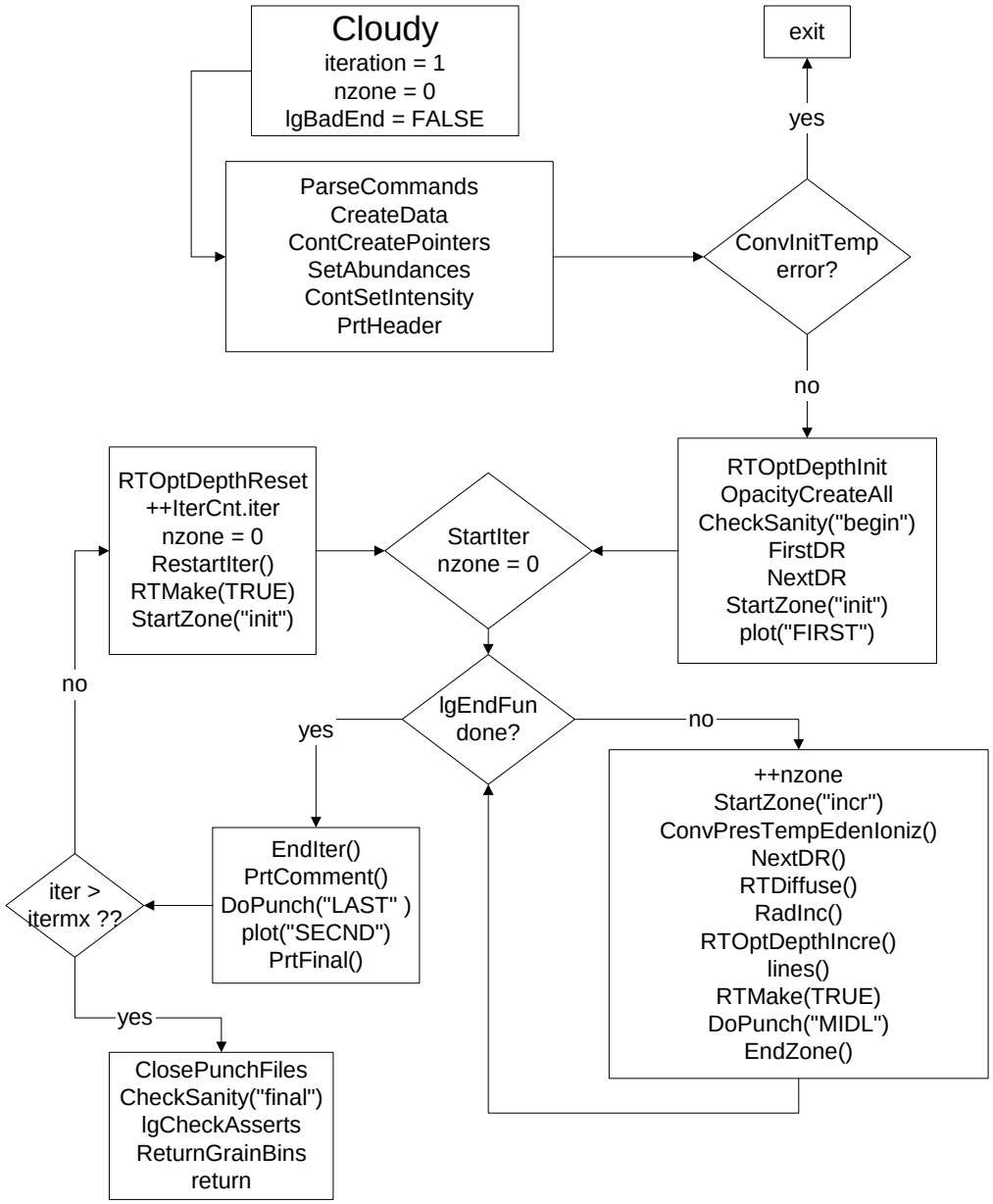

Figure 3 This figure shows the structure of subroutine Cloudy.

1.5.4. The convergence ladder

Many quantities must be simultaneously converged. The following table, and the following sections, outlines the nested group of routines that converges each type of ingredient. At the highest level the pressure is converged, and that solver assumes that the temperature, ionization, etc, are known. Below that is the temperature solver, which is not concerned with the pressure, but assumes that the ionization and electron density are known. Below that is the electron density solver, which assumes that the level of ionization and the OTS rates are known.

Routine	Ionization OTS	Electron density	Temperature	Pressure	Trace convergence keyword
ConvPresTempEdenIoniz	Stable	Stable	Stable	Solve	Pressure
ConvTempEdenIoniz	Stable	Stable	Solve	NA	Temperature
ConvEdenIoniz	Stable	Solve	NA	NA	Eden
ConvIoniz	Solve	NA	NA	NA	ioniz
ConvBase	Drive	NA	NA	NA	

1.5.5. ConvPresTempEdenIoniz converge pressure

ConvPresTempEdenIoniz, shown in Figure 4, is the routine that converges the local pressure or satisfies some other specification of the gas density. Its major loop calls routine ***PressureChange***, which determines what the local density/pressure should be, changes the density if necessary, and sets the variable ***conv.lgConvPres*** to true if the current pressure is correct. It then calls routine ***ConvTempEdenIoniz*** to determine the local temperature, electron density, and level of ionization at the new density. ***ConvPresTempEdenIoniz*** loops until the pressure is declared converged (by the value of the flag ***conv.lgConvPres***) as determined by routine ***PressureChang.***

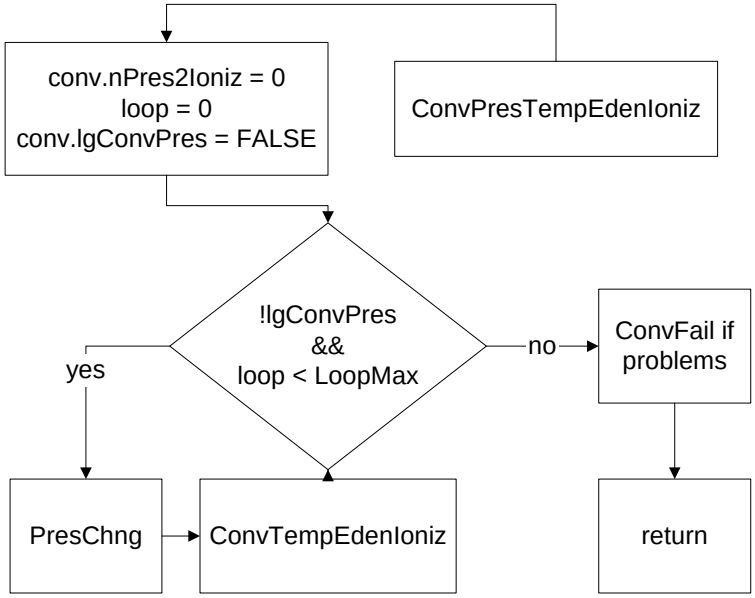

Figure 4 The structure of routine ConvPresTempEdenIoniz..

1.5.6. ConvTempEdenIoniz – converge temperature

ConvTempEdenIoniz is the routine that calls ***ConvEdenIoniz*** to converge the electron density and ionization, and simultaneously determines the electron temperature by balancing heating and cooling. An overview is shown in Figure 5. ***Ionte*** totally controls the value of ***lgDoPhoto***. When ***lgDoPhoto*** is true the code completely reevaluates all opacities and photoionization rates. When false the rates are left at previous values, safe for second iterations.

ConvTempEdenIoniz returns when the heating and cooling match (the variable ***conv.lgConvTemp l*** is set TRUE), or a temperature failure occurs (***tfail*** is set true). The Boltzmann factors are evaluated next in routine ***boltgn***.

A great deal of the code within ***ConvTempEdenIoniz*** deals with identifying temperature oscillations or problems in obtaining temperature convergence. The upshot of this is an estimate of the partial derivative of the difference in heating and cooling with respect to temperature. Many tricks are used to establish this estimate. Routine ***MakeDeriv*** can recall previous values of the heating and cooling and make numerical estimates of their change with respect to temperature. Analytical estimates are also made from the functional form of various heating and cooling constituents.

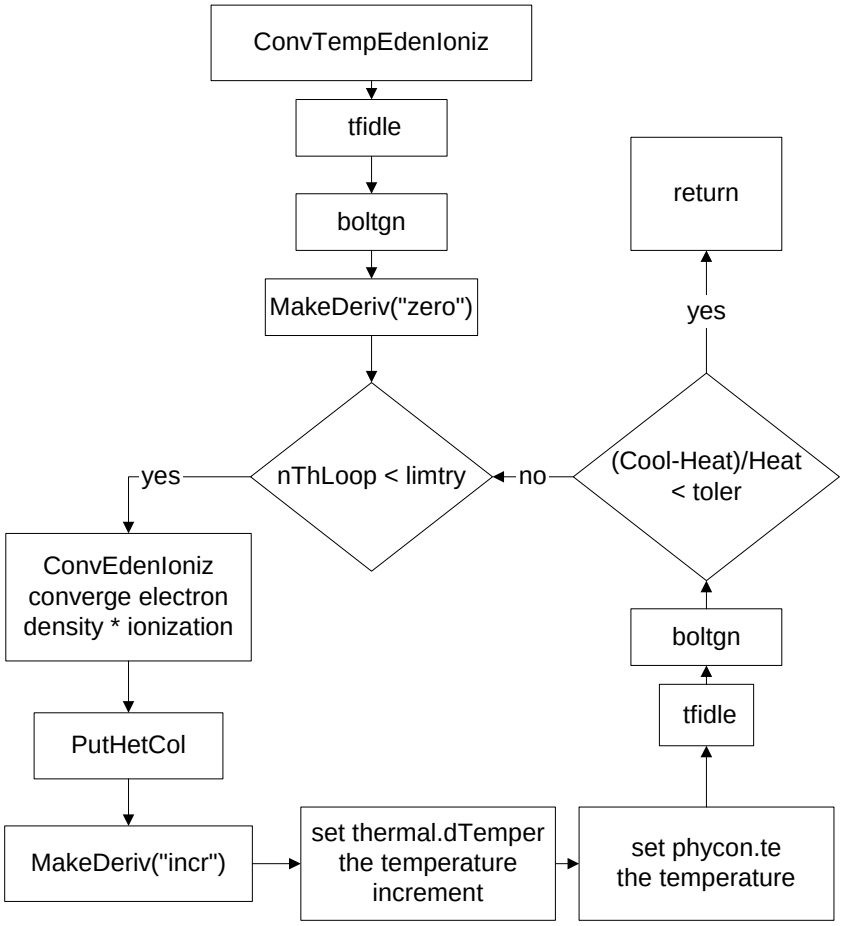

Figure 5 The structure of routine ConvTempEdenIoniz.

1.5.7. ConvEdenIon – converge the electron density

The electron density is actually converged by routine ***ConvEdenIon,*** called by ***ConvTempEdenIon*** as described above. The structure of the routine is shown in Figure 6.

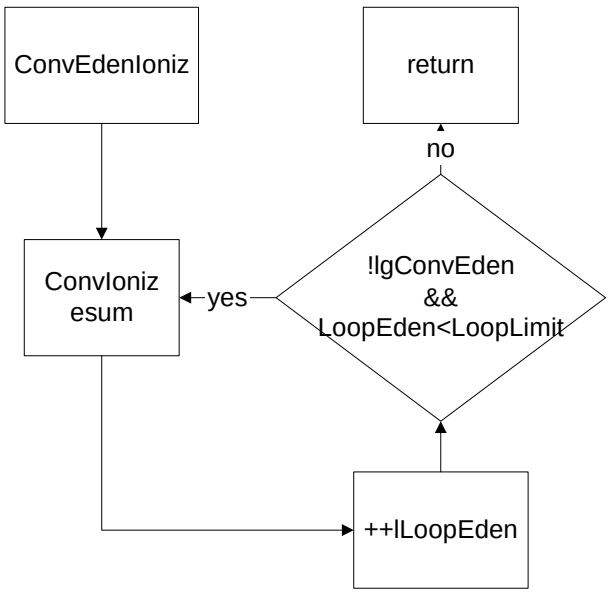

Figure 6 The structure of routine ***ConvEdenIoniz***.

1.6. Line radiative transfer routines

Figure 7 shows the series of routines that are called to evaluate line radiative transfer.

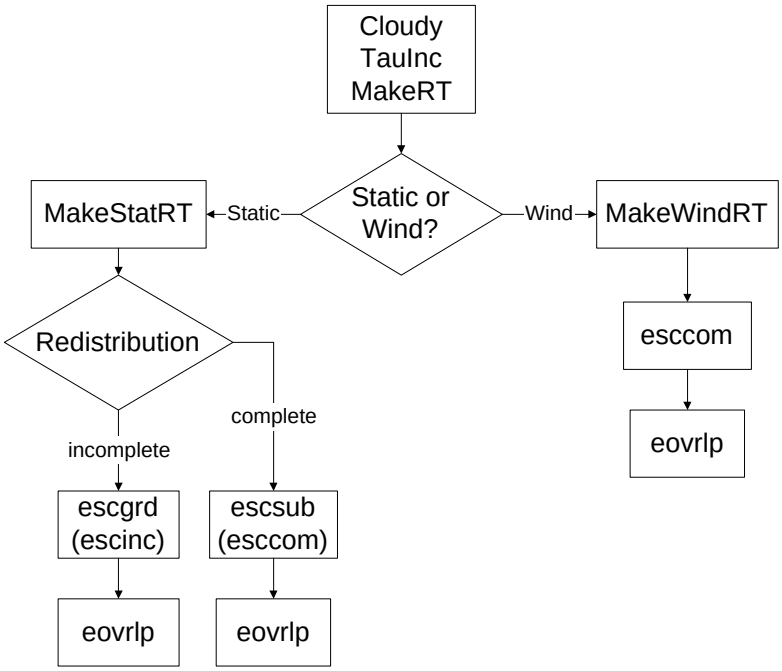

Figure 7 This figure shows the structure of the radiative transfer routines. radtrn

1.7. Geometry

This section defines the internal variables used to describe the geometry. The geometry is always spherical, but can be made effectively plane parallel by making the inner radius of the cloud much larger than its thickness.

Most variables having to do with the geometry are members of the structure *radius*, contained in *radius.h*, and are set and incremented in routine ***ZoneStart***. The

following gives the variable name and a brief description of its intentions. Variables are contained within the structure radius.

***rinner*, $\mathbf{r_o}$** This is the separation between the center of symmetry (i.e., the center of the central object) and the inner edge of the cloud. It remains constant throughout the calculation. If an inner radius is not specified then it is given the default value of 10^{30} cm. This will usually result in a plane parallel geometry.

drad*, δr** This is the thickness of the current zone. Note that the zone size changes continuously throughout the calculation. Upper or lower limits to ***drad can be set with the **`drmax`** and **`drmin`** commands described in Part I.

radius*, r** This is the distance between the center of symmetry and the *outer* edge of the current zone. For the first zone, ***radius has the value ***rinner* + *drad***.

depth*, Δr** This is the distance between the inner edge of the cloud and the *outer* edge of the current zone. For the first zone, ***depth has the value ***drad***.

A problem can arise under certain extreme circumstances. The depth variable ***depth*** must be increased for every zone by adding the zone thickness ***drad***. Both variables are double precision. If the radio ***drad/depth*** falls below ~ 10^{-14} then the depth cannot be updated on most machines. The problem is that the sum ***depth*** + ***drad*** will be equal to ***depth*** because of numerical underflow. If this occurs (i.e., the zone thickness ***drad*** falls below ***depth***/10^{14}) the code will stop, with the comment than the zone thickness is too small relative to the depth. There is no obvious solution to this problem.

drNext This will be the thickness of the next zone. The thickness of the zones is adjusted continuously during a calculation. Adaptive logic is used to ensure that the zones are large enough to be economical, but small enough to follow changes in the physical conditions across the nebula. This choice of the next zone thickness is done in routine ***radius_next***. The logic behind the choice of the zone thickness can be followed with either the **`trace dr`** or **`punch dr`** commands.

router[iteration] This is the limit to the outer radius of the structure, as set before the calculation begins. The default value is effectively infinite, actually 10^{31} cm.

r1r0sq This is the sphericity ratio

$$\mathrm{R1R0SQ} = \left[\frac{\text{outer radius of zone}}{\text{radius of face}}\right]^2 = \left(\frac{\mathrm{RADIUS}}{\mathrm{RINNER}}\right)^2 \qquad (1)$$

dReff This is the effective radius, $\delta r_{eff} = \delta r \times f\left(r\right)$ where $f(r)$ is the filling factor.

dVeff This is the effective volume relative to the inner radius. The units of ***dVeff*** are cm, and it is equal to ***dReff*** if the geometry is plane parallel.

$$\mathrm{dVeff} = \left(\frac{radius - dRad/2}{rinner}\right)\left(\frac{\min\left(radius - dRad/2, \mathrm{cylind}\right)}{rinner}\right) dRad \times f\left(r\right) \qquad (2)$$

pirsq This is the log of the inner area ($4\pi r_o^2$).

lgFourPi – set true if quantities like line intensities are into 4π sr.

1.8. Physical Conditions

1.8.1. Densities

These are contained in structure ***dense***.

xMassDensity The gas mass density in gm cm^{-3}.

pden This is the number of particles per cubic centimeter. It is evaluated in ***TotalPressure***.

wmole This is a quantity related to the mean molecular weight, the mean AMU per particle. It is evaluated in ***TotalPressure***.

$$wmole = \frac{\sum n_i m_i}{n_{tot}} \tag{3}$$

With these definitions the density ***densty*** (gm cm^{-3}) is the product of ***pden*** and ***wmole***.

TotalNuclei – total number of nuclei

eden This is the electron density, as evaluated in routine ***esum***. ***eden*** is also controlled by other parts of the code, which allow it to change only gradually while looking for a new solution.

EdenTrue This is the correct electron density, and is evaluated in ***esum***. The electron density has converged when ***EdenTrue*** and ***eden*** are within ***EdenError*** of one another. ***EdenError*** is set in the large block data to 0.01. This variable is the sole member of the common block of the same name.

edensqte This is the ratio

$$edensqte = \left[n_e + n\left(\mathrm{H}^0\right) 1.7\times10^{-4} \right] T_e^{-0.5} \tag{4}$$

used in many collision rate equations across the code. It is evaluated in routine ***tfidle***. The second term in parenthesis approximately accounts for neutral collisions (Darwin 1969).

cdsqte This is the ratio

$$cdsqte = edsqte \times 8.629\times10^{-6} = \left[n_e + n\left(\mathrm{H}^0\right) 1.7\times10^{-4} \right] T_e^{-0.5} 8.629\times10^{-6} \ [\mathrm{cm^{-3}\ s^{-1}}] \tag{5}$$

used in many collision rate equations across the code. It is evaluated in routine ***tfidle***.

1.8.2. Temperatures

These are all contained in structure ***phycon***.

te This is the local electron temperature.

tlast is the final temperature of the last computed zone. It is only meaningful for the second or greater zone.

alogte, alogete These are the base 10 and natural logs of the electron temperature. The array ***telogn*** contains powers of the base 10 log of the temperature.

telogn[i] This is a vector dimensioned 7 long. The n^{th} member of the array contains $\log(T_e)^n$.

alogete is the natural log of the temperature.

Routine ***StartZone*** will propose a temperature for the next zone, the variable ***TeProp***, if the model is a constant density model. Routine ***tfidle*** sets all ancillary variables related to the temperature, such as alogte.

1.8.3. Structure

The *struc* structure. This saves information about the structure of the model. It has several elements, each containing a saved quantity for a zone.

ednstr The electron density of each zone is saved in this vector.

hiistr The H^+ density of each zone is saved in this vector.

histr The H^0 density of each zone is saved in this vector.

heatsrt This is the total heating.

pdenstr This save the total number of particles per cubic centimeter.

radstr The effective thickness ***dReff*** (cm) of each zone is saved in this vector. This includes a filling factor if one was specified.

testr The temperature structure of the nebula is saved in this vector.

volstr The volume ***dVeff*** (cm^3) of each zone is saved in this vector. This includes a filling factor if one was specified.

1.9. Optical depths and iterations

1.9.1. RTOptDepthInit

Routine ***RTOptDepthInit*** is called soon after the initial boundary conditions are established, to estimate the initial total line and continuum optical depths. It uses various methods to estimate these.

1.9.2. RTOptDepthIncre

Routine ***RTOptDepthIncre*** is called once during each zone to increment the optical depth scale.

1.9.3. RTOptDepthReset

Routine ***RTOptDepthReset*** is after the iteration is complete to reset the optical depth scale.

1.9.4. lgTauOutOn

This logical variable indicates whether or not the outward optical depths have been estimated. It is false on the first iteration and true thereafter.

1.10. Zones and Iterations

iteration This global variable is the counter for the current iteration. It is set to one at the start of the first iteration, and is incremented in routine Cloudy after the

last printout, just after the limiting optical depths are updated by calling routine ***RTOptDepthReset***. The calculation stops when ***iteration*** is greater than ***itermx*** *after* the iteration is complete, but before the counter is incremented.

ITRDIM This is the limit to the total number of iterations that can possibly be performed. It is used to declare the dimension of the vectors that store iteration information. It currently is set to 200.

itermx This is the limit to the number of iterations to be performed and is set by the user. ***itermx*** is part of the structure ***IterCnt***. ***itermx*** is initialized to 0 so that the code normally stops after the first iteration. The value of ***itermx*** can be changed with the **`iterate`** command. ***itermx*** is set equal to the number entered on the command *minus one*. This is so that "**`iterate 1`**" will cause the code to stop after a single iteration (***iteration*** is equal to 1 at the end of the first iteration, and the code will only stop if ***iteration*** is greater than ***itermx*** after the iteration is complete).

nzone This is a global variable and gives the current zone number. It is equal to one for the first zone. ***nzone*** is set and incremented in routine Cloudy. ***nzone*** is equal to zero during the search for the initial conditions, on all iterations. After the search has identified a solution the conditions in the first zone are computed with ***nzone*** set to unity.

nend[I] This is the limit to the number of zones in the current (i^{th}) iteration and is part of the structure *ZoneCnt*. It is a vector of dimension 200 (as set by ***ITRDIM***). Individual elements of the vector are set with the **`stop zone`** command. The current iteration stops when ***nzone*** is greater than or equal to ***nend[iteration***].

lgLastIt This logical variable indicates whether (true) or not this is the last iteration. It is controlled by routine ***startr*** and is set true if ***iter*** is greater than ***itermx***, and false otherwise.

1.11. Search phase?

The logic used during the search for the initial conditions at the illuminated face of the cloud is quite different from that used when going from zone to zone across the cloud. Usually no good estimate of the initial conditions exists, but within the cloud conditions do not vary by much from zone to zone. One way to check whether the code has a valid estimate of the physical conditions, or whether the first step in the initial search for parameters is taking place, is to check the status of the variable ***conv.lgSearch***. The initial search is underway if this variable is true. Another is to check whether ***nzone*** is greater than 0.

Some quantities are totally unknown while the various routines are being called for the very first time during a calculation. The variable *nPres2Ioniz*, part of *conv*, is zero before the ionization has been determined the first time, since it counts the number of times the pressure routine has called the ionization routine.

1.12. Composition variables

All variables that hold information concerning abundances and composition are contained in the structure *abund*, defined in the header file *abundances.h*.

Routine ***SetAbundances*** is called by routine ***cloudy*** after all commands have been entered. This routine sets the final abundances to be used in the first zone of the calculation. The following variables are used.

Routine ***SetAbundances*** first modifies the contents of *solar* by the scale factors. The helium abundance is altered by both *depset* and *scalem*, while all heavier elements are modified by these and *dmetal* as well. Then *abund.gas_phase[nelem]* is set to the density (cm^{-3}) of each element, the product *hden* and *solar[nelem]*. This is the total abundance of that element, in all stages of ionization and molecular forms.

The initial chemical composition is printed by routine ***PrintElem***, which is called by ***SetAbundances***.

Default abundances are stored in several arrays. Solar abundances are stored in the array *SolarSave[nelem]*, where *nelem* is the atomic number on the C scale. Other mixtures, such as ISM, HII Region, etc, are also entered in this structure, in other arrays. Each array is dimensioned *LIMELM* (currently 30), the number of elements included in the code.

When the code is initialized the contents of *SolarSave* are copied to the array *solar*, which will contain the initial abundance mix for the current calculation. Gas phase depletion factors, used to modify the final abundance, are stored in the array *depset[nelem]* and are set to unity in routine ***zero*** when the calculation is initialized. The final contents of *solar* will be absolute abundances by number, on a scale with hydrogen at unity.

When an element with atomic number *nelem+1* is turned off, the logical variable ***lgElmtOn[nelem]*** is set to false.

ScaleMetals This is the scale factor entered with the **`metals`** command when a number but no keyword appears on the line. This multiplies the abundances of all elements heavier than helium. It has no effect on hydrogen or helium.

depset If the **`metals`** command is entered and no numbers appear, but the keyword **`deplete`** occurs instead, then this array of scale factors is set to the contents of the array *deplon*.

ScaleElement This is an array of *LIMELM* scale factors, and is set when the **`element scale`** command is entered.

lgAbnSolar This logical variable is false if the default abundances have been altered, and is true if they are left at the default solar mixture. It is used for sanity checks within the code.

xIonDense This is a two dimensional vector containing the gas-phase ionic abundances. *xIonDense[nelem][n]* is the gas-phase density of the *n*th ionization stage of that element, where the atom is 0.

gas_phase This is a one-dimensional array containing the total gas-phase abundances of all elements included in the calculation. This does not include material locked in grains, but does include ices that form on the surfaces of grains.

1.13. Covering factors

Two covering factors enter into the calculations. These are referred to as the geometric covering factor, and the radiative transfer covering factor. All covering factors are part of the structure *sphere*, defined in the header file *sphere.h*.

1.13.1. Geometric covering factor

This covering factor linearly affects the luminosity of emission lines. The nebula intercepts a fraction $\Omega_{geo}/4\pi$ of the luminosity radiated by the central object. Within the code the geometric covering factor is referred to by the variable *covgeo*.

The code actually works in units of intensity radiated by a unit area of illuminated face of the cloud to avoid exponential range problems with IEEE machines. If the predicted intensity of a line (erg s^{-1} cm^{-2}) is given by I then the line luminosity will be

$$L = 4\pi \quad r_{inner}^2 \frac{\Omega_{geo}}{4\pi} I \ \text{[erg s}^{-1}\text{]} \qquad (6)$$

where r_{inner} is the inner radius.

The default value of the geometric covering factor is unity, and it can be changed with the **`covering factor`** and **`sphere`** commands.

1.13.2. Radiative transfer covering factor

The radiative transfer covering factor has only second order effects on the intensity of emission lines. This is the covering factor which takes into account interactions with diffuse fields produced on the symmetric far side of the nebula. Within the code it is referred to by the variable *covrt*.

The default value of the radiative transfer covering factor is zero, appropriate for an open geometry. For a closed geometry it is set to unity. The radiative transfer covering factor only affects the model through the diffuse fields. For a closed geometry all radiation is included in the outward beam, and for an open geometry only half. This covering factor has no effects on the calculations, other than the amount of diffuse fields transferred outward. Physically for an open geometry the fraction of radiation escaping in the inward direction is then lost to the system. In an open geometry the nebula is symmetric, and escaping radiation is exactly matched by radiation impinging from the far side of the geometry.

1.14. Floating Point Environment

The floating-point environment should be set to ignore floating-point underflow but crash on any other floating-point error. Floating-point underflow is an unavoidable consequence of the attenuation of radiation as a beam of light is extinguished by an absorbing medium; underflow error checking should be disabled.

Floating point overflow or division by zero *must never* occur, nor should library function domain errors (i.e., the log of a negative number). I would appreciate hearing about these errors. I can't fix it if I don't know it is broken. The code's web site, www.nublado.org, has a discussion board for this purpose. Please include the input file and version number.

1.15. Reliability in the face of complexity

The real challenge in software development is to prevent mistakes from happening in the first place, catch mistakes as soon as they are produced, then validate all results every time anything changes (Ferland 2001b). You can help by keeping on the lookout for suspicious results.

2. RUNNING A SINGLE MODEL

Cloudy can be used to run a single model or to create grids of calculations. This section describes how to read in the parameters for a single model and compute the result. The next goes into grid calculations, in which the code is called as a subroutine of another larger code.

2.1. Running a single model with a shell script

The easiest way to do this is to create a small file that contains the input commands for that model. As a typical case consider a simple planetary nebula:

```
hden 4 // this is the log of the hydrogen density (cm^-3)
radius 17 // log of the inner radius in cm
black body 100,000K, luminosity 38 // black body temperature and total luminosity
```

Assume this is saved as the file *pn.in*. Cloudy stops reading the input steam when it reaches either an empty line or the end of file. No special end of input sentinel is needed.

I have a shell script named *run* which is in my "bin" directory, which I include on my path. The shell script *run* consists of the following:

```
echo reading input file $1.in
case $# in
0) echo there must be an input file ;;
1) /homeb/uwc0/gary/cloudy/c.sun4<$1.in >$1.out
  echo created output file $1.out ;;
2) /homeb/uwc0/gary/cloudy/c.sun4 < $1.in >$2.out
  echo created output file $2.out ;;
esac
echo $p
exit
```

If *run* is executed with no input parameters it will complain that at least one argument is needed and then stop. If there is one parameter it is treated as the name of the input and output files. So in the above example, typing

```
run pn
```

would read the input stream in *pn.in* and create an output file of results called *pn.out*. When two parameters occur the first is the name of the input stream and the second is the name of the output steam. The example

```
run pn test
```

would read the file *pn.in* and create the file *test.out* .

2.2. Running a single model from the command line

The code also has a command-line option that will accomplish the same thing as the shell script described in the previous section. If you create an executable called *cloudy.exe*, then the command

```
cloudy.exe -p model
```

will read input from *model.in*, write output to *model.out*, and add the prefix *model* to all the punch files. This option was added by Robin Williams.

3. CLOUDY AS A SUBROUTINE

3.1. Overview

Cloudy is designed to be used as a subroutine of other, much larger, codes. When used this way a series of subroutine calls, described next, are used to initialize the code, specify the initial conditions, do the simulation, and finally examine the predictions.

It is said to be possible to call a C program like Cloudy from a Fortran program by using the *cfortran.h* header file described at http://www-zeus.desy.de/~burow/cfortran/ . I have never tried this. Good luck.

A common strategy is to call the code to compute line intensities for a large matrix of parameters. The results of one such calculation is shown in Figure 8 (Baldwin et al. 1995; Ferland 2003). Such grids can be computed in a few dozen hours on modern workstations, and offer far greater insight to physical effects of changing model parameters than does a single model.

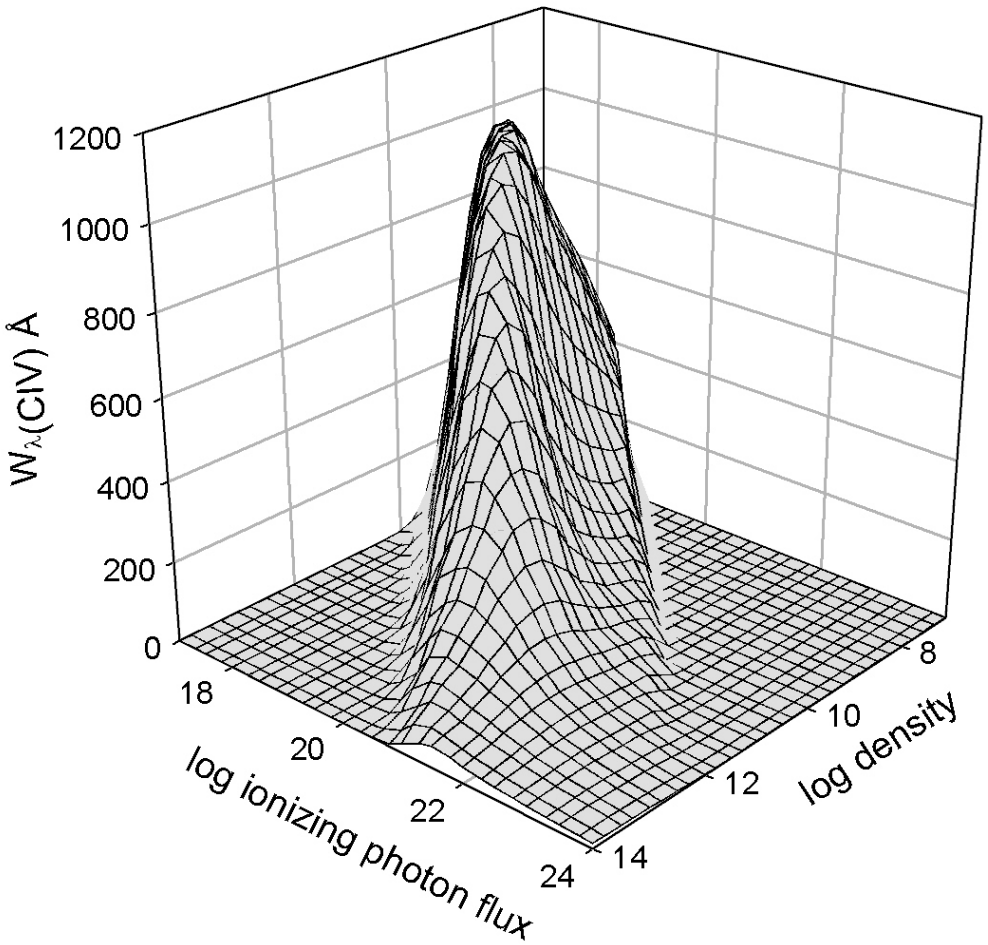

Figure 8 The results of a large grid of quasar emission-line cloud calculations are shown. The x-y plane shows the logs of the hydrogen density (cm^3) and flux of ionizing photons (cm^{-2} s^{-1}). The z axis is the predicted line equivalent width.

This chapter gives an overview of all the routines that are intended to be "public", that is, needed to be accessed by programs that will call Cloudy. The definitions for

all public routines are contained in the header file *cddrive.h*, which gives the best current description of all these routines. That file is the definitive reference source for all of the material in this chapter.

3.1.1. Creating a new main program

In C there must be exactly one main program and it must be called ***main***. This routine is within the file *maincl.c* in the source downloaded from the web. You need to replace the existing Cloudy main program with one that you write. The file *maincl.c* that is included in the distribution must be deleted so that the program you write will be loaded instead. The remaining routines are then compiled with a command like the following:

```
gcc -c *.c
```

which will create a large number of object files. Often the new main program will be linked with these object files with a command something like

```
gcc newmain.c *.o -lm
```

The following subsections outline how to write code for this new main program.

3.1.2. The cddefines.h and cddrive.h header files

The file *cddrive.h* contains definitions of all public routines, the routines that a user would call to drive Cloudy. That file is the definitive reference for the material contained in this section and is more up to date than this document. Comments within that file explain all routines and their parameters.

The header *cddefines.h* should come before *cddrive.h* since it includes many definitions and includes the standard C header files that are needed to drive the code. The first two header files in the new main routine should be the following:

```
#include “cddefines.h”
#include “cddrive.h”
```

3.1.3. A note on return conditions

Some of the routines return a value to indicate success or failure. I try to follow the C and Unix conventions to indicate success with zero and trouble with a non-zero return. This rule is not always followed (it is not followed by the important routine ***cdLine***), however, and *cddrive.h* should be consulted to make sure the return conditions are understood.

3.2. Initializing the code

Many variables must be initialized at the beginning of the calculation. Calling routine ***cdInit*** does this.

```
cdInit();
```

Routine ***cdInit*** must be called every time a new calculation is to be performed, *before* calling any of the following subroutines, but after the results of any previous calculations have been read. (The results of any previous calculations are lost when ***cdInit*** is called.)

cdMPI When the code is executed using MPI (Message Passing Interface, used on parallel machines) the code must call a specific exit handler, MPI_finalize, upon exit. Routine ***cdMPI*** should be called after ***cdInit*** but before the main program is called to do this.

3.3. Handling input and output

3.3.1. cdTalk - produce output??

Cloudy normally speaks what's on its mind. This would generate too much output in a large grid. It does have a quiet mode in which nothing at all is printed. This quiet mode is set by the logical argument to subroutine ***cdTalk***.

```
#include "cddefines.h"
#include "cddrive.h"
   cdInit();
   /*set no output at all*/
   cdTalk( FALSE )
   /*have the code produce the normal printout*/
   cdTalk( TRUE )
```

The default is for Cloudy to produce output, and ***cdTalk*** does not have to be called if this is desired. However, it does need to be called with the logical variable ***FALSE*** if the quiet mode is desired. (***TRUE*** and ***FALSE*** are 1 and 0 and are defined in *cddrive.h*).

3.3.2. cdOutp - sending output to a file

Cloudy normally writes its standard output on the system's **`stdout`**. This can be changed to another file by calling routine ***cdOutp***, which has a file handle to an open file as its single argument. By combining this redirection with the C **`fopen`** statement it is possible to have the standard output sent into any file.

```
#include "cddefines.h"
#include "cddrive.h"

       /* this defines a standard C file handle */
       FILE *ioData;

       /* open the file output.txt for writing */
       ioData = fopen("output.txt","w");

       /* ioData is equal to NULL if we failed to open the file */
       if( ioData==NULL )
       {
              exit(1);
       }

       /* send output to this file*/
       cdOutp( ioData ) ;
       -   - - code goes here
       /* at end of calculation we need to close the file */
       fclose(ioData);
```

3.3.3. cdRead - entering Commands

Command lines are entered by successive calls to routine ***cdRead***. The argument of ***cdRead*** is a null-terminated string containing valid commands. These commands must obey all the rules outlined in Part I.

In the examples below some commands are directly entered as strings (this works when the string is a constant) while others are created by writing variables through ***sprintf*** (a standard C io function – this is necessary when the value of a variable needs to be placed into a string).

```
char chLine[132];/* this vector will hold the command lines we will generate*/

/* this example sends the string straight to cdRead */
nleft = cdRead("title a series of constant pressure models" );

/* write variable to a string then sends the string to cdRead */
hden = 5.4;
sprintf( chLine , "hden %5.2f ", hden );
nleft = cdRead(chLine );

/* this example sends a string that contains double quotes,
 * and so must “escape” them with doubled backslashes */
nleft = cdRead("set path\"d:\\projects\\cloudy\\ccloudy\\data\" " );

sprintf( chLine , "coronal %5.2f ", temp );
nleft = cdRead(chLine );

nleft = cdRead("stop zone 1 " );
```

cdRead returns the number of commands that can still be entered before exceeding the size of the storage arrays. The return value was ignored in the examples above. So this routine is an exception to the general rule that a zero return condition indicates success – here it indicates a problem – no further commands can be entered.

It is not now possible to read in more than 4000 command lines because of limits to the size of the character arrays used to store them. This limit is stored as the variable ***NKRD***. If more than 4000 lines are read in by calling ***cdRead*** then ***cdRead*** will stop after explaining why. It will be necessary to increase ***NKRD*** if more than 4000 command lines are needed.

3.4. Executing the code

3.4.1. cdDrive - calling the Code

The calculation is performed when routine ***cdDrive*** is called. ***cdDrive*** returns an int indicating whether the calculation was successful. The value 0 indicates a successful calculation. The following shows an example of its use.

```
if( cdDrive() )
{
          printf(“problems!\n”);
          exit(1);
}
```

If problems occurred and the results cannot be trusted then the return value is non-zero. This will only be set if the calculation suffered a complete meltdown. Routine ***cdNwcns*** (see page 428 below) can be called to find out about any problems.

3.4.2. cdNoExec - checking without Computing

If routine ***cdNoExec*** is called after ***cdInit*** but before ***cdDrive*** then only the initial parts of a calculation will be performed when routine ***cdDrive*** is called.

```
cdInit();

/*read in commands */
cdRead( . . .);

/*tell it not to execute */
cdNoExec();

/*call the code */
lgBad = cdDrive();
```

When ***cdDrive*** is called after ***cdNoExec*** the code will generate the incident continuum, set the initial density, and derive the chemical composition. It will then stop just before the initial search for the physical conditions in the first zone. All of the initial printout, summarizing properties of the composition and continuum, will be generated. This provides a quick way to check that a large grid of models will be specified correctly, without actually fully computing the grid.

Table 1 Special cases Column Densities

Excited states		molecules
Label	column	Label
He1*	He^0 2^3S	H2
CII*	C^+ $J = 3/2$	H-
C11*	C^0 $J = 0$	H2+
C12*	C^0 $J = 1$	H3+
C13*	C^0 $J = 2$	H2g
C30*	C^{2+} $J = 0$	H2*
C31*	C^{2+} $J = 1$	HeH+
C32*	C^{2+} $J = 2$	CO
O11*	O^0 $J = 2$	OH
O12*	O^0 $J = 1$	H2O
O13*	O^0 $J = 0$	O2
Si2*	Si^+ J=3/2	SiO
C2	C_2	C2
C3	C_3	C3
H2vJ	H_2 any v,J	H2

3.5. Checking Predictions

This section describes a series of routines that allow predicted quantities to be obtained after the calculation is complete.

3.5.1. cdB21cm – mean magnetic field

The return value is the mean magnetic field weighted by $n(H^0)\ dr/T_{spin}$. This is the field measured with 21 cm Zeeman observations. A tangled magnetic field is assumed. A magnetic field is not included by default but can be added with the **`magnetic field`** command, described in Part 1 of this document.

3.5.2. cdCO_colden – column density in CO

This routine returns the column density of a rotation level within the ground vibrational level of CO. It has two arguments, the carbon isotope, which must be 12 or 13, and the rotation quantum number. It returns the column density in that rotation level. Some caveats – the chemistry network does not now independently solve for the 13CO abundance, but rather it uses a preset 13CO/12CO ratio (see the description of the **`atom co`** command), and only the ground vibrational state is done. Any number of rotation states can be done. The routine has two integer arguments. The first is the carbon isotope and the second is the rotation level.

```
/* total column density in J=0 of 13CO*/
total = cdCO_colden( 13 , 0 );
/* total column density in J=2 of 12CO */
ortho = cdCO_colden( 12 , 2 );
```

3.5.3. cdColm - the computed column densities

The predicted column densities of some species can be obtained by calling routine ***cdColm***:

```
/* want C+2 */
if(cdColm("carb", 3 , &colum))
{
              printf(" could not find C+2\n");
}
else
{
       printf("The predicted C+2 column density is %e\n", column );
}
```

The routine returns zero if it found the species, and 1 if it could not. It returns the predicted column density (linear, cm^{-2}) as the third argument. The first argument ***chLabel*** is a four-character identifier that must agree with the first four characters (upper or lower case) of the name used to indicate the element in the printout. The integer variable ***ion*** is the spectroscopic designation of the level of ionization, i.e., 1 indicates C I or C^0, 3 indicates C III or C^{+2}, etc.

The ion stage of 0 indicates a special case, a molecule or excited level of an atom or ion. The label determines the species in this case. Table 1 gives the levels and molecules that are recognized. Many of the molecules have fewer than four characters. The label must still contain four characters and spaces are used to fill out the four.

It is possible to obtain column densities in any *v,J* level of H_2 when the large molecule is included with the **`atom H2`** command. Call routine ***cdColm*** with an ion stage of zero but with the *v,J* quantum levels given by single digits after the "H2" in the four-character label giving *v* and *J* as "H2vJ". For instance, "H218" would find the column density in the *v*=1, *J*=8 level. The command works by subtracting the character '0' from the third and fourth characters in the label. Levels v and J greater than 9 can be specified by following the character-coding for your computer. For ASCII characters (used on nearly all of today's systems) the colon, semicolon, and less than sign follow 9 and so would be used for 10, 11, and 12. Consult a character table for your computer system.

3.5.4. cdCooling_last- last zone's cooling

The return value is the total cooling rate (erg cm^{-3} s^{-1}) for the last computed zone.

3.5.5. cdDepth_depth –the depth structure of the cloud

This routine returns a vector giving the zone depths (in cm) of the previous iteration. The code uses adaptive logic to control the radial zoning of the model. Neither the number of depth points nor their structure is known in advance. This routine is called with a double precision vector with enough space to hold the structure. The number of depth points is determined by calling ***cdnZone*** and space must be allocated by the calling routine. Each element of the vector is the depth from the illuminated face to the center of zone *n*.

3.5.6. cdDLine – emergent line intensities

This form of the ***cdLine*** routine has the same arguments and return values, but returns the intensity emergent from the illuminated face of a layer in front of an optically thick scattering/absorbing layer. These are the lines that are printed with

the heading *Emergent Line Intensities*. They are only predicted for an open geometry when grains are present and are discussed on page 459 below.

3.5.7. cdEmis - emissivity of lines

cdEmis functions much the same as ***cdLine*** (page 420 above) but returns the local emissivity (erg cm^{-3} s^{-1} for unit filling factor) of the line for the last computed zone. The return value is the index of the line within the line stack if it was found, and the negative of the number of lines in the stack if the line could not be found.

3.5.8. cdGetLineList - sets of emission lines

The routine ***cdGetLineList*** provides a way to access a large number of emission lines in an automatic manner.

A list of emission lines can be entered into a data file. Routine ***cdGetLineList*** is called with the name of this file. The set of lines is entered into a pair of vectors. One vector will give the set of line labels, which are strings like "H 1". The second vector gives the corresponding wavelengths. The lists can then be used to call ***cdLine*** to obtain intensities of the lines.

cdInit must be called to initialize needed variables before ***cdGetLineList*** is called. Next ***cdGetLineList*** is called, and finally, the actual grid of calculations begins with another call to ***cdInit***. The predicted intensities of a set of lines are extracted by calls to ***cdLine***. So the first call to ***cdInit*** followed by a call to ***cdGetLineList*** rather than the actual execution of the code.

The first argument to routine ***cdGetLineList*** is the name of the file containing the line list. A set of such files is included in the data directory of the distribution files. They have names *LineList*.dat*. The last part of the name indicates its purpose. If a null string is passed ("") then *LineList_BLR.dat* is used. The code will first try to open the file in the current directory, and if is not present, will try on the path as set with the **`path`** command or in *path.c*.

The second two parameters are a pair of pointers that are defined by the calling program. When routine ***cdGetLineList*** is called it uses these pointers to create a pair of vectors giving the labels and wavelengths. Space for the lines is allocated by ***cdGetLineList*** after it determines how many lines are in the file. These string and integer vectors will then contain the label and wavelength used to identify the lines. The function returns the number of lines in the list. If problems occurred then a -1 is returned.

The following shows an example of getting the lines from *LineList_BLR.dat*, executing the code and then obtaining the predicted intensities of all lines listed in *LineList_BLR.dat* by calling ***cdLine***.

```
/* define variables */
char **chLabel;
float *wl;
/* initialize the code */
cdInit();
/* get list of lines from standard data file */
if( (nLines=cdGetLineList("",&chLabel,&wl)) < 0 )
{
              /* this is the error exit – could not obtain the lines */
              exit(1);
}
- - - - - - missing code
/* now set up the actual call to the code */
cdInit();
/* missing commands here, then call the code */
- - - - - - missing code
cdDrive();
- - - - - - missing commands go here
/* now print the predicted emission lines */
for( n=0; n<nLines; ++n )
{
       lgOK = cdLine( cdGetchLabel[n], cdGetnWL[n] , &relative , &absolute );
              if( lgOK<= 0 )
              {
                            fprintf(stderr,"did not find
%4s%5li\n",cdGetchLabel[n],cdGetnWL[n]);
                            fprintf(ioDATA,"\ndid not find line.\n”);
              }
              print(“%.3e\n”, relative);
}
```

3.5.9. *cdH2_colden – state-specific column densities of H_2*

This routine returns the column density of any level in the ground electronic state of H_2. This command only works when the large H_2 molecule is included with the **`atom H2`** command. It has two integer arguments, the vibration and rotation quantum numbers of a level in X. If both are zero or greater the routine returns the column density in that level. If the vibration quantum number is negative then a summed column density is turned. If v<0 and J=0 it returns the total H_2 column density, if J=1 it returns the ortho column density, and if J=2 the para column density. If the indices do not make sense the routine prints a message and returns -1.

Here are some examples:

```
/* total H2 column density */
total = cdH2_colden( -1 , 0 );
/* ortho column density */
ortho = cdH2_colden( -1 , 1 );
/* para column density */
para = cdH2_colden( -1 , 2 );
/* column density in 0, 0 */
total00 = cdH2_colden( 0 , 0 );
```

3.5.10. *cdH2_Line – an H2 emission line intensity*

More than half a million H_2 lines are predicted and there will be instances where two H_2 lines have nearly the same wavelength. Identification of a particular transition within the list of lines can be ambiguous. This command determines the intensity and luminosity of a transition by specifying its upper and lower n, v, J levels. The first six arguments give the n, v, J indices of the upper and lower levels in that order. The last two variables are double pointers that return the intensity and

luminosity of the transition. The function returns 1 if it finds the line and 0 if it did not. (This behavior follows that of ***cdLine*** rather than the standard C++ conventions on function return values.) Currently this only works for the ground electronic state.

Here is an example:

```
double xInten , xLumin;
/* the 1-0 S(1) at 2.121 microns */
If( cdH2_Lines( 0,1,3 , 0,0,1 , &xInten , &xLumin ) == 0 )
{
        Printf("could not find line.\n");
}
```

3.5.11. cdHeating_last – last zone's heating

The total heating rate (erg cm^{-3} s^{-1}) for the last computed zone is returned.

3.5.12. cdIonFrac - the computed ionization fractions

The predicted ionization fractions[2], averaged over radius or volume, can be accessed by calling the subroutine ***cdIonFrac***. These are defined as follows – the average over radius is defined as

$$\left\langle \frac{n\left(S^{+n}\right)}{n\left(S_{gas}\right)} \right\rangle = \frac{\int n(S^{+n})\, f(l)\, dl}{\int n(S_{gas})\, f(l)\, dl} \qquad (400)$$

Where S_{gas} is the total gas phase density of the element. The average over volume is defined as

$$\left\langle \frac{n\left(S^{+n}\right)}{n\left(S_{gas}\right)} \right\rangle = \frac{\int n(S^{+n})\, f(r)\, dV}{\int n(S_{gas})\, f(r)\, dV} \; . \qquad (400)$$

Two sample calls to the routine follow:

```
/* FALSE below means to not include electrons in the mean */
if( cdIonFrac( "carb" , 2 , &frac , "radius" , FALSE) )
{
        exit(1);
}
printf("The predicted ionization fraction over radius is is%g\n", frac);
/* TRUE below means to include electrons in the mean */
if( cdIonFrac( "carb" , 2 , &frac , "radius" , TRUE) )
{
        exit(1);
}
printf("Ionization fraction wrt radius end elec den is is%g\n", frac);
```

The routine returns the predicted ionization fraction A_{ion}/A_{tot}. ***chLabel*** is a four-character identifier that must agree with the first four characters (upper or lower case) used to indicate the element in the printout. The integer variable ***ion*** is the spectroscopic designation of the level of ionization, i.e., 1 indicates C^0 or C I, 3

[2] Before version 96 the ionization fractions only included atoms and ions. They now also include molecules. The sum of the atomic and ionic fractions will not add up to unity if a significant fraction of the element is in molecules.

indicates the second ion C^{+2} or C III, etc. ***chWeight*** is a six-character variable (plus end of string sentinel) which must be either "**radius**" or "**volume**" (either upper or lower case). This string determines whether the ionization fraction returned is weighted with respect to radius or volume. The last variable determines whether (TRUE) or not (FALSE) the ionization fraction is also weighted with respect to the electron density. The function returns zero if the ion was found and non-zero if an error occurred.

The ionization stage of zero will request the fraction of an element within a molecule. If the element name is "H2 " (the letters H2 followed by two spaces) then the fraction of hydrogen in H_2, $2n(H_2)/n(H_{tot})$, will be returned. Currently only H_2 is done.

3.5.13. cdLine – emission-line intensities

subroutine ***cdLine*** returns the line intensity or luminosity. The label and wavelength of the line are specified in the call and the routine returns the relative intensity and the log of the absolute intensity or luminosity. The following is an example.

```
#include "cddefines.h"
#include "cddrive.h"
double relint , absint;

if( cdLine( "totl" , 4861 , &relint , &absint ) <= 0)
   printf("did not find this line\n");
```

The first variable in the call is the line label, the four-character null-terminated string (upper or lower case) as used by the code to identify the line in the main emission line printout. The second variable gives the wavelength of the line in Angstroms. Both of these must exactly match the label and wavelength used by Cloudy to identify the line (see the chapter "Lines" for a full description). The third variable (***relint*** in the above example) is a double precision pointer to the relative intensity of the line (relative to the normalization line, usually Hβ, and reset with the **normalize** command). The log of the intensity (erg cm^{-2} s^{-1}) or luminosity (erg s^{-1}) of the line is returned as the last double precision pointer (***absint*** in the above example). If the intensity of the line is zero or the line was not found then this variable will be set to -37.

If ***cdLine*** finds the line it returns the index of the line within the stack of emission lines. So a positive return value indicates success. It returns the negative of the total number of lines in the stack if the line is not found. This may occur if the line wavelength or label was mistyped. This is an exception to the C++ function return convention in which a normal return is zero and an abnormal return is non-zero. A positive value indicates a successful return.

The emission lines returned by this routine are those printed with the heading *Intrinsic Intensities* when grains are present in an open geometry. This does not include the effects of possible reflection off a background molecular cloud. See this discussion on page 459 below for more information.

3.5.14. cdnZone – how many zones in the last iteration?

The routine returns the number of zones in the previous iteration.

3.5.15. cdPressure_depth – pressure structure of the last iteration

The pressure as a function of depth, for the last iteration, is obtained by calling routine ***cdPressure_depth***. This routine has three arguments, pointers to vectors giving the total (gas plus radiation) pressure, the gas pressure, and the radiation pressure. All are double precision vectors and the calling routine must have allocated space for these before calling this routine. The total number of elements needed for each vector is the number of zones in the last iteration and is obtained by calling routine ***cdnZone***.

3.5.16. cdPressure_last – pressure of the last zone

The pressure for the last zone is obtained by calling routine ***cdPresure_last***. This routine has three arguments, pointers to the total (gas plus radiation) pressure, the gas pressure, and the radiation pressure. All are double precision variables.

3.5.17. cdSPEC – get predicted spectrum

This routine provides an interface between Cloudy and Keith Arnaud's X-Ray spectral analysis program XSPEC. It is called after ***cdDrive*** has computed a model. Depending on which option is used, it will return the incident continuum, the attenuated incident continuum, the reflected continuum, the diffuse continuous continuum, outward direction diffuse continuous emission, reflected lines, or outward lines. All are $4\pi\nu J_\nu$ [erg cm^{-2} s^{-1}] and assume full coverage of the continuum source. Details are given in *cddrive.h.*

3.5.18. cdTemp - the computed mean temperature

Routine ***cdTemp*** returns the mean electron temperature weighted with respect to some species. The first parameter is a four character null-terminated string giving the first four letters (upper or lower case) of the name of an element as spelled by the code. The second parameter is the ionization stage, with 1 for the atom, 2 the first ion, etc. The third parameter will be the computed mean temperature. The last parameter is a six-character null-terminated string, either "radius" or "volume", that says whether the temperature should be weighted with respect to radius or volume. The mean temperature weighted by ion $+n$ of element S over radius is defined as

$$\left\langle T\left(S^{+n}\right)\right\rangle = \frac{\int T\, n(S^{+n})\, f(l)\, dl}{\int n(S^{+n})\, f(l)\, dl} \text{ [K]} \qquad (400)$$

and the average over volume is

$$\left\langle T\left(S^{+n}\right)\right\rangle = \frac{\int T\, n(S^{+n})\, f(r)\, dV}{\int n(S^{+n})\, f(r)\, dV} \text{ [K]} \, . \qquad (400)$$

The routine returns 0 if it finds the species, and 1 if it could not find the species. The following is an example of a call:

```
if( cdTemp( "carb" , 2 , &temp , "radius") )
{
       exit(1);
}
printf("The mean C+2 temperature is%g\n", temp);
```

An ionization stage of zero requests one of the following special temperatures:

21 cm-related temperatures: If the ion stage is zero then the routine will return one of three temperatures related to 21 cm observations. The label "**21cm**" will return the mean of $n(H^0)/T_{kin}$, the harmonic mean gas kinetic temperature weighted with respect to the atomic hydrogen density, averaged over radius. The label "**spin**" will return the mean of $n(H^0)/T_{spin}$, the harmonic mean of the 21 cm spin temperature weighted with respect to the atomic hydrogen density, averaged over radius. Finally the label "**opti**" returns the temperature derived from the ratio of Lα to 21 cm optical depths. This is the temperature measured by combined 21 cm – Lα observations. The spin temperature T_{spin} is calculated with Lα radiative processes included.

Molecular hydrogen: The label "**H2__**" and an ionization stage of zero will return the mean temperature weighted (over volume or radius) with respect to the H_2 density.

Simple mean temperature: If the label consists of four spaces, as in " ", and the ionization stage is zero the routine will return the mean temperature averaged over radius or volume, but not weighted by any species.

3.5.19. cdTemp_last - the temperature of the last zone

The kinetic temperature of the last zone is obtained by called the function ***cdLastTemp***. The function has no arguments and its return value is the temperature.

3.5.20. cdTimescales – several timescales.

This routine has three arguments, pointers to doubles that return the timescales [s] for several processes. These are the thermal timescale, the hydrogen recombination timescale, and the H_2 formation timescale.

3.6. Other information

3.6.1. cdDate(cdString)

The date when the current version of the code was released will be placed as a null-terminated string. The string is passed as an argument and the calling program must have allocated enough room for the string.

3.6.2. cdVersion(cdString)

The code's version number will be placed as a null-terminated string into the string passed as an argument. The version number is a string rather than a float since it can end with a letter of the alphabet. The calling program must allocate enough space for the string.

3.6.3. double cdExecTime(void)

This returns the time that has elapsed since the previous call to ***cdInit***.

3.7. Printing comments

After the calculation is complete, but before the emission lines are printed, the code generates a series of statements that indicate warnings, cautions, comments, and surprises. These should be examined to confirm that the calculation is likely to be valid. A series of public routines allows the driving code to determine whether these comments were generated, what type they were, and to print then into an arbitrary open file.

3.7.1. Were comments generated?

Routine ***cdNwcns*** will return the number of warnings, cautions, surprises, notes, and temperature and pressure failures:

```
cdNwcns( &lgAbort , &nw , &nc , &nn , &ns , &nte , &npe , &nione, &neden )
```

where the first variable is a flag indicating whether the calculation aborted, ***nw*** is the number of warnings generated (if this number is non-zero, then the calculation has serious problems), ***nc*** is the number of cautions generated (these are less severe than warnings, but are still a cause of concern), and ***nn*** and ***ns*** are the number of notes and surprises. The next two arguments are the number of temperature and pressure failures. The last two are the number of ionization and electron density failures. All failures will add up to zero in a successful calculation (there should not be any failures).

If either of the first two variables are non-zero then the code returned with an indication of serious failure. An abort is far more serious than a warning since it indicates catastrophic meltdown. I would appreciate learning about these. Please post details on the code's discussion board.

3.7.2. Printing the comments.

A series of comments normally appear after the last zone. These may be printed into any file by calling the series of subroutines described here. In all cases the routines take as an argument a file handle which must point to a file that has already been opened for writing.

```
/* output the comments into a file, but first open it */
/* first define the file handle, then open the file for writing */
FILE *ioOUT;
If( (IoOUT = fopen( "comments.txt", "w") ) == NULL )
{
       printf("error creating comments.txt file\n");
       exit(1);
}
/*print the reason the calculation stopped, and geometry*/
 cdReasonGeo( ioOUT )
/*print the warnings*/
 cdWarnings(ioOUT)
/*next print the cautions*/
 cdCautions(ioOUT)
/*now print any surprising results*/
 cdSurprises(ioOUT)
/*now print the notes
 cdNotes(ioOUT)
fclose( ioOUT );
```

***cdReasonGeo*(*FILE *io*)** It is very important to understand why the calculation stopped. The first two lines after the last zone results give the reason the calculation stopped and the type of geometry. This information will be printed into the file whose handle is the argument.

***cdWarnings*(*FILE *io*)** All warnings (denoted by "W-") will be printed.

cdCautions (***FILE *io*)** All cautions (denoted by a "C-") will be printed.

***cdSurprises*(*FILE *io*)** All surprises (denoted by a "!") are printed.

***cdNotes*(*FILE *io*)** The notes concerning the calculation will be printed.

*3.7.3. cdErrors(FILE *io) - printing a summary of any problems*

Routine ***cdErrors***(***FILE *io***) will generate a summary of any problems that happened during a calculation. The argument is a file pointer to the output file where the summary will be placed. The calling program must have already opened the file for writing. If problems occurred in the calculation, such as temperature or pressure failures, warnings, or cautions, these will be printed following the title for the calculation.

*3.7.4. cdPrintCommands(FILE *io) – print the command stack*

The entire series of input commands will be written into the file. The single argument is a file handle that points to a previously opened file. The commands are preceded and followed by lines that begin with "c =====" to easily identify their start and end.

3.7.5. setbuf or the no buffering command

Programs produce output by writing into a buffer and place information on the disk once the buffer is nearly full. If a C program crashes before this buffer is "flushed" the information within the buffer will be lost. This poses a problem if the printout generated just before the crash is needed for debugging. The C io library provides a routine, ***setbuf***, that can turn file buffering off. The following sequence would open a file and turn buffering off:

```
ioDATA = fopen("d:\\projects\\cloudy\\run2\\test.out","w");
/* turn off buffering so we see results as then happen */
setbuf( ioDATA , NULL );
```

The **`no buffering`** command will accomplish the same thing. Note that turning off buffering has a severe performance penalty – the code will run far more slowly.

3.8. Example Call as a Subroutine

The following is an example of a very simple use of Cloudy as a subroutine.

```
/*main program that calls cloudy when used as a stand-alone program */
#include "cddefines.h"
#include "cddrive.h"

int main( void )
{
        int lgOK ;

        /* first create an open file */
        FILE *ioDATA ;
        ioDATA = fopen("d:\\projects\\cloudy\\run2\\test.out","w");
        if( ioDATA == NULL )
        {
                printf(" could not open test.out for writing.\n");
                exit(1);
        }

        /* initialize the code */
        cdInit();
        /* divert the output to this file */
        cdOutp(ioDATA);
        /* enter commands for this run */
        cdRead( "hden 10.5 ");
        cdRead( "agn 6.00 -1.40 -0.50 -1.0 ");
        cdRead( "phi(h) 23 ");
        cdRead( "stop column density 21.860889 ");
        cdRead( "*constant temper 727,000 ");
        cdRead( "background z=0 ");
        cdRead( "failures 3 no map ");
        /* actually call the code */
        lgOK = cdDrive();
        /* close the file then exit */
        fclose( ioDATA);
        exit(0);
}
```

3.9. Computing Grids of Calculations

Today I usually use the code to compute results, extract information on the fly, and then save desired quantities. The following example illustrates producing a series of models with increasing stellar temperature. The stellar temperature and the [O III] λ5007/Hβ intensity ratio are written to a file.

This example only gets results for a single line. Often a large number of lines are needed. A call to ***cdLineList*** (page 422 above) provides an easy way to obtain large numbers of lines whose labels are stored in a file.

```
/* very simple main program to call cloudy as a stand-alone program */
#include "cddefines.h"
#include "cddrive.h"

/*int main( int argc, char *argv[] )*/
int main( void )
{
   /* this will hold images of the command lines */
   char chCard[200];
   double TStar , rel , absol;
   int lgFail;
   int nFail;
   FILE *ioDATA ;

   /* open file for writing some results */
   if( (ioDATA = fopen("1DGrid.out","w")) == NULL )
   {
      printf(" could not open 1DGrid.out for writing.\n");
      exit(1);
   }

   TStar = 3e4;
   nFail = 0;
   while( TStar < 5e4 )
   {
      /* initialize the code */
      cdInit();
      /* redirect output to the file we opened above */
      cdOutp(ioDATA);
      /* but also say we want no output by passing 0, for FALSE (defined in cddefines.h)*/
      cdTalk(FALSE);
      /* write variables into strings and send string as input file */
      cdRead( "hden 5 ");
      cdRead( "ionization parameter -2 ");
      cdRead( "stop zone 1 ");
      /* this is example of writing a variable into the string then passing
       * the string to cloudy */
      sprintf( chCard , "blackbody, T=%f" , TStar );
      cdRead( chCard );
      /* actually call the code */
      lgFail = cdDrive();
      if( lgFail )
      {
         printf("Beware: Cloudy returned error condition, so exit with 1.\n");
         /* this counts how many failures occurred */
         ++nFail;
      }
      /* get intensity of [OIII] relative to Hbeta - remember cdLine is different
       * from most cd routines since it returns element within line stack, 0 for failure */
      if( !cdLine( "o 3" , 5007 , &rel , &absol ) <=0 )
      {
         printf("could not find 5007\n");
         exit(1);
      }
      /* now print stellar temperature and 5007/Hbeta ratio */
      fprintf(ioDATA , "%.0f %.2f\n", TStar , rel );
      /* now increment TStar by 5000K */
      TStar += 5000.;
   }
   /* exit with number of error returns – this should be zero */
   exit(nFail);
}
```

4. OUTPUT

4.1. Overview

This section defines the output produced by Cloudy. Each section begins with a sample of the output described, and then goes on to describe the meaning of the printout in greater detail. The output actually shown is from the Orion H II Region / PDR / molecular cloud test case (*orion_hii_pdr_pp.in*).

4.2. Header Information

Several lines of output echo the input commands and outline some properties of the initial continuum.

```
                                     Cloudy 06.01.02

************************************06Jan02****************************************
*                                                                                 *
* title the Orion HII Region / PDR / Molecular cloud with an open geometry        *
* c                                                                               *
* c commands controlling continuum =========                                      *
* c the incident continuum is two parts                                           *
* c kurucz continuum and flux of photons striking cloud                           *
* c this is the photosphere of the OVI star, its temperature and phi(H)           *
* table star kurucz 39,600K                                                       *
* phi(H) 13                                                                       *
* c this adds the observed hot brems                                              *
* c its temperature (as log of T) and the flux of                                 *
* c photons striking the cloud                                                    *
* brems 6                                                                         *
* phi(h) 10                                                                       *
* c                                                                               *
* c cosmic rays are important for pdr chemistry                                   *
* cosmic rays, background                                                         *
* c                                                                               *
* c commands controlling geometry  =========                                      *
* c this turns off the stop temperature option                                    *
* c so the sim will not stop due to temperature                                   *
* stop temperature off                                                            *
* c this sets the thickness of the HII region & PDR                               *
* stop thickness 0.5 linear parsec                                                *
* c this will result in a milli gauss B-field in molecular region                 *
* magnetic field -5 gauss                                                         *
* c assume constant pressure                                                      *
* constant pressure                                                               *
* set nend 2000                                                                   *
* c                                                                               *
* c other commands for details     =========                                      *
* failures 3                                                                      *
* c mimic existance of unmodeled molecular gas                                    *
* double                                                                          *
* c iterate since lines optically thick                                           *
* iterate                                                                         *
* c set microturbulence in equipartition with B field                             *
* turbulence equipartition                                                        *
* c set the line width so lines appear on the punch continuum                     *
* set punchLwidth 10 km/s                                                         *
* c                                                                               *
* c commands for density & abundances =========                                   *
* c this is the log of the initial H density, cm-3                                *
* hden 4                                                                          *
* c this will speed up the calculation a bit                                      *
* init file="ism.ini"                                                             *
* c this uses HII region abundances, but no grains                                *
* abundances hii region no grains                                                 *
* c this uses orion grains                                                        *
* grains orion                                                                    *
* >>>> mie_read_opc reading file -- graphite_orion_10.opc                  <<<< *
* >>>> mie_read_opc reading file -- silicate_orion_10.opc                  <<<< *
* c turn on PAHs, with an abundance that depends on H0 fraction,                  *
* c as suggested by long-slit observations of Orion bar,                          *
* c with an abundance 3x larger than default built into the code                  *
* grains pah function 3                                                           *
* >>>> mie_read_opc reading file -- pah1_bt94_10.opc                       <<<< *
* c                                                                               *
* c commands controlling output    =========                                      *
* c print lots of faint CO lines                                                  *
* print line faint -4                                                             *
* c normalize to Ha                                                               *
```

```
* normalize to "H  1" 6563                                                      *
* c                                                                             *
* c orion hii pdr pp.in                                                         *
* c class hii pdr                                                               *
*                                                                               *
*********************************************************************************
```

This begins with the version number of Cloudy, the date that the version was released in the form yy.mm.dd. The following line gives this date in another form.

All of the input command lines, with the exception of those starting with a #, %, or *, are echoed before the calculation begins, and are saved to be reprinted after the calculation is completed.

```
3198CellPeak1.00E+00   Lo 9.99e-09=912.21cm   Hi-Con:1.20E+02 Ryd   E(hi):7.35E+06Ryd     E(hi):     100.01 MeV
I(nu>1ryd):   2.4792   Average nu:1.382E+00   I( X-ray):  -1.6194   I(BalC):   2.8255     Phi(BalmrC):  13.7081
phi(1.0-1.8):12.9508   phi(1.8-4.0): 12.033   phi(4.0-20):  9.388   phi(20--):  7.634     Ion pht flx:1.001E+13
I(gam ray):   0.0000   phi(gam r):   0.0000   I(Infred):   1.5064   Alf(ox):   0.0000     Total inten:   3.0012
U(1.0----):3.339E-02   U(4.0----):8.293E-06   T(En-Den):4.586E+01   T(Comp):3.532E+04     nuJnu(912A):5.422E+02
Occ(FarIR):2.911E+08   Occ(H n=6):1.326E-11   Occ(1Ryd):2.470E-14   Occ(4R):5.400E-20      Occ (Nu-hi):1.201E-32
Tbr(FarIR):4.835E+05   Tbr(H n=6):5.816E-08   Tbr(1Ryd):3.905E-09   Tbr(4R):3.413E-14      Tbr (Nu-hi):2.269E-25
```

A large block of information describes the continuum that strikes the illuminated face of the cloud. The full block of information is shown above, and in the following discussion each line will be given again just before it is described.

```
3198CellPeak1.00E+00 Lo 9.99e-09=912.21cm Hi-Con:1.20E+02 Ryd E(hi):7.35E+06Ryd  E(hi):  100.01 MeV
```

This line gives the number of numerical frequency cells in the continuum followed by the energy (in Ryd) of the peak of hydrogen-ionizing continuum[3]. This is the point with the largest flux density per unit energy interval (J_ν). Next is the energy of the low-energy limit of the continuum mesh, both in Ryd and cm. The last two numbers are the energies of the high-energy limit of the continuum mesh in Ryd and MeV.

```
I(nu>1ryd): 2.4792 Average nu:1.382E+00 I( X-ray): -1.6194 I(BalC): 2.8255  Phi(BalmrC): 13.7081
```

This line gives the intensity or luminosity of the continuum source. Luminosities are printed if the inner radius of the cloud is specified. The units will be energy radiated by the central object into 4π sr [erg s^{-1}]. If an inner radius is not set then the code will compute the intensity case and give the emission per unit area of cloud surface. This is loosely called the intensity but is more formally $4\pi J$ where J is the proper mean intensity [erg cm^{-2} s^{-1} sr^{-1} for an emission line; AGN3 Appendix 1].

The line gives the log of the energy (erg s^{-1} cm^{-2} or erg s^{-1}, depending on whether a flux or luminosity was specified) in the hydrogen-ionizing continuum (1 Ryd $\le h\nu <$ 100 MeV), and the average energy of the hydrogen-ionizing continuum, in Ryd, weighted by photon number;

$$\langle h\nu \rangle = \frac{\int_{1\,Ryd}^{\infty} 4\pi\, J_\nu \, d\nu}{\int_{1\,Ryd}^{\infty} 4\pi\, J_\nu / h\nu \, d\nu} \text{ [Ryd] .} \qquad (400)$$

---

[3] The printed number was incorrect in versions 80 through 88.01, but had no other effects on computed results.

The log of the energy in the X-ray continuum (20.6 Ryd ≤ $h\nu$ ≤ 7676 Ryd), the log of the energy (erg s^{-1} cm^{-2} or erg s^{-1}), and the number of photons (cm^{-2} s^{-1} or s^{-1}) in the Balmer continuum (0.25 Ryd to 1.0 Ryd) is then printed.

```
phi(1.0-1.8):12.9508 phi(1.8-4.0): 12.033 phi(4.0-20): 9.388 phi(20--): 7.634  Ion pht flx:1.001E+13
```

The third line gives the log of the number of photons (cm^{-2} s^{-1} or s^{-1}) in four frequency bins (1.0 Ryd ≤ $h\nu$ < 1.807 Ryd, 1.807 Ryd ≤ $h\nu$ < 4.0 Ryd, 4.0 Ryd ≤ $h\nu$ < 20.6 Ryd, and 20.6 Ryd ≤ $h\nu$ < 7676 Ryd). The last number "Ion pht flx" is the flux of hydrogen ionizing photons;

$$\Phi\left(H^0\right)=\frac{Q\left(H^0\right)}{4\pi r^2}\ \ [\mathrm{cm^{-2}\ s^{-1}}]. \qquad (401)$$

In this equation $Q(H^0)$ is the total number of hydrogen-ionizing photons emitted by the central object (s^{-1}), and r is the separation between the center of the central object and the illuminated face of the cloud. Unlike the majority of the quantities printed in the header, $\Phi(H^0)$ (per unit area) is always printed, never $Q(H^0)$ (into 4π sr).

```
I(gam ray): 0.0000 phi(gam r): 0.0000 I(Infred): 1.5064 Alf(ox): 0.0000  Total inten: 3.0012
```

The fourth line of the header gives some information about the low and high energy portions of the incident continuum. The first number is the log of the luminosity or intensity in the gamma-ray (~ 100 keV to ~ 100 MeV) continuum. The second number is the log of the number of photons over this energy range. The third number is the log of the luminosity in the continuum between 0.25 Ryd and the lowest energy considered, presently an energy of 1.001×10^{-8} Ryd. All of these entries are either per unit area, or radiated into 4π sr, depending on whether the intensity or luminosity case was specified.

The entry "Alf(ox)" is the spectral index α_{ox}, defined as in Zamorani et al. (1981), except for the difference in sign convention. This is the spectral index which would describe the continuum between 2 keV (147 Ryd) and 2500Å (0.3645 Ryd) if the continuum could be described as a single power-law, that is,

$$\frac{f_\nu\left(2\ \mathrm{keV}\right)}{f_\nu\left(2500\ \text{Å}\right)}=\left(\frac{\nu_{2\,\mathrm{keV}}}{\nu_{2500\,\text{Å}}}\right)^{\alpha}=403.3^{\alpha}\ \ . \qquad (402)$$

The definition of α_{ox} used here is slightly different from that of Zamorani et al. since implicit negative signs are *never* used by Cloudy. Typical AGN have α_{ox} ~ -1.4 . If no X-rays are present then α_{ox} = 0. The last number on the line is the log of the total energy in the continuum between 1.001×10^{-8} Ryd and 100 MeV.

```
log L/Lsun: 3.9743 Abs bol mg: -5.1858 Abs V mag: 2.4170 Bol cor: -7.6028  nuFnu(Bbet): 34.5867
```

The next line is optional, depending on whether the continuum is specified as the total luminosity or photon number radiated into 4π sr or as an incident surface flux. (It was not printed in this model since we are working in the intensity case but a sample is shown). This optional line is generated if the continuum is specified in the luminosity case. First comes the log of the total luminosity in the continuum in solar units. The absolute bolometric magnitude, absolute *V* magnitude, and the

bolometric correction, are then given, followed by the log of the continuum specific luminosity [$\nu F_\nu(\mathrm{H}\beta)$] at the wavelength of H$\beta$ [erg s^{-1}].

```
U(1.0----):3.339E-02 U(4.0----):8.293E-06 T(En-Den):4.586E+01 T(Comp):3.532E+04  nuJnu(912A):5.422E+02
```

The next line begins with two ionization parameters. The first is the dimensionless ratio of ionizing photon to hydrogen densities, defined as

$$U \equiv \frac{\Phi\left(\mathrm{H}^0\right)}{n_\mathrm{H} c} \tag{403}$$

where n_H is the total hydrogen density. The second number is defined in a similar way, but the numerator is the number of photons with energies greater than 4 Ryd (i.e., helium-ionizing). The third number is the equivalent black-body temperature corresponding to the energy density u at the illuminated face of the cloud, from the incident continuum and Stefan's radiation density constant a;

$$T_u \equiv \left(L / 4\pi r^2 ac\right)^{1/4} \text{ [K]} , \tag{404}$$

and T(Comp) is the Compton temperature of the incident radiation field[4]. The last number is $4\pi\,\nu J_\nu$(912 Å), the flux at 912Å (erg cm^{-2} s^{-1}). In this equation J_ν is the mean intensity of the incident continuum as defined by Mihalas (1978).

```
Occ(FarIR):2.911E+08 Occ(H n=6):1.326E-11 Occ(1Ryd):2.470E-14 Occ(4R):5.400E-20  Occ(Nu-hi):1.201E-32
Tbr(FarIR):4.835E+05 Tbr(H n=6):5.816E-08 Tbr(1Ryd):3.905E-09 Tbr(4R):3.413E-14  Tbr(Nu-hi):2.269E-25
```

The next two lines give dimensionless photon occupation numbers $\eta(\nu)$, for the incident continuum at several energies,

$$\eta(\nu) \equiv J_\nu(\nu)\left(\frac{2h\nu^3}{c^2}\right)^{-1} , \tag{405}$$

and the incident continuum brightness temperature $T_b(\nu)$, (K), defined as

$$T_b(\nu) \equiv J_\nu(\nu)\left(\frac{2k\nu^2}{c^2}\right)^{-1} \text{ [K]}, \tag{406}$$

for five energies. These energies correspond to the lowest frequency considered (presently an energy of 1.001×10^{-8} Ryd); the ionization potential of the n = 6 level of hydrogen (1/36 Ryd); one Rydberg; four Rydbergs, and the high energy limit of the incident continuum (this depends on the continuum shape; the energy is given by the fifth number on the first line of the continuum output).

4.3. Chemical composition

[4]For a blackbody radiation field $T_{Compton}$ is roughly 4% lower than the blackbody color temperature T_{color} when the energy density temperature T_u is $\ll T_{color}$. Only when $T_u \equiv T_{color}$ does induced Compton heating cause $T_{Compton} \equiv T_{color}$. If $T_u > T_{color}$ then $T_{Compton} > T_{color}$ because of induced Compton heating. All of the relevant physics is included in the Compton temperature printed here.

```
                                    Gas Phase Chemical Composition
 H :  0.0000  He: -1.0223  C : -3.5229  N : -4.1549  O : -3.3979  Ne: -4.2218  Mg: -5.5229  Si: -5.3979  S : -5.0000
                                   Cl: -7.0000  Ar: -5.5229  Fe: -5.5229

                                     Grain Chemical Composition
                          C : -3.6259  O : -3.9526  Mg: -4.5547  Si: -4.5547  Fe: -4.5547

                                    Number of grains per hydrogen
                                 Carbonaceous: -14.166  silicate: -14.103
```

The chemical composition of the gas comes next. There are three blocks of numbers, the first giving the gas-phase abundances of the elements, the second the abundances contained in grains, and the third the number of each type of grains per unit hydrogen. The numbers are the logs of the number densities of the elements, relative to the gas-phase hydrogen abundance of unity (so, 0 on the log scale). Only the active elements are included (those turned off with the **`elements off`** command are not printed). If grains are not present then the second two blocks are not printed.

4.4. Zone Results

Next comes a summary of the conditions in the first and last zone. This print out is done in routine ***PrtZone*** which should be consulted if there are any questions. The following is the output produced for one zone. Details follow.

```
####  1  Te:9.361E+03 Hden:1.000E+04 Ne:1.101E+04 R:1.000E+30 R-R0:5.223E+11 dR:1.045E+12 NTR:  3 Htot:3.461E-16 T912: 1.48e-05###
 Hydrogen      1.47e-04 1.00e+00 H+o/Hden 1.00e+00 4.12e-12 H-    H2 8.43e-17 4.10e-13 H2+ HeH+ 1.13e-12 Ho+ ColD 1.54e+12 1.04e+16
 Helium        6.57e-04 9.45e-01 5.47e-02 He I2SP3 3.52e-06 Comp H,C 1.75e-22 4.64e-23 Fill Fac 1.00e+00 Gam1/tot 1.00e+00
 He singlet n  6.54e-04 2.35e-11 6.59e-18 2.09e-18 3.18e-18 2.52e-18 He tripl 3.52e-06 9.32e-16 7.41e-18 4.77e-17 7.56e-18
 Pressure      NgasTgas 2.06e+08 P(total) 2.84e-08 P( gas ) 2.84e-08 P(Radtn) 1.79e-11 Rad accl 3.51e-05 ForceMul 3.33e+03
               Texc(La) 4.21e+03 T(contn) 4.59e+01 T(diffs) 2.03e+00 nT (c+d) 1.16e+07 Prad/Gas 6.30e-04 Pmag/Gas 2.80e-04
 gra-orion01*  DustTemp 2.12e+02 Pot Volt 5.32e+00 Chrg (e) 1.21e+02 drf cm/s 4.83e+03 Heating: 4.26e-18 Frac tot 1.23e-02
 gra-orion02*  DustTemp 2.02e+02 Pot Volt 5.08e+00 Chrg (e) 1.43e+02 drf cm/s 5.26e+03 Heating: 3.69e-18 Frac tot 1.07e-02
 gra-orion03*  DustTemp 1.91e+02 Pot Volt 4.86e+00 Chrg (e) 1.70e+02 drf cm/s 5.60e+03 Heating: 3.21e-18 Frac tot 9.26e-03
 gra-orion04*  DustTemp 1.81e+02 Pot Volt 4.66e+00 Chrg (e) 2.01e+02 drf cm/s 5.86e+03 Heating: 2.79e-18 Frac tot 8.06e-03
 gra-orion05   DustTemp 1.70e+02 Pot Volt 4.47e+00 Chrg (e) 2.39e+02 drf cm/s 6.07e+03 Heating: 2.43e-18 Frac tot 7.03e-03
 gra-orion06   DustTemp 1.60e+02 Pot Volt 4.30e+00 Chrg (e) 2.85e+02 drf cm/s 6.22e+03 Heating: 2.13e-18 Frac tot 6.16e-03
 gra-orion07   DustTemp 1.50e+02 Pot Volt 4.15e+00 Chrg (e) 3.40e+02 drf cm/s 6.33e+03 Heating: 1.87e-18 Frac tot 5.41e-03
 gra-orion08   DustTemp 1.40e+02 Pot Volt 4.02e+00 Chrg (e) 4.07e+02 drf cm/s 6.42e+03 Heating: 1.65e-18 Frac tot 4.77e-03
 gra-orion09   DustTemp 1.31e+02 Pot Volt 3.91e+00 Chrg (e) 4.89e+02 drf cm/s 6.48e+03 Heating: 1.46e-18 Frac tot 4.21e-03
 gra-orion10   DustTemp 1.22e+02 Pot Volt 3.80e+00 Chrg (e) 5.89e+02 drf cm/s 6.54e+03 Heating: 1.29e-18 Frac tot 3.73e-03
 sil-orion01*  DustTemp 1.55e+02 Pot Volt 2.85e+00 Chrg (e) 6.44e+01 drf cm/s 1.45e+04 Heating: 2.44e-18 Frac tot 7.06e-03
 sil-orion02*  DustTemp 1.49e+02 Pot Volt 2.70e+00 Chrg (e) 7.58e+01 drf cm/s 1.62e+04 Heating: 2.09e-18 Frac tot 6.03e-03
 sil-orion03*  DustTemp 1.43e+02 Pot Volt 2.57e+00 Chrg (e) 8.92e+01 drf cm/s 1.77e+04 Heating: 1.78e-18 Frac tot 5.15e-03
 sil-orion04   DustTemp 1.37e+02 Pot Volt 2.44e+00 Chrg (e) 1.05e+02 drf cm/s 1.91e+04 Heating: 1.53e-18 Frac tot 4.42e-03
 sil-orion05   DustTemp 1.31e+02 Pot Volt 2.33e+00 Chrg (e) 1.24e+02 drf cm/s 2.02e+04 Heating: 1.32e-18 Frac tot 3.81e-03
 sil-orion06   DustTemp 1.26e+02 Pot Volt 2.24e+00 Chrg (e) 1.47e+02 drf cm/s 2.11e+04 Heating: 1.14e-18 Frac tot 3.30e-03
 sil-orion07   DustTemp 1.20e+02 Pot Volt 2.15e+00 Chrg (e) 1.76e+02 drf cm/s 2.18e+04 Heating: 9.93e-19 Frac tot 2.87e-03
 sil-orion08   DustTemp 1.15e+02 Pot Volt 2.08e+00 Chrg (e) 2.10e+02 drf cm/s 2.23e+04 Heating: 8.67e-19 Frac tot 2.50e-03
 sil-orion09   DustTemp 1.10e+02 Pot Volt 2.01e+00 Chrg (e) 2.52e+02 drf cm/s 2.26e+04 Heating: 7.60e-19 Frac tot 2.20e-03
 sil-orion10   DustTemp 1.06e+02 Pot Volt 1.96e+00 Chrg (e) 3.03e+02 drf cm/s 2.28e+04 Heating: 6.69e-19 Frac tot 1.93e-03
 pah-bt9401 *  DustTemp 3.41e+02 Pot Volt 6.60e+00 Chrg (e) 1.06e+00 drf cm/s 1.97e+02 Heating: 9.29e-22 Frac tot 2.68e-06
 pah-bt9402 *  DustTemp 3.44e+02 Pot Volt 6.64e+00 Chrg (e) 1.28e+00 drf cm/s 2.13e+02 Heating: 1.01e-21 Frac tot 2.92e-06
 pah-bt9403 *  DustTemp 3.47e+02 Pot Volt 6.61e+00 Chrg (e) 1.49e+00 drf cm/s 2.37e+02 Heating: 1.07e-21 Frac tot 3.08e-06
 pah-bt9404 *  DustTemp 3.50e+02 Pot Volt 6.54e+00 Chrg (e) 1.70e+00 drf cm/s 2.67e+02 Heating: 1.09e-21 Frac tot 3.16e-06
 pah-bt9405 *  DustTemp 3.53e+02 Pot Volt 6.44e+00 Chrg (e) 1.92e+00 drf cm/s 3.02e+02 Heating: 1.09e-21 Frac tot 3.16e-06
 pah-bt9406 *  DustTemp 3.55e+02 Pot Volt 6.45e+00 Chrg (e) 2.22e+00 drf cm/s 3.29e+02 Heating: 1.13e-21 Frac tot 3.26e-06
 pah-bt9407 *  DustTemp 3.57e+02 Pot Volt 6.47e+00 Chrg (e) 2.54e+00 drf cm/s 3.60e+02 Heating: 1.17e-21 Frac tot 3.38e-06
 pah-bt9408 *  DustTemp 3.59e+02 Pot Volt 6.43e+00 Chrg (e) 2.87e+00 drf cm/s 4.00e+02 Heating: 1.18e-21 Frac tot 3.40e-06
 pah-bt9409 *  DustTemp 3.61e+02 Pot Volt 6.46e+00 Chrg (e) 3.27e+00 drf cm/s 4.35e+02 Heating: 1.20e-21 Frac tot 3.46e-06
 pah-bt9410 *  DustTemp 3.63e+02 Pot Volt 6.48e+00 Chrg (e) 3.71e+00 drf cm/s 4.74e+02 Heating: 1.22e-21 Frac tot 3.52e-06
 Carbon        6.76e-07 1.91e-02 9.70e-01 1.10e-02 1.77e-04 2.36e-09 0.00e+00 H2O+/O   0.00e+00 OH+/Otot 0.00e+00 Hex(tot) 0.00e+00
 Nitrogen      1.60e-06 1.72e-02 9.69e-01 1.41e-02 4.77e-05 1.34e-07 9.81e-14 0.00e+00 O2/Ototl 0.00e+00 O2+/Otot 0.00e+00
 Oxygen        9.23e-06 1.17e-01 8.59e-01 2.47e-02 6.97e-05 9.60e-08 4.83e-11 0.00e+00 0.00e+00
 Neon          5.77e-05 3.93e-01 5.95e-01 1.17e-02 7.25e-05 5.08e-08 1.99e-12 1.47e-16 0.00e+00 0.00e+00 0.00e+00
 Magnesium     6.41e-06 7.31e-03 9.65e-01 2.74e-02 1.76e-04 5.41e-07 2.86e-10 3.72e-14 9.96e-19 0.00e+00 0.00e+00 0.00e+00 0.00e+00
 Silicon    0  1.13e-07 8.39e-03 8.16e-01 1.56e-01 1.86e-02 4.68e-05 3.08e-08 5.13e-12 1.63e-16 0.00e+00 0.00e+00 0.00e+00 0.00e+00
 Sulphur    0  7.25e-08 7.46e-03 9.03e-01 8.81e-02 1.60e-03 1.67e-04 5.91e-06 9.11e-10 3.49e-14 3.20e-19 0.00e+00 0.00e+00 0.00e+00
 Chlorine   0  2.51e-07 1.32e-02 9.57e-01 2.92e-02 7.57e-04 5.50e-05 7.07e-07 9.54e-09 2.94e-13 2.17e-18 0.00e+00 0.00e+00 0.00e+00
 Argon      0  9.50e-08 2.83e-03 9.69e-01 2.73e-02 4.35e-04 2.65e-05 3.24e-07 1.53e-09 1.16e-11 8.21e-17 0.00e+00 0.00e+00 0.00e+00
 Iron       0  1.78e-08 2.88e-04 1.08e-01 8.56e-01 3.26e-02 2.33e-03 2.33e-05 2.30e-07 1.28e-10 1.94e-14 9.07e-19 0.00e+00 0.00e+00
```

The results of calculations for the first and last zones are always printed. Results for intermediate zones can be printed if desired (see the **`print every`** command). The following is a line-by-line description of the output produced for each printed zone.

```
#### 1 Te:9.361E+03 Hden:1.000E+04 Ne:1.101E+04 R:1.000E+30 R-R0:5.223E+11 dR:1.045E+12 NTR: 3 Htot:3.461E-16 T912: 1.48e-05###
```

The line begins with a series of #### characters to make it easy to locate with an editor. The zone number is the first number and it is followed by the electron temperature of the zone ("Te"). A lower case "u" will appear before the "Te" if the temperature solution is possibly thermally unstable (i.e., the derivative of the net

cooling with respect to temperature is negative. See the section on thermal stability problems starting on page 483 below). The total hydrogen ("Hden") and electron ("Ne") densities (cm^{-3}) follow. The next number ("R") is the distance from the center of the central object to the center of the zone. The depth, the distance between the illuminated face of the cloud and the center of the zone, ("R-R0", or "r-r_o"), and the thickness of the zone ("dR", or δr), (all are in cm), follow. The inner edge of the zone is $(r - r_o) - \delta r / 2$ from the illuminated face of the cloud. The line ends with a number indicating how many ionization iterations were needed for this zone to converge (NTR), followed by the total heating[5] ("Htot"; photoelectric and otherwise, erg cm^{-3} s^{-1}), and the optical depth between the *illuminated* face of the cloud and the *outer* edge of the zone at the Lyman limit (T912; the number is the *total absorption* optical depth at 912Å, and *not* the hydrogen Lyman-limit optical depth).

```
WIND; V:-7.000e+00km/s G:-0.00e+00 Accel: 8.62e-06 Fr(cont): 1.000 Fr(line): 0.000 Fr(dP): 0.000
```

A line describing the velocity and acceleration of the zone is printed if the **wind** option is used. The numbers are the wind velocity at the outer edge of the current zone (km s^{-1}), inward gravitational acceleration (cm s^{-2}), total outward radiative acceleration (cm s^{-2}), and the fraction of this acceleration caused by the incident continuum, line driving, and the gradient of the radiation pressure.

```
P(Lines):(Mg 2 2796A 0.32)(Mg 2 2803A 0.20)(H 1 6563A 0.13)(H 1 1.875m 0.10)(Fe 2 1786A 0.06)(H 1 4861A 0.05)
```

If the geometry is a wind and the ratio of line radiation to gas pressure, P(radiation)/P(gas), is greater than 5%, then a line describing the source of the radiation pressure is generated. The line begins with the label **P(Lines)** and continues with the fraction of the total radiation pressure produced by that emission line, the spectroscopic designation of the line, and its wavelength. Up to twenty lines can be printed, although in most cases only Lα and a few others will dominate.

```
Hydrogen   1.47e-04 1.00e+00 H+o/Hden 1.00e+00 4.12e-12 H-  H2 8.43e-17 4.10e-13 H2+ HeH+ 1.13e-12 Ho+ ColD 1.54e+12 1.04e+16
```

The line begins with the abundance of neutral and ionized hydrogen relative to all hydrogen (i.e., the ratios H^0/ H and H^+/ H^0 where H is the total hydrogen density in all forms (including molecular). If **print h-like departure coefficients** has been specified then departure coefficients are also printed on the following line. Neutral hydrogen H^0 is defined to be the total population of atomic hydrogen in all explicitly computed bound levels. Next comes "H+o/Hden", the ratio of the density of hydrogen in atomic or ionic form (this is indicated by the label "H+o") to the total hydrogen density.

The following five numbers give densities of the negative hydrogen ion and several molecules (H^-, H_2, H_2^+, and HeH^+) relative to the total hydrogen density. Note that, with this definition of the hydrogen density, a fully molecular gas will have $n(H_2)/n(H)=0.5$. These molecular abundances are also expressed as departure

---

[5]Cloudy defines heating as the energy input by the freed photoelectron, or $h\nu$ - IP, where IP is the ionization potential of the atom or ion, and hν is the energy of the photon. See AGN3 for more details.

coefficients if this option is set with the **print departure coefficients** command. The last number on the line is the H^0 and H^+ column densities (cm^{-2}).

```
H  1 1S-12    1.39e-01 3.43e-04 1.02e-03 1.02e-03 1.24e-03 1.62e-03 2.12e-03 2.73e-03 3.43e-03 4.23e-03 5.12e-03 6.12e-03 7.20e-03
H  1  rest    8.39e-03 9.66e-03 1.10e-02 1.25e-02 1.41e-02 1.57e-02 1.75e-02 1.93e-02 2.13e-02 2.33e-02 2.54e-02 2.77e-02 3.00e-02
              3.24e-02 3.49e-02 3.75e-02 4.02e-02 4.30e-02 4.59e-02 4.89e-02 5.20e-02 5.51e-02 5.84e-02 6.18e-02 6.52e-02 6.88e-02
              7.24e-02 7.62e-02 8.00e-02 8.39e-02 8.79e-02 9.21e-02 9.63e-02 1.01e-01 1.05e-01 1.09e-01 1.14e-01 1.19e-01
```

This information is only printed if it is explicitly requested with the **print H-like populations** command. The numbers give the populations of the H^0 levels relative to the ionized hydrogen density. All of these populations usually are relative to the ionized hydrogen density, but can also be printed as LTE departure coefficients if the **print departure coefficients** command is given.

```
Helium    6.57e-04 9.45e-01 5.47e-02 He I2SP3 3.52e-06 Comp H,C 1.75e-22 4.64e-23 Fill Fac 1.00e+00 Gam1/tot 1.00e+00
```

The first three numbers are the total populations of the three ionization stages of helium relative to the total helium abundance. The population of atomic helium is the sum of the total population in the triplets and singlets, including the population of all explicitly computed levels of each. These populations can also be expressed as departure coefficients if this option is set with the **print departure coefficients** command. The population of He 2^3 S, relative to the total helium abundance, follows. The Compton heating and cooling rates (both erg cm^{-3} s^{-1}) are next, followed by the gas filling factor. The last number is the fraction of the total hydrogen ionizations that are caused by photoionization from the ground state.

```
He singlet n 6.54e-04 2.35e-11 6.59e-18 2.09e-18 3.18e-18 2.52e-18 He tripl 3.52e-06 9.32e-16 7.41e-18 4.77e-17 7.56e-18
```

The first group are the level populations of the populations of the 6 *l*-levels from *n*=1 to 3 of the He^0 singlets. The next group consists of He^0 triplets populations of 2*S*, the three 2^3P_j, levels and the 3*S*, 3*P*, and 3*D* levels. Both sets of populations are relative to the total helium abundance. Departure coefficients are also printed if requested.

```
Pressure      NgasTgas 2.06e+08 P(total) 2.84e-08 P( gas ) 2.84e-08 P(Radtn) 1.79e-11 Rad accl 3.51e-05 ForceMul 3.33e+03
              Texc(La) 4.21e+03 T(contn) 4.59e+01 T(diffs) 2.03e+00 nT (c+d) 1.16e+07 Prad/Gas 6.30e-04 Pmag/Gas 2.80e-04
```

Some information concerning the pressure is printed. The gas equation of state includes thermal gas pressure, the radiation pressure due to trapped line emission, magnetic and turbulent pressure, and the radiation pressure due to absorption of the incident continuum. The first number is the gas pressure n_{gas} T_{gas} (with units cm^{-3} K), followed by the total pressure (dynes cm^{-2}), and followed by the gas pressure (n_{gas} kT_{gas}) in dynes cm^{-2}. The radiation pressure follows. The second to last number is the radiative acceleration (cm s^{-2}) at the inner edge of this zone. The radiative acceleration is computed with all continuous scattering and absorption opacities included. The last number is a force multiplier, defined as in Tarter and McKee (1973), and is the ratio of total opacity to electron scattering opacity.

The second line gives further information. The line starts with "Texc(La)", the excitation temperature T_{exc} of Lα, defined as

$$\frac{n(2p)/g(2p)}{n(1s)/g(1s)} = \exp\left[-h\nu / kT_{exc}(L\alpha)\right] \quad (407)$$

is given. This is followed by the temperature corresponding to the energy density of the attenuated incident continuum ("T(contn)") and the diffuse continua ("T(diffs)"). This includes all trapped lines and diffuse continuous emission. The entry "nT (c+d)"is the energy density of the sum of these two continua expressed as an equivalent pressure nT [cm^{-3} K] The line ends with the ratios of the radiation to gas pressure "Prad/Gas" and the ratio of magnetic to gas pressure "Pmag/Gas".

```
gra-orion01*  DustTemp 2.12e+02 Pot Volt 5.32e+00 Chrg (e) 1.21e+02 drf cm/s 4.83e+03 Heating: 4.26e-18 Frac tot 1.23e-02
gra-orion02*  DustTemp 2.02e+02 Pot Volt 5.08e+00 Chrg (e) 1.43e+02 drf cm/s 5.26e+03 Heating: 3.69e-18 Frac tot 1.07e-02
gra-orion03*  DustTemp 1.91e+02 Pot Volt 4.86e+00 Chrg (e) 1.70e+02 drf cm/s 5.60e+03 Heating: 3.21e-18 Frac tot 9.26e-03
gra-orion04*  DustTemp 1.81e+02 Pot Volt 4.66e+00 Chrg (e) 2.01e+02 drf cm/s 5.86e+03 Heating: 2.79e-18 Frac tot 8.06e-03
gra-orion05   DustTemp 1.70e+02 Pot Volt 4.47e+00 Chrg (e) 2.39e+02 drf cm/s 6.07e+03 Heating: 2.43e-18 Frac tot 7.03e-03
gra-orion06   DustTemp 1.60e+02 Pot Volt 4.30e+00 Chrg (e) 2.85e+02 drf cm/s 6.22e+03 Heating: 2.13e-18 Frac tot 6.16e-03
gra-orion07   DustTemp 1.50e+02 Pot Volt 4.15e+00 Chrg (e) 3.40e+02 drf cm/s 6.33e+03 Heating: 1.87e-18 Frac tot 5.41e-03
gra-orion08   DustTemp 1.40e+02 Pot Volt 4.02e+00 Chrg (e) 4.07e+02 drf cm/s 6.42e+03 Heating: 1.65e-18 Frac tot 4.77e-03
gra-orion09   DustTemp 1.31e+02 Pot Volt 3.91e+00 Chrg (e) 4.89e+02 drf cm/s 6.48e+03 Heating: 1.46e-18 Frac tot 4.21e-03
gra-orion10   DustTemp 1.22e+02 Pot Volt 3.80e+00 Chrg (e) 5.89e+02 drf cm/s 6.54e+03 Heating: 1.29e-18 Frac tot 3.73e-03
sil-orion01*  DustTemp 1.55e+02 Pot Volt 2.85e+00 Chrg (e) 6.44e+01 drf cm/s 1.45e+04 Heating: 2.44e-18 Frac tot 7.06e-03
sil-orion02*  DustTemp 1.49e+02 Pot Volt 2.70e+00 Chrg (e) 7.58e+01 drf cm/s 1.62e+04 Heating: 2.09e-18 Frac tot 6.03e-03
sil-orion03*  DustTemp 1.43e+02 Pot Volt 2.57e+00 Chrg (e) 8.92e+01 drf cm/s 1.77e+04 Heating: 1.78e-18 Frac tot 5.15e-03
sil-orion04   DustTemp 1.37e+02 Pot Volt 2.44e+00 Chrg (e) 1.05e+02 drf cm/s 1.91e+04 Heating: 1.53e-18 Frac tot 4.42e-03
sil-orion05   DustTemp 1.31e+02 Pot Volt 2.33e+00 Chrg (e) 1.24e+02 drf cm/s 2.02e+04 Heating: 1.32e-18 Frac tot 3.81e-03
sil-orion06   DustTemp 1.26e+02 Pot Volt 2.24e+00 Chrg (e) 1.47e+02 drf cm/s 2.11e+04 Heating: 1.14e-18 Frac tot 3.30e-03
sil-orion07   DustTemp 1.20e+02 Pot Volt 2.15e+00 Chrg (e) 1.76e+02 drf cm/s 2.18e+04 Heating: 9.93e-19 Frac tot 2.87e-03
sil-orion08   DustTemp 1.15e+02 Pot Volt 2.08e+00 Chrg (e) 2.10e+02 drf cm/s 2.23e+04 Heating: 8.67e-19 Frac tot 2.50e-03
sil-orion09   DustTemp 1.10e+02 Pot Volt 2.01e+00 Chrg (e) 2.52e+02 drf cm/s 2.26e+04 Heating: 7.60e-19 Frac tot 2.20e-03
sil-orion10   DustTemp 1.06e+02 Pot Volt 1.96e+00 Chrg (e) 3.03e+02 drf cm/s 2.28e+04 Heating: 6.69e-19 Frac tot 1.93e-03
pah-bt9401 *  DustTemp 3.41e+02 Pot Volt 6.60e+00 Chrg (e) 1.06e+00 drf cm/s 1.97e+02 Heating: 9.29e-22 Frac tot 2.68e-06
pah-bt9402 *  DustTemp 3.44e+02 Pot Volt 6.64e+00 Chrg (e) 1.28e+00 drf cm/s 2.13e+02 Heating: 1.01e-21 Frac tot 2.92e-06
pah-bt9403 *  DustTemp 3.47e+02 Pot Volt 6.61e+00 Chrg (e) 1.49e+00 drf cm/s 2.37e+02 Heating: 1.07e-21 Frac tot 3.08e-06
pah-bt9404 *  DustTemp 3.50e+02 Pot Volt 6.54e+00 Chrg (e) 1.70e+00 drf cm/s 2.67e+02 Heating: 1.09e-21 Frac tot 3.16e-06
pah-bt9405 *  DustTemp 3.53e+02 Pot Volt 6.44e+00 Chrg (e) 1.92e+00 drf cm/s 3.02e+02 Heating: 1.09e-21 Frac tot 3.16e-06
pah-bt9406 *  DustTemp 3.55e+02 Pot Volt 6.45e+00 Chrg (e) 2.22e+00 drf cm/s 3.29e+02 Heating: 1.13e-21 Frac tot 3.26e-06
pah-bt9407 *  DustTemp 3.57e+02 Pot Volt 6.47e+00 Chrg (e) 2.54e+00 drf cm/s 3.60e+02 Heating: 1.17e-21 Frac tot 3.38e-06
pah-bt9408 *  DustTemp 3.59e+02 Pot Volt 6.43e+00 Chrg (e) 2.87e+00 drf cm/s 4.00e+02 Heating: 1.18e-21 Frac tot 3.40e-06
pah-bt9409 *  DustTemp 3.61e+02 Pot Volt 6.46e+00 Chrg (e) 3.27e+00 drf cm/s 4.35e+02 Heating: 1.20e-21 Frac tot 3.46e-06
pah-bt9410 *  DustTemp 3.63e+02 Pot Volt 6.48e+00 Chrg (e) 3.71e+00 drf cm/s 4.74e+02 Heating: 1.22e-21 Frac tot 3.52e-06
```

Some properties of the grain populations are printed if they are present. Each line gives the results of calculations for a specific type and size of grain. Graphite and silicate are normally included when grains are present. Each line begins with the name of the grain and an asterisk appears if quantum heating was important for the species. Quantum heating is only computed if it is significant due to its computational expense. The remainder of the line gives the equilibrium temperature of the grain, the potential in volts, the charge, the drift velocity, the gas heating (erg cm^{-3} s^{-1}) due to grain electron photoemission, and the dimensionless fraction of the total gas heating due to grain electron photoemission. For quantum-heated grains the temperature is the average weighted by T^4.

```
Molecules   CH/Ctot: 3.65e-04 CH+/Ctot 5.82e-13 CO/Ctot: 5.52e-01 CO+/Ctot 1.95e-14 H2O/Otot 3.27e-09 OH/Ototl 4.18e-11
```

A line giving relative abundances of some molecules is printed if the molecular fraction is significant. All molecular abundances are relative to either the total carbon or total oxygen abundance (this is indicated in the label for each). In order, the molecules are CH, CH$^+$, CO, CO$^+$, H_2O, and OH.

```
Lithium    8.94e-02 9.11e-01 9.53e-10 0.00e+00 Berylliu 9.99e-01 6.40e-04 6.38e-05 7.06e-10 0.00e+00 sec ion: 7.66e-15
```

Abundances of each stage of ionization of lithium and beryllium relative to the total gas-phase abundance of the element are followed by the secondary ionization rate [s^{-1}].

```
Carbon    6.76e-07 1.91e-02 9.70e-01 1.10e-02 1.77e-04 2.36e-09 0.00e+00 H2O+/O  0.00e+00 OH+/Otot 0.00e+00 Hex(tot) 0.00e+00
```

The abundances of the seven stages of ionization of carbon relative to the total gas-phase carbon abundance begin the line. The abundance of H_2O^+ and OH^+ relative to the total gas-phase oxygen abundance are given. These are followed by "Hex(tot)", the extra heat (erg cm^{-3} s^{-1}) due to fast neutrons, dissipation of turbulence, or added with the **hextra** command.

```
Nitrogen  1.60e-06 1.72e-02 9.69e-01 1.41e-02 4.77e-05 1.34e-07 9.81e-14 0.00e+00 O2/Ototl 0.00e+00 O2+/Otot 0.00e+00
```

The relative populations of the eight ionization stages of nitrogen are printed first. The relative abundance of O_2 and O_2^+ (relative to the total oxygen abundance) follows.

```
Silicon    0  1.13e-07 8.39e-03 8.16e-01 1.56e-01 1.86e-02 4.68e-05 3.08e-08 5.13e-12 1.63e-16 0.00e+00 0.00e+00 0.00e+00 0.00e+00
Sulphur    0  7.25e-08 7.46e-03 9.03e-01 8.81e-02 1.60e-03 1.67e-04 5.91e-06 9.11e-10 3.49e-14 3.20e-19 0.00e+00 0.00e+00 0.00e+00
Chlorine   0  2.51e-07 1.32e-02 9.57e-01 2.92e-02 7.57e-04 5.50e-05 7.07e-07 9.54e-09 2.94e-13 2.17e-18 0.00e+00 0.00e+00 0.00e+00
Argon      1  9.50e-08 2.83e-03 9.69e-01 2.73e-02 4.35e-04 2.65e-05 3.24e-07 1.53e-09 1.16e-11 8.21e-17 0.00e+00 0.00e+00 0.00e+00
Iron       3  1.78e-08 2.88e-04 1.08e-01 8.56e-01 3.26e-02 2.33e-03 2.33e-05 2.30e-07 1.28e-10 1.94e-14 9.07e-19 0.00e+00 0.00e+00
```

There are too many ionization stages to print across the line for elements more massive than neon. Although all stages with non-trivial abundances are computed, only the highest twelve stages of ionization are printed. The first number is an integer indicating how many stages are "off the page to the left". If the number is 2, then the first printed stage of ionization is twice ionized, i.e., Fe^{+2}.

4.5. Comments about the calculation

```
 the Orion HII Region / PDR / Molecular cloud with an open geometry
Calculation stopped because outer radius reached. Iteration 1 of 2
```

A series of messages appear after the printout of the last zone. The first will say why the calculation stopped. In a valid calculation the model will stop because one of the specified stopping criteria specified was met. If no other criteria are specified then the calculation usually stops when the default lowest temperature of 4000 K is reached. If the code stops because of an unintended reason (i.e., internal errors, or reaching the default limit to the number of zones) then a warning is printed saying that the calculation may have halted prematurely.

Only one stopping criterion message will be printed. The possible messages, and their interpretations, are:

... because of radiation pressure The default density law is for a constant density. If constant pressure is specified instead (with the **constant pressure** command), then Cloudy will try to keep the total pressure, particle and radiation, constant. The radiation pressure is small at the boundaries of the cloud, so the cloud will be unstable if the ratio of radiation to total pressure exceeds 0.5. The calculation stops, and this message is generated, if $P_{rad}/P_{tot} > 0.5$ occurs after the first iteration.

... because lowest EDEN reached. The calculation can be forced to stop when the electron density (**eden**) falls below a certain value, as set by the **stop eden** command. This can be used to stop the calculation at an ionization front. The

default lowest electron density is negative, so this stopping criterion applies only when the command is entered.

... because low electron fraction. The calculation can be forced to stop when the ratio of electron to hydrogen densities falls below a certain value, as set by the **stop efrac** command. This can be used to stop the calculation at an ionization front when the hydrogen density there is not known (for instance, in a constant pressure model). The default lowest electron density is negative, so this stopping criterion applies only when the command is entered.

... because low H_2/H fraction The calculation can be forced to stop when the ratio of densities of molecular hydrogen to total hydrogen falls below a certain value, as set by the **stop mfrac** command. The molecular fraction is defined as $2n(H_2)/n(H_{tot})$. This can be used to stop the calculation at some depth into a PDR. The default lowest molecular density is negative, so this stopping criterion applies only when the command is entered.

... because wind veloc too small The code can perform a wind calculation which includes the outward force due to radiation pressure and the inward force of gravity. This message is printed if the gas is decelerated to a stop.

... because code returned BUSTED The calculation stopped because something bad happened. The results are suspect. I would appreciate learning about this - please send the input script and version number.

... because DRAD small - set DRMIN The Strömgren radius of the H^+ zone is estimated at the start of the calculation, and the smallest allowed zone thickness is then set as a very small fraction of this. The calculation will stop if the zone thickness falls below this smallest thickness. This can occur because of any of several logical errors within Cloudy (adaptive logic is used to continuously adjust the zone thickness), although it can rarely occur for physical reasons as well. The smallest thickness can be reset to any number with the **set drmin** command, but it should not be necessary to do this. I would appreciate learning about this - please send the input script and version number.

... because DR small rel to thick. The depth into the cloud is stored as the double precision variable *depth* and the zone thickness is stored as the double precision variable *drad*. If the zone size becomes too small relative to the depth ($drad/depth < 10^{-14}$) then the depth variable will underflow such that $depth + drad = depth$. The calculation will stop in this case and give the above reason if this problem prevents the density from being properly evaluated.

... because optical depth reached. The largest allowed continuous absorption optical depth can be set with the **stop optical depth** command. The command specifies both the absorption optical depth, and the energy at which it is to be evaluated. All absorption opacity sources included in the calculation contribute to the computed optical depths and scattering opacities are not included. If the calculation stops because the largest continuum optical depth is reached, then this line is printed. This line is also printed if the **stop effective column density**

command is used to stop the calculation, since this command is actually a form of the **stop optical depth** command.

... because outer radius reached. The default outer radius is unphysically large, but can be changed with the **radius** or **stop thickness** commands. If the calculation stops because the outer radius set by one of these commands is reached, then this line is printed.

... because column dens reached. The default values of the largest allowed neutral, ionized, and total hydrogen column densities are unphysically large. They can be reset with the commands **stop column density**, **stop neutral column density**, or **stop ionized column density**. This message will be printed if one of these criteria stops the calculation.

... because lowest Te reached. The default value of the lowest temperature allowed is 4000 K. This is reasonable when only emission from warm ionized gas is of interest. The limit can be changed with the **stop temperature** command. This message is printed if the calculation stops because the lowest temperature is reached.

... because highest Te reached. The default value of the highest temperature allowed is 10^{10} K. The limit can be changed with the **stop temperature exceeds** command. This message is printed if the calculation stops because the highest allowed temperature is exceeded.

... because freeze out fraction. Nick Abel incorporated the condensation of molecules onto grain surfaces. Currently CO, H_2O, and OH condensation are treated. The chemistry network will become unstable when oxygen is highly depleted from the gas phase. The code stops when a certain fraction of oxygen is in the form of molecules frozen out on grain surfaces. By default the code stops when 99% of the oxygen abundance has condensed out of the gas phase.

... because NZONE reached. By default the code will stop after computing 1400 zones. This can be reset with the **stop zone** command. This message is printed if the calculation stops because the limiting number of zones is reached. A warning will be printed at the end of the calculation if it stops because it hits the default limit to the number of zones allowed, presently 1400, since this was probably not intended.

The default limit to the number of zones can be increased, while retaining the check that the default limit is not hit, by using the **set nend** command.

... because line ratio reached. It is possible to set a limit to the largest value of an emission-line intensity ratio with the **stop line** command. This message is printed if the calculation stops because the largest value of the ratio is reached.

... because internal error - DRAD. An internal logical error caused this message to be printed. Please report the problem, including the command lines and the version number of Cloudy, on the discussion board at the code's web site, www.nublado.org.

... because initial conditions out of bounds. The temperature of the first zone was not within the temperature bounds of the code. This is probably due to the incident continuum not being set properly.

... because zero electron density The electron density fell to zero because there was no source of ionization. This is unphysical and usually occurs because the cloud boundary conditions were not set properly. Consider adding at least galactic background cosmic rays with the **`cosmic ray background`** command and perhaps the galactic or extragalactic background.

... because reason not specified. I would appreciate learning about this internal error. Please post the input and version number on the code's discussion board.

4.6. Geometry

```
The geometry is plane-parallel.
```

The code will next say whether the geometry is plane parallel ($\Delta r/r_o < 0.1$), a thick shell ($\Delta r/r_o < 3$), or spherical ($\Delta r/r_o \geq 3$), where r_o is the inner radius and Δr is the thickness of the cloud.

4.7. Warnings, Cautions, Surprises, and Notes

```
C-Cloud thicker than smallest Jeans length=3.51e+16cm; stability problems? (smallest Jeans mass=2.58e-01Mo)
 !Magnetic field & cosmic rays both present. Their interations are not treated.
 !Some input lines contained underscores, these were changed to spaces.
 !Suprathermal collisional ionization of H reached 83.84% of the local H ionization rate.
 !H2 vib deexec heating reached 6.68% of the local heating.
 !Charge transfer ionization of H reached 95.8% of the local H ionization rate.
 !The largest continuum brightness temperature was 4.835e+05K at 1.052e-08 Ryd.
 !Both constant pressure and turbulence makes no physical sense???
 !AGE: Cloud age was not set. Longest timescale was 8.43e+15 s = 2.67e+08 years.
 !The excitation temp of Lya exceeded the electron temp, largest value was 4.60e+03K (gas temp there was 1.01e+03K, zone 310)
 !Line absorption heating reached 13.45% of the local heating - largest by level 1 line Si 2 34.8m
 !Some infrared fine structure lines are optically thick: largest tau was 2.05e+03
 !Local grain-gas photoelectric heating rate reached 98.8% of the total.
 !The local H2 photodissociation heating rate reached 12.8% of the total heating.
 !The CMB was not included. This is added with the CMB command.
 !The fraction of H in H2  reached 100.0% at some point in the cloud.
 !The fraction of C in CO  reached 100.0% at some point in the cloud.
 !The fraction of N in N2  reached 99.7% at some point in the cloud.
 !The fraction of S in CS  reached 100.0% at some point in the cloud.
 !The fraction of S in SO  reached 56.9% at some point in the cloud.
 !The fraction of S in OCS  reached 36.3% at some point in the cloud.
 !The fraction of Cl in HCl  reached 24.5% at some point in the cloud.
 !The fraction of O in H2Ogrn reached 58.3% at some point in the cloud.
 !A signficant amount of molecules condensed onto grain surfaces.
 !These are the molecular species with "grn" above.
 !The optical depth in the H I 21 cm line is 6.84e-01
 !The optical depth in the 12CO J=1-0 line is 2.79e+05
 !The radiation pressure jumped by 123% at zone 334, from 5.28e-11 to 3.67e-11 to 3.73e-11
 !The H2 density varied by 12.6% between two zones
 Continuum fluorescent production of H-beta was significant.
 Te-ne bounds of Case B lookup table exceeded, H I Case B line intensities set to zero.
 Te-ne bounds of Case B lookup table exceeded, He II Case B line intensities set to zero.
 Destruction of He 2TriS reached 3.4% of the total He0 dest rate at zone 236, 3.4% of that was photoionization.
 Critical density for l-mixing of He I not reached. More resolved levels are needed for accurate He I line ratios.
 The largest continuum occupation number was 2.911e+08 at 1.052e-08 Ryd.
 The continuum occupation number fell below 1 at 1.944e+04 microns.
 The continuum brightness temperature fell below 10,000K at 1.433e+06 microns.
 Ratio of computed diffuse emission to case B reached 2.30168 for iso 1 element 2
 Global grain photoelectric heating of gas was 9.9% of the total.
 Local grain-gas cooling of gas rate reached 90.4% of the total.
 The local H2 cooling rate reached 7.2% of the local cooling.
 Local CO rotation cooling reached 83.0% of the local cooling.
 The Balmer continuum optical depth was 3.68e+03.
 The Balmer continuum stimulated emission correction to optical depths reached 7.64e-02.
 The Paschen continuum optical depth was 1.69e+03.
 The continuum optical depth at the lowest energy considered (1.052e-08 Ryd) was 3.213e+03.
 The optical depth to Rayleigh scattering at 1300A is 4.36e-02
 3 body rec coef outside range 1
 The fraction of Cl in CCl+  reached 0.103% at some point in the cloud.
 The fraction of N in HNC  reached 0.312% at some point in the cloud.
 The fraction of C in C2H  reached 2.60% at some point in the cloud.
 The fraction of C in COgrn reached 0.379% at some point in the cloud.
```

The next messages fall into four categories: warnings beginning with W-; cautions beginning with C-; surprising results beginning with an explanation mark (!), and notes.

Cloudy checks that its range of validity was not exceeded in the calculation and does many internal sanity checks (Ferland 2001b). Warnings are issued to indicate that the program has not treated an important process correctly. For instance, warnings occur if the temperature was high enough for the electrons to be relativistic, if the global heating - cooling balance is off by more than 20%, or if the code stopped for an unintended reason. I would like to hear about warnings – the web site has a discussion board to place comments. Cautions are less severe, and indicate that Cloudy is on thin ice. Examples are when the optical depths in excited states of hydrogen change during the last iteration. Surprises begin with "!" and indicate that, while the physical process has been treated correctly, the result is surprising. An example is when induced Compton heating is more that 5 percent of the total Compton heating. Notes indicate interesting features about the model, such as maser effects in lines or continua, or if the fine structure lines are optically thick. The messages are usually self-explanatory.

4.8. Optional Plot

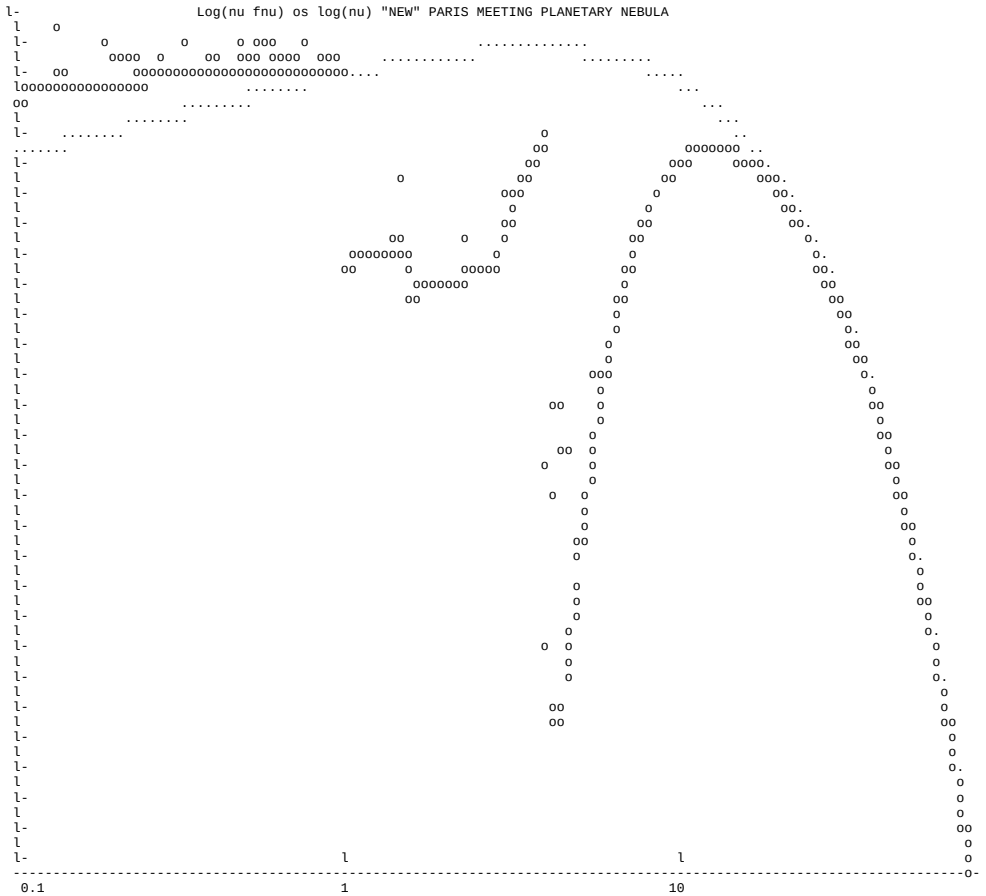

If any of the optional plots are requested with the **`plot - -`** command then they will appear next. This option is seldom used today since it is much easier to create data files with **punch** commands, described in Part 1, and then use other software to make plots.

4.9. Final Printout

```
   ********************************> Cloudy 06.01.02 <*********************************
   * title the Orion HII Region / PDR / Molecular cloud with an open geometry        *
   * c                                                                               *
   * c commands controlling continuum =========                                      *
-                                                                                    
-                                                                                    
-                                                                                    
-                                                                                    
   * assert line luminosity "12CO" 235.4m  -2.80 error 0.15                         *
   * assert line luminosity "12CO" 215.7m  -2.84 error 0.15                         *
   * assert nzone < 1400                                                            *
   * assert itrzn < 24                                                              *
   * c orion hii pdr pp.in                                                          *
   * c class hii pdr                                                                *
   * c ======================================                                       *
   ********************************> Log(U): -1.48 <*********************************
   >>>>>>>>>> Cautions are present.
```

The final printout begins by reprinting the input commands. The box surrounding it gives both the version number of Cloudy (at the top) and the log of the ionization parameter (the ratio of ionizing photon to hydrogen densities) at the bottom.

```
      Emission Line Spectrum.  Constant  Pressure Model.    Open geometry.  Iteration 2 of 2.
                                  Intensity (erg/s/cm^2)
```

This line summarizes some properties of the model and output. The first part indicates whether the energy in the emission lines is given as the luminosity case (the energy radiated by a spherical shell covering Ω sr [erg s^{-1}] where $\Omega / 4\pi$ is the covering factor) or the intensity case (emission produced by a unit area of gas [erg s^{-1} cm^{-2}]). Which of the two choices is printed is determined by whether the luminosity of the continuum was specified as the luminosity radiated by the central object into 4π sr or the intensity ($4\pi J$) of the incident continuum (erg cm^{-2} s^{-1}) at the illuminated face of the cloud. If the cloud is spherical and the intensity case is computed then the emergent emission-line spectrum will be per unit area in units of the inner radius r_o (that is, the total line luminosity radiated by a shell covering 4π sr will be the listed intensity $4\pi J$ times 4π r_o^2). The second part of thes line indicates the density structure (i.e., wind, constant density, constant pressure, constant gas pressure, power-law density distribution, etc). The next section tells whether the geometry was open or closed (these are defined in Part I of this document). The last part indicates the iteration number.

```
                                        Emergent line intensities
 TOTL  4861A     0.132   1.0000      12CO 517.8m  -3.749   0.0001      12CO 431.5m  -3.474   0.0002      12CO 369.8m  -3.268   0.0004
13CO 353.6m  -3.709   0.0001      13CO 309.4m  -3.605   0.0002      13CO 275.0m  -3.547   0.0002      13CO 247.5m  -3.544   0.0002
 13CO 225.0m  -3.641   0.0002      H  1  1216A   0.547   2.6028           H  1  1026A  -1.178   0.0490      H  1 972.5A  -1.350   0.0330
-                                                                                    
-                                                                                    
-                                                                                    
C  3 398.4A  -3.773   0.0001      N  1 980.7A  -3.567   0.0002      N  2 916.3A  -2.513   0.0023      N  2 646.4A  -2.307   0.0036
 N  3 348.7A  -3.763   0.0001       O  1  7950A  -2.869   0.0010       O  2  4188A  -3.756   0.0001      O  2 386.3A  -1.774   0.0124
 O  2 385.7A  -1.955   0.0082      O  3 300.5A  -3.653   0.0002                                                                    
                                        Intrinsic line intensities
 general properties.........      H  1 1.500m  -2.042   0.0010      +Col 1.278m  -1.666   0.0024      O  2 833.8A  -1.615   0.0027
 TOTL  4861A   0.473   0.3311      H  1 7.458m  -1.094   0.0090      Ca B 1.870m  -1.760   0.0019      O 2r  4651A  -2.135   0.0008
 TOTL  1216A   0.740   0.6119      H  1 4.653m  -1.299   0.0056      +Col 1.870m  -1.757   0.0019      O 2r  4341A  -2.413   0.0004
 Inci     0    3.001 111.7791      H  1 3.740m  -1.487   0.0036      Ca B 1.279m  -2.153   0.0008      TOTL  4341A  -2.413   0.0004
 TotH     0    1.727   5.9400      H  1 3.296m  -1.650   0.0025      +Col 1.279m  -2.149   0.0008      TOTL  1665A  -1.363   0.0048
-                                                                                    
 -                                                                                   
 -                                                                                   
H  1 1.513m  -2.287   0.0006      Ca B 1.869m  -1.283   0.0058      O 2r  2471A  -2.363   0.0005      hyperfine structure.........
 H  1 1.508m  -1.964   0.0012       +Col 1.869m  -1.275   0.0059       O 2r  7323A  -2.536   0.0003       inner shell.................
 H  1 1.504m  -1.999   0.0011      Ca B 1.278m  -1.676   0.0024      O 2r  7332A  -2.657   0.0002
```

A series of predicted quantities follow. These are mainly emission-line intensities although the output also includes other predicted quantities.

Two blocks of output may occur. The block "Emergent line intensities" is the observed intensity as viewed from the illuminated face of a layer that has a large column beyond the shielded face. It is only printed in the case of a dusty open geometry and is discussed further in the section on page 459 below. The second block "Intrinsic line intensities" is the intrinsic emission from the cloud.

Some continua and various indications of contributors to lines and continua are included. The section of this document describing observed quantities (page 455 below) tells how to convert these into some observed quantities. Not all are printed by default – the **`print`** commands described in Part I and also in section 6.3.2 starting on page 470 tell how to get more or fewer predictions. This list of emission lines can also be sorted by wavelength or intensity, and can be printed as a single column so that they can be entered into a spreadsheet (see the **`print lines`** command in Part I of this document).

The organization and meaning of the different of lines in the printout is discussed on page 463 below.

A list of emission lines with negative intensities may follow the main block of lines. These are lines which heat rather than cool the gas (heating is negative cooling). This is not a problem, but occurs if the line collisional de-excitation rate exceeds the line collisional excitation rate. This usually occurs when the line is radiatively excited but collisionally de-excited.

```
the Orion HII Region / PDR / Molecular cloud with an open geometry
Cooling:  HFBc     0 :0.110 HFFc     0 :0.077 TOTL  3727A:0.074 O  3  5007A:0.210 O  3  4959A:0.070 S  3  9532A:0.074
Heating:  BFH1     0 :0.817 BFHe     0 :0.074 GrGH     0 :0.099
```

Cooling: This line indicates the fraction of the total cooling (defined here as the energy of the freed photoelectron as in AGN3) carried by the indicated emission lines. The line label is followed by the ratio of the energy in the line to the total cooling. This is an important indication of the fundamental power-losses governing conditions in the model. The labels used are the same as those in the line array.

Heating: This line indicates the fraction of the total heating produced by various processes. The format is the same as the line giving the cooling.

```
IONIZE PARMET: U(1-) -1.4764 U(4-): -5.0813 U(sp): -4.46 Q(ion):  -4.574 L(ion)-13.505  Q(low): 15.158   L(low) 1.121
```

The line begins with the log of the H "U(1-)" and He^+ "U(4-)" ionization parameters. The third number "U(sp)" is the log of a spherical ionization parameter often used in spherical geometries, such as H II regions or planetary nebulae. It is defined as

$$U_{sph} = \frac{Q\left(\mathrm{H}^0\right)}{4\pi R_s^2 n_{\mathrm{H}} c} \qquad (408)$$

where R_S is the Strömgren radius, defined as the point where the hydrogen neutral fraction falls to $H^0/H = 0.5$. If no ionization front is present then U_{sph} is evaluated at the outer edge of the cloud. The next two numbers are the log of the number of

hydrogen ionizing photons ($h\nu \geq 1$ Ryd) exiting the nebula "Q(ion)", and the log of the energy in this ionizing continuum "L(ion)". The next two numbers are the equivalent quantities, for non-ionizing ($h\nu < 1$ Ryd) radiation. These are either per unit area or by a shell covering 4π sr. These have been corrected for the r^{-2} dilution if per unit area, and so are directly comparable with the numbers given at the start of the calculation.

```
ENERGY BUDGET: Heat: 1.725 Coolg: 1.725 Error: 0.0% Rec Lin: 1.462 F-F H -5.612 P(rad/tot)mx:1.10E-01
```

This line gives an indication of the energy budget of the nebula. The first number "Heat" is the log of the total heating (in ergs s^{-1}, but again either into 4π sr or cm^{-2}). The second number "Coolg" is the log of the total cooling, in the same units. Cooling, as defined in Osterbrock & Ferland (2006; hereafter AGN3), is the total energy in collisionally excited lines and part of the recombination energy, but *does not* include recombination lines. The percentage error in the heating–cooling match "Error" follows. The next numbers give "Rec Lin", the log of the total luminosity in recombination lines, "F-F H", the log of the amount of energy deposited by free-free heating, and "P(rad/tot)mx", the largest value of the ratio of radiation to gas pressures that occurred.

```
Col(Heff):  1.031E+25 snd travl time 5.06E+13 sec Te-low: 1.69E+01 Te-hi: 1.08E+04 G0TH85:3.54E+05 G0DB96:4.54E+05
```

The effective column density "Col(Heff)", as defined in the section on the **`stop effective column density`** command, is printed. This is followed by "snd travl time", the sound travel time across the nebula in seconds. Constant pressure is only valid if the cloud is static for times considerably longer than this. The last two numbers are the lowest "Te-low" and highest "Te-hi" electron temperatures found in the computed structure. The last numbers "G0TH85" and "GHBD96" give the intensity of the ultraviolet radiation field relative to the background Habing value, as defined by Tielens & Hollenbach (1985) and Bertoldi & Draine (1996).

```
Emiss Measure  n(e)n(p) dl   2.205E+25 n(e)n(He+)dl    1.962E+24 En(e)n(He++) dl   1.402E+21
```

This gives several line-of-sight emission measures. The definition of the line of sight emission measure of a species X is (AGN3 section 5.4)

$$E(X) = \int n(e)\, n(X)\, f(r)\, dr \quad [\mathrm{cm}^{-5}] \tag{409}$$

where $f(r)$ is the filling factor. This is given for H^+, He^+, and He^{2+}.

```
He/Ha:9.61E-02 = 1.01*true Lthin:1.81E+01 itr/zn: 9.78 H2 itr/zn: 0.00 File Opacity: F Mass 62.573
```

This line gives some quantities deduced from the predicted emission-line spectrum. The first (He/Ha) number is the apparent helium abundance He/H, measured from the emission-line intensities using techniques similar to those described in AGN3 (Chapter 5);

$$\left(\frac{\mathrm{He}}{\mathrm{H}}\right)_{apparent} = \frac{0.739 \times I(5876) + 0.078 \times I(4686)}{I(\mathrm{H}\beta)} \quad . \tag{410}$$

The intensities of all lines are the total predicted intensities and include contributions from collisional excitation and radiative transfer effects. The second number (i.e., 1.07*true), is the ratio of this deduced abundance to the true abundance. This provides a simple way to check whether ionization correction factors, or other effects, would upset the measurement of the helium abundance of the model nebula. This is followed by the longest wavelength in centimeters "Lthin" at which the nebula is optically thin. Generally the largest FIR opacity source is bremsstrahlung, and the number will be 10^{30} if the nebula is optically thin across the IR. The number "itr/zn" is the average number of iterations needed to converge each zone while "H2 itr/zn" is the number of iterations required to converge the large H_2 model if it is included. "Mass" gives the log of the total mass of the computed structure in grams if the inner radius was specified. If the inner radius was not specified then this is the log of the mass per unit area [gm cm^{-2}].

```
Temps(21 cm)   T(21cm/Ly a)  8.40E+02       T(<n(H0)/T>)  1.04E+03         T(<n/Tspin>)    1.29E+03         TB21cm       5.32E+02
     <Tspin>  1.29E+03       N(H0/Tspin)     5.22E+18      N(OH/Tkin)       2.01E+13
```

This line gives various quantities related to the H I 21 cm line. "T(21cm/Ly a)" gives the temperature deduced from the ratio of the 21 cm to Lα line optical depths (AGN3 Section 5.5). The opacity within the 21 cm line is proportional to $n\left(\mathrm{H}^0\right)\chi/kT$ where χ is the excitation energy of the line. "T(<n(H0)/T>)" gives the harmonic mean temperature

$$<T>=\frac{\int Tn\left(\mathrm{H}^0\right)\chi/kT\,dr}{\int n\left(\mathrm{H}^0\right)\chi/kT\,dr} \qquad (411)$$

where T is the electron or gas kinetic temperature. "T(n/Tspin)" is the temperature derived from the n/T_{spin} ratio using the 21 cm spin temperature. The spin and kinetic temperatures are often assumed to be equal although they are not in practice. The number "TB21cm" is an estimate of the brightness temperature of the 21 cm line as viewed from the illuminated face of the cloud. It is the spin temperature at a depth where the 21 cm line becomes optically thick at line center.

On the next line "<Tspin>" gives the mean spin temperature of the 21 cm transition. The is the mean of the actual ratio of populations of the ground fine structure levels, which is computed including the effects of Lyα scattering. The next two numbers are the H^0 and OH column densities divided by the 21 cm spin temperature in the case of H^0 and by the kinetic temperature in the case of OH. These ratios are proportional to the optical depth of a line at radio frequencies.

```
<a>:0.00E+00 erdeFe0.0E+00 Tcompt1.90E+06 Tthr1.19E+13 <Tden>: 2.38E+01 <dens>:2.00E-17 <Mol>:2.31E+00
```

The mean radiative acceleration <a> [cm s^{-2}] is printed if the geometry is a wind model and zero otherwise. This is followed by some time scales. "erdeFe" is the time scale, in seconds, to photoerode Fe (Boyd and Ferland 1987; this number is 0s if the γ -ray flux is zero). The next gives the Compton equilibrium timescale "Tcompt" and the thermal cooling timescale "Tthr" [s]. The density (gm cm^{-3}) weighted mean

temperature "<Tden>", radius-weighted mean density "<dens>" (gm cm^{-3}), and mean molecular weight "<Mol>", follow.

```
Mean Jeans l(cm)4.19E+16 M(sun)4.36E-01 smallest:  len(cm):3.53E+16 M(sun):2.61E-01 Alf(ox-tran):  0.0000
```

This line gives the mean Jeans length "l(cm)" (cm) and Jeans mass "M(sun)" (in solar units), followed by the smallest Jeans length "smallest len(cm)" and the smallest Jeans mass "M(sun)" which occurred in the calculation. The last quantity "Alf(ox-tran)" is the spectral index α_{ox}, defined as in the header, but for the transmitted continuum (attenuated incident continuum plus emitted continuum produced by the cloud).

```
Hatom level 26 NHtopoff: 22 HatomType: add HInducImp F He tot level: 63 He2 level:  26 ExecTime 2233.72
```

This line gives the number of levels of the model hydrogen atom, the "topoff" level, above which the remainder of the recombination coefficient is added, the type of topping off used for this calculation, and the number of levels used for the helium singlets and ion. The last number on the line is the execution wall-clock time in seconds.

```
ConvrgError(%)  <eden>  0.075  MaxEden  0.543  <H-C>   0.20  Max(H-C)    0.50  <Press>   0.042 MaxPres  2.535
 Continuity(%)  chng Te   3.9  elec den   5.8  n(H2)   12.8  n(CO)        8.5
```

The first line gives some estimates of the errors that occurred in several quantities that the code determines. A pair of numbers gives the mean and largest percentage errors for the electron density, the heating-cooling balance, and the pressure. The second line gives the percentage changes that occurred from one zone to the next for the temperature, the electron density, and the H_2 and CO densities.

```
                                                Averaged Quantities
           Te      Te(Ne)   Te(NeNp)  Te(NeHe+)Te(NeHe2+) Te(NeO+)  Te(NeO2+)  Te(H2)     N(H)     Ne(O2+)   Ne(Np)
Radius:  6.86e+02  9.19e+03  9.27e+03  9.18e+03  9.09e+03  9.65e+03  8.86e+03  2.28e+01  8.30e+06  1.43e+04  1.50e+04
```

This begins with several temperature and density averages, over either radius or volume. The volume averages are only printed if the **sphere** command is entered. The quantity which is printed is indicated at the top of each column. The averaged quantity is the first part of the label, and the weighting used is indicated by the quantity in parenthesis. For instance, **Te(NeO2+)** is the electron temperature averaged with respect to the product of the electron and O^{2+} densities.

```
Peimbert T(OIIIr)9.08E+03 T(Bac)0.00E+00 T(Hth)0.00E+00 t2(Hstrc) 6.01e-03 T(O3-BAC)0.00E+00 t2(O3-BC) 0.00e+00 t2(O3str) 1.81e-03
 Be careful: grains exist.  This spectrum was not corrected for reddening before analysis.
```

This series of quantities deal with temperature fluctuations (t^2, Peimbert 1967; AGN3 section 5.11) . The code analyzes the predicted emission line and continuum spectrum using the same steps that Manuel outlined in this paper. The code does not attempt to correct the predicted emission line intensities for collisional suppression or reddening, so this line is only printed if the density is below the density set with the **set tsqden** command - the default is 10^7 cm^{-3}. This code does not attempt to deredden the spectrum: a caution is printed if grains are present.

The nature of temperature fluctuations is, in my option, the biggest open question in nebular astrophysics. Theory (Cloudy too) predicts that they should be very small, because of the steep dependence of the cooling function on the temperature, while some observations indicate a very large value of t^2 (see Liu et al. 1995, Kingdon & Ferland 1995, and Ferland 2003 for discussions). If something is missing from our current understanding of the energy source of photoionized nebulae then the entire nebular abundance scale (for both the Milky Way and the extragalactic nebulae) is in error by as much as 0.5 dex.

Two fundamentally different t^2s enter here - the "structural" t^2 and the "observational" t^2. The structural value comes from the computed ionization and thermal structure of the nebula while the observational value comes from an analysis of the predicted emission-line spectrum following the methods outlined in Peimbert's 1967 paper.

The structural t^2 for the H^+ ion is defined as

$$t^2\left(\mathrm{H}^+\right)=\left\langle\left[\frac{T(r)-\langle T\rangle}{\langle T\rangle}\right]^2\right\rangle=\frac{\int\left[T(r)-\langle T\rangle\right]^2 n_e n\left(\mathrm{H}^+\right) f(r)\,dV}{\langle T\rangle^2\int n_e n\left(\mathrm{H}^+\right) f(r)\,dV} \tag{412}$$

where <*T*> is the density-volume weighted mean temperature

$$\langle T\rangle=\frac{\int T(r)\,n_e n\left(\mathrm{H}^+\right) f(r)\,dV}{\int n_e n\left(\mathrm{H}^+\right) f(r)\,dV}. \tag{413}$$

This quantity is given in the averaged quantities block as the column "Te(NeNp)".

The observational t^2 - related quantities are the following: "T(OIIIr)" is the electron temperature indicated by the predicted [OIII] 5007/4363 ratio in the low-density limit. This number is meaningless for densities near or above the critical density of these lines. "T(Bac)" is the hydrogen temperature resulting from the predicted Balmer jump and Hβ. "T(Hth)" is the same but for optically thin Balmer continuum and case B Hβ emission. "t2(Hstrc)" is the structural H II t^2. The entries "T(O3-BAC)" and t2(O3-BC)" are the mean temperature and t^2 resulting from the standard analysis of the [O III] and H I spectra (Peimbert 1967). Finally "t2(O3str)" is the structural t^2 over the O^{2+} zone. Only the structural t^2s are meaningful for high densities. This section was developed in association with Jim Kingdon, and Kingdon and Ferland (1995) provide more details.

```
Average Grain Properties (over radius):
   gra-orion01* gra-orion02* gra-orion03* gra-orion04* gra-orion05* gra-orion06* gra-orion07 gra-orion08 gra-orion09 gra-orion10
  nd:   0     1     2     3     4     5     6     7     8     9
<Tgr>: 3.659e+01  3.592e+01  3.522e+01  3.450e+01  3.377e+01  3.306e+01  3.236e+01  3.170e+01  3.106e+01  3.045e+01
<Vel>: 4.177e+02  4.780e+02  5.483e+02  6.279e+02  7.223e+02  8.327e+02  9.572e+02  1.095e+03  1.241e+03  1.396e+03
<Pot>: 3.072e-01  2.905e-01  2.736e-01  2.575e-01  2.423e-01  2.281e-01  2.151e-01  2.036e-01  1.932e-01  1.842e-01
<D/G>: 1.202e-04  1.337e-04  1.486e-04  1.653e-04  1.837e-04  2.043e-04  2.271e-04  2.525e-04  2.808e-04  3.122e-04

   sil-orion01* sil-orion02* sil-orion03* sil-orion04* sil-orion05 sil-orion06 sil-orion07 sil-orion08 sil-orion09 sil-orion10
  nd:  10     11     12     13     14     15     16     17     18     19
<Tgr>: 3.303e+01  3.261e+01  3.216e+01  3.173e+01  3.130e+01  3.090e+01  3.051e+01  3.015e+01  2.981e+01  2.950e+01
<Vel>: 1.093e+03  1.237e+03  1.385e+03  1.532e+03  1.676e+03  1.817e+03  1.953e+03  2.086e+03  2.215e+03  2.342e+03
<Pot>: 1.693e-01  1.598e-01  1.509e-01  1.427e-01  1.352e-01  1.283e-01  1.220e-01  1.163e-01  1.109e-01  1.062e-01
<D/G>: 2.031e-04  2.259e-04  2.511e-04  2.792e-04  3.104e-04  3.451e-04  3.837e-04  4.267e-04  4.744e-04  5.274e-04

   pah-bt9401 * pah-bt9402 * pah-bt9403 * pah-bt9404 * pah-bt9405 * pah-bt9406 * pah-bt9407 * pah-bt9408 * pah-bt9409 * pah-bt9410 *
  nd:  20     21     22     23     24     25     26     27     28     29
<Tgr>: 4.620e+01  4.634e+01  4.650e+01  4.662e+01  4.675e+01  4.683e+01  4.691e+01  4.697e+01  4.702e+01  4.706e+01
<Vel>: 9.565e+00  1.100e+01  1.255e+01  1.426e+01  1.617e+01  1.819e+01  2.029e+01  2.261e+01  2.516e+01  2.779e+01
<Pot>: 2.697e+00  2.424e+00  2.181e+00  1.964e+00  1.768e+00  1.594e+00  1.442e+00  1.307e+00  1.188e+00  1.084e+00
<D/G>: 9.119e-08  9.556e-08  1.002e-07  1.050e-07  1.100e-07  1.153e-07  1.208e-07  1.266e-07  1.327e-07  1.391e-07
Dust to gas ratio (by mass): 5.457e-03, A(V)/N(H)(pnt):5.543e-22, (ext):4.024e-22, R:3.647e+00 AV(ext):5.152e+03 (pnt):7.097e+03
```

The next lines give some information concerning grains if these were included in the calculation. These lines give the mean temperature, drift velocity, and potential, for all of the grain populations included in the calculation. An asterisk will appear to the right of the name of any species with quantum heating included. In this case the mean temperature is weighted by T^4.

The last line gives some information related to the grain abundance and optical properties. The first number is the dust to gas ratio by mass. The next two are the total visual extinction per unit hydrogen column density for a point and extended source. These are different because of the different effects of forward scattering (AGN3 section 7.6). The next gives the ratio of total to selective extinction. The line ends with A_V for both an extended and point source.

```
 Contin Optical Depths: COMP: 1.07e-03  H-: 1.90e-04  R(1300): 4.53e-02 H2+: 1.12e-06 Pfa:1.55E+02
          Pa: 7.89e+02  Ba: 3.98e+03  Hb: 5.31e+03  La: 1.07e+04  1r:1.151E+05 1.8:3.79E+07 4.:4.382E+06
 Line Optical Depths: 10830: 8.12e+02 3889: 3.49e+01  5876: 1.91e-04 7065: 2.62e-05 2.06m: 1.29e-02 21c: 5.29e-01
```

The first two lines give the continuum optical depths at various energies. These are the total optical depths, including the correction for stimulated emission, and will be negative if maser action occurs. These include grain opacity if grains are present. The labels, and their interpretation, are as follows. COMP is Thomson scattering. H- is the negative hydrogen ion at maximum cross section. R(1300) is Rayleigh scattering at 1300Å, H_2^+ is the molecular hydrogen ion. Pfa is the optical depth at the wavelength of the Pfund α transition (5-4).

The next line gives total continuous optical depths at the energies of various hydrogen and helium ionization edges and lines. These are evaluated at the energies of the Paschen α, Balmer α and β, and Lα lines, and the ionization edges of hydrogen, atomic helium, and the helium ion.

The third line gives optical depths of some He I lines. These are computed with a full model of the He^0 atom (Porter et al. 2004).

```
Old, new H 1 continuum optical depths:
     1 1.13e+05     2 3.68e+03     3 1.69e+03     4 8.24e+02     5 4.03e+02     6 2.12e+02     7 1.24e+02     8 8.47e+01
     9 7.60e+01    10 3.02e+02    11 2.24e+02    12 1.05e+02    13 9.80e+01    14 1.31e+02    15 1.16e+02    16 9.21e+01
    17 7.61e+01    18 6.54e+01    19 5.68e+01    20 4.88e+01    21 4.19e+01    22 3.55e+01    23 3.00e+01    24 2.55e+01
    25 2.17e+01
     1 1.13e+05     2 3.61e+03     3 1.66e+03     4 8.08e+02     5 3.95e+02     6 2.08e+02     7 1.22e+02     8 8.31e+01
     9 7.46e+01    10 2.96e+02    11 2.20e+02    12 1.03e+02    13 9.61e+01    14 1.28e+02    15 1.14e+02    16 9.03e+01
    17 7.46e+01    18 6.41e+01    19 5.57e+01    20 4.78e+01    21 4.11e+01    22 3.48e+01    23 2.95e+01    24 2.50e+01
    25 2.12e+01
```

```
Old, new H  1 line optical depths:
 2- 1 2.59e+09  3- 2 1.58e-01  4- 3 9.14e-08  5- 4 5.27e-08  6- 5-1.66e-08  7- 6-1.39e-07  8- 7-5.70e-07
 9- 8-1.24e-06 10- 9-1.79e-06 11-10-3.40e-06 12-11-4.47e-06 13-12-4.36e-06 14-13-3.91e-06 15-14 9.70e-06 16-15-6.04e-05
17-16-1.08e-04 18-17-1.88e-04 19-18-3.44e-04 20-19-6.90e-04 21-20 1.37e-02 22-21 2.07e-02 23-22 6.52e-02 24-23 8.91e-02
25-24 1.18e-01
 2- 1 1.16e+09  3- 2 7.08e-02  4- 3 6.02e-08  5- 4 2.67e-08  6- 5-2.15e-08  7- 6-1.51e-07  8- 7-5.76e-07
 9- 8-1.23e-06 10- 9-1.78e-06 11-10-3.35e-06 12-11-4.41e-06 13-12-4.30e-06 14-13-3.81e-06 15-14 4.83e-06 16-15-5.97e-05
17-16-1.07e-04 18-17-1.85e-04 19-18-3.39e-04 20-19-6.74e-04 21-20 6.72e-03 22-21 1.01e-02 23-22 3.20e-02 24-23 4.38e-02
25-24 5.79e-02

Old, new He 2 continuum optical depths:
    1 4.47e+06     2 1.12e+05     3 4.60e+03     4 3.68e+03     5 2.54e+03     6 1.69e+03     7 1.17e+03     8 8.24e+02
    9 5.77e+02    10 4.03e+02    11 2.88e+02    12 2.12e+02    13 1.61e+02    14 1.24e+02    15 1.01e+02    16 8.47e+01
   17 7.13e+01    18 7.60e+01    19 1.43e+02    20 3.02e+02    21 3.11e+02    22 2.24e+02    23 1.54e+02    24 1.05e+02
   25 8.75e+01
    1 4.38e+06     2 1.13e+05     3 4.52e+03     4 3.61e+03     5 2.50e+03     6 1.66e+03     7 1.15e+03     8 8.08e+02
    9 5.66e+02    10 3.95e+02    11 2.82e+02    12 2.08e+02    13 1.57e+02    14 1.22e+02    15 9.93e+01    16 8.31e+01
   17 7.00e+01    18 7.46e+01    19 1.40e+02    20 2.96e+02    21 3.05e+02    22 2.20e+02    23 1.51e+02    24 1.03e+02
   25 8.58e+01

Old, new He 2 line optical depths:
 2- 1 7.60e+06  3- 2 6.42e-07  4- 3 2.62e-13  5- 4-1.24e-12  6- 5-5.54e-12  7- 6-1.45e-11  8- 7-2.98e-11
 9- 8-5.02e-11 10- 9-7.50e-11 11-10-9.49e-11 12-11-9.32e-11 13-12-3.54e-11 14-13 2.08e-10 15-14 1.07e-09 16-15-1.24e-09
17-16-2.30e-09 18-17-3.80e-09 19-18-6.67e-09 20-19-1.30e-08 21-20 2.38e-07 22-21 3.59e-07 23-22 1.20e-06 24-23 1.63e-06
25-24 2.15e-06
 2- 1 4.03e+06  3- 2 3.21e-07  4- 3 1.31e-13  5- 4-1.23e-12  6- 5-5.53e-12  7- 6-1.44e-11  8- 7-2.97e-11
 9- 8-5.01e-11 10- 9-7.48e-11 11-10-9.47e-11 12-11-9.29e-11 13-12-3.54e-11 14-13 1.04e-10 15-14 5.32e-10 16-15-1.23e-09
17-16-2.30e-09 18-17-3.80e-09 19-18-6.66e-09 20-19-1.30e-08 21-20 1.18e-07 22-21 1.78e-07 23-22 5.96e-07 24-23 8.09e-07
25-24 1.07e-06

Old He Is optical depths:   1 3.86e+07   2 4.04e+03   3 3.94e+03   4 3.80e+03   5 3.80e+03   6 3.80e+03   7 3.67e+03   8 2.16e+03
New He Is optical depths:   1 3.79e+07   2 3.96e+03   3 3.86e+03   4 3.72e+03   5 3.72e+03   6 3.72e+03   7 3.60e+03   8 2.12e+03
        Old He Is Lines: 2-1 9.19e+11 3-2 6.78e-09
        New He Is Lines: 2-1 4.51e+11 3-2 3.44e-09
```

Hydrogen and helium optical depths in continua and $\alpha(n \rightarrow n\text{-}1)$ transitions follow. The first blocks of lines are the optical depths assumed at the start of the present iteration, and the second block of lines gives the newly computed total optical depths. Negative optical depths indicate maser action. For each of the pairs of lines, the first block is the optical depth at thresholds of levels of hydrogen. The second line gives the optical depths in the α $(n \rightarrow n\text{-}1)$ transitions of hydrogen or helium.

```
  Line Optical Depths: 10830: 3.52e+01  3889: 1.51e+00    5876: 2.11e-08 7065: 2.88e-09  2.06m: 2.86e-05  21c: 5.35e-05
  H  1 1215A 5.15e+05 H  1 1025A 8.26e+04 H  1  972A 2.87e+04 H  1  949A 1.35e+04 H  1  937A 7.45e+03 H  1  930A 4.56e+03
  H  1  926A 3.00e+03 H  1  923A 2.08e+03 H  1  920A 1.51e+03 H  1  919A 1.12e+03 H  1  918A 8.62e+02 H  1  917A 6.75e+02
  H  1  916A 5.39e+02 H  1  915A 4.37e+02 H  1  915A 3.59e+02 H  1  914A 2.99e+02 H  1  914A 2.52e+02 H  1  914A 2.14e+02
  H  1  914A 1.83e+02 H  1  913A 1.58e+02 H  1  913A 1.37e+02 H  1  913A 1.20e+02 H  1  913A 1.06e+02 H  1  913A 9.34e+01
 --------
```

Line optical depths are not normally printed, but will be if the **`print line optical depths`** command is entered.

```
                                                Log10 Column density (cm^-2)
  Htot  : 25.107   HII   : 21.167   HI    : 21.830   H-    : 12.687   H2g   : 24.806   H2*   : 16.421   H2+   : 11.203   HeH+  : 11.485
  H3+   : 13.820
  CH    : 17.799   CH+   : 12.136   OH    : 14.764   OH+   : 11.763   O2    : 17.909   CO    : 21.489   CO+   : 10.423   H2O   : 17.459
  H2O+  : 11.049   O2+   : 11.735   H3O+  : 14.429   CH2+  : 11.869   CH2   : 17.534   HCO+  : 15.394   CH3+  : 13.437   SiH2+ : 11.835
  SiH   : 15.523   HOSi+ : 14.069   SiO   : 17.953   SiO+  :  9.222   CH3   : 20.296   CH4   : 20.207   CH4+  : 11.132   CH5+  : 13.562
  N2    : 20.644   N2+   : 12.546   NO    : 15.954   NO+   : 12.873   S2    :  4.242   S2+   :  0.565   OCN   : 12.648   OCN+  :  9.954
  NH    : 14.634   NH+   :  9.266   NH2   : 16.135   NH2+  :  9.125   NH3   : 16.966   NH3+  : 12.225   NH4+  : 13.243   CN    : 18.325
  CN+   :  7.814   HCN   : 18.107   HCN+  :  8.175   HNO   :  8.826   HNO+  : 10.277   HS    : 14.673   HS+   : 13.458   CS    : 19.929
  CS+   : 10.371   NO2   : 10.136   NO2+  :  4.356   NS    : 13.418   NS+   : 12.254   SO    : 19.303   SO+   : 14.554   SiN   : 13.857
  SiN+  : 10.516   N2O   : 10.072   HCS+  : 15.996   OCS   : 19.077   OCS+  : 14.312   C2    : 20.023   C2+   : 11.133   CCl   : 14.010
  ClO   :  2.369   HCl+  : 11.968   HCl   : 17.061   H2Cl+ : 12.002   CCl+  : 12.258   H2CCl+: 10.100   ClO+  : -1.084   HNC   : 18.151
  HCNH+ : 14.265   C2H   : 19.590   C2H+  : 10.670   C2H2  : 16.355   C2H2+ : 15.324   C3H   :  4.558   C3H+  : -0.848   C2H3+ : 11.612
  C3    :  3.013   C3+   : -6.584   COgrn : 17.793   H2Ogrn: 21.202   OHgrn :  8.957


             1      2      3      4      5      6      7      8      9     10     11     12     13     14     15     16     17

Hydrogen   21.830 21.167 25.107 (H2)               Log10 Column density (cm^-2)
Helium     24.085 20.117 17.105
Carbon     17.950 18.459 17.563 14.609 13.216  3.870
Nitrogen   19.044 16.241 16.933 14.065 11.478  5.692 -1.143
Oxygen     20.608 17.460 17.476 14.327 11.487  6.302  2.306
Neon       20.885 16.857 16.224 13.324 10.890  5.202  0.097
Magnesium  19.584 16.541 15.619 12.650 10.152  4.929  0.953
Silicon    19.701 16.932 15.711 14.515 13.010 10.127  3.809 -0.668
Sulphur    19.036 17.151 16.136 14.583 12.601 11.685 10.014  2.678 -2.437
Chlorine   18.066 14.800 14.129 11.924 10.392  9.305  4.190  1.698 -3.512
Argon      19.584 14.672 15.606 13.401 11.627 10.513  5.326  2.378 -0.441
Iron       19.584 16.655 15.236 15.417 12.498 11.847  9.292  5.178  1.303 -3.214
Exc state    He1* 14.756   CII* 18.248   C11* 17.606   C12* 17.569   C13* 17.067   O11* 20.607   O12* 18.042   O13* 17.426
             Si2* 16.187   C30* 12.885   C31*  8.857   C32* 13.149
```

This lists the column densities (cm^{-2}) of some atoms, ions, and molecules. The first number "Htot" is the total column density of hydrogen in all forms (including atoms, ions, and molecules). The following two numbers are the column densities in H^+ and H^0 only. The last four numbers are column densities in four ions and molecules (H^-, H_2^g, H_2^*, H_2^+, H_3^+, and HeH^+). The remaining lines give column densities in various

molecules containing heavy elements. Molecules with names ending in "grn" are solids that have condensed onto grain surfaces.

The next block gives column densities in atoms and ions of the heavy elements. For hydrogen the last number is the H_2 column density. Column densities within certain excited states of the heavy elements, listed in Table 1 on page 420 above, are also printed. The label gives the element, ionization stage, and level within the ground term. The meaning of the labels is given in Table 1 on page 420 above.

```
              1      2      3      4      5      6      7      8      9     10     11     12     13     14     15     16

Hydrogen    -3.278 -3.940 -0.000 (H2)                Log10 Mean Ionisation (over radius)
Helium      -0.000 -3.968 -6.980
Carbon      -3.635 -3.126 -4.021 -6.975 -8.368-17.715
Nitrogen    -1.908 -4.712 -4.019 -6.887 -9.474-15.261-22.096
Oxygen      -1.101 -4.249 -4.234 -7.382-10.222-15.407-19.403
Neon        -0.000 -4.028 -4.662 -7.561 -9.996-15.684-20.788
Magnesium   -0.000 -3.044 -3.966 -6.934 -9.432-14.656-18.631
Silicon     -0.008 -2.778 -3.999 -5.194 -6.700 -9.582-15.900-20.377
Sulphur     -1.071 -2.956 -3.971 -5.524 -7.507 -8.423-10.093-17.429-22.545
Chlorine    -0.041 -3.307 -3.978 -6.184 -7.716 -8.802-13.918-16.410-21.619
Argon       -0.000 -4.912 -3.979 -6.183 -7.957 -9.071-14.259-17.206-20.025
Iron        -0.001 -2.929 -4.348 -4.167 -7.086 -7.737-10.292-14.406-18.282-22.799

              1      2      3      4      5      6      7      8      9     10     11     12     13     14     15     16

Hydrogen    -1.292 -0.090 -0.864 (H2)          Log10 Mean Ionisation (over radius*electron density)
Helium      -0.622 -0.119 -3.265
Carbon      -2.105 -0.549 -0.176 -3.188 -4.552-14.000
Nitrogen    -0.770 -0.843 -0.174 -3.101 -5.664-11.546-18.381
Oxygen      -0.813 -0.378 -0.405 -3.646 -6.501-11.692-15.688
Neon        -0.730 -0.171 -0.855 -3.828 -6.272-11.969-17.073
Magnesium   -1.269 -0.741 -0.117 -3.184 -5.702-10.941-14.916
Silicon     -1.764 -0.643 -0.148 -1.382 -2.932 -5.840-12.185-16.662
Sulphur     -2.018 -0.696 -0.122 -1.719 -3.712 -4.627 -6.332-13.714-18.829
Chlorine    -0.856 -0.966 -0.130 -2.390 -3.910 -4.994-10.203-12.695-17.904
Argon       -0.732 -1.160 -0.130 -2.396 -4.146 -5.259-10.544-13.491-16.310
Iron        -1.472 -0.778 -0.478 -0.331 -3.339 -3.971 -6.562-10.691-14.567-19.083
```

The next blocks of output give the mean ionization, averaged over volume (if the model is spherical), and over radius. The numbers printed are the log of the mean ionization fraction in the various stages. The volume-averaged ionization fraction for ion i of element a is given by

$$\left\langle \frac{n_a^i}{n_a} \right\rangle_{vol} = \frac{\int n_a^i f(r)\ dV}{\int n_a f(r)\ dV}. \tag{414}$$

and the radius average by

$$\left\langle \frac{n_a^i}{n_a} \right\rangle_{rad} = \frac{\int n_a^i f(r)\ dr}{\int n_a f(r)\ dr}. \tag{415}$$

Where n_a is the total gas-phase density and $n_a{}^i$ is the density in ionization stage i. Similar blocks of information will give the mean ionization weighted by electron density and radius or volume, and mean electron temperature weighted by volume, radius, and electron density and volume and radius.

```
              1      2      3      4      5      6      7      8      9     10     11     12

Hydrogen    3.127  3.965  1.357 (H2)                Log10 Mean Temperature (over radius)
Helium      1.372  3.961  3.937
Carbon      1.485  3.097  3.957  3.945  3.948  3.972
Nitrogen    1.949  4.004  3.956  3.945  3.951  3.972  3.972
Oxygen      1.586  3.983  3.946  3.956  3.963  3.972  3.972
```

```
Neon        1.370  3.968  3.944  3.956  3.961  3.972  3.972
Magnesium   1.357  2.953  3.963  3.951  3.957  3.972  3.972
Silicon     1.354  2.714  3.963  3.945  3.946  3.950  3.972  3.972
Sulphur     1.463  2.867  3.964  3.943  3.946  3.946  3.944  3.972  3.972
Chlorine    1.348  3.198  3.962  3.944  3.947  3.947  3.972  3.972  3.972
Argon       1.370  3.922  3.960  3.945  3.948  3.948  3.972  3.972  3.972
Iron        1.357  2.822  3.984  3.950  3.953  3.947  3.957  3.972  3.972  3.972

              1      2      3      4      5      6      7      8      9     10     11     12

Hydrogen    3.223  3.967  2.109 (H2)    Log10 Mean Temperature (over radius*electron density)
Helium      3.430  3.963  3.959
Carbon      2.234  3.742  3.958  3.945  3.949  3.972
Nitrogen    2.664  4.006  3.958  3.945  3.952  3.972  3.972
Oxygen      2.826  3.985  3.947  3.956  3.963  3.972  3.972
Neon        2.675  3.971  3.944  3.956  3.961  3.972  3.972
Magnesium   2.041  3.498  3.965  3.951  3.957  3.972  3.972
Silicon     1.496  3.474  3.965  3.945  3.946  3.950  3.972  3.972
Sulphur     1.721  3.369  3.966  3.944  3.946  3.946  3.943  3.972  3.972
Chlorine    2.140  3.842  3.964  3.944  3.947  3.948  3.972  3.972  3.972
Argon       2.631  4.016  3.962  3.945  3.949  3.949  3.972  3.972  3.972
Iron        1.803  3.140  3.986  3.952  3.953  3.947  3.956  3.972  3.972  3.972
```

The next block gives the mean temperature weighted by radius, volume, and these multiplied by the electron density.

```
Cloudy ends: 196 zones,   1 iteration,  1 caution.  ExecTime(s) 86.97
[Stop in maincl, Cloudy exited OK]
```

The code ends by listing the number of zones and iterations that were performed and the number of warnings and cautions that occurred. Next comes the elapsed wall-clock time [s].

5. OBSERVED QUANTITIES

5.1. Overview

This section describes how to convert the quantities actually used or predicted by Cloudy into commonly observed ones.

5.2. Intensities of various continua

5.2.1. Incident continuum

The incident continuum is the continuum striking the cloud. The emission-line printout gives the intensity of the incident continuum with the label **Inci**. The total continuum integrated over all energies [with units erg s^{-1} or erg cm^{-2} s^{-1}] is given with a wavelength of 0. The incident continuum is also evaluated at two wavelengths, 4860 Å and 1215 Å, as λF_λ or νF_ν, [also with units erg s^{-1} or erg cm^{-2} s^{-1}].

The entire incident continuum can be obtained with the output of the **punch continuum** command.

5.2.2. Emitted or diffuse continuum

The continuum at specific wavelengths The diffuse continuum, the continuum emitted by the cloud, is not normally included in the line output. The **print diffuse continuum** command will evaluate the diffuse continuum at a series of energies and add the total emitted continuum to the emission line list. These have units λF_λ or νF_ν, are evaluated at the indicated wavelengths, and have the label **nFnu**. The entry with the label **nTnu** is the sum of the reflected plus attenuated incident continuum. The inward total emission and the reflected incident continua will be printed if this command appears together with the **print line inward** command. Two contributors to the inward emission are predicted. That labeled **InwT** is the total inwardly emitted continuum, and includes both diffuse emission and the back-scattered incident continuum. The component labeled **InwC** is the back-scattered incident continuum alone. See the description of the **print diffuse continuum** command in Part 1 to learn more. The number of points and their wavelengths are set in routine ***zerologic.c***. Search for the variable *EnrPredCont*. The code can easily be modified to add more continuum points.

The continuum integrated over a range of wavelengths The emitted continuum integrated over a series of bands is also in the main set of emission line. The file *bands_continuum.dat* in the data directory specifies a series of wavelength bands. A label and a wavelength that will be printed in the emission-line output are also specified. The code will integrate over the continuum and lines within these bands to find the total radiated luminosity and enter this into the main emission-line stack. The file can be edited to change the number of bands or their detailed properties.

5.3. Line Equivalent Widths

The equivalent width of an emission or absorption line is defined as the number of Angstroms of the continuum that is equivalent to the energy in the line. It is defined as

$$W_\lambda = \int \frac{F_\lambda^c - F_\lambda^l}{F_\lambda^c} \; d\lambda \approx -\lambda \frac{F_{line}}{\lambda F_\lambda^c} \;\; [\text{units of } \lambda] \qquad (416)$$

where the fluxes are in the interpolated continuum (F_λ^c) and the integrated line (F_{line}). By this convention the equivalent width of an emission line is negative.

The code's output can be used to predict a line's equivalent width. The previous section describes several of the continua that predicted. The code prints both the log of the intensity or luminosity of all lines and continua and also the intensity of each relative to a normalization line.

The ratio of a line to continuum intensity or luminosity will be the dimensionless ratio $F_{line}/\lambda F_\lambda^c$, part of the last term in equation 416. The line equivalent width is this ratio multiplied by the wavelength where the continuum is evaluated. For instance, you could trick the code into printing the relative intensities of the lines as an equivalent width relative to the incident continuum at 1215 Å by including the command **`normalize to "Inci" 1215 scale factor = 1215`**. This has two effects – it gives the intensities relative to the incident continuum at 1215 Å and multiplies this by the continuum wavelength in Angstrom, producing the rightmost ratio in equation 416.

A covering factor will complicate this slightly. (Covering factors are defined in the section ***Definitions*** in Part I of this document and in Section 5.9 of AGN3.) If luminosities are predicted then partial coverage of the source is taken into account with the **`covering factor`** command, and the luminosities are correct for this coverage. The ratio of line to continuum given in equation 416 will represent what is observed. If intensities are predicted then the line intensity is given per unit area of cloud, no matter what covering factor is specified. In this second case the ratio in equation 416 must be scaled by the covering factor.

5.4. Emission Line Asymmetries

The inward fraction of the total emission of each line is always predicted by the code, but not normally printed out. Many lines are significantly inwardly beamed, and this can lead to emission line asymmetries if the envelope is expanding. The inward part of the lines will be printed if the **`print line inward`** command is entered. The effects of this line beaming are very geometry dependent.

5.5. Line to Continuum Contrast

The code has several **`punch`** commands that will produce ancillary files containing the predicted line and continuum spectra. There is an ambiguity in how strong the lines should appear to be relative to the continuum in a plot where the lines are not resolved. This is described in Part I of this document where the **`punch continuum`** and **`set PunchLWidth`** commands are introduced.

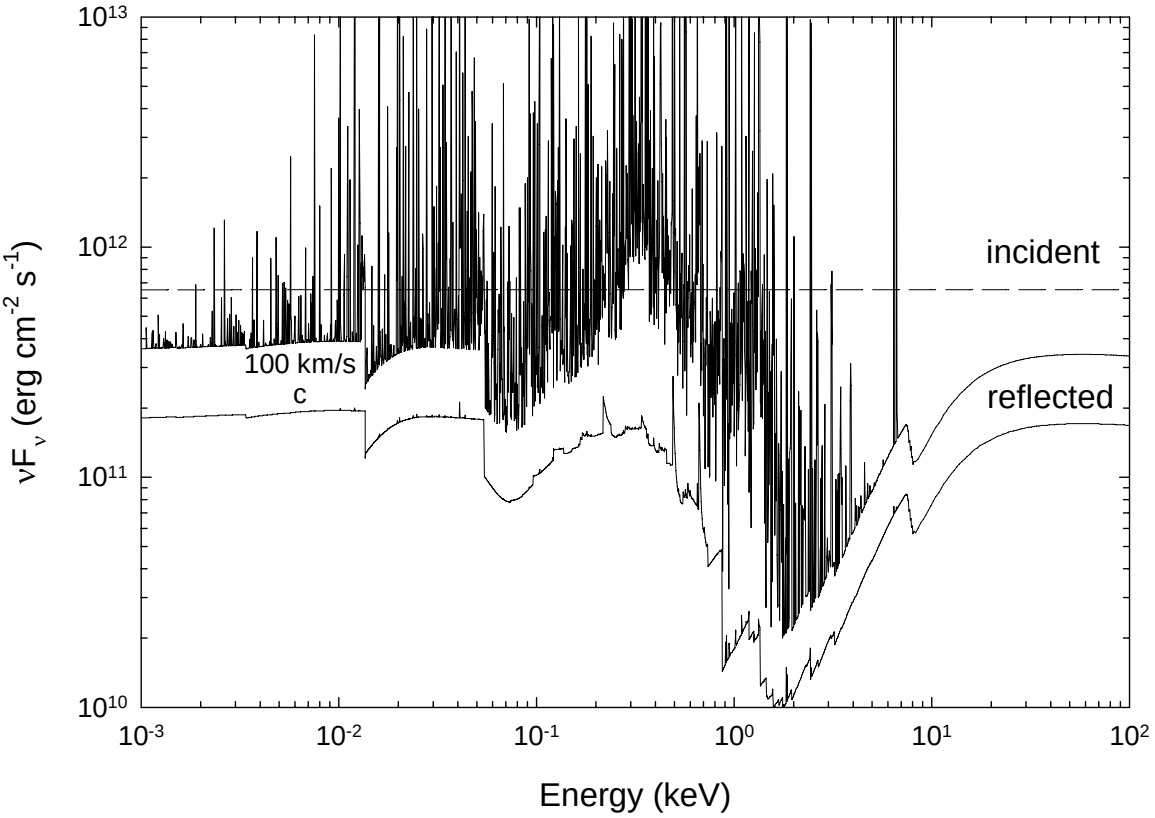

Figure 9 This shows the continua predicted by the input file reflector.in. The lowest curve has been divided by two and shows the total spectrum produced by setting the line width to the speed of light The middle curve shows the 100 km s^{-1} case. The upper curve shows the incident continuum. reflector

Figure 9 shows the continuum predicted with the **`agn_reflector.in`** test case. The dashed upper curve is the incident continua and the two lower curves give the reflected continua for cases where the linewidth is 100 km s^{-1} and the speed of light[6]. With a linewidth of *c* lines are added to the continuum such that the difference between νF_ν at the line peak and νF_ν for the underlying diffuse continuum is equal to the line flux. As a result the resulting line to continuum contrast is very small. The middle curve shows the same model but with the line contrast enhanced by entering the command **`set PunchLWidth 100 km/s`**. The entire spectrum of the c linewidth case is shifted by a factor of two to make the two continua appear separated. The default line width is 1000 km s^{-1}.

The only effect of the **`set PunchLWidth`** command is to change the contrast in the punch output. The computed results and line intensities in other output are not affected. If the width is set to the speed of light then the intensities in the punch output will be correct but the line to continuum contrast too small. If the width is set to a small value the contrast is increased but the total intensity in the punch output will be greater than the actual emission. (Energy *will not* appear to have been conserved in this punch output).

[6] The speed of light was the default for version 90.00 through version 90.03. In C90.04 the default was changed to 1000 km/s. Before version 90 the line to continuum contrast depended on the cell width at the particular energy.

5.6. Surface Brightness

Cloudy will normally predict a line's intensity as $4\pi J$, the intensity radiated into 4π sr by a unit area of cloud, with units erg s^{-1} cm^{-2}. Observations of resolved sources often measure the surface brightness, with units erg s^{-1} cm^{-2} $arcsec^{-2}$. Be careful! Some workers may report surface brightness with units erg s^{-1} cm^{-2} $arcsec^{-2}$ sr^{-1}. Remove the sr^{-1} before continuing by multiplying by 4π.

To obtain the predicted surface brightness we must divide the intensity $4\pi J$ by the number of square seconds of arc in 4π sr. One radian is $360/2\pi = 57.29578$ deg, so 1 sr is $(180/\pi)^2 = 3282.806$ deg^2. There are $(60\times 60)^2$ square seconds in a square degree, so there are 5.3464×10^{11} square arc seconds in 4π sr. The surface brightness (per square second of arc) is the intensity $4\pi J$ multiplied by the inverse of this, or 1.8704×10^{-12} $arcsec^{-2}$.

Note that this is only correct for a line that is emitted isotropically, because the code predicts $4\pi J$ while an observer measures I along a particular direction. (The code does predict the fraction of a line that is emitted from the illuminated face of the cloud.) This discussion is only formally correct if $I = J$.

There is a **`print line surface brightness`** command, described in Part I of this document, which will change the intensity into surface brightness units. By default the final units will then be erg s^{-1} cm^{-2} sr^{-1}, but the command has an arcsec keyword to specify the surface brightness in erg s^{-1} cm^{-2} $arcsec^{-2}$.

5.7. Flux to luminosity

The luminosity is the flux of a line multiplied by the total area of the shell. For full coverage this is $4\pi r^2$ where r is the radius of the shell. If the shell only partially covers the continuum source then this should be multiplied by the covering factor.

5.8. Flux at the Earth

If the distance to the object is specified with the **`distance`** command, and the simulation specifies enough information for the source luminosity to be predicted, then the flux observed at the Earth will be predicted if the **`print flux at Earth`** command also appears.

5.9. Relative hydrogen line intensities

Hydrogen line intensities can be predicted with great precision when Case B applies. Ferguson and Ferland (1997) describe Cloudy's hydrogen atom. It gives good results for levels below 10 in the code's default state, which uses a 26 level atom. The number of levels can be increased by using the **`atom H-like levels`** command, and this gives better results at the expense of more compute time. The larger atom should give results accurate to better than 5% for lines arising from below principal quantum number 10, and 10% accuracy for lines with upper levels between 10 and 15.

All levels except for 2*s* and 2*p* are assumed to be well *l*-mixed. So no attempt to resolve the n levels into l levels is made for $n > 2$. This approximation should be

nearly exact at medium to high densities ($n_H > 10^6$ cm^{-3}) but is approximate (but certainly better than 10%) at low densities, as Ferguson and Ferland (1997) describe.

The accuracy of Cloudy's H I line emissivities is limited by the size of the model hydrogen atom that can be computed on the fly. The definitive calculation for hydrogen recombination is that of Hummer and Storey (1987) and Storey and Hummer (1995), who used a 1000 level atom with all *l*-states explicitly considered (that works out to something like a million levels!). The code prints their Case A and Case B predictions within the main emission line list. These predictions are more accurate than Cloudy's in cases where the Case A or Case B approximation is valid.

The Hummer and Storey (1987) calculation is for case B conditions, which assume that many processes are unimportant (see Ferguson and Ferland 1997). Neglected processes include collisional excitation from the ground or first excited states, induced processes where the incident continuum causes the atom to fluoresce, and line transfer in all non-Lyman lines. This is an excellent assumption for conventional nebulae, such as planetary nebular or H II regions. They are questionable for gas denser than 10^6 cm^{-3} or when x-rays are present. When any of these processes are important the hydrogen spectrum is far more model dependent and Cloudy's results are more realistic than the case B results.

5.10. Helium line intensities

The code includes a model of the He^0 atom that is applied all along the helium iso-electronic sequence, and which can be made to have an arbitrarily large number of levels (Bauman et al. 2005; Porter et al. 2005). The predictions become more exact as the number of levels is increased. This model does not collapse *L* and *S* levels into single *n* levels, so its predictions should be exact if the atom is made large enough.

5.11. Line Intensities in a dusty open geometry

Two sets of line intensities are printed when a dusty open geometry is computed. The second block of lines (with the title *Intrinsic Intensities*) is the conventional set of intrinsic emission-line intensities. When grains are present these intensities would need to be corrected for line-of-sight reddening to be compared with observations.

The first block of emission-line intensities (with the title *Emergent Intensities*) would be that emitted from the illuminated face of a molecular cloud. The geometry is appropriate for the Orion Nebula, a blister H II region on the surface of Orion Molecular Cloud 1 (OMC1). An idealized geometry is shown in Figure 10. The code computes the fraction of the line emission that is directed towards the illuminated face. The remainder is emitted towards the neutral gas, which is assumed to have an infinite optical depth due to grains. The albedo of the gas-grain mixture is computed and the fraction reflected is passed back towards the illuminated face. The total intensities are roughly half what would be expected were the cloud emitting from both sides. Something like 10% of the light striking the molecular cloud will be reflected back to the observer, and so slightly more than 50% of isotropically emitted lines will emerge from the illuminated face. The code uses the albedo of the gas at the wavelength of the line to predict this reflected portion.

So, for the illustrated blister the first block of lines gives what would be seen by an observer a large distance off to the left.

5.12. Continuum pumping contribution to line intensities

Continuum pumping or fluorescence is included for all lines. The contribution is only explicitly printed if the **`print line pump`** command is entered. Whether or not this contribution actually adds to the observed line emission depends on the geometry. Continuum pumping increases the line emission if no related continuum absorption occurs. This will be the case if the continuum source is either not observed or not covered by absorbing gas. If absorbing gas covers an observed continuum source then the situation is like the P Cygni problem, and pumping may not increase the net intensity of the line at all (the absorption component will have the same equivalent width as the associated emission). The printed line intensity includes this contribution unless the **`no induced processes`** command is entered. (The **`no induced processes`** command has many other effects and so should not be used except as a test.)

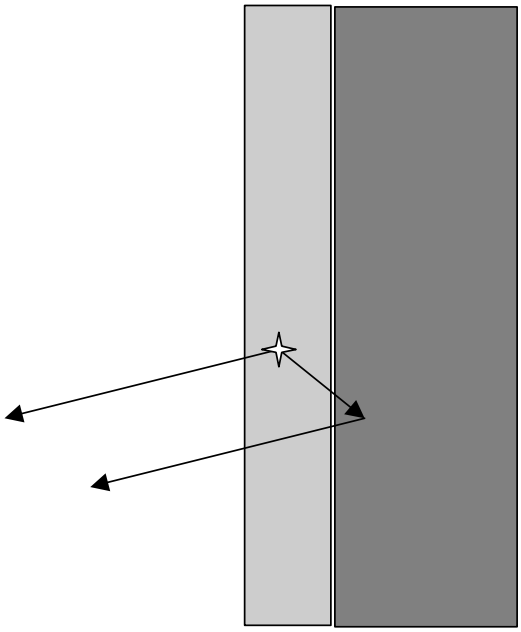

Figure 10 The geometry assumed when in an open dusty geometry. The lightly shaded area is the H^+ region, and is a layer on the surface of an infinitely optically thick molecular cloud, the dark area on the right. Light can be emitted from the illuminated face of the cloud. A fraction of the light emitted towards the molecular cloud is reflected back towards the illuminated face.

The output produced by the **`punch continuum`** commands does not include the pumped part of the line contribution. This is correct if the continuum source is included in the beam, but is not if only the gas is observed.

5.13. Column densities

The column densities of all constituents are saved and printed at the end of the calculation. Column densities within many excited states are also printed. In the column density printout the excited states are identified with a '*', while the table that accompanies the description of the ***cdColm*** command, see Table 1 on page 422 above, identifies the various labels.

5.14. A synthetic spectrum

A table of emission-line intensities is part of the normal output. Sometimes a synthetic spectrum, rather than a table, is desired. Very coarse spectra can be generated with the **`punch continuum`** or **`punch spectrum`** commands, but a detailed synthetic spectrum is not the main purpose of this output.

The best course is to save the emission-line spectrum at the end of the calculation, and then post-process this data using your own software. Then blends of lines can be synthesized at any spectral resolution desired. The spectrum can be save two ways. The main block of emission-line intensities in the final printout can be printed

as a single column, which can be sorted by intensity or intensity (see the **print lines** command in Section 1 of this document). The **punch spectrum** command includes a set of all lines with non-zero intensities. Write a small program or script to read these tables and create a final synthesized spectrum.

5.15. Line profiles

The observed line profile can be predicted by integrating the emissivity of the line over the computed structure, taking the local velocity structure into account. The emissivity is obtained with the **punch lines emissivity** command, described in Part 1 of this document. This gives the net emission, with units erg cm^{-3} s^{-1}, emitted by a unit volume of gas and emergent from the cloud surface. The total emission is the integrated sum of this emission. An integral over radius will give the line surface brightness while an integral over volume will give the luminosity.

The observed profile will depend on the velocity field at each point in the integration. For static models this will be the Voigt function at the local temperature and microturbulence. For a dynamical model it will include bulk motion of the gas.

5.16. Hydrogen recombination lines

The following table gives the strongest H I $\delta n = 1$ lines of the lowest series. All lines have the label "H 1". The wavelength column gives the string as it appears in the printout. "m" indicated a wavelength in μm and A in Angstroms. The Case B intensity is taken from the test case *h_caseb_lon*.

Table 2
Hydrogen emission lines

Series	$n' \rightarrow n$	Wavelength	I(Case B)
Lyman	2 - 1	1216A	23.3
Balmer	3 – 2	6563A	1.00
Paschen	4 – 3	1.875m	0.343
Brackett	5 – 4	4.051m	0.0813
Pfund	6 – 5	7.458m	0.0258
Humphreys	7 – 6	12.37m	0.0098
	8 – 7	19.06m	0.0042
	9 - 8	27.80m	0.0020

5.17. Molecular hydrogen lines

The following table gives some of the stronger or more frequently observed H_2 lines. These are only predicted when the model H_2 molecule is included with the **atom H2** command. The wavelength column gives the string as it appears in the printout. "m" indicated a wavelength in μm. All lines have the label "H2 ".

Table 3
Molecular hydrogen emission lines

Line	$(v,J)_{upper}$	$(v,J)_{lower}$	Wavelength
0-0 S(1)	0,3	0,1	17.03m
0-0 S(2)	0,4	0,2	12.28m
1-0 S(4)	1,6	0,4	1.891m
1-0 S(3)	1,5	0,3	1.957m
1-0 S(2)	1,4	0,2	2.033m
1-0 S(1)	1,3	0,1	2.121m
1-0 S(0)	1,2	0.0	2.223m
1-0 Q(2)	1,2	0,2	2.413m
1-0 Q(1)	1,1	0,0	2.406m

6. THE EMISSION LINES

6.1. Overview

The following sections outline the emission lines predicted by Cloudy. Before version 90 of the code all lines were listed in the sub-section immediately following this section. The code is being modified to bring all lines into a common line class, as the code moves to C++ and objects. This chapter will remain incomplete until this work is finished.

6.2. The main emission line printout

The main emission line printout was briefly described on page 445 above. This section goes into more detail.

Output organization. The printed list is sorted into four large groups of columns, with each large column sub-divided into four smaller sub-columns. The first sub-column is either the spectroscopic designation of the ion producing the line or an indication of how the line is formed. The second sub-column is the line wavelength, with a 0 to indicate a continuum. The third sub-column is the log of the power in the line, in the units given in the header (erg s^{-1} into either 4π sr or cm^{-2}). The last sub-column is the intensity of the line relative to the reference line, usually Hβ, unless this is reset with the **`normalize`** command.

These lines can be printed as a single large column, and can be sorted by wavelength or intensity. These options are controlled by the **`print line`** command described in Part I of this document.

Line intensities when grains are present. The computed emission-line spectrum follows. Emission lines are divided into two large groups. The first includes the effects of grain scattering and absorption, and is indicated by the header "Emergent Line Intensities". This first group is only printed if grains are present and the geometry is open (i.e., **`sphere`** not set). The intensities are the *total* intensities observed from the illuminated face, including both absorption and scattering by grains. This is discussed on page 459 above.

The second, larger, group of lines, called "Intrinsic line intensities", is always printed. This usually gives the intrinsic intensity of the lines, and does not include the reddening effects of internal grains due to the photon's passage out of the nebula (unlike the first group). This second group usually gives the total intrinsic intensity of the lines. Although reddening effects of internal (or external) dust are not taken into account, photon destruction by background opacity sources during the transfer process is. This distinction is only important for forbidden lines, which have no local destruction since they are optically thin, but can be absorbed along their way out. This predicted spectrum should be compared with the reddening-corrected observed spectrum.

Line wavelengths. These are given in various units. Numbers ending in "A" are wavelengths in Angstroms. For instance, Hβ is given by "H 1 4861A".

Wavelengths in microns are indicated by "m", an example, the strong [O III] IR line, is "O 3 51.80m".

The code follows the contention that wavelengths longward of 2000Å are given in air and shorter wavelengths in vacuum. Continua are usually indicated by a wavelength of zero.

6.2.1. Blocks of lines....

Lines are organized by common origin with a comment, ending in a series of periods ".....", beginning the section. As an example, the first commented block of lines begins with "general properties.....". The following subsections give overviews of the lines.

6.2.2. General properties....

This mainly summarizes heating and cooling agents for the model.

TOTL 4861 and ***TOTL*** 1216, are the total intensities of Hβ and Lα, as predicted by the multi-level H atom. These intensities are the results of calculations that include all collisional, radiative, and optical depth effects.

Inci - The total energy in the incident continuum.

TotH and ***TotC*** give the total heating and cooling. These will be nearly equal in equilibrium.

BFH1 and ***BFHx*** are the heating due to photoionization of ground state and excited state hydrogen respectively.

He1i, 3He1, heating due to ground state He and the triplets.

BFHe and ***TotM*** are the heating due to helium and metal photoionization.

Pair – heating due to pair production.

ComH , ***ComC***, – Compton heating, cooling.

CT H ***CT C*** – charge transfer heating and cooling.

extH ***extC*** "extra" heating or cooling added to model.

e-e+ 511 The positron line.

Expn, expansion, or adiabatic, cooling

H FB, H radiative recombination cooling

HFBc, ***HFBc***, hydrogen net free-bound cooling and heating

Iind, cooling due to induced recombination of hydrogen

3He2, cooling due to induced recombination of fully ionized helium

Cycn, cyclotron cooling

6.2.3. Continua....

These give intensities of various continua. These are either the total integrated continuum or the product νF_ν at certain energies.

The file *bands_continuum.dat* in the data directory can be used to specify a series of wavelength bands. A label and a wavelength that are printed in the emission-line output is also specified. The code will integrate over these bands to find the total radiated luminosity and enter this into the main emission-line stack. The file can be edited to change the number of bands or their detailed properties. The following table lists the bands in the file at the time of this writing. Please consult the file to see its current contents and feel free to add your own bands. The first and second columns give the label and wavelength as they appear in the printout. The last column gives the wavelength range for the integration.

Table 4
Default continuum bands

Label	Wavelength	Wavelength Range
Bcon	3650A	911.6 Å – 3636.4 Å
Pcon	5000A	3646.4 Å – 8204.4 Å
NIRa	2.85m	0.7 μm – 5.0 μm
NIRb	3.0m	1.0 μm – 5.0 μm
MIRa	15.0m	5.0 μm – 25.0 μm
NMIR	21.75m	0.7 μm – 42.5 μm
MIRb	22.5m	5.0 μm – 40.0 μm
FIR	83μm	42.5 μm – 122.5 μm
TIR	550m	3.0 μm – 1100.0 μm
TFIR	611.25m	122.5 μm – 1100.0 μm

Bac 3646 residual flux at head of Balmer continuum, νF_ν

cout 3646 cref 3646, outward, reflected continuum at peak of Balmer Jump

thin 3646, residual flux at head of Balmer continuum, optically thin limit

Inci 4860, ***Inci 1215***, incident continua near Hβ and Lα

Ba C 0, integrated Balmer continuum

PA C 0, integrated Paschen continuum

HeFF 0, He brems emission

HeFB 0, He recombination cooling

MeFB 0, heavy element recombination cooling

MeFF 0, metal brems emission

ToFF 0, total brems emission

FF x, part of H brems, in x-ray beyond 0.5KeV

eeff, electron - electron brems

nFnu 122m, ***nInu 122m***, ***InwT 122m***, ***InwC 122m***, a large list of continua at selected wavelengths will be printed if the **`print diffuse continuum`** command is entered. The first is the total continuum at the wavelength, given as νF_ν. ***nInu*** is the transmitted and reflected incident continuum. ***InwT*** is the total reflected continuum. ***InwC*** is the reflected incident continuum.

6.2.4. Molecules….

H2dC, is the cooling due to collisional dissociation of H_2.

H2dH, heating by H_2 dissociation by Lyman continuum

H2vH, heating by coll deexcit of vib-excited H_2

H2vC, cooling by coll deexcit of vib-excited H_2

H2 v, line emission by vib-excited H_2

H-FB and ***H-FF*** are the free-bound and free-free continua of the H^- ion.

H-CT 6563, H-alpha produce by H- mutual neutralization

H- H 0, H- heating

H-Hc 0, H- heating

H2+ and ***HEH+*** are the cooling due to formation of H_2^+ and HeH^+.

Codh, carbon monoxide photodissociation heating

CO C 12, C12O16 cooling

CO C 13, C13O16 cooling

12CO 2588m, ***Inwd 2588m***, ***Coll 2588m***, ***Pump 2588m***, ***Heat 2588m***, et al. Next follows intensities and contributors to the ^{12}CO and ^{13}CO lines included in the calculation.

6.2.5. Grains….

Information in this block concerns emission, absorption, heating, and cooling by any grains included in the calculation.

GrGH, gas heating by grain photoionization

GrTH, gas heating by thermionic emissions of grains

GrGC, gas cooling by collisions with grains

GraT, This is the total grain heating by all sources, lines, collisions, incident continuum. If the grain emission is optically thin limit then this is equal to the total intensity in grain emission.

GraI, grain heating by incident continuum

GraL 1216, grain heating due to destruction of Lα

GraC, grain heating due to collisions with gas

GraD, grain heating due to diffuse fields, may also have grain emission

Grain emission is included in the predicted total emitted continuum. The continuum is not printed by default (it makes the printout longer) but can be included in the emission line array with the **`print continuum`** command, described in Part I of this document. A machine readable form of the continuum can be produced with the punch continuum command, also described in Part I of this document.

6.2.6. H-like iso-seq....

This block includes all hydrogen-like isoelectronic species.

HFFc 0, net free-free cooling, nearly cancels with cooling in lte

HFFh 0, net free-free heating, nearly cancels with cooling in lte

H FF 0, H brems (free-free) cooling

FF H 0, total free-free heating

Clin 912, total collisional cooling due to all hydrogen lines

Hlin 912, total collisional heating due to all hydrogen lines

Cool 1216, collisionally excited La cooling

Heat 1216, collisionally de-excited La heating

Crst 960, cooling due to n>2 Lyman lines

Hrst 960, heating due to n>2 Lyman lines

Crst 4861, cooling due to n>3 Balmer lines

Hrst 4861, heating due to n>3 Balmer lines

Crst 0, cooling due to higher Paschen lines

Hrst 0, heating due to higher Paschen lines

LA X 1216, Lα contribution from suprathermal secondaries from ground

Ind2 1216, Lα produced by induced two photon

Pump 4861, Hβ produced by continuum pumping in optically thin ld limit

CION 0, net col ionz-3 body heat collision ionization cooling of hydrogen

3bHt 0, heating due to 3-body recombination

Strk 1216, Stark broadening component of line

Dest 1216, part of line destroyed by background opacities

Fe 2 1216, part of Lα absorbed by Fe II

Q(H) 4861 is the intensity of Hβ predicted from the total number of ionizing photons, $Q(H^0)$, assuming that each hydrogen-ionizing photon produces one hydrogen atom recombination.

Q(H) 1216 indicates the Lα intensity produced if each hydrogen ionizing photon results in one Lα photon in the high density limit (i.e., no two-photon emission).

CaBo 4861 These are the "old" case B predictions, as printed in versions 90 and before of the code.

Ca B 6563A The entries starting with Ca B are the Case B intensities computed from the actual model ionization and temperature structure, but assuming that Hβ emits with its case B emissivity.

Next the predicted intensities of all lines of the hydrogenic iso-electronic sequence are given. The lines have labels that identify the species and stage of ionization, such as H 1, He 2, Li 3, C 6, etc. The entries with a wavelength of zero are the total intensities of the 2*s*-1*s* two-photon emission.

6.2.7. He iso-sequence....

Atoms and ions of the helium-like iso-electronic sequence are treated as multi-level atoms. All species and stages of ionization are specified by labels like He 1, Li 2, C 5, etc. A wavelength of zero indicates the two-photon continuum.

6.2.8. level 1 lines....

In the current version of the code, the lines printed under this title include both the lines that have been moved to the common *EmLine* class, but also older lines that are still scalar quantities. This part of the code is still in a state of flux, and this is reflected in the current documentation. The remaining part of this subsection outlines the methods used for most of the heavy element atoms. The method for producing a list of transferred lines, those that have been moved to the *EmLine* class, is described in the section beginning on page 469 below. The old-style scalar lines are described in the section beginning on page 471 below, although this is not totally up to date.

These lines have accurate collision strengths and wavelengths. Many are two-level atoms, but some are the result of multi-level atoms. The following is a summary of the general approach.

Li-sequence. Examples include C IV λ1549, O VI λ1034, and Mg II λ2798. A three-level atom, with full treatment of optical depths and collisional excitation, is used. The "TOTL" intensity is the sum of both lines in the doublet, and is followed by the individual intensities of each member.

Be-sequence. Examples include C III] λ1909, O V] λ1215, and Si III] 1895. A four-level atom, solving for populations of the individual ^3P_j states, is used. The first printed intensity is the total intensity of the multiplet (both j=0,1 decays), and this is followed by the intensities of individual lines. The intensity of the permitted ^1P_o - ^1S transition is also calculated. Optical depth and collisional effects on both the permitted and intercombination lines are included.

B-sequence. Examples include C II and O IV. The ground term is treated as a two level atom, with optical depth and collisional effects included, when the gas is too cool to excite the UV lines. The ^4P -^2P_o lines are also predicted with a full multi-level

atom that resolves fine structure. The TOTL intensity printed is the total intensity of the multiplet and is followed by individual lines. Pumping by all level two lines of the same ion is included as an excitation process.

^{3}P- ground term. Examples include such spectra as [O III] and [O I]. The infrared fine structure lines are computed with full treatment of collisional and optical depth effects. A comment is printed at the end of the model if these lines mase or become optically thick. The populations of ^1D and ^1S are computed with a three-level atom. The intensity of the ^1D - ^3P transition is only that of the individual line (i.e. 5007), not the doublet.

^{4}S^0 - ground term. Examples include [O II] and [S II]. They are treated as a five-level atom. Intensities of all individual lines, as well as co-added multiplets, are given.

6.2.9. Recombination .. .

These are a set of heavy-element recombination lines that are predicted assuming that they are optically thin. This consists of all recombination lines of C, N., and O, with coefficients taken from Nussbaumer and Storey (1984) and Péquignot, Petitjean, and Boisson (1991).

These are all predictions for optically thin pure recombination. These should be accurate for classical nebulae, such as planetary nebulae and H II regions. They will not be accurate for dense environments where optical depths and collisional effects come into play. There are several instances where more than one line of an ion will have the same wavelength due to the integer Angstrom format used for wavelengths. The worst case is O V 4953, where three lines of the same multiplet have the same wavelength.

6.2.10. Level 2 lines . ..

These are resonance lines that use Opacity Project wavelengths, which are generally accurate to about 10%. These lines have g-bar collision strengths, which are not very accurate at all.

6.3. The transferred lines

The group of "transferred lines" includes all those that have been moved to the *EmLine* class, in anticipation of the code's move to C++ and objects.

In versions of HAZY for Cloudy versions 90 and before, this section included descriptions of all predicted lines, and was automatically generated by the code. Today there is no limit to the number of lines the code is capable of predicting, since the iso-electronic sequences can now have a nearly arbitrarily large number of levels. Rather than waste paper by including the iso-electronic sequences here, instructions are given for creating your own automatic list of lines.

6.3.1. Punch line data output

To generate a line list, set up a calculation with the atoms set to whatever size is desired (see the **`atom`** command in Part I). Then execute this script with the **`punch`**

`line data` command included (described in Part I). The punch output will include the line list. This will include the level 1 ,level 2, CO, and recombination lines, but not the scalar forbidden lines. These are described in a list following this subsection.

In previous versions of this document a large list of emission lines appeared here. This list is now far too large to include here. Rather, the list can be generated by executing the code with the command **`punch line data "filename.txt"`** included. This will create a file that includes the full set of lines that are predicted. Note that the lines that are output are only those that exist when the code is run. It is possible to make many of the model atoms and molecules as large or small as you like, and the actual lines that exist when the **`punch`** command is entered will be output.

This contains several groups of lines. All quantities were evaluated at 10^4 K. The description of the command in Part I of this document explains how to evaluate the quantities at other temperatures.

The ion is the first column of the table. This is in a uniform format, beginning with the two character element symbol and followed by an integer indicating the level of ionization. "C 2" is C^+ or C II. This is followed by the integer wavelength label used to identify the line in the printout. The third column, with the label "WL", is the correct wavelength of the line, with units of microns ("m"), Angstroms ("A"), or cm ("c"). The remaining columns give the statistical weights of the lower and upper levels, the product of the statistical weight and the oscillator strength, and then the transition probability.

The last column is the electron collision strength. Exceptions are lines whose collision strengths are only evaluated for temperatures far from 10^4 K, for instance, a Fe XXV transition. Usually these collision strengths are for only the indicated transition, although in some cases (the Be sequence) the value is for the entire multiplet.

6.3.2. Output produced for the transferred lines

Because the lines have a common format within their storage vectors, the output has a common format too. Generally only the total intensity of the transition, the result of the solution of a multi-level atom with all processes included, is printed. The approach used to compute the level populations is described in Part II of Hazy, and includes continuum pumping, destruction by background opacities, and trapping.

The total intensity of the transition is printed in a form like "C 2 1335", with the spectroscopic identification given by the first part, as found in the first column of the table, and the wavelength as indicated by the number in the second column of the table.

In a few cases (for instance, the C 4 λλ1548, 1551 doublet), a total intensity is also derived. In these cases the label "Totl" will appear together with an average

wavelength (1549 in this case). These lines are all explicitly shown in a following section.

It is possible to break out various contributors to the lines with options on the **`print line`** command, described in Part I of this document and in the following. These contributors are printed following the total intensity.

`print line heating` An emission line will heat rather than cool the gas if it is radiatively excited but collisionally de-excited. The print out will include this agent, with the label "Heat", when this command is given.

`print line collisions` The collisional contribution to the lines will be printed, with the label "Coll".

`print line pump` The contribution to the total line, produced by continuum pumping, is printed with the label "Pump". What is observed? Whether or not this is a net emission process contributing to the observed line intensity depends on the geometry, mainly whether or not continuum source is in the beam. At some velocities within the line profile this can be a net emission process, due to absorption at other velocities. If the continuum source is in the beam and gas covers it, this is not a *net* emission process, since photons are conserved.

`print line inward` The inwardly directed part of the total emission is printed with the label "Inwd". This can be greater than half of the line intensity if the line is optically thick since these lines tend to be radiated from the hotter illuminated face of the cloud.

`print line optical depths` At the end of the calculation the optical depths for all optically thick lines will be printed. This is not done by default since it can be quite long.

6.4. Forbidden Lines

These are a series of entries that contain most of the optical forbidden lines, some continua, and identify various contributors to the main lines. These are older lines that have not yet been moved to the *EmLine* class. This description is not totally up to date since this is a part of the code that is slowly being removed as lines go to the new style.

For this set of lines, the first column gives the four character label printed in the final array listing and the second column gives the wavelength of the line, using the conventions described above. The label in the first column is the one used to access the line using the ***cdLine*** routine described elsewhere.

The third character indicates whether the entry in the column is a heat source (indicated by h), a coolant (c), a recombination line (r), or an intensity entered for information only (i). The last column gives a brief description of the meaning of the line prediction.

Label	λ		Description
Mion	0	c	cooling due to collisional ionization of heavy elements
Li3r	19	i	these lines added to outlin in metdif - following must be false
Be4r	19	i	these lines added to outlin in metdif - following must be false

```
Bo5r  19 i  these lines added to outlin in metdif - following must be false
REC  1656 i  C 1 1656 recomb; n.b. coll deexcitation not in

C Ic 9850 c  C 1 9850, coll excit
C Ir 9850 i  was a big mistake
TOTL 9850 i  total intensity, all processes, C I 9850
C  1 8727 c  C 1 8727; equivalent to 4363
C  1 4621 c  1S - 3P

Phot 2326 i  photoproduction, Helfand and Trefftz
REC  1335 i  C 2 1335 recombination,
C II 3134 c  C 2 intercombination line with same upper state as 1335
C3 R  977 i  dielectronic recombination contribution to C 3 977
P386  977 r  C 3 977 pumped by continuum near 386A

TOTL 1909 i  C 3  1909 collision, both lines together
C  3 1907 i  C 3 1908 j-2 to ground
C3 R 1909 i  C 3 1909 recombination from Storey
Phot 1909 i  C 3 1909 following relax following inner shell photoionization
Rec  1175 i  dielectronic recombination contribution to C 3 1175

TOTL 1549 i  total intensity of C 4 1549, all processes
Inwd 1549 i  inward part of C 4
DEST 1549 i  part of line destroyed by photoionization of Balmer continuum
C4 r 1549 i  recombination C 4 1549 from CV
C 6r  34 i  these lines added to outlin in metdif - following must be false

N  1 5200 i  N 1 5200, both 5198, 5200, collisions and recombination
Coll 5200 c  N 1 5200, both 5198, 5200, collisions and recombination
REC  5200 i  recombination contributon to [NI] 5200
N  1 3466 c  [N 1] 3466, 3 - 1 transition, whole multiplet
N  1 10400 c  [N 1] 10400 3 - 2 transition, whole multiplet

N  2 6584 c  N 2 6584 alone
N  2 6548 c  N 2 6548 alone
REC  6584 i  N 2 6584 alone, recombination contribution
N  2 5755 i  N 2 5755 total, collisions plus charge transfer
Coll 5755 c  N 2 5755 collisional contribution

C T  5755 c  N 2 5755 charge transfer contribution
Rec  1085 i  dielectronic recombination contribution to N 2 1085
N2cn   1 i  continuum pumped N 2 6584
N2cn 5755 i  continuum pumped N 2 5755
N3cn 4640 i  continuum pumped "Bowen" N 3, optically thin excited line

N3cn 4634 i  continuum pumped "Bowen" N 3, optically thin excited line
N3cn 4642 i  continuum pumped "Bowen" N 3, optically thin excited line
extr  990 i  total N 3 990, both electron excitation and continuum pumping
rec  990 i  part of N 3 990 due to recombination
N 3p  990 r  N 3 989.8, continuum pumped

TOTL 1486 i  N 4] 1486, total intensity of both lines
N  4 1485 i  the N 4] slow transition by itself
rec  765 i  N 4 765 recombination,
TOTL 1240 i  N 5 1240, total emission, collisions plus pumping
Inwd 1240 i  inward part of N 5

N 7r  25 i  these lines added to outlin in metdif - following must be false
Fl7r  19 i  these lines added to outlin in metdif - following must be false
O  1 6300 c  total Oxygen I 6300, including line optical depth
O  1 6363 c  total Oxygen I 6363, including line optical depth
O  1 5577 c  auroral OI

TOIc   0 c  total collisional cooling due to 6-level OI atom
TOIh   0 h  total collisional heating due to 6-level OI atom
6lev 8446 i  be moved to call PutLine
6lev 1304 i  OI 1304 from six level atom
6lev 1039 i  OI 1039 from six level atom

6lev 4368 i  OI 4368 from six level atom
6lev  13 i  OI 1.3 micron from six level atom
6lev  11 i  OI 1.1 micron from six level atom
6lev  29 i  OI 2.9 micron from six level atom
6lev  46 i  OI 4.6 micron from six level atom

TOTL 3727 c  O II 3727, all lines of multiplet together
```

```
TOTL 7325 c  O II 7325, all lines of multiplet together
IONZ 3727 i  line produced by photoionization of Oo; already in TOTL
IONZ 7325 i  line produced by photoionization of Oo; already in TOTL
O II 3729 i  five level atom calculations; D5/2 - S3/2

O II 3726 i  D3/2 - S3/2 transition
O II 2471 c  both 2P 1/2 and 3/2 to ground
O II 7323 i  P1/2-D5/2 and P3/2-D5/2 together
O II 7332 i  P1/2-D3/2 and P3/2-D3/2 together
TOTL 1665 i  total intensity of OIII] 1665, all processes

Phot 1665 i  contribution to OIII 1665 due to inner shell (2s^2) ionization
Augr 1665 i  contribution to OIII 1665 due to K-shell ionization
O 3 5007 c  fac = c5007/(1.+1./2.887)
O 3 4959 c  O III 4959 alone, collisions, tot OIII is this times 4
LOST 5007 i  O III 5007 lost through excit photo

TOTL 4363 i  O III 4363, sum of rec, coll, ct excitation
Coll 4363 c  O III 4363,collisions from five level atom
Rec  4363 i  O III 4363 recombination, coef from Burgess and Seaton
O 3 2321 c  collisional excitation of 2321, 5-level atom
C EX 4363 i  charge exchange, Dalgarno+Sternberg ApJ Let 257, L87.

C EX 5592 i  charge exchange rate, D+S
rec  835 i  O III 834A, dielectronic recombination only
InSh 1401 i  inner shell photoionization, relaxation
rec  789 i  O IV 789A, dielectronic recombination only
rec  630 i  O V 630A, dielectronic recombination only

TOTL 1218 i  O V 1218], total intensity of both lines
O 5 1211 i  the slow transition by itself
O 5 5112 i  BS O V 5112, recombination
TOTL 1035 i  O VI 1035, total of pumping and collisional excitation
Inwd 1035 i  inward part of OVI line

O 8r  19 i  recombination from fully stripped ion
Ne 3 3869 c  Ne III 3869, of 3968+3869 doublet
Ne 3 3968 c  Ne III 3968, of 3968+3869 doublet
Ne 3 3343 c  NeIII auroral line
Ne 3 1815 c  NeIII auroral line

Ne 4 2424 c  Ne IV 2424, collisional excitation
Ne 4 4720 c  Ne IV N=3 lines, three level atom approx
Ne 4 1602 c  Ne IV N=3 lines, three level atom approx
Ne 5 3426 c  Ne V 3426 of 3426, 3346 doublet
Ne 5 3346 c  Ne V 3346 of 3426, 3346 doublet

Ne 5 2976 c  auroral line
Ne 5 1575 c  collisionally excited
Ne 5 1141 c  both components of 5S-3P 1146.1, 1137.0 doublet
TOTL  895 i  Ne VII 895, collisionally excited, both lines
Ne 7  890 i  Ne VII 890, single line

TOTL  774 i  Ne VIII 774, collisionally excited
Inwd  774 i  inward part of NeVIII 774 line
NeLr  12 i  these lines added to outlin in metdif - following must be false
Na 5 1365 c  [NaV] 1365, sum of 1365.1+1365.8; cs only guess
Na 5 2067 c  [NaV] 2067, sum of 2066.9+2068.4; cs only guess

Na 5 4017 c  [NaV] 4017, sum of 4010.9+4016.7+4022.7; cs only guess
Na 6 2569 c  [Na VI] 2568.9
Na 6 1357 c  [Na VI] 1356.6
Na 6 2972 c  [Na VI] 2971.9
Na 6 2872 c  [Na VI] 2872.7

NaLr  10 i  these lines added to outlin in metdif - following must be false
TOTL 2798 i  Mg II 2798
Inwd 2798 i  inward part of Mg II 2798
Mg 6 1806 c  MG VI
TOTL  615 i  Mg 10 614.9 bothof doublet, li seq 2s 2p

MgLr  7 i  these lines added to outlin in metdif - following must be false
totl 2665 i  total emission in Al II] 2669.7, 2660 doublet
Al 2 2660 i  emission in Al II] 2669 alone
TOTL 1860 i  Al III
Inwd 1860 i  inward part of AlIII line
```

```
Al 6 2428 c  [Al VI] 2428.4
Al 6 2601 c  [Al VI] 2601.0
Al 6 1170 c  [Al VI] 1169.86
Al 6 2125 c  [Al VI] 2124.95
TOTL  556 i  Al 11, Li seq 2s2p

AlLr   6 i  these lines added to outlin in metdif - following must be false
diel 1260 i  SI II 1260, rough guess of dielec contribution
diel 1909 i  dielectronic recombination SiII 1909
rec  1207 i  Si III 1207, dielectronic recombination only
TOTL 1888 i  Si III] 1892+1883, total intensity of both lines

Si 3 1883 i  Si III] 1883 by itself
PHOT 1895 i  photoproduction by inner shell removal
TOTL 1397 i  Si IV 1397, collisionally excited
Inwd 1397 i  inward part of SiIV 1397
Si 7 2148 c  SI VII, 2148, O III like, collisionally excited

Si 7 2148 c
Si 8 1446 c  SI VIII 1446, OIII like, collisionally excited
Si 9 1985 c  SI IX 1985, 2150, collisionally excited
Si 9  949 c  collisionally excited
Si 9 1815 c  collisionally excited

Si 9  691 c  both components of 5S-3P doublet
Si10  606 c  SI 10 606A, actually group of 4 intercombination lines.
Si11  583 c  SI XI 582.9, collisionally excited
TOTL  506 i
SiLr   6 i  these lines added to outlin in metdif - following must be false

P15r  19 i  these lines added to outlin in metdif - following must be false
S 1R 1807 i  this is to check whether photoexcit of S II is ever important
S 2 6720 c  S II 6731 + 6716 together
S 2 4074 c  S II 4070 +4078 together
S 2 10330 c  S II N=3 lines, all four lines together

S II 6731 i  individual line from five level atom
S II 6716 i  individual line from five level atom
S II 4070 i  individual line from five level atom
S II 4078 i  individual line from five level atom
S II 10323 i  individual line from five level atom

S II 10289 i  individual line from five level atom
S II 10373 i  individual line from five level atom
S II 10339 i  individual line from five level atom
S 3 9532 c  [S III] 9532 alone
S 3 9069 c  [S III] 9069 alone

S 3 6312 c  [S III] 6312, transauroral temperature sensitive
S 3 3722 c  [S III] 3722, same upper level as 6312
TOTL 1198 i  S V 1198] both lines together
S 5 1188 i  Be seq, weaker of the two transitions
TOTL  933 i  total S VI 933+944

S 9 1715 c  S IX 1715, 1987, collisionally excited
S10 1213 c  S X 1213, 1197, collisionally excited
S11 1826 c  S XI 1615, 1826, collisionally excited
S12  520 c  group of four intercombination lines
S13  488 c  S XIII 488.4, 1909 like, collisionally excited

TOTL  427 i  S 14 506 li seq 2s2p
S LR   5 i  these lines added to outlin in metdif - following must be false
S LR   5 i
Cl 2 8579 c  Chlorine II 8581, 9127 doublet
Cl 2 9127 c  Chlorine II 8581, 9127 doublet

Cl 2 9127 c
Cl 2 6164 c  Chlorine II 6164 auroral line
Cl 2 3676 c  Chlorine II 3679 auroral line
TOTL 5525 c  Cl III 5519, 5539 doublet, both together
TOTL 3350 c  Cl III 3354, 3344 doublet, both together

TOTL 8494 c  Cl III 8504, 8436, 8552, 8483 multiplet, all together
Cl 3 5538 i  Cl III 5538
Cl 3 5518 i  Cl III 5518
```

```
Cl 3 3354 i  Cl III 3354
Cl 3 3344 i  Cl III 3344

Cl 3 8504 i  Cl III 8504
Cl 3 8436 i  Cl III 8436
Cl 3 8552 i  Cl III 8552
Cl 3 8483 i  Cl III 8483
Cl 4 8047 c  ClIV 8047

Cl 4 7532 c  ClIV 7532
Cl 4 3119 c  ClIV 3119
Cl 4 5324 c  ClIV 5324
Cl 4 5324 c
ClRr   4 i  Cl 17 ly a recombination 3.7A from fully stripped ion

Ar 3 7135 c  Argon III 7135
Ar 3 7751 c  Argon III 7751
Ar 3 5192 c  Argon III 5192
Ar 3 3109 c  Argon III 3109
Ar 3 3005 c  Argon III 3005

TOTL 4725 i  Argon IV 4711 + 4740 together, 4740=90%
TOTL 2860 i  [AvIV] 2868, 2854 together
TOTL 7250 i  [AvIV] auroral lines, 7237, 7331, 7171, 7263
Ar 4 4740 c  [Ar IV] 4740
Ar 4 4711 c  [Ar IV] 4711

Ar 4 2868 c  [Ar IV] 2868
Ar 4 2854 c  [Ar IV] 2854
Ar 4 7263 c  [Ar IV] 7263
Ar 4 7171 c  [Ar IV] 7171
Ar 4 7331 c  [Ar IV] 7331

Ar 4 7237 c  [Ar IV] 7237
Ar 5 7005 c  Argon V, 3P lines, 7005, collisionally excited
Ar 5 6435 c  Argon V, 3P lines, 6435, collisionally excited
Ar 5 6435 c
Ar14 4413 c  Ar XIV 4413, predicted lambda, not observed(??)

Ar15  409 c  collisionally excited
ArRr   4 i  these lines added to outlin in metdif - following must be false
K19r   4 i  these lines added to outlin in metdif - following must be false
Ca 2 3933 c  coll excit calcium k+h
Ca 2 8579 c  infrared triplet

Ca 2 7306 c  forbidden lines, 7291+7324 together
Phot 3933 i  fraction H Ly-alpha destruction of excited levels
Phot 7306 i  fraction H Ly-alpha destruction of excited levels
Ca2K 3934 i  individual lines from five level atom
Ca2H 3969 i  individual lines from five level atom

Ca2X 8498 i  individual lines from five level atom
Ca2Y 8542 i  individual lines from five level atom
Ca2Z 8662 i  individual lines from five level atom
CaF1 7291 i  individual lines from five level atom
CaF2 7324 i  individual lines from five level atom

Rec  3933 i  reccombination contribution to CaII emission
Ca 5 6087 c  Ca V optical and uv lines, collisional excitation, 3-level atom
Ca 5 5311 c  Ca V optical and uv lines, collisional excitation, 3-level atom
Ca 5 2414 c  Ca V optical and uv lines, collisional excitation, 3-level atom
Ca 5 3997 c  Ca V optical and uv lines, collisional excitation, 3-level atom

Ca 7 5620 c  Ca VII optical and uv lines, collisional excitation, 3-level atom
Ca 7 4941 c  Ca VII optical and uv lines, collisional excitation, 3-level atom
Ca 7 2112 c  Ca VII optical and uv lines, collisional excitation, 3-level atom
Ca 7 3688 c  Ca VII optical and uv lines, collisional excitation, 3-level atom
CaLr   3 i  these lines added to outlin in metdif - following must be false

ScLr   3 i  these lines added to outlin in metdif - following must be false
Sc 2  21 c  Sc II 2.08 (1-3)
Sc 2  41 c  Sc II 4.1 mic (1-2)
Sc 2  42 c  Sc II 4.22 (2-3)
Sc 3 3933 c  Sc III 3936

Sc 6 5054 c  Sc VI 5054 (1-2)
```

```
Sc 6 3592 c  Sc VI 3595 (2-3)
Sc 6 2100 c  Sc VI 2100 (1-3)
TiLr   3 i  these lines added to outlin in metdif - following must be false
Ti 3  12 c  Ti III 1.21 micron, (actually multiplet) 2-1 transition from model atom

Ti 3 9594 c  Ti III 9594, 3-1 transition, (actually multiplet) from model atom
Ti 3  45 c  Ti III 4.57 micron, 3-2 transition, (actually multiplet) from model atom
V Lr   3 i  these lines added to outlin in metdif - following must be false
V 3 8823 c  V III 8823
V 3 8507 c  V III 8507

V 3 8507 c
V 4 7735 c  V IV 7741 1-3
V 4 9489 c  V IV 9496 2-1
V 4  42 c  V IV 4.19 mic 3-2
CrLr   3 i  these lines added to outlin in metdif - following must be false

Cr 3 5828 c  [CrIII] multiplet blend at 5828A
Cr 4 7267 c  [CrIV] 2 - 1 multiplet blend at 7272
Cr 4 6801 c  [CrIV] 3 - 1 multiplet blend at 6806
Cr 5 7979 c  [CrV] 2 - 1 multiplet blend at 7985
Cr 5 6577 c  [CrV] 3 - 1 multiplet blend at 6582

Cr 5  37 c  [CrV] 3 - 2 multiplet blend at 3.75 microns
MnLr   3 i  these lines added to outlin in metdif - following must be false
Fe 2 6200 i  Fe 2 the 3-2 transition of Netzer's atom
Fe 2 4300 i  Fe 2 forbidden 2-1 transition from Netzer's atom
Fe 2 2400 i  Fe 2 UV3, 3-1 transition from Netzer's atom

Fe2c   0 c  total of all UV+optical Fe 2 cooling
Fe2h   0 h
Fe 2 1100 i  1 to 6 transition of Fred's Fe 2 atom
Fe 2 1500 i  2 to 6 transition of Fred's Fe 2 atom
Fe 2 11500 i  3 to 4 transition of Fred's Fe 2 atom

Fe 2 2500 i  3 to 5 transition of Fred's Fe 2 atom
Fe 2 2300 i  4 to 6 transition of Fred's Fe 2 atom
Fe 2 8900 i  5 to 6 transition of Fred's Fe 2 atom
Fe 2   0 c  all cooling due to 16 level atom
Fe 2  166 i  Fe 2 1.664 microns 8-13

Fe 2  160 i  Fe 2 1.599 microns 7-12
Fe 2  153 i  Fe 2 1.534 microns 6-11
Fe 2  164 i  Fe 2 1.644 microns 6-10
Fe 2  128 i  Fe 2 1.279 microns 12-4
Fe 2  130 i  Fe 2 1.295 microns 11-3

Fe 2  133 i  Fe 2 1.328 microns 11-4
Fe 2  126 i  Fe 2 1.257 microns 10-1
Fe 2  132 i  Fe 2 1.321 microns 10-2
Fe 2  259 i  Fe 2 25.988 microns 2-1
Fe 2  353 i  Fe 2 35.348 microns 3-2

Fe 2  178 i  Fe 2 17.936 microns 7-6, label is 178 to be unique
Fe 2  245 i  Fe 2 24.518 microns 8-7
Fe 2  358 i  Fe 2 35.776 microns 9-8
Fe 2  181 i  Fe 2 1.810 microns 10-7
Fe 2  168 i  Fe 2 1.677 microns 11-7

Fe 2  180 i  Fe 2 1.800 microns 11-8
Fe 2  171 i  Fe 2 1.712 microns 12-8
Fe 2  179 i  Fe 2 1.798 microns 12-9
Fe 2  229 i  Fe 2 22.902 microns 11-10
Fe 2  347 i  Fe 2 34.660 microns 12-11

Fe 2 8619 i  Fe 2 8619A 14-06
Fe 2 8894 i  Fe 2 8894A 15-07
Fe 2 9229 i  Fe 2 9229A 15-08
Fe 2 9270 i  Fe 2 9270A 16-09
Fe2b   2 i  emission from lage FeII atom, integrated over band

Fe 3   0 c  sum of 3p and 3g states together
Fe 3 5270 c  Fe 3 5270, predictions from garstang et al 78
Fe 3 4658 c  Fe 3 5270, predictions from garstang et al 78
Fe 4   0 c  total cooling due to 12-level Fe 4 atom
Fe 4 3096 i  Fe 4 3096.A, 4-1 and 5-1 transitions together
```

```
Fe 4 2836 i  Fe 4 2835.7A, 6-1 transition, 4P5/2 - 6S5/2
Fe 4 2829 i  Fe 4 2829.4A, 7-1 transition, 4P3/2 - 6S5/2
Fe 4 2567 i  Fe 4 2567.6+ 2567.4. 11-1 and 12-1 transitions
Fe 4  277 i  Fe 4 2.774 microns 12-7 transition
Fe 4  271 i  Fe 4 2.714 microns 12-6 transition

Fe 4  272 i  Fe 4 2.716 microns 11-6 transition
Fe 4  281 i  Fe 4 2.806 microns 10-7 transition
Fe 4  287 i  Fe 4 2.865 microns 10-8 transition
Fe 4  284 i  Fe 4 2.836 microns 9-6 transition
Fe 5 3892 c  Fe 5  3892+3839

Fe 6   0 c  all of 2G lines together first
Fe 6 5177 c  Fe 6 5177, approximate correct
Fe 7 6087 c  [Fe 7] 6087
Fe 7 5722 c  [Fe 7] 5722
Fe 7  242 c  Fe 9 242 j=1 slower decay

Fe11 2649 c  Fe 11 2649 collisional excitation
Fe11 1467 c  Fe 11 1467 collisional excitation
Fe12 1242 c  Fe 12, 1242, 1349 together, collisional excitation
Fe12 2170 c  Fe 12, 2170, 2406 together, collisional excitation
Fe12 2568 c  Fe12 2904, 2567, 3567, 3073 together, collisional excitation

Fe14 5303 i  Fe 14 optically thin in line 344
Coll 5303 c  contribution from collisional excitation
Pump 5303 r  continuum fluorescense
 347 5303 c66 error  - put this in
Fe19  592 c  Fe 19 from loulergue et al '85

Fe19 7082 c  Fe 19 from loulergue et al '85
Fe19 1118 c  Fe 19 from loulergue et al '85
Fe19 1328 c  Fe 19 from loulergue et al '85
Fe22  846 c  Fe 22 845.6A
Fe23  263 c  Fe 23 1909-like 262.6

FeKa   2 i  total intensity of K-alpha line
FeLr   2 i  recombination from fully stripped ion
TotH   2 i  total hot iron Ka; Auger "hot" iron, plus recom
AugC   2 i  Auger production of "cold" iron, less than or 17 times ionized
CoLr   1 i  these lines added to outlin in metdif - following must be false

NiLr   1 i  these lines added to outlin in metdif - following must be false
CuLr   1 i  these lines added to outlin in metdif - following must be false
ZnLr   1 i  these lines added to outlin in metdif - following must be false
Stoy   0 i  optional sum of certain emission lines, set with "print sum"
```

7. CODING CONVENTIONS

Cloudy is large, complex, and as is any large code, it is the result of many hands. It is essential that clarity and integrity of purpose be sustained (Ferland 2001b). This can only be achieved by having the *self-restraint* to follow a coherent set of standards. These standards are outlined in this section. All are arbitrary standards, but these are the standards Cloudy follows. It is far better to follow a single set of standards than to have total anarchy.

7.1. Variable names and strong typing

Cloudy is evolving towards a simple formulation of the Hungarian naming convention (Simonyi 1977). In this convention the first few characters of a variable name indicate the type and function of that variable.

The naming convention used in the code today looks back to an under appreciated advantage in the FORTRAN II and FORTRAN 66 languages - the fully implicit designation of variable types by the first letter of its name. The naming convention forced by early versions of FORTRAN (integers begin with i-n, real numbers begin with other characters) is still useful since the type can be determined at a glance.

7.1.1. Integers

Integers begin with the characters i, j, k, l, m, or n.

Counters begin with n. Examples include ***nLevel*** or ***nLoop***.

Loop indices are generally i, j, or k. Sometimes they are counters.

Indices within arrays begin with ip. Examples include ***ipContinuum*** or ***ipCIV1549***.

7.1.2. Double or float variables

These begin with letters between a through h, and o through z. Examples include ***PumpRate***, ***DestRate***, or ***CollisIoniz***.

At this time the naming convention does not distinguish between floats and doubles. Eventually the code will be totally double precision.

In some cases floating numbers naturally will have names beginning with one of the letters reserved for integers. In this case a lower case x is used as the first character. Examples include ***xJumpDown***, ***xMoleDen***.

7.1.3. Character strings

Character variables begin with "***ch***". Examples are ***chName*** or ***chReadInput***.

7.1.4. Logical variables

These begin with "l***g***". Examples are ***lgOK***, ***lgDone***. These are of intrinsic type int.

7.2. Structure names

Variables with a common purpose are grouped together into structures. For instance, the electron density variable *eden* is an element of the structure *dense* and so has the name *dense.eden*. The declaration for a structure occurs within an included file with the same name ending with ".h" – the *dense* structure is in *dense.h*.

7.3. Braces

The format of braces consumes a staggering amount of on-line debate and is important since the format must be followed consistently across the code for it to be instantly legible. There are three major styles of braces:

Style 1;

```
if( a>0 )
{
              b = 0.;
}
else
{
              b = 1.;
}
```

Style 2:

```
if( a>0 )
       {
              b = 0.;
       }
else
       {
              b = 1.;
       }
```

Style 3:

```
if( a>0 ) {
              b = 0.; }
else {
              b = 1.;}
```

The code uses the first style. Any one of the three could have been chosen, but the first one was chosen. We must have the *self-restraint* to follow this arbitrary choice, for the clarity of the overall code.

7.4. Changes to the code

Changes to logical flow or the physics are indicated by a comment line just before the affected line. These have the following style:

```
/* >>chng 05 dec 20 eden had eold, was undefined here, affect electron density */
```

The flag **>>chng yy mmm dd** indicates a change. Here **yy** are the last two digits of the year, **mmm** is a 3-character abbreviation of the month, all in lower case, and **dd** is a two-digit date. It is important that this style be followed consistently so that changes within the code can be extracted with a pattern matcher such as

grep, and then sorted by date (as in, why did the Compton temperature change on March 21?).

7.5. Atomic data references

Codes such as Cloudy only exist because of the foundation of basic atomic and molecular data. It is important to the survival of this field that the original sources of the basic data be cited, since this in turn affects their ability to generate support. The code follows the convention of preceding all uses of atomic data with a citation to the original paper in the following form:

```
/* >>refer Si+2 AS Berrington, K., AtData Nuc Data Tab 33, 195.
```

This information is extracted from the source with a Perl script that creates a file giving all atomic data references.

The flag "**>>refer**" indicates a reference. The fields are delimited by the tab character, and indicate the species (c4, he2, etc) and process (cs for collision strength, As for transition probabilities, etc). If the reference cannot fit on a single line it may continue on the following line, starting with the flag "**>>refercon**" which is followed by a tab. This style must be followed consistently so that a pattern search will generate a list of references used.

7.6. Asserts

Asserts are tests that variable values are valid (Maguire 1993). Examples include negative collision strengths or electron temperatures. A major improvement to Cloudy version 86 and later is the inclusion of large numbers of sanity checks, while in version 94 and later the C *assert* macro is used. These checks do not have a major impact on performance but they do slow the code down a bit. For production runs with a gold version of the code it is reasonable to not include these checks.

The asserts can be neglected so that the code will run slightly faster, by defining the macro NDEBUG on the compiler command line, as in

```
cc -DNDEBUG file.c
```

For most compilers this happens automatically when higher levels of optimization are used.

Asserts are also present in the test suite. They tell the code values of various quantities that the code has found in the past or are expected from theoretical grounds. These do not slow down the code.

7.7. Code in need of attention

broken() It is sometimes necessary to physically break the code, either by writing specific code to override the correct behavior or disable a physical

process. Such code should be accompanied by a call to routine ***broken***. This routine sets a flag showing that broken code is present. This flag generates a warning after the calculation is complete, to serve as a reminder of the presence of the broken code. This routine is not normally used.

TestCode() Trial code is identified by a call to routine ***TestCode***. This routine does nothing but set a flag that test code is present. This flag generates a comment after the calculation is complete, to serve as a reminder of the presence of the test code. This routine is not normally used.

fixit() sets a flag saying that the code needs to be fixed. A comment is generated at the end of the calculation.

/*TODO <tab> priority <tab> comment*/ This is a comment within the source that indicates something that needs attention, but not serious enough to cause a comment to be generated. This format must be followed so that a list of issues and priorities can be automatically parsed.

TotalInsanity() This routine announces that total insanity has been encountered, and exits with appropriate warnings. This is called when a test indicates that an impossible condition has occurred. It causes the calculation to stop and indicate that a catastrophic condition has occurred.

cdEXIT(condition) This routine must be called to exit the code. It does several chores, including calling the MPI exit handler and closing open file handles. The argument is the exit condition – if the exit was intended and the calculation is valid then the argument should be the standard macro *EXIT_SUCCESS*. If the exit is the result of a failure then the argument should be *EXIT_FAILURE*.

NB – it is essential that the code exit with this routine when running in a multiprocessor environment – the version of MPI on our HP cluster will hang and require a reboot, resulting in a nasty phone call from the system manager, if the code exists with a without this call.

7.8. Version numbers

Cloudy uses version numbers to keep track of changes to the code. The version number is stored in ***version***, in the structure ***date***. The variable ***chDate*** contains the date of the last major revision, and the variable ***chVersion*** is a string giving the version of the code.

8. PROBLEMS

8.1. Overview

This section describes some of the errors that can cause Cloudy to stop. Floating point errors should never occur. Several other internal errors, which the code is designed to catch and then complain about, can occur. Finally, it is possible that the code will stop because of thermal stability problems. If the calculation aborts it will conclude with a request to post the information on the web site's discussion board – please do – I can't fix it if I don't know it's broken.

The most important single thing to understand about any calculation is why it stopped, and whether this affects the predictions. This is discussed further in the section ***Stopping Criteria*** in Part I of this document.

8.2. Thermal stability and temperature convergence

This section describes thermal stability problems, how to identify them, and what to do about them.

8.2.1. Types of thermal maps

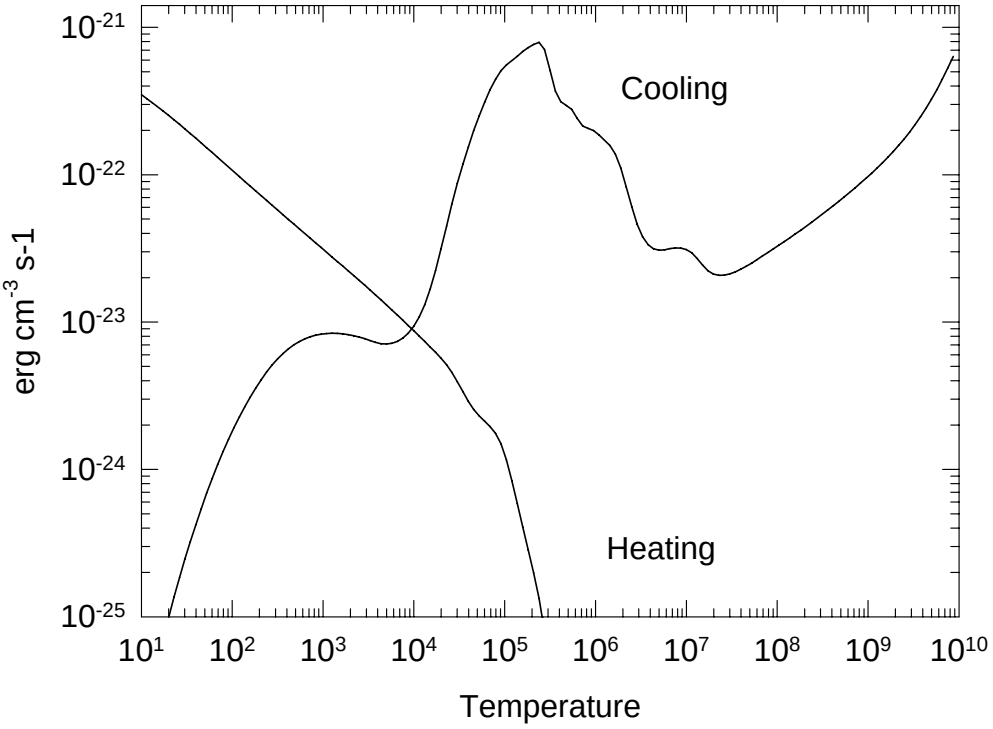

Figure 11 A typical heating - cooling function for low density photoionized gas. The cooling and heating rates (erg cm^{-3} s^{-1}) are shown.

Three types of thermal maps, showing the heating or cooling of gas as a function of temperature, can be produced by Cloudy. Each is the answer to a different question.

Figure 11 shows the heating and cooling rates as a function of temperature for a photoionized gas in which the electron temperature was varied. The data for this figure was produced by running the test case **`func_map.in`**, one of the standard test

cases included in the code distribution. Both the gas density and the flux of ionizing photons were held constant, so only one temperature, the point where the two curves cross, occurs in equilibrium. The **`func_map.in`** file uses the **`punch map`** command to determine heating and cooling rates at a variety of temperatures. This is exactly what the code does to determine the equilibrium temperature, so this plot can be useful to find out why the code ran into problems. This is why the command was introduced.

Gas in collisional equilibrium has a well-defined cooling rate that is only a function of temperature. The sample program **`hazy_coolingcurve.c`** (included in the *programs* file on the web site) does such a calculation, and Figure 12 shows the results. Here the kinetic temperature is set by some physics external to the calculation. The entire ionization solution is valid for each temperature under this assumption. The unspecified heat source would have to provide a local heating rate that is equal to the calculated cooling rate for the solution to be time steady.

The third map is the type of thermal stability map shown by Krolik, McKee, and Tarter (1981) and plotted in Figure 13. The program that generated these results is given in the file **`hazy_kmt.c`**. Here the equilibrium temperature is determined self-consistently for gas over a wide range of densities, but for a single flux of ionizing photons (or equivalently, distance from the central object).

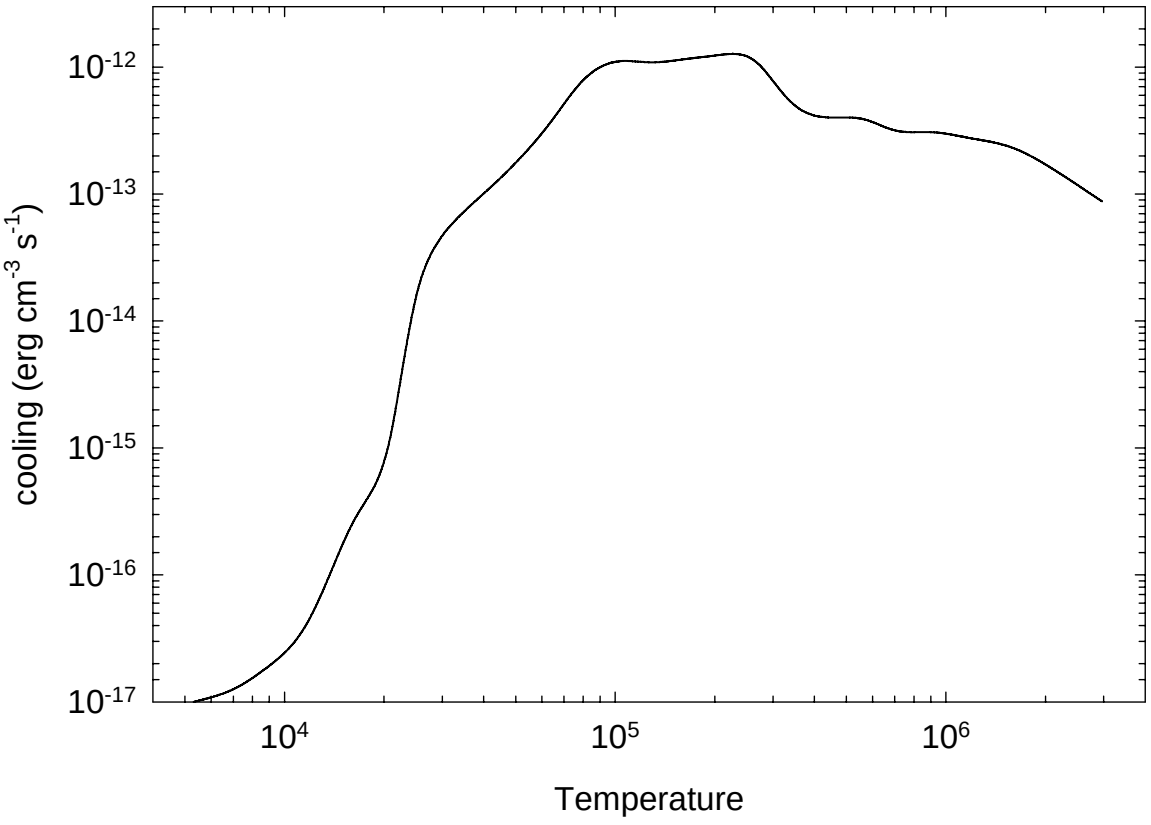

Figure 12 A typical cooling function for low density collisionally ionized gas. coolcurve

8.2.2. No Temperature Convergence

A temperature failure occurs when the heating-cooling balance is not within a certain tolerance, set by the **`set temperature error`** command, after 20 tries.

Normally Cloudy will punt after an excessive number of temperature failures occur. The limit to the number of failures is reset with the **failures** command. The default value is 20. (If the **failures map** command is entered then the code will first produce a map of heating-cooling space to give an indication of where the equilibrium temperature should have been when excessive failures occur.)

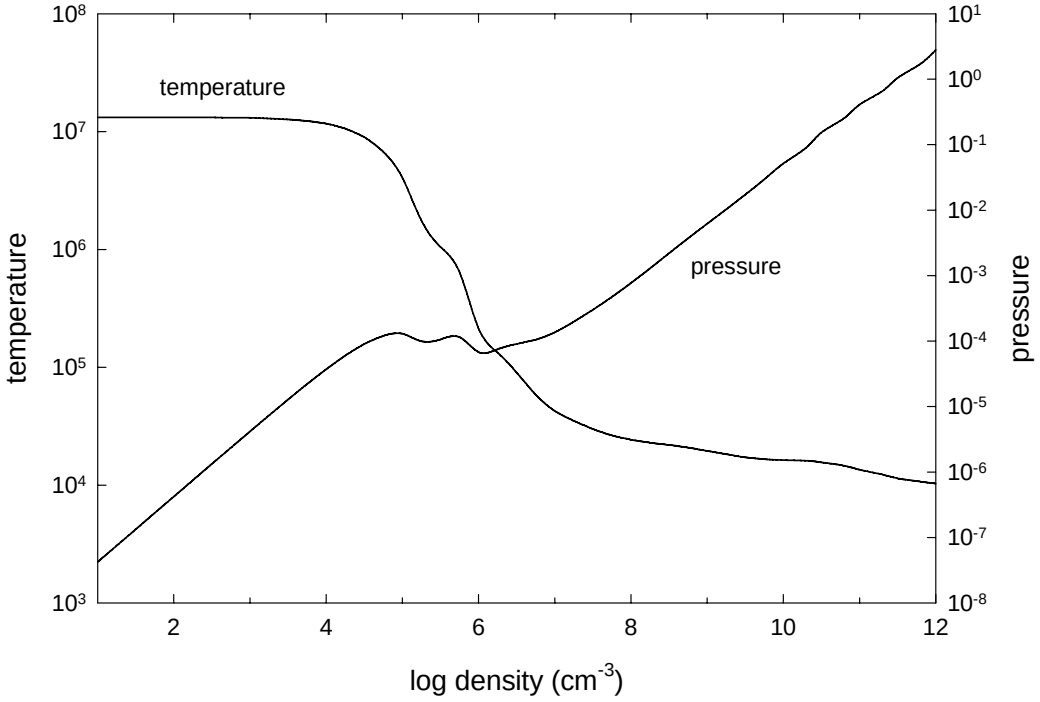

Figure 13 Equilibrium temperate as a function of density. hazy_kmt

Temperature failures most often occur for temperatures in the range 10^2 to 4×10^3 K, and 10^5 to 10^6 K. These are ranges where the cooling function permits more that one thermal solution (see, for example, Williams 1967; Dalgarno & McCray 1972). Figure 11 shows a typical cooling function for gas in photoionization equilibrium, and there are regions where the gas is unstable.

A peak is reached at a temperature near 10^3 K. This occurs when the fine-structure lines are major coolants. At lower temperatures their cooling rate increases exponentially (as expected), until roughly 10^3 K, when their Boltzmann factors are near unity. Above this temperature their cooling rate is nearly proportional to the Coulomb focusing factor $T^{-1/2}$, and the cooling *decreases* until the temperature is high enough for optical forbidden lines to become important (at roughly 4000 K). A similar phenomenon occurs near the ~ 10^5 to 10^6 K peak in the cooling function.

When failures occur because more than one temperature solution is possible, the reported failures are a physical (not numerical) problem. Cloudy will try to deal with this problem by forcing the temperature to values below the peak in the cooling function. Increasing the number of allowed failures (with the **failures** command) to prevent the code from stopping prematurely is permissible as long as the global

energy balance is preserved. A warning will be issued at the end of the calculation if the heating-cooling balance is not preserved.

8.2.3. Thermal Stability

The thermal solution may be unstable when the temperature derivative of the net cooling function (cooling minus heating) is negative (Field 1965). Possibly unstable solutions are indicated by a "u" just before the equilibrium temperature in the zone printout. The temperature derivative is for isochoric (constant density), not isobaric (constant pressure), conditions. Comments are printed at the end of the calculation if possibly unstable thermal solutions are present in the calculation.

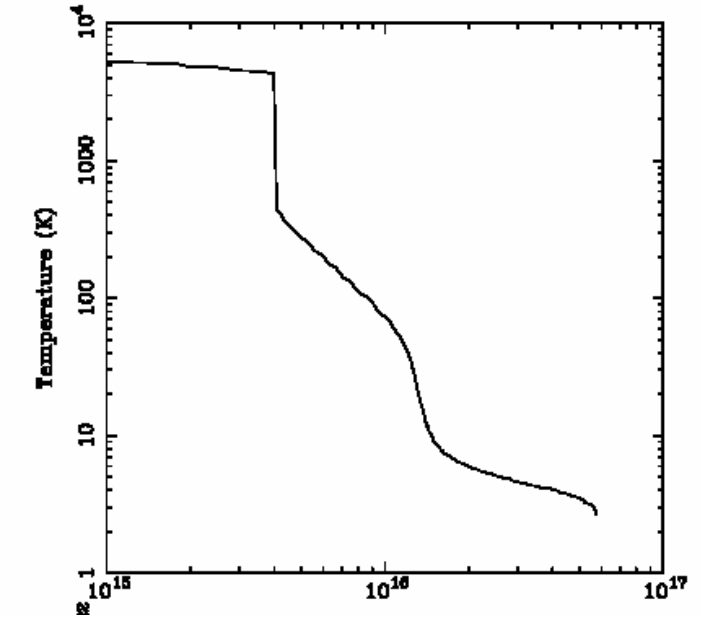

Figure 14 An example of a thermal front in a cooling flow cloud (Ferland, Fabian, & Johnstone 2001). The x-axis is the depth into the cloud. The thermal front at ~4×10^{15} cm is unresolved.

8.2.4. Thermal fronts

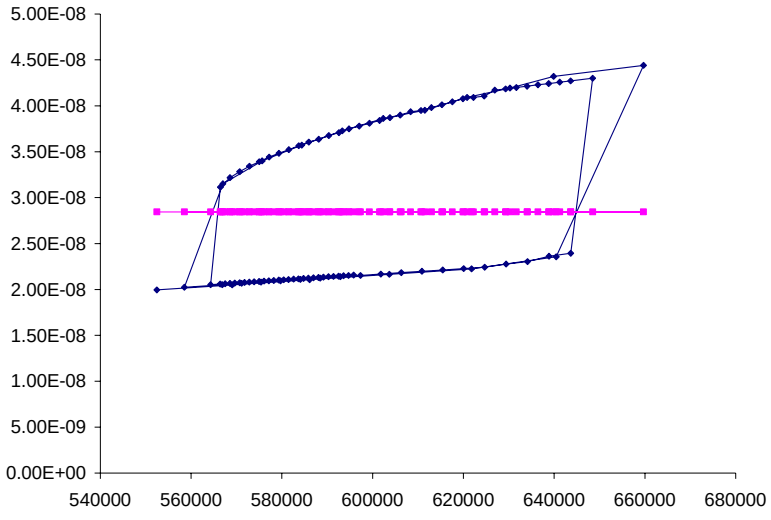

Figure 15 A thermal front in a constant pressure simulation. The x-axis gives the hydrogen density [cm^{-3}] and the y-axis is the pressure [dynes cm^{-2}]. The points forming the large box are the resulting total gas pressure and the horizonal points are the correct pressure. The solution jumps above and

below the equilibrium value as the temperature jumps above and below the thermal front, leading to a pressure failure.

Just as an ionization front is a region where the level of ionization changes dramatically over a small scale, a thermal front occurs where the temperature changes dramatically over a small scale. This can be caused by a real physical change of state of the gas such as those that occur near the peaks in the cooling curve. An example of a thermal front, taken from Ferland, Fabian, & Johnstone (2001), is shown in Figure 14. This type of jump is physical. The gas changes phase and moves to different branches of the cooling curve. The code will generate a caution or comment if the electron temperature changes discontinuously from one zone to the next.

A thermal front can lead to pressure convergence failures when the solution jumps between the high and low temperature branches. Figure 15 shows an example case, taken from *orion_hii_pdr_pp.in* in the test suite. This shows the pressure history (output with the **`punch pressure history`** command). The solver adjusts the density trying to make the resulting pressure agree with the desired pressure. The pressure changes continuously with density up to the point where the temperature jumps over the peak in the cooling curve. No solution is possible, and the code announces a pressure failure. In nature the presence of a magnetic field (added with the **`magnetic field`** command) will cushion the front from large changes in density.

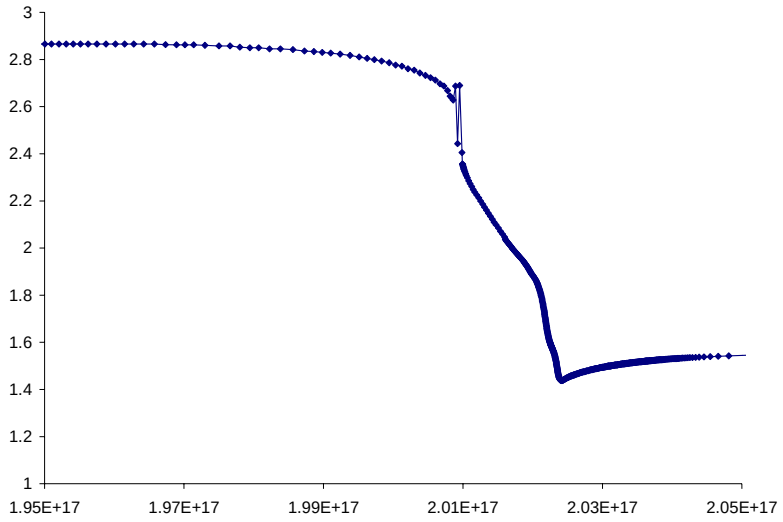

Figure 16 A constant-pressure thermal front in a temperature – radius plot. The x-axis gives the radius (cm). The y-axis gives the log of the temperature (K). The solution jumps above and below the equilibrium value, leading to a series of pressure failures, near a depth of 2×10^{17} cm, as it soldiers on through the thermal front.

A serious of pressure failures occur in this simulation when the gas falls to a temperature of ~300 K, as shown in Figure 16. The code tries to simply press on with the goal of reaching the cold side of the front.

8.2.5. Map Output

If an excessive number of temperature failures occur (the default limit is 20) then the program stops. It will produce a map of the heating and cooling as a function of temperature for the last computed zone if the **map** option on the **failures** command is given. The limit to the number of failures allowed before the code punts is reset with the **failures** command. The map is described here. The start of the output from the test case **func_map** is shown below.

```
90.02x map of heating vs cooling
 te, heating, cooling.
 Cloudy punts, Te= 9.254E+03 HTOT= 9.123E-24 CTOT= 9.118E-24 nzone=   1
 COOLNG array is
     O  4    25  0.340 O  3  5007  0.182 O  3    88  0.075 H FB     0  0.057 S  4    10  0.048 O  3    51  0.042 S  3  9532 0.035
     H ff     0  0.022 S  3    33  0.020 Ne 3    15  0.019 Hefb     0  0.015 N  3    57  0.015 Ne 3  3869  0.013 S  3    18 0.013
     Ne 5    24  0.010 Ne 5    14  0.009 C  3  1910  0.008 Heff     0  0.007 Si 2    34  0.006 Fe 5  3892  0.006 O  2  3727 0.005
 Line heating array follows
    Te     Heat-------------------> Cool---------------------->    dH/dT    dC/DT       Ne         NH      HII       Helium
1.0000E+01 3.4774E-22   1   1 0.636 4.6095E-26 H FB    0A 0.723 -8.19E-24  1.56E-27 9.1178E-01 1.0000E+00 -0.07 -0.40 -0.24 -1.75
1.0209E+01 3.4490E-22   1   1 0.635 4.6814E-26 H FB    0A 0.720 -7.98E-24  1.65E-27 9.1353E-01 1.0000E+00 -0.07 -0.40 -0.23 -1.73
1.0423E+01 3.4233E-22   1   1 0.635 4.7510E-26 H FB    0A 0.717 -7.74E-24  1.74E-27 9.1491E-01 1.0000E+00 -0.07 -0.41 -0.23 -1.73
```

The output begins with a listing of the strongest coolants for the last zone. Then the program steps through increasing temperatures and prints the heating, cooling, and ionization of the gas. From this information it should be possible to determine the temperature where the equilibrium thermal solution should have been. Each solution is completely self-consistent, except that heating and cooling do not balance. Both the local attenuated radiation field and collisional ionization contribute to the ionization balance at each temperature. All processes contribute to the thermal balance, including collisional ionization. The map is at constant density.

The first column gives the temperature. Columns 2 and 6 give the volume heating and cooling. Both have units erg s^{-1} cm^{-3}. Columns 3 and 4 constitute an indication of the main heating source. Columns 7 and 8 give the label and wavelength of the strongest coolant. Columns 5 and 9 give the fraction of the total heating or cooling due to these agents. Columns 10 and 11 give the heating and cooling derivatives. Columns 12 and 13 give the electron and hydrogen densities (cm^{-3}) and the remaining columns give the logs of the hydrogen and helium ionization fractions. The location of the probable thermal solution is indicated by a comment surrounded by dashed lines.

8.3. Convergence problems with dust-free static sphere

Ionization convergence problems can occur with a dust-free static spherical geometry. The default geometry when the **sphere** command is entered is for lines to freely escape after crossing the central hole due to some level of expansion. In a static spherical geometry (set with the **sphere static** command) the total Lα optical depth at the illuminated face of the shell will be very large since the line is scattered by the matter that lies across the entire shell. The line is destroyed when dust is present but if dust is not present the Lα intensity J will become very large. If the total optical depth in Lα is also large then the dominant escape / destruction process for the line will be absorption by atoms of third-row elements or the n=2 level of hydrogen. This can lead to ionization convergence problems due to the extremely large Lα intensity J.

The first question to ask is whether this geometry is appropriate. Dust is nearly always present in the ISM. In dense stellar environments it is unlikely that a spherical geometry will be static. Add dust or use the default spherical geometry – the problem will go away.

8.4. Optical depth convergence problems

The code generally will not converge if it has not done so within ten or so iterations. Convergence problems most commonly occur when the specified column density or thickness is very near a prominent ionization front. In this case very small changes in the physical conditions results in large changes in the optical depths. The code will not have convergence problems if an optical depth is used as a stopping criterion instead.

8.5. Negative populations

It is possible that the code will stop because negative level populations were predicted for atoms, ions, or molecules. This is not supposed to occur, but sometimes happens because of numerical instabilities in the matrix inversion routine. Please post the input stream and version of Cloudy on the code's web site.

8.6. Floating Point Errors

The code should be compiled and linked with options enabled so that the code will crash on overflow or division by zero, but ignore underflow. *Floating point errors should never occur.* The logic within the code is designed to identify problems, and complain, but not fail. The logic is only as good as the tests they were designed to pass. It is inevitable that circumstances will occur for which the logic now in the code is not sufficient. It is possible that the code will fail when these circumstances occur. I would be grateful for reports of any such failures, since they inevitably identify shortcomings in the code, and lead to its improvement. Please post comments on the discussion board on the code's web site.

8.7. I can't fix it if I don't know it's broken

Machines are growing faster far more rapidly than people are getting smarter. Reliability in the face of complexity is the major challenge to the development of any large-scale computer code (Ferland 2001b). There can be little doubt that Cloudy contains bugs.

The code is well tested in many limits, and behaves in the correct manner. Simulations of H II regions, planetary nebulae, and other simple objects, are in good agreement with predictions of other photoionization codes (Ferland et al. 1995; Ferland & Savin 2001).

Bugs can be discovered by strange behavior or crashes in situations where the code has not been well-tested. The discovery of the existence of problems is itself a major challenge. If problems arise or the code crashes then it is likely that a problem has been isolated. I would appreciate learning about such problems since they identify shortcomings which usually lead to improvements in the code (or the

documentation). Please post queries and bug reports on the discussion board on the code's web site.

9. COMPARISON CALCULATIONS

9.1. Overview

This section presents comparisons between the current predictions of the code, and results from other independent calculations. The "other" calculations are from the compendium resulting from the Lexington meeting on model nebulae (Ferland et al. 1995 and Péquignot et al. 2001).

The scatter among the calculations, as well as the changes that have occurred in the predictions made by Cloudy, are in some sense an indication of the stability and reliability of these types of extreme non-LTE calculations. The largest discrepancies between current predictions made by Cloudy and the other models from the Meudon meeting (which were computed in 1985) are due to changes which have occurred in the atomic data base between 1985 and the present. In general, the strongest lines are in very good agreement (as they must because of energy conservation) while weak lines (which are very sensitive to changes in the computed temperature and ionization structure) scatter by nearly a factor of two.

9.2. Cool HII Region

This is an HII region ionized by a very cool star. It is one of the Lexington Meeting test cases and is computed with the input script *hii_coolstar.in* in the code's test suite. This is the simplest model since helium is predominantly neutral. The entry ***L(total)*** comes from the "Stoy" printed entry.

Table 5 HII Region Ionized by Cool Star

		Mean	Ferland	Harrington	Netzer	Péquignot	Rubin
L(Hβ)	E36	4.90	4.98	4.93	4.85	4.83	4.93
[N II]	6584+	0.87	0.91	0.82	0.97	0.82	0.84
[O II]	3727+	1.21	1.16	1.22	1.32	1.14	1.21
[Ne II]	12.8 μm	0.30	0.35	0.29	0.29	0.29	0.29
[S II]	6720+	0.57	0.64	0.55	0.61	0.52	0.52
[S III]	18.7 μm	0.31	0.27	0.36	0.17	0.37	0.37
[S III]	34 μm	0.51	0.47	0.60	0.27	0.61	0.62
[S III]	9532+	0.57	0.48	0.55	0.64	0.60	0.56
L(total)	E36	21.3	21.3	21.7	20.7	21.0	21.8
T(in)		6860	6952	6749	6980	6870	6747
T(H+)		6767	6740	6742	6950	6660	6742
<He+>/<H+>		0.047	0.041	0.044	0.068	0.048	0.034
R(out)	E18	8.96	8.93	8.94	9.00	8.93	9.00

Table 6 Cool HII Region vs Cloudy

		Mean	STD	90.05	94.00	96.00
L(Hβ)	E36	4.90	0.06	4.91	5.03	4.85
[N II]	6584	0.65	0.05	0.64	0.63	0.57
[O II]	3727+	1.21	0.07	1.08	1.04	1.01
[Ne II]	12.8 μm	0.30	0.03	0.26	0.26	0.26
[S II]	6720+	0.57	0.05	0.45	0.44	0.49
[S III]	18.7 μm	0.31	0.09	0.43	0.45	0.44
[S III]	34 μm	0.51	0.15	0.61	0.64	0.90
[S III]	9532	0.43	0.05	0.42	0.42	0.36
L(total)	E36	21.29	0.45	21.0	21.7	21.2
T(in)		6860	110	7261	7188	6790
T(H+)		6767	108	6600	6530	6622
<He+>/<H+>		0.047	0.01	0.048	0.043	0.046
R(out)	E18	8.96	0.04	8.81	8.92	8.83

9.3. Paris HII Region

This compares current predictions of the code with those of other participants at the Meudon meeting on photoionization calculations for the case of a simple spherical H II region. The input used to generate this model H II region is contained in the sample input file *hii_paris.in*.

Table 7 Paris Meeting HII Region

		Meu	Lex	Ferland	Harrington	Netzer	Péquignot	Rubin
L(Hβ)	E37	2.06	2.04	2.06	2.04	2.02	2.02	2.05
He I	5876	0.116	0.111	0.109	0.119	0.101	0.116	
Cl I	2326+	0.17	0.17	0.19	0.17	0.16	0.14	0.18
C III]	1909+	0.051	0.07	0.059	0.059	0.078	0.065	0.076
[N II]	122 μm		0.031	0.033			0.036	0.031
[N II]	6584+	0.73	0.80	0.88	0.74	0.87	0.78	0.73
[N III]	57 μm	0.30	0.28	0.27	0.29	0.26	0.30	0.30
[O II]	3727+	2.01	2.20	2.19	2.14	2.3	2.11	2.26
[O III]	51.8 μm	1.10	1.06	1.04	1.11	0.99	1.08	1.08
[O III]	88.4 μm	1.20	1.20	1.07	1.28	1.16	1.25	1.26
[O III]	5007+	2.03	2.09	1.93	1.96	2.29	2.17	2.10
[Ne II]	12.8 μm	0.21	0.21	0.23	0.19	0.22	0.20	0.20
[Ne III]	15.5 μm	0.44	0.41	0.43	0.43	0.37	0.42	0.42
[Ne III]	3869+	0.096	0.091	0.103	0.086	0.100	0.079	0.087
[S II]	6720+	0.14	0.18	0.23	0.16	0.22	0.17	0.13
[S III]	18.7 μm	0.55	0.53	0.48	0.56	0.5	0.55	0.58
[S III]	34 μm	0.93	0.87	0.82	0.89	0.81	0.88	0.94
[S III]	9532+	1.25	1.31	1.27	1.23	1.48	1.27	1.30
[S IV]	10.5 μm	0.39	0.38	0.37	0.42	0.36	0.41	0.33
Sum	Sum	11.59	11.87	11.58	11.70	12.17	11.90	12.01
L(total)	E37	24.1	24.4	24.1	24.1	24.8	24.3	24.6
T(in)		7378	7655	7815	7741	7670	7650	7399
T(H+)		7992	8052	8064	8047	8000	8060	8087
<He+>/<H+>			0.76	0.71	0.77	0.76	0.75	0.83
R(out)	E18	1.45	1.46	1.46	1.46	1.47	1.46	1.46

Table 8 Paris HII Region vs Cloudy

		Mean	STD	76.03	80.06	84.15	90.05	94.00	96.00
L(Hβ)	E37	2.04	0.02	2.06	2.04	2.01	2.05	2.02	2.04
HeI	5876	0.11	0.01	0.12	0.12	0.12	0.11	0.117	0.113
C II]	2326+	0.17	0.02	0.24	0.17	0.17	0.15	0.145	0.195
C III]	1909+	0.07	0.01	0.06	0.11	0.09	0.063	0.060	0.051
[N II]	122 μm	0.03	0.00			0.03	0.028	0.028	0.027
[N II]	6584	0.60	0.05	0.58	0.60	0.58	0.58	0.57	0.519
[N III]	57 μm	0.28	0.02			0.29	0.289	0.297	0.302
[O II]	3727+	2.20	0.08	2.29	2.43	2.31	2.02	1.996	2.00
[O III]	51.8 μm	1.06	0.05	1.15	1.09	1.11	1.22	1.24	1.27
[O III]	88.4 μm	1.20	0.09			1.06	1.11	1.13	1.16
[O III]	5007	1.57	0.11	1.83	1.62	1.50	1.66	1.62	1.57
[Ne II]	12.8 μm	0.21	0.02	0.22	0.23	0.23	0.18	0.18	0.17
[Ne III]	15.5 μm	0.41	0.02	0.47	0.45	0.45	0.28	0.29	0.29
[Ne III]	3869	0.0689	0.008	0.098	0.090	0.082	0.063	0.061	0.059
[S II]	6720+	0.18	0.04	0.27	0.29	0..129	0.126	0.12	0.153
[S III]	18.7 μm	0.53	0.04	0.54	0.53	0.52	0.61	0.61	0.62
[S III]	34 μm	0.87	0.05			0.88	0.85	0.86	1.21
[S III]	9532	0.98	0.07	1.04	1.04	1.05	0.90	0.89	0.77
[S IV]	10.5 μm	0.38	0.04	0.09	0.11	0.36	0.53	0.53	0.56
Sum	Sum	11.87	0.24	10.0	9.9	11.8	11.9	11.8	12.1
L(total)	E37	24.44	0.31	20.9	20.4	23.9	24.5	24.3	24.1
T(in)		7655	157			6547	7822	7746	7524
T(H+)		8052	32			7530	7970	7920	7980
<He+>/<H+>		0.76	0.04			0.75	0.72	0.74	0.76
R(out)	E18	1.46	0.00			1.45	1.45	1.46	1.44

9.4. Blister HII Region

This is one of the Lexington Meeting test cases, and is meant to be similar to inner regions of the Orion Nebula and is called *hii_blister.in* in the test suite.

Table 9 Blister HII Region

		Mean	Ferland	Harrington	Netzer	Péquignot	Rubin
I(Hβ)		4.69	4.59	4.81	4.69	4.67	4.70
He I	5876	0.12	0.13	0.11	0.12	0.12	
C II	2326+	0.16	0.14	0.20	0.10	0.15	0.23
C II	1335+	0.15	0.17	0.14	0.13	0.16	
C III]	1909+	0.18	0.22	0.17	0.18	0.15	0.20
[N II]	6584+	0.81	0.58	0.94	0.74	0.90	0.87
[N III]	57 μm	.033	.035	.033	.033	.032	.034
[O II]	7330+	0.12	0.10	0.13	0.09	0.12	0.14
[O II]	3727+	0.86	0.73	0.98	0.69	0.86	1.04
[O III]	51.8 μm	0.29	0.31	0.29	0.28	0.28	0.28
[O III]	5007+	4.18	4.74	3.90	4.40	3.90	3.96
[Ne II]	12.8 μm	0.34	0.32	0.33	0.35	0.33	0.35
[Ne III]	15.5 μm	1.06	1.24	1.07	0.96	1.04	1.00
[Ne III]	3869+	0.34	0.48	0.32	0.35	0.26	0.29
[S III]	18.7 μm	0.33	0.31	0.34	0.31	0.33	0.35
[S III]	9532+	1.46	1.41	1.46	1.51	1.42	1.53
[S IV]	10.5 μm	0.51	0.54	0.52	0.51	0.53	0.43
Sum	Sum	10.78	11.32	10.80	10.63	10.46	10.71
I(total)		51.3	52.6	52.4	50.4	49.4	50.3
T(in)		7911	8206	7582	8200	8200	7366
T(H+)		8303	8324	8351	8310	8200	8328
<He+>/<H+>		0.85	0.94	0.78	0.93	0.79	0.84
ΔR	E17	2.99	2.88	3.08	2.93	2.98	3.09

Table 10 Blister HII Region vs Cloudy

		Mean	STD	90.05	94.00	96.00
I(Hβ)		4.69	0.08	4.71	4.64	4.91
HeI	5876	0.12	0.01	0.129	0.132	0.132
C II]	2326+	0.16	0.05	0.133	0.124	0.135
C II	1335+	0.15	0.02	0.179	0.171	0.18
C III]	1909+	0.18	0.03	0.222	0.234	0.26
[N II]	6584	0.54	0.09	0.468	0.417	0.40
[N III]	57 μm	0.03	0.00	0.037	0.038	0.038
[O II]	7330+	0.12	0.02	0.115	0.113	0.127
[O II]	3727+	0.86	0.15	0.737	0.713	0.794
[O III]	51.8 μm	0.29	0.01	0.303	0.309	0.307
[O III]	5007	3.13	0.28	3.74	3.84	3.88
[Ne II]	12.8 μm	0.34	0.01	0.140	0.141	0.14
[Ne III]	15.5 μm	1.06	0.11	0.458	0.462	0.466
[Ne III]	3869	0.34	0.08	0.157	0.159	0.166
[S III]	18.7 μm	0.255	0.015	0.301	0.304	0.349
[S III]	9532	1.09	0.037	0.950	.955	0.87
[S IV]	10.5 μm	0.51	0.04	0.68	0.68	0.665
Sum	Sum	10.78	0.32	10.6	10.7	10.8
I(total)		51.29	1.39	50.9	50.2	50.0
T(in)		7910	406	8447	8370	8430
T(H+)		8302	59	8325	8330	8429
<He+>/<H+>		0.85	0.07	0.895	0.90	0.916
ΔR	E17	2.99	0.09	2.99	2.94	2.94

9.5. Paris Planetary Nebula

This compares current predictions of the code with those of other participants at the Meudon (1985) and Lexington (1993) meetings on photoionization calculations, for the case of ionization by a very hot black body. The input used to generate this model planetary nebula is shown in the sample input section and is called *pn_paris.in* in the test suite. The model results are very sensitive to the detailed transfer of HeII Lα; this line is the dominant heat source across the He^{++} region of the model nebula. The parameters were chosen to be roughly similar to NGC 7027, a very well studied object.

Table 11 Paris Meeting Planetary Nebula

Line		Meudon	Lexington	Ferland	Harrington	Netzer	Péquignot
L(Hβ)	E35	2.60	2.68	2.63	2.68	2.73	2.68
HeII (35)	erg/s	0.87	0.88	0.83	0.88	0.94	0.85
He I	5876	0.11	0.11	0.11	0.10	0.10	0.11
He II	4686	0.33	0.33	0.32	0.33	0.35	0.32
C II]	2326+	0.38	0.33	0.33	0.43	0.27	0.30
C III]	1909+	1.70	1.77	1.82	1.66	1.72	1.87
C IV	1549+	1.64	2.33	2.44	2.05	2.66	2.18
[N II]	6584+	1.44	1.49	1.59	1.45	1.47	1.44
N III]	1749+	0.11	0.12	0.13	0.13	0.11	0.13
[NIII]	57 μm		0.13	0.12	0.13	0.13	0.13
N IV]	1487+	0.12	0.19	0.20	0.15	0.21	0.19
N V	1240+	0.09	0.17	0.18	0.12	0.23	0.15
[O I]	6300+	0.15	0.14	0.15	0.12	0.14	0.14
[O II]	3727+	2.23	2.25	2.23	2.27	2.31	2.18
[O III]	5007+	20.9	20.76	21.1	21.4	19.4	21.1
[O III]	4363	0.16	0.15	0.16	0.16	0.14	0.16
[O III]	52 μm	1.43	1.43	1.42	1.44	1.40	1.46
[O IV]	26 μm	3.62	3.67	3.52	3.98	3.32	3.86
O IV]	1403+	0.13	0.26	0.20	0.23	0.26	0.33
O V]	1218+	0.09	0.20	0.20	0.11	0.29	0.19
[Ne III]	15.5 μm	2.51	2.78	2.75	2.76	2.80	2.81
[Ne III]	3869+	2.59	2.69	3.33	2.27	2.74	2.44
Ne IV]	2423+	0.56	0.78	0.72	0.74	0.91	0.74
[Ne V]	3426+	0.73	0.67	0.74	0.60	0.73	0.61
[Ne V]	24.2 μm	1.67	0.87	0.94	0.76	0.81	0.99
Mg II	2798+	1.48	1.58	2.33	1.60	1.22	1.17
[Mg IV]	4.5 μm	0.09	0.12	0.12	0.13		0.12
[Si II]	34.8 μm	0.13	0.19	0.16	0.26	0.19	0.17
Si II]	2335+	0.11	0.16	0.15		0.16	0.16
Si III]	1892+	0.20	0.41	0.39	0.32	0.46	0.45
Si IV	1397+	0.15	0.18	0.20	0.15	0.21	0.17
[S II]	6720+	0.39	0.35	0.21	0.45	0.33	0.43
[S III]	18.7 μm	0.49	0.48	0.48	0.49	0.46	0.49
[S III]	9532+	2.09	1.96	2.04	1.89	2.05	1.87
[S IV]	10.5 μm	1.92	1.98	1.92	2.21	1.81	1.98
L(total)	E35	129	137	139	136	135	136
T(in)	E4		1.81	1.83	1.78	1.84	1.78
T(H+)	E4		1.25	1.22	1.21	1.35	1.21
<He+>/<H+>			0.72	0.74	0.74	0.71	0.71
R(out)	E17		4.06	4.04	4.04	4.07	4.07

Table 12 Paris Planetary vs Cloudy

Line		Lexington	STD	74.23	76.03	80.06	84.15	90.05	94.00	96.00
L(Hβ)	E35	2.68	0.04	2.57	2.66	2.52	2.34	2.62	2.55	2.56
HeII (35)	erg/s	0.88	0.05				0.83	0.83	0.866	.873
He I	5876	0.11	0.01	0.11	0.11	0.11	0.11	0.111	0.108	0.108
He II	4686	0.33	0.01	0.29	0.32	0.35	0.36	0.319	0.343	0.345
C II]	2326+	0.33	0.07	0.36	0.35	0.37	0.35	0.286	0.289	0.294
C III]	1909+	1.77	0.09	1.57	1.48	1.72	1.72	1.88	1.83	1.90
C IV	1549+	2.33	0.27	2.24	2.76	2.48	2.19	2.65	2.63	2.61
[N II]	6584	1.12	0.05	1.06	1.05	1.08	1.11	0.978	1.00	0.885
N III]	1749+	0.12	0.01	0.10	0.08	0.10	0.11	0.123	0.118	0.121
[NIII]	57 μm	0.13	0.00				0.12	0.128	0.125	0.127
N IV]	1487+	0.19	0.03	0.16	0.12	0.11	0.15	0.242	0.238	0.241
N V	1240+	0.17	0.05	0.14	0.09	0.06	0.09	0.175	0.18	0.18
[O I]	6300	0.105	0.007	0.11	0.11	0.12	0.12	0.116	0.118	0.119
[O II]	3727+	2.25	0.06	2.24	2.19	2.35	2.40	2.22	2.32	2.36
[O III]	5007	15.6	0.68	15.9	15.8	15.3	15.6	17.0	16.3	16.4
[O III]	4363	0.15	0.01	0.14	0.13	0.15	0.16	0.174	0.166	0.167
[O III]	52 μm	1.43	0.03	1.40	1.35	1.37	1.35	1.32	1.28	1.28
[O IV]	26 μm	3.67	0.30			3.42	3.65	3.42	3.59	3.64
O IV]	1403+	0.26	0.05	0.19	0.22	0.11	0.15	0.248	0.25	0.225
O V]	1218+	0.20	0.07	0.17	0.11	0.07	0.11	0.200	0.20	0.20
[Ne III]	15.5 μm	2.78	0.03	2.77	2.70	2.67	2.71	1.90	1.87	1.87
[Ne III]	3869	2.01	0.35	2.41	2.25	2.43	2.49	2.15	2.09	2.11
Ne IV]	2423+	0.78	0.09	0.62	0.51	0.51	0.63	0.823	0.827	0.829
[Ne V]	3426	0.50	0.06	0.48	0.40	0,40	0.48	0.589	0.614	0.621
[Ne V]	24.2 μm	0.87	0.11	0.24	0.25	1.01	1.04	1.03	1.09	1.098
Mg II	2798+	1.58	0.54	0.83	1.82	1.96	2.33	2.26	2.27	2.29
[Mg IV]	4.5 μm	0.12	0.00	0.12	0.13	0.14	0.13	0.118	0.12	0.123
[Si II]	34.8 μm	0.19	0.04	0.16	0.16	0.16	0.17	0.157	0.16	0.159
Si II]	2335+	0.16	0.01	0.15	0.14	0.16	0.18	0.150	0.15	0.173
Si III]	1892+	0.41	0.07	0.32	0.42	0.42	0.42	0.526	0.49	0.499
Si IV	1397+	0.18	0.03	0.17	0.24	0.22	0.15	0.235	0.223	0.229
[S II]	6720+	0.35	0.11	0.38	0.68	0.66	0.36	0.354	0.354	0.356
[S III]	18.7 μm	0.48	0.02	0.58	0.71	0.67	0.47	0.467	0.472	0.556
[S III]	9532	1.47	0.075	1.27	1.58	1.55	1.48	1.34	1.35	1.17
[S IV]	10.5 μm	1.98	0.17	1.64	1.32	1.53	1.78	2.20	2.04	2.04
L(total)	E35	137	1.60	117	124	128	121	135		
T(in)	E4	1.81	0.03				1.49	1.828	1.80	1.808
T(H+)	E4	1.25	0.07				1.28	1.22	1.22	1.23
<He+>/<H+>		0.72	0.02				0.72	0.74	0.72	0.72
R(out)	E17	4.06	0.02				3.90	4.03	3.99	4.00

9.6. Paris NLR Model

This compares current predictions of the code with those of other participants at the Meudon meeting on photoionization calculations, for a model similar to the NLR of active nuclei. Results for other codes are from the 1985 Meudon meeting. The input stream is the file *nlr_paris.in* in the test suite.

Table 13 Paris Meeting NLR Model

Line		Netzer	Pequignot	Binette	Kraemer	Mean
Hβ	erg/s/cm^2	0.129	0.134	0.124	0.12	0.127±0.006
Hβ	4861	1.00	1.00	1.00	1.00	1.00
Lα	1216	35.3	33.1	-	24.0	30.8±6.0
He I	5876	0.095	0.098	0.092	0.090	0.094±0.004
He II	4686	0.36	0.32	0.38	0.37	0.358±0.026
C II]	2326	0.96	0.77	1.70	1.06	1.12±0.40
C II	1335	0.14	0.14	0.20	0.08	0.14±0.05
C III]	1909	4.59	4.99	6.50	4.91	5.25±0.85
C IV	1549	7.03	7.20	5.30	7.20	6.68±0.93
[N I]	5200	0.31	0.33	0.82	0.37	0.46±0.24
[N II]	6548	2.68	1.52	1.77	1.63	1.90±0.53
N III]	1749	0.40	0.40	0.43	0.48	0.428±0.038
N IV]	1487	0.45	0.43	0.51	0.48	0.468±0.035
N V	1240	0.32	0.30	0.32	0.28	0.305±0.019
[O I]	63.2 μm	-	0.62	0.14	0.10	0.29±0.29
[O I]	6300	1.32	0.90	1.62	1.04	1.22±0.32
[O II]	7325	0.11	0.094	0.16	0.10	0.116±0.03
[O II]	3727	3.4	2.62	4.41	2.73	3.29±0.82
[O III]	52μm	2.5	2.54	2.31	2.65	2.50±0.14
[O III]	5007	27.36	27.36	23.28	27.76	26.44±2.11
[O III]	4363	0.42	0.41	0.44	0.44	0.428±0.015
O III]	1663	0.97	0.95	0.92	1.01	0.963±0.038
[O IV]	25.9μm	5.69	5.19	5.49	-	5.46±0.25
O IV]	1403	0.53	0.44	0.51	0.66	0.534±0.092
O V]	1218	0.33	0.32	0.45	0.24	0.335±0.086
O VI	1035	0.17	0.17	0.22	0.10	0.165±0.049
[Ne II]	12.8μm	0.28	0.18	0.48	0.13	0.268±0.155
[Ne III]	15.5μm	2.8	2.62	1.83	1.25	2.13±0.72
[Ne III]	3869	2.70	2.59	2.27	1.67	2.31±0.46
Ne IV]	2423	0.82	0.79	1.03	1.12	0.94±0.16
[Ne V]	24.2μm	3.54	2.64	3.54	-	3.24±0.52
[Ne V]	3426	1.17	1.02	1.13	1.05	1.095±0.066
Mg II	2798	1.58	1.43	1.51	1.10	1.40±0.21
Si II	34.8μm	1.73	0.97	0.51	-	1.07±0.62
Si II	2335	0.21	0.17	0.09	-	0.16±0.06
Si III]	1892	0.15	0.19	0.69	0.14	0.29±0.26
Si IV	1397	0.21	0.14	0.02	0.13	0.13±0.08
S II	6720	1.00	0.62	1.29	0.37	0.82±0.41
S II	4070	0.07	0.04	0.078	0.03	0.055±0.023
S III	18.7μm	0.75	0.49	0.68	0.65	0.64±0.11
S III	9532	2.25	1.38	1.73	1.62	1.74±0.37
S IV	10.5μm	1.39	0.73	0.94	1.57	1.16±0.39

Table 14 Paris NLR Model vs Cloudy

Line		Mean	84.15	90.05	94.00	96.00
Hβ	erg/s/cm^2	0.127±0.006	0.133	0.136	0.131	0.136
Hβ	4861	1.00	1.00	1.00	1.00	1.00
Lα	1216	30.8±6.0	32.3	32.3	33.8	33.0
He I	5876	0.094±0.004	0.104	0.103	0.100	0.107
He II	4686	0.358±0.026	0.351	0.34	0.330	0.330
C II]	2326	1.12±0.40	0.766	0.652	0.693	0.754
C II	1335	0.14±0.05	0.126	0.141	0.142	0.145
C III]	1909	5.25±0.85	5.02	4.64	4.54	4.49
C IV	1549	6.68±0.93	8.42	7.47	7.15	6.84
[N I]	5200	0.46±0.24	0.14	0.144	0.151	0.154
[N II]	6548	1.90±0.53	2.32	2.36	2.50	2.52
N III]	1749	0.428±0.038	0.45	0.388	0.376	0.369
N IV]	1487	0.468±0.035	0.553	0.544	0.518	0.500
N V	1240	0.305±0.019	0.391	0.302	0.272	0.269
[O I]	63.2 μm	0.29±0.29	0.36	0.439	0.464	0.476
[O I]	6300	1.22±0.32	1.02	1.02	1.08	1.19
[O II]	7325	0.116±0.03	0.111	0.106	0.117	0.125
[O II]	3727	3.29±0.82	2.99	2.69	2.97	3.32
[O III]	52μm	2.50±0.14	2.34	2.23	2.20	2.10
[O III]	5007	26.44±2.11	25.3	26.05	25.4	24.4
[O III]	4363	0.428±0.015	0.45	0.441	0.428	0.414
O III]	1663	0.963±0.038	1.05	1.03	1.00	0.973
[O IV]	25.9μm	5.46±0.25	5.76	5.91	5.79	5.59
O IV]	1403	0.534±0.092	0.54	0.517	0.490	0.419
O V]	1218	0.335±0.086	0.453	0.292	0.264	0.260
O VI	1035	0.165±0.049	0.222	0.142	0.120	0.123
[Ne II]	12.8μm	0.268±0.155	0.220	0.168	0.172	0.227
[Ne III]	15.5μm	2.13±0.72	3.13	2.12	2.12	2.13
[Ne III]	3869	2.31±0.46	3.99	3.22	3.19	3.12
Ne IV]	2423	0.94±0.16	1.19	1.16	1.12	1.09
[Ne V]	24.2μm	3.24±0.52	2.74	2.69	2.69	2.59
[Ne V]	3426	1.095±0.066	1.45	1.25	1.20	1.17
Mg II	2798	1.40±0.21	1.76	1.66	1.62	1.79
Si II	34.8μm	1.07±0.62	1.12	1.03	1.07	1.20
Si II	2335	0.16±0.06	0.218	0.191	0.201	0.239
Si III]	1892	0.29±0.26	0.401	0.501	0.474	0.464
Si IV	1397	0.13±0.08	0.140	0.215	0.188	0.185
[S II]	6720	0.82±0.41	1.50	0.988	0.958	1.21
[S II]	4070	0.055±0.023	0.1004	0.095		0.114
[S III]	18.7μm	0.64±0.11	0.625	0.685	0.715	0.837
[S III]	9532	1.74±0.37	1.92	1.67	1.74	1.57
[S IV]	10.5μm	1.16±0.39	1.73	1.44	1.32	1.27

9.7. Lexington NLR Model

This is the NLR model computed at the 1994 Lexington meeting, and is called *nlr_lex00.in* in the test suites.

Table 15 Lexington NLR Model

		Lexington	Binette	Ferland	Netzer	Péquignot	Viegas
I(Hβ)	E0	1.36	1.33	1.31	1.37	1.43	1.34
Lyα	1216	33.70	38.3	32.1	32.4	31.5	34.2
HeI	5876	0.12	0.11	0.13	0.12	0.13	0.13
HeII	4686	0.24	0.25	0.25	0.25	0.23	0.24
HeII	1640	1.62	1.60	1.74	1.53	1.56	1.67
CIII]	1909+	2.90	2.90	2.99	2.87	2.83	2.90
CIV	1549+	3.35	2.70	3.85	3.69	3.17	3.36
[NII]	6584+	2.55	1.40	3.20	3.10	2.67	2.40
NIII]	1749+	0.23	0.24	0.24	0.22	0.22	0.22
NIV]	1487+	0.21	0.20	0.23	0.22	0.21	0.21
[OI]	6300+	1.65	2.20	1.61	1.67	1.31	1.46
[OI]	63 μm	1.12	0.25	1.13		1.44	1.64
[OII]	3727+	1.42	1.60	1.44	1.58	1.30	1.20
OIII]	1663+	0.56	0.35	0.63	0.61	0.57	0.63
[OIII]	5007+	33.54	31.4	34.5	33.0	32.8	36.0
[OIII]	4363	0.32	0.30	0.34	0.31	0.30	0.33
OIV	1403+	0.36	0.49	0.30	0.36	0.42	0.25
[NeIII]	15.5 μm	1.89	1.50	2.01	1.94	2.05	1.95
[NeIII]	3869+	2.13	1.90	2.51	2.16	1.72	2.34
[Ne IV]	2423+	0.44	0.52	0.42	0.47	0.41	0.38
[NeV]	3426+	0.52	0.59	0.55	0.53	0.44	0.50
MgII	2798+	1.84	3.50	1.72	1.23	1.12	1.61
[SiII]	34.8 μm	0.90	1.00	0.96	1.07	0.96	0.52
[SII]	6720+	1.29	2.40	1.01	0.93	0.99	1.10
[SIII]	9532+	1.91	1.60	2.15	2.06	1.67	2.08
[SIII]	18.7 μm	0.49	0.36	0.61	0.57	0.52	0.37
[SIV]	10.5 μm	1.02	0.86	1.24	0.82	0.94	1.22
I(total)	E0	130	131	128	128	131	133
T(in)	E4	1.70	1.71	1.70	1.72	1.68	1.68
T(H+)	E4	1.18		1.24	1.06	1.20	1.23

Table 16 Lexington NLR vs Cloudy

		Mean	STD	90.05	94.01	96.00
I(Hβ)	E0	1.36	0.05	1.38	1.33	1.39
Lα	1216	33.70	2.76	30.0	31.6	29.7
HeI	5876	0.12	0.01	0.128	0.12	0.129
HeII	4686	0.24	0.01	0.24	0.24	0.232
HeII	1640	1.62	0.09	1.76	1.68	1.63
CIII]	1909+	2.90	0.06	2.62	2.55	2.52
CIV	1549+	3.35	0.45	3.99	3.78	3.64
[NII]	6584	1.91	0.52	2.26	2.39	2.448
NIII]	1749+	0.23	0.01	0.20	0.20	0.192
NIV]	1487+	0.21	0.01	0.286	0.27	0.260
[OI]	6300+	1.65	0.34	1.63	1.73	1.96
[OI]	63 μm	1.12	0.61	0.77	0.79	0.784
[OII]	3727+	1.42	0.17	1.33	1.45	1.60
OIII]	1663+	0.56	0.12	0.62	0.60	0.584
[OIII]	5007+	33.54	1.76	34.4	33.4	32.1
[OIII]	4363	0.32	0.02	0.327	0.32	0.306
OIV	1403+	0.36	0.09	0.35	0.38	0.326
[NeIII]	15.5 μm	1.89	0.22	1.43	1.44	1.42
[NeIII]	3869+	2.13	0.32	1.96	1.98	1.92
[Ne IV]	2423+	0.44	0.06	0.47	0.45	0.437
[NeV]	3426+	0.52	0.06	0.60	0.60	0.544
MgII	2798+	1.84	0.96	1.48	1.48	1.63
[SiII]	34.8 μm	0.90	0.22	0.87	0.90	0.935
[SII]	6720+	1.29	0.63	0.91	0.91	1.18
[SIII]	9532+	1.91	0.26	2.02	2.04	1.85
[SIII]	18.7 μm	0.49	0.12	0.68	0.72	0.928
[SIV]	10.5 μm	1.02	0.20	1.14	1.06	1.02
I(total)		130	1.86	125	125	124
T(in)	E4	1.70	0.02	1.7	1.69	1.70
T(H+)	E4	1.18	0.08	1.24	1.23	1.02

9.8. The DQ Her Shell

This is more or less the model of the DQ Her nebula proposed by Ferland et al. (1984). The input stream for this model is called *nova_dqher.in* in the test suite. The big difference between C90 and previous versions is in the intensity of Hβ predicted. The code no longer assumes case B when the temperature is too low to do the matrix solution. The nebula is optically thin to many Lyman lines and they escape, robbing flux from Hβ.

Table 17 The DQ Her Shell

Line		80.09	84.15	90.05	94.00	96.00
Hβ (+30)	4861	1.65	1.62	0.879	1.07	1.07
Totl	4861			0.649	0.883	0.887
Case B	4861			1.00	1.00	1.00
Lα	1216	40.9	20.7	20.6	27.9	28.7
He I	5876	0.786	0.315	0.246	0.274	0.273
He II	4686	0.166	0.085	0.0877	0.052	0.054
C II	158μ	0.777	0.62	0.092	0.102	0.103
C II	1335		0.062	0.0195	0.021	0.677
[N I]	5200	0.144		0.078	0.087	0.087
[N II]	122μm	7.85	3.43	3.22	3.58	3.603
[N III]	57μm	5.30	3.78	9.20	10.2	10.4
[O II]	3727	1.16	0.304	0.294	0.325	0.331
[O III]	88μm	12.1	6.36	4.95	5.45	5.40
[O III]	52μm	12.4	6.60	5.51	6.06	6.00
[Si II]	35μm	0.586	0.79	0.83	0.92	0.93
[S III]	34μm	0.114	0.167	0.230	0.258	0.398
[Fe II]		0.121	0.187	0.137	0.151	0.154
<Te>	K		643	862	853	860

9.9. The Kwan and Krolik Standard Model

Table 18. The Kwan and Krolik Standard Model.

Line	KK81	80	84.15	90.05	94.00	96.00
Lα 1216	5.512+7[7]	5.78	5.59	6.03	5.98	6.03
Lα 1216	100	100	100	100	100	100
Hβ 4861	10.3	6.37	6.05	5.85	5.55	5.97
Hα 6563	42.8	19.9	19.56	24.4	17.2	18.2
BaC	47.0	38.8	39.5	59.6	58.5	64.6
PaC	30.7	20.2	20.0	37.4	34.1	39.8
2s-1s	3.3	2.35	3.19	2.70	2.95	2.78
free-free	29.0	25.3	23.3	40.5	39.2	43.9
He I 10830	4.4	2.86	2.84	3.30	2.96	3.30
He I 5876	0.9	0.697	0.845	0.68	0.64	0.690
He II 4686	-	0.365	0.316	0.29	0.27	0.272
He II 1640	2.5	3.17	2.77	2.49	2.29	2.29
C II] 2326	3.3	2.70	0.686	3.17	3.70	4.83
C II 1335	-	0.661	0.611	0.68	0.71	0.587
C III 977	5.1	7.53	6.52	5.58	5.47	5.76
C III] 1909	13.0	20.7	15.9	13.5	13.2	13.2
C IV 1549	67.0	95.7	76.3	70.2	68.1	68.1
N III] 1750	1.5	4.26	4.95	4.23	4.17	3.67
N III 990	-	0.324	1.35	1.40	1.35	1.35
N IV] 1486	5.8	4.88	5.24	5.27	5.13	5.13
N V 1240	8.4	3.61	4.95	3.78	3.72	3.72
O I 1304	6.9	4.01	3.93	5.13	8.21	6.44
O III] 1663	9.5	18.4	18.3	18.6	18.3	18.6
O IV] 1402	5.2	4.81	5.84	6.20	6.04	5.15
O V] 1218	6.7	3.07	4.63	3.23	3.15	3.25
O VI 1034	15.0	2.85	4.71	2.92	2.85	2.98
Mg II 2798	18.0	17.6	9.71	30.0	33.8	34.6
Si III] 1892	-	14.6	15.7	11.6	12.2	12.6
Si IV 1397	5.5	14.2	9.77	8.54	7.60	7.75
Fe II	23.9	9.58	11.3	13.6	15.5	13.2
Fe Kα		2.11	1.74	1.78	1.81	1.80

Table 18 gives the spectrum of the Kwan and Krolik (1981) standard model, called *blr_kk.in* in the test suite.

[7]Line intensity in erg s^{-1} cm^{-2}. The entries which follow are relative to a scale where Lyα=100.

9.10. Rees, Netzer, and Ferland, low density

This is the lower density model listed in Table 1 of Rees et al. (1989). It is *blr_rnfa.in* in the sample input streams.

Table 19 Rees, Netzer, and Ferland, low density case.

	1989	90.05	94.00	95.00	Ion
log n = 10					
Lα	1.000	100	100	100	1.000
Hβ	0.030	2.76	3.18	3.44	0.026
Hα	0.197	13.0	12.1	12.5	0.180
Pα	0.022	1.45	1.43	1.31	0.020
Ba C	0.127	13.3	12.1	12.9	0.125
Pa C	0.052	5.01	4.54	4.90	0.025
ff	0.082	8.38	8.24	8.61	0.089
HeI 5876	0.007	0.656	0.584	0.623	0.008
HeII 4686	0.005	0.39	0.392	0.397	0.004
HeII 1640	0.039	3.44	3.38	3.42	0.034
CII 1335	0.009	1.04	1.00	0.880	0.008
CII] 2326	0.014	1.05	0.96	1.59	0.011
CIII 977	0.030	2.59	2.52	2.58	0.035
CIII] 1909	0.106	9.91	9.66	9.96	0.103
CIV 1549	0.424	44.8	42.9	42.3	0.453
NIII] 1750	0.012	1.31	1.26	1.06	0.014
NIV] 1486	0.009	1.19	1.14	1.13	0.009
NV 1240	0.002	0.235	0.22	0.225	0.003
OI 1304	0.033	0.91	0.915	1.27	0.013
OI 8446	0.005	0.0579	0.064	0.066	0.005
OIII] 1663	0.055	6.17	5.92	6.00	0.060
OIV] 1402	0.011	1.41	1.35	1.18	0.017
Mg II 2798	0.076	19.2	18.4	21.5	0.160
SiIII 1207	0.012	1.04	1.05	1.07	0.013
SiIII] 1892	0.085	8.56	8.51	9.13	0.090
SiIV 1397	0.048	4.47	4.10	4.16	0.044
FeII	0	1.79	2.77	3.46	0.052
Kα	0	0.098	0.102	0.103	0.001
sum	2.492	254.2169	248.787	255.764	2.602
Lα	4.85E+07	4.54+07	4.42+7	4.39	4.55+07
I(total)	6.03E+07	1.15+8	1.09+8		6.02+07

9.11. Rees, Netzer, and Ferland, high density

Table 20 Rees, Netzer, and Ferland, high density case.

	1989	90.05	94.00	96.00	Ion
	log n = 12				
Lα	1.000	100	100	100	1.000
Hβ	0.063	1.99	1.66	1.62	0.054
Hα	0.175	5.87	3.00	2.94	0.134
Pα	0.009	0.45	0.22	0.212	0.008
Ba C	2.938	230	234	233	2.680
Pa C	1.313	104	104	107	0.590
ff	1.563	114	120	119	1.300
HeI 5876	0.038	3.13	3.42	3.27	0.032
HeII 4686	0.030	2.78	2.76	2.69	0.017
HeII 1640	0.266	17.5	18.3	17.8	0.140
CII 1335	0.082	4.67	4.84	4.34	0.099
CII] 2326	0.003	0.14	0.18	0.312	0.002
CIII 977	0.225	9.95	11.5	11.2	0.150
CIII] 1909	0.023	0.85	0.92	0.895	0.014
CIV 1549	0.938	55.4	62.7	59.9	0.860
NIII] 1750	0.006	0.26	0.28	0.182	0.004
NIV] 1486	0.006	0.35	0.36	0.341	0.004
NV 1240	0.031	2.15	2.34	2.20	0.021
OI 1304	0.033	2.01	1.98	2.05	0.028
OI 8446	0.006	0.26	0.27	0.276	0.005
OIII] 1663	0.039	1.77	1.90	1.82	0.024
OIII 835	0.041	1.90	0.043	2.03	0.002
OIV] 1402	0.023	1.62	1.69	1.60	0.020
Mg II 2798	0.088	12.6	13.6	13.0	0.170
SiIII 1207	0.088	4.46	4.70	4.37	0.068
SiIII] 1892	0.113	3.37	3.72	6.79	0.061
SiIV 1397	0.300	17.5	18.9	18.3	0.230
FeII		0.77	0.99	0.832	0.015
Kα		0.38	0.42	0.405	0.003
sum	8.188	700.13	718.693	718.375	7.521
Lα	8.54+08	1.17+09	1.08+09	1.11+09	1.08+09
I(total)	7.00+09	8.19+09	7.74+09		7.04+09

This is the higher density model listed in Table 1 of Rees et al. (1989). It is *blr_rnfb.in* in the sample input streams.

10. SAMPLES - THE TEST SUITE

The code must be completely tested every time anything is changed (Ferland 2001b). This is done with the test suite that is included in the distribution. In versions 90 and before this section listed all the test cases and discussed the motivations for each. Now each input file is self-descriptive, and should be consulted to use as examples and understand how the code is run.

The test suite contains a series of Perl scripts that automate several tasks. The *readme_tests.htm* file included with the tests describes these. The script *doc_tsuite.pl* extracts the test names and the description of each, and creates two files, *doc_tsuite.htm*, a formatted description of each test, and *doc_tsuite.txt*, the table that follows this discussion. The file *doc_tsuite.htm* documents each of the test cases. The next page is an example of the contents for one test case. The large table that follows this example is contained in *doc_tsuite.txt*. Column 1 of the table lists the name of each test case and the second column gives a brief description of it.

`agn_blr_albedo.in` *measure rayleigh scattering of Lya*

```
title measure rayleigh scattering of Lya
c model from Korista, K., & Ferland, G. 1998, ApJ, 495, 672
c
c commands controlling continuum =========
agn 6.683 -1.20 -1.20 -0.90
ionization parameter 1.0
c
c commands for density & abundances =========
init file = "ism.ini"
abundances old solar 84
hden 11.0
c
c commands controlling geometry =========
stop total column density = 23.75
c
c other commands for details =========
iterate
c
c commands controlling output =========
normalize to "feka" 2
print line faint -1
*print last iteration
print diffuse continua
print lines inward
punch continuum last "agn_blr_albedo.con" units kev
punch dr "agn_blr_albedo.dr"
punch reflected continuum last "agn_blr_albedo.ref"
punch emitted continuum last "agn_blr_albedo.emt"
c
c line would appear to change the rest of the spectrum
c agn_blr_albedo.in
c class blr
c ======================================
```

This model computes the albedo of a fairly standard BLR cloud. This is the type of model that was presented in the BLR albedo paper by Korista & Ferland, 1998, ApJ 495, 672.

The print diffuse continua command enters continuum fluxs into the emission line stack. The asserts then check that these continua have the expected brightness.

The following table was generated by the perl script *doc_tsuite.pl*. This is a copy of the generated file *doc_tsuite.txt*.

Table 21 The single-model standard test cases

agn_blr_albedo.in	measure rayleigh scattering of Lya
agn_reflector.in	model of Compton reflector
agn_S_u000.in	temperature across Spitzer thermal stability S curve
agn_S_u050.in	temperature across Spitzer thermal stability S curve
agn_S_u100.in	temperature across Spitzer thermal stability S curve
agn_S_u150.in	temperature across Spitzer thermal stability S curve
agn_S_u200.in	temperature across Spitzer thermal stability S curve
agn_S_u225.in	temperature across Spitzer thermal stability S curve
agn_S_u250.in	temperature across Spitzer thermal stability S curve
agn_S_u275.in	temperature across Spitzer thermal stability S curve
agn_S_u300.in	temperature across Spitzer thermal stability S curve
agn_warm_absorber.in	simple warm absorber model
aperture_beam_int.in	test aperture beam command with intensity
aperture_beam_lum.in	test aperture beam command with luminosity
aperture_slit.in	test aperture slit command with luminosity
blr_f92.in	standard blr cloud in Ferland et al. 1992
blr_fp89.in	final F+P 1989 BLR model table 3
blr_hizqso.in	high Z quasar cloud
blr_kk81.in	old blr
blr_level2.in	test dominant blr_level2 lines
blr_n09_p18.in	BLR model, density 1e09 cm-3, flux of H-ion phots 1e18 cm2 s-1
blr_n09_p18_Z20.in	BLR model, density 1e09 cm-3, flux of H-ion phots 1e18 cm2 s-1, Z=20
blr_n09_p20.in	BLR model, density 1e09 cm-3, flux of H-ion phots 1e20 cm2 s-1
blr_n09_p20_Z20.in	BLR model, density 1e09 cm-3, flux of H-ion phots 1e20 cm2 s-1, Z=20
blr_n09_p22.in	BLR model, density 1e09 cm-3, flux of H-ion phots 1e20 cm2 s-1
blr_n09_p22_Z20.in	BLR model, density 1e09 cm-3, flux of H-ion phots 1e22 cm2 s-1, Z=20
blr_n11_p20.in	BLR model, density 1e11 cm-3, flux of H-ion phots 1e20 cm2 s-1
blr_n11_p20_Z20.in	BLR model, density 1e11 cm-3, flux of H-ion phots 1e20 cm2 s-1, Z=20
blr_n12_p19.in	BLR model, density 1e12 cm-3, flux of H-ion phots 1e19 cm2 s-1
blr_n12_p19_Z20.in	BLR model, density 1e12 cm-3, flux of H-ion phots 1e19 cm2 s-1, Z=20
blr_n13_p18.in	BLR model, density 1e13 cm-3, flux of H-ion phots 1e18 cm2 s-1
blr_n13_p18_Z20.in	BLR model, density 1e13 cm-3, flux of H-ion phots 1e18 cm2 s-1, Z=20
blr_n13_p22.in	BLR model, density 1e13 cm-3, flux of H-ion phots 1e22 cm2 s-1
blr_n13_p22_Z20.in	BLR model, density 1e13 cm-3, flux of H-ion phots 1e18 cm2 s-1, Z=20
blr_nf84.in	early model of blr
blr_nf84_45deg.in	early model of BLR, with illumination at 45 degree angle
blr_rnfa.in	table 1 of Rees et al. ApJ 347, 648
blr_rnfb.in	table 1 of Rees et al. ApJ 347, 648
c6_caseb.in	c6_caseb C VI case B
coll_coronal.in	model of active region of solar corona
coll_heat_only.in	test code in limit where ONLY mechanical heating is present
coll_t4.in	coronal equilibrium at 10^4 K
coll_t5.in	coronal equilibrium at 10^5 K
coll_t6.in	coronal equilibrium at 10^6 K
coll_t7.in	coronal equilibrium at 10^7 K
feii_hin.in	test feii in high density limit
feii_hirad.in	feii in case of high radiation density limit
feii_pump.in	test feii in continuum pumped limit
feii_ste.in	thermal equilibrium of FeII in STE limit
func_abund_fluc.in	this runs the standard, one command, test, which contains many asserts
func_distance.in	check that distance and "print flux earth" commands work

func_globule.in	test of globule command
func_hotgas_coolstar.in	test very soft continuum, very hot gas
func_ion_increase.in	test model where ionization increases with depth
func_map.in	map of heating vs cooling
func_set_ion.in	test impact of setting ionization
func_stopline.in	test stop line command
func_t10.in	test very soft continuum, very hot gas
func_t30.in	test very soft continuum, very hot gas
func_test.in	this runs the standard, one command, test, which contains many asserts
func_trans_punch.in	first of func_trans_punch/transread pair, punch continuum
func_trans_read.in	second of transpunch/transread pair, used transmitted continuum
grains_hot.in	test temperature of gas and dust in high energy density environment
grains_lte.in	check that grains equilibriate at correct temp in ste limit
grains_qheat.in	cool atomic ISM with Si grain quantum heating
grains_temp.in	test all grain species temperature
grains_temp_all.in	test all grain species temperature
h2_cr.in	background cosmic ray ionization by suprathermal electrons only
h2_cr_grains.in	background cosmic ray ionization by suprathermal electrons only
h2_hminus.in	H2 populations in H- dominated limit
h2_pdr_leiden_f1.in	low density flux model 1 as defined in e-mail
h2_solomon.in	H2 populations in solomon dominated limit
h2_t2000.in	test large H2 molecule in shock-like conditions
h2_t500.in	test large H2 molecule in PDR-like conditions
h_casea.in	case A
h_caseb_lon.in	low density case b
h_caseb_lot.in	log density case B, T=5000, log n=2
h_caseb_n8.in	h_caseb_n8 high density case B
h_casebn2.in	log density case B, T=5000, log n=2
h_casec.in	case C
h_induc.in	constant temper black body limit from Ferland and Rees 1988
h_lrg_atom.in	h_lrg_atom case B with largest possible H atom
h_lym_thin.in	H only optically thin in Lyman continuum
h_otsopen.in	test ots, inward fractions for pure hydrogen, open geo, filling factor
h_otspp.in	plane parallel conservation and hydrogenic emission for pure hydrogen
h_otssp.in	spherical conservation and hydrogenic emission for pure hydrogen
h_outopen.in	test inward fractions, open geo, filling factor, 2-photon emission
h_outpp.in	plane parallel H-only, close, test hydrogenic emission
h_outsp.in	spherical conservation and hydrogenic emission for pure hydrogen
h_t4_conemis.in	test continuous emission from model H atom
h_t4_conemis.in	punch continuum "h_t4_conemis.con" last no units microns
h_t4_conemis.in	punch spectrum "h_t4_conemis.ncon" last no units microns
h_t4_conemis_lon.in	test low-den continuous emission from H atom, 2-nu is important
h_t4_conemis_thick.in	test hydrogen atom continuous emissivity, used for plot in hazy
he1n2t4.in	test hei atom vs Benjamin et al. 99
he1n2t4_best.in	test hei atom vs Benjamin et al. 99
he1n2t4_Smits96.in	test hei atom vs Smits 96
he1n4t4.in	test hei atom vs Benjamin et al. 99
he1n4t4.in	punch diffuse continuum "he1n4t4.dif" last no units microns
he1n4t4.in	punch continuum "he1n4t4.con" last no units microns
he1n4t4_best.in	the best we can do to predict the HeI emission spectrum
he1n4t4_best.in	punch diffuse continuum "he1n4t4_best.dif" last no units microns
he1n4t4_best.in	punch continuum "he1n4t4_best.con" last no units microns
he1n6t4.in	test hei atom vs Benjamin et al. 99
he1n6t4_best.in	test hei atom vs Benjamin et al. 99
he1n6t4_Smits96.in	test hei atom vs Smits 96

he2_caseb.in	he2_caseb He II case B
heatomt10.in	continuous emission from HeI
heatomt10.in	punch spectrum "heatomt10.spc" last no units microns
heatomt10.in	punch continuum "heatomt10.con" last no units microns
heatomt10.in	punch diffuse continuum "heatomt10.dif" last no units microns
heatomt10lon.in	test low-den continuous emission from H atom, 2-nu is important
heiont10.in	continuous emission from HeII
heiont10.in	punch continuum "heiont10.con" last no units microns
heiont10.in	punch spectrum "heiont10.spc" last no units microns
helike_ar.in	test he-like argon ion
helike_c.in	test he-like carbon ion
helike_co.in	test he-like cobalt ion
helike_cu.in	test he-like copper ion
helike_fe.in	test he-like iron ion
helike_mg.in	test he-like magnesium ion
helike_n.in	test he-like nitrogen ion
helike_ne.in	test he-like neon ion
helike_ni.in	test he-like nickel ion
helike_o.in	test he-like oxygen ion vs. Bautista & Kallman 2000 Table 1, column 3
helike_si.in	test he-like silicon ion
helike_zn.in	test he-like zinc ion
hhe_otspp.in	plane parallel conservation and hydrogenic emission for pure H, He
hhe_otssp.in	pherical conservation and hydrogenic emission for hydrogen and helium
hhe_outpp.in	plane parallel conservation and H, He emission for pure H, He gas
hhe_outppff.in	plane parallel filling factor for pure H, He gas
hhe_outsp.in	spherical conservation and hydrogenic emission for hydrogen and helium
hii_blister.in	conditions similar to Orion nebula hii_blister
hii_coolstar.in	cool HII region model from Lexington Meeting
hii_icf.in	HII region with negative He/H ICF
hii_paris.in	"New" Paris meeting HII region
igm_lalpha.in	Ly alpha forest cloud
igm_primal.in	cloud with primordial abundances exposed to background at Z=10
igm_z3.in	redshift 1000 recombination epoch
ism.in	interstellar cloud irradiated by ism background
ism_cosmicray.in	background cosmic ray ionization by suprathermal electrons only
ism_hot_brems.in	generate continuum due to hot ism in high Z,z starburst
ism_hot_brems.in	punch continuum last "ism_hot_brems.con" no title, units keV
ism_jura.in	check rate H2 forms on grain surfaces
ism_opacity.in	generate standard ISM opacity curve
ism_set_cr_rate.in	background cosmic ray ionization by suprathermal electrons only
limit_compton_hi_t.in	compton exchange in high temper limit
limit_compton_lo_t.in	compton exchange near low temperature limit
limit_compton_mid_t.in	Compton limit, test continuum partition
limit_conserve.in	test that energy is limit_conserved
limit_eden.in	Martin Gaskell's funny model
limit_laser_1.in	test of H ionization in optically thin limit
limit_laser_2.in	test of H and HeI ionization in optically thin limit
limit_laser_200.in	test of ionization in optically thin Auger-dominated limit
limit_laser_200_low.in	test of ionization in optically thin Auger-dominated limit
limit_laser_3.in	test of H, HeI, and HeII ionization in optically thin limit
limit_lowd0.in	test low density limit, this and lowdm6 should get same results
limit_lowden.in	test optically thin model that extends to very low densities
limit_lowdm6.in	test low density limit, this and limit_lowdm6 should get same results
limit_lowion_low.in	test conditions of very low ionization matrix/simple solver
limit_lowion_pops.in	test conditions of very low ionization matrix/simple solver

limit_lte_h_t50_cion.in	test collisional ionization only, no excitation, should be in LTE
limit_lte_h_t50_coll.in	test collisional excitation only, very high density to force H to LTE
limit_lte_he1_coll.in	test hei atom at high densities
limit_lte_he1_ste.in	test He I atom LTE at high densities
limit_lte_hhe.in	thermal equil black body LTE limit from Ferland and Rees 1988
limit_lte_hhe_coll_t50.in	high electron density approach to LTE
limit_lte_hhe_induc.in	half H, He gas with induced BF processes dominate, go to LTE
limit_lte_hminus.in	hminus test of LTE
limit_lte_metal.in	LTE (actually strict thermodynamic equilibrium) with metals
limit_recoil_ion.in	test compton recoil ionization of hydrogen
limit_strom.in	check pure hydrogen Stromgren sphere
limit_supra.in	test very high levels of seciondary ionization, like SN envelope
limit_vbhum.in	test against Van Blerkom and Hummer, fig 4
limit_veryfast.in	very fast dusty windy model
limit_veryveryfast.in	very fast model for running with debuggers
limit_wind.in	test of equations of motion in a wind
lines.in	create output file with list of lines
nlr_lex00.in	Hagai's nlr_lex00 model for Lexington Meeting
nlr_liner.in	nlr_liner model
nlr_liner_grains.in	liner model with grains
nlr_paris.in	paris meeting NLR model
nova_dqher.in	(roughly) Ferland et al. DQ Her model
nova_photos.in	dense nova_photos shell
o8_caseb.in	o8_caseb O VIII case B
optimal.in	test optimizers, spectrum computed with hden 5, temp 4
optimize_amoeba.in	test optimizers, spectrum computed with hden 5, temp 4
optimize_phymir.in	test optimizers, spectrum computed with hden 5, temp 4
optimize_powell.in	test optimizers, spectrum computed with hden 5, temp 4
optimize_subplex.in	test optimizers, spectrum computed with hden 5, temp 4
orion_hii_dist_grn.in	conditions similar to Orion nebula blister
orion_hii_open.in	conditions similar to Orion nebula blister
orion_hii_pdr.in	constant gas pressure orion into pdr
orion_hii_pdr_fast.in	constant gas pressure orion into pdr
orion_hii_pdr_pp.in	the Orion HII Region / PDR / Molecular cloud with an open geometry
orion_hii_single_grn.in	conditions similar to Orion nebula blister
orion_wind.in	Orion nebula blister with wind
pdr_co_fully.in	test case where H2 and CO go into fully molecular limit
pdr_dense_persei.in	dense phase model of zeta persei cloud, Table 3
pdr_HTT91.in	Hollenbach et al. 1991 low-density PDR
pdr_leiden_f1.in	model 1 as defined in e-mail
pdr_leiden_f2.in	model 2 as defined in e-mail
pdr_leiden_f3.in	model 3 as defined in e-mail
pdr_leiden_f4.in	model 4 as defined in e-mail
pdr_leiden_hack_f1.in	model 1 as defined in e-mail
pdr_leiden_hack_f2.in	model 2 as defined in e-mail
pdr_leiden_hack_f3.in	model 3 as defined in e-mail
pdr_leiden_hack_f4.in	model 4 as defined in e-mail
pdr_leiden_hack_v1.in	model 5 as defined in e-mail
pdr_leiden_hack_v2.in	model 6 as defined in e-mail
pdr_leiden_hack_v3.in	model 7 as defined in e-mail
pdr_leiden_hack_v4.in	model 8 as defined in e-mail
pdr_leiden_v1.in	model 5 as defined in e-mail
pdr_leiden_v2.in	model 6 as defined in e-mail
pdr_leiden_v3.in	model 7 as defined in e-mail
pdr_leiden_v4.in	model 8 as defined in e-mail

pdr_orion_veil.in	model like Orion's veil
pdr_th85ism.in	Tielens and Hollenbach pdr model with ism grains, Table 2, paper b
pdr_th85ism_cgto.in	Tielens and Hollenbach pdr with ism grains and C > O
pdr_th85orion.in	Tielens and Hollenbach pdr model with orion grains, Table 2, paper b
pn_fluc.in	Paris meeting Planetary nebula with density fluctuations
pn_ots.in	Paris meeting Planetary nebula with ots
pn_paris.in	pn_paris.in Meudon Planetary nebula
pn_paris_fast.in	pn_paris_fast.in Meudon Planetary nebula
pn_sqrden.in	test with density falling as R^-2, and filling factor
stars_atlas.in	Model of a Compact HII Region
stars_costar.in	test costar continuum
stars_costarhalo.in	test costar halo abundances continuum
stars_kurucz.in	Model of a Compact HII Region
stars_mihalas.in	Model of a Compact HII Region
stars_rauch.in	hot PN model
stars_rauchold.in	very hot PN model
stars_starburst99.in	demonstrate use of Starburst 99 spectrum
stars_werner.in	test run with Werner stellar atmosphere

11. ATOMIC DATA SOURCES

Codes like Cloudy can only exist because of the large body of work done by the atomic and molecular physics community. This work will only continue to be supported if it is cited in the literature whenever it is used. The following is a partial list of citations for the atomic data used within the code.

This table is generated by the perl script *doc_atomic_data.pl*. This generates the file *doc_atomic_data_refer.txt* which is pasted below.

21cm	cs	Liszt, H. A&A, 371, 698
abundance	D/H	Pettini, M., & Bowen, D.V., 2001, ApJ, 560, 41
AGN	cont	Mathews and Ferland ApJ Dec15 '87
Al	CT	Pequignot, D., & Aldrovandi, S.M.V., 1986, A&A, 161, 169-176
al10	cs	Keenan, F.P. Berrington, K.A., Burke, P.G., Dufton, P.L Kingston
al11	cs	Cochrane, D.M., & McWhirter, R.W.P. 1983, PhyS, 28, 25
al2	cs	Tayal, S.S., Burke, P.G., Kingston, A.E. 1985, J.Phys. B, 18, 4321
al2	cs	Tayal, S.S., Burke, P.G., Kingston, A.E. 1984, J.Phys. B, 17, 3847
al2	cs	Keenan, F.P., Harra, L.K., Aggarwal, K.M., Feibelman, W.A. 1992
al3	as	Dufton, P.L., Brown, P.J.F., Lennon, D.J., Lynas-Gray, A.E. 1986 M
al3	cs	Dufton, P.L., & Kingston, A.E. 1987, J.Phys. B, 20, 3899
al5	cs	Saraph, H.E. & Tully, J.A. 1994, A&AS, 107, 29
al6	cs	Butler, K., & Zeippen, C.J. 1994, A&AS, 108, 1
al8	cs	Lennon, D.J. Burke, V.M. 1994, A&AS, 103, 273
all	all	Mendoza, C. 1982, in Planetary Nebulae, IAU Symp No. 103 ed b Holland), 143
all	atomic weight	Coplen, T.B. 2001, J. Phys. Chem REf Data, 30, 701
all	auger	Kaastra, J.S., & Mewe, R. 1993, A&AS, 97, 443-482
all	auger	Kaastra, J.S., & Mewe, R. 1993, 97, 443-482
all	Auger	Kaastra, J.S., & Mewe, R., 1993, A&AS, 97, 443
all	Auger	Kaastra, J.S., & Mewe, R., 1993, A&AS, 97, 443
all	coll_ion	Voronov G.S., 1997, At. Data Nucl. Data Tables 65, 1
all	collion	Voronov, G. S., 1997, At. Data Nucl. Data Tables, 65, 1
all	cs	Mendoza, C. 1982, in Planetary Nebulae, IAU Symp No. 103 ed b Holland), 143
all	cs	Mendoza, C. 1982, in Planetary Nebulae, IAU Symp No. 103 ed b Holland), 143
all	diel	Ali, B., Blum, R. D., Bumgardner, T. E., Cranmer, S. R., Ferland, G 1991, PASP, 103, 1182
all	DR	Kraemer, S.B., Ferland, G.J., & Gabel, J.R. 2004, ApJ, 604, 556
all	dr	Mazzotta, P., Mazzitelli, G., Colafrancesco, S & Vittorio, N. 1998,
all	photocs	Verner, Ferland, Korista, Yakovlev, 1996, ApJ, in press
all	photoerode	Boyd, R., & Ferland, G.J. ApJ, 318, L21
all	reccoef	Verner & Ferland, 1996, ApJS, 103, 467
all	recom	Shull & Van Steenberg, 1982, ApJS, 48, 95
Ar+1	CT	Butler, S.E., & Dalgarno, A., 1980b, ApJ, 241, 838
Ar+2	CT	Butler, S.E., & Dalgarno, A., 1980b, ApJ, 241, 838

Ar+3	CT	Butler, S.E., & Dalgarno, A., 1980b, ApJ, 241, 838
Ar+4	CT	Butler, S.E., & Dalgarno, A., 1980b, ApJ, 241, 838
Ar10	cs	Saraph, H.E. & Tully, J.A. 1994, A&AS, 107, 29
Ar14	as	Froese Fischer, C. 1983, J.Phys. B, 16, 157
Ar14	cs	Keenan, F.P., Katsiyannis, A.C., Reid, R.H.G., Pradhan, A.K Zhang, H.
ar16	??	Cochrane, D.M., & McWhirter, R.W.P. 1983, PhyS, 28, 25
Ar2	as	Nussbaumer, H., & Storey, P.J. 1988, A&A, 200, L25
Ar2	cs	Pelan, J., & Berrington, K.A. 1995, A&A Suppl, 110, 209
ar3	cs	Galavis, M.E., Mendoza, C., & Zeippen, C.J. 1995, A&AS, 111, 347
ar3	cs	Galavis, M.E., Mendoza, C., & Zeippen, C.J. 1995, A&AS, 111, 347
ar4	cs	Zeippen, C.J., Le Bourlot, J., Butler, K. 1987, A&A, 188, 251
ar4	cs	Ramsbottom, C.A., Bell., K.L., & Keenan, F.P., 1997 MNRAS 284, 754
ar4	cs	Ramsbottom, C.A., & Bell, K.L. 1997, At. Data Nucl. Data Tables, 66, 6
Ar5	as	Mendoza, C., & Zeippen, C.J. 1982, MNRAS, 199, 1025
Ar5	as	Mendoza, C. 1982, in Planetary Nebulae, IAU Symp No. 103 ed by D.F Holland), 143
Ar5	cs	Galavis, M.E., Mendoza, C., & Zeippen, C.J. 1995, A&AS, 111, 347
Ar5	cs	Galavis, M.E., Mendoza, C., & Zeippen, C.J. 1995, A&AS, 111, 347
ar6	cs	Saraph, H.E., & Storey, P.J. A&AS, 115, 151
background	continuum	Haardt, F. & Madau, P. 1996, ApJ, 461, 20
background	continuum	Haardt, F. & Madau, P. 1996, ApJ, 461, 20
blr	cloud	Kwan, J., & Krolik, J. 1981, ApJ, 250, 478
blr	model	Netzer, H., & Ferland, G. J. 1984, PASP, 96, 593
blr	model	Netzer, H., & Ferland, G. J. 1984, PASP, 96, 593
blr	model	Rees, M. J., Netzer, H Ferland, G. J. 1989, ApJ, 347, 640
blr	model	Rees, M. J., Netzer, H., & Ferland, G. J 1989, ApJ, 347, 640
C	abund	Allende Prieto, C Lambert, D.L., & Asplund, M., 2002, ApJ, 573, L137
C	DR	Nussbaumer H. & Storey, P 1983, A&A, 126, 75
c	hei	intensity
c	test	model Hollenbach, D., Takahashi, T
C+1	CT	Butler, S.E., Heil,T.G., & Dalgarno, A. 1980, ApJ, 241, 442
C+3	CT	Butler, S.E., & Dalgarno, A., 1980b, ApJ, 241, 838
C+4	CT	Butler, S.E., & Dalgarno, 1980b
c1	as	Mendoza, C. 1982, in Planetary Nebulae, IAU Symp No. 103 ed by D.F Holland), 143
c1	cs	Tielens, A.G.G., & Hollenbach, D. 1985, ApJ, 291, 722
c1	cs	Johnson, C.T., Burke, P.G., Kingston, A.E. 1987, JPhB, 20, 2553
c1	cs	Launay & Roueff 1977, A&A 56, 289
C1	cs	Roueff, E. & Le Bourlot, J. 1990, A&A 236, 515
c1	cs	Schroeder et al. 1991, J.Phys.B 24, 2487
C1	rec	Escalante, Vladimir, & Victor, G.A., 1990, ApJS 73, 513
c2	as	Froese Fischer, C. 1983, J.Phys. B, 16, 157
c2	as	Nahar, S.N. 2003, ADNDT, 80, 205
c2	as	Nahar, S.N. 2003, ADNDT, 80, 205
c2	as	Lennon, D.J., Dufton, P.L., Hibbert, A., Kingston, A.E. 1985, ApJ, 294, 2
c2	cs	Blum, R.D., & Pradhan, A.K. 1992, ApJS 80, 425

c2	cs	Tielens, A.G.G., & Hollenbach, D. 1985, ApJ, 291, 722
c2	cs	Wilson, N.J., & Bell, K.L. 2002, MNRAS, 337, 1027-1034
c2	cs	Barinovs, G., van Hemert, M., Krems, R. & Dalgarno, A. 2005, Ap
c2	cs	Lennon, D.J., Dufton, P.L., Hibbert, A., Kingston, A.E. 1985, ApJ,
c2	cs	Blum, R.D., & Pradhan, A.K. 1992, ApJS 80, 425
c2	cs	Blum, R.D., & Pradhan, A.K., 1992, ApJS 80, 425
c2	cs	Lennon, D.J., Dufton, P.L., Hibbert, A., Kingston, A.E. 1985, ApJ,
c2	cs	Blum, R.D., & Pradhan, A.K., 1992, ApJS 80, 425
C3	13C As	Clegg, R.E.S., Storey, P.J., Walsh, J.R., & Neale, L 1997, MNRAS,
c3	as	Kwong, V., Fang, Z., Gibbons, T.T., Parkinson, W.H., Smith, P.L
c3	as	Fleming, J., Bell, K.L, Hibbert, A., Vaeck, N., Godefroid, M.R 199
c3	cs	Berrington, K.A., Burke, P.G., Dufton, P.L., Kingston, A.E. 1985 A
c3	cs	Berrington, K.A., Burke, P.G., Dufton, P.L., Kingston, A.E. 1985 A
c3	cs	Berrington, K.A. 1985, J.Phys. B, 18, L395
c4	cs	Cochrane, D.M., & McWhirter, R.W.P. 1983, PhyS, 28, 25
c6	cs	Aggarwal, K.M., & Kingston, A.E. 1991, J Phys B, 24, 4583
ca12	cs	Saraph, H.E. & Tully, J.A. 1994, A&AS, 107, 29
ca18	cs	Cochrane, D.M., & McWhirter, R.W.P. 1983, PhyS, 28, 25
ca2	as	Zeippen, C.J. 1990, A&A, 229, 248
ca2	cs	Saraph, H.E. 1970, J.Phys. B, 3, 952
ca2	cs	Chidichimo, M.C. 1981, J.Phys. B, 14, 4149
ca20	cs	Aggarwal, K.M., & Kingston, A.E. 1992, J Phys B, 25, 751
ca4	as	Mendoza, C. 1982, in Planetary Nebulae, IAU Symp No. 103 ed b Holland), 143
ca4	cs	Pelan, J., & Berrington, K.A. 1995, A&A Suppl, 110, 209
ca5	as	Mendoza, C. 1982, in Planetary Nebulae, IAU Symp No. 103 ed b Holland), 143
ca5	as	Mendoza, C. 1982, in Planetary Nebulae, IAU Symp No. 103 ed b Holland), 143
ca5	cs	Galavis, M.E., Mendoza, C., & Zeippen, C.J. 1995, A&AS, 111, 34
ca5	cs	Galavis, M.E., Mendoza, C., & Zeippen, C.J. 1995, A&AS, 111, 34
ca7	cs	Galavis, M.E., Mendoza, C., & Zeippen, C.J. 1995, A&AS, 111, 34
ca72	cs	Galavis, M.E., Mendoza, C., & Zeippen, C.J. 1995, A&AS, 111, 34
ca8	cs	Saraph, H.E., & Storey, P.J. A&AS, 115, 151
Cl	CT	Pequignot, D., & Aldrovandi, S.M.V., 1986, A&A, 161, 169-176
Cl1	cs	Hollenbach, D. & McKee, C.F. 1989, ApJ, 342, 306
cl2	as	Mendoza, C., & Zeippen, C.J. 1983, MNRAS, 202, 981
Cl2	As	Mendoza, C., & Zeippen, C.J. 1983, MNRAS, 202, 981
cl2	cs	Wilson, N.J., & Bell, K.L. 2002, MNRAS, 331, 389
Cl2	cs	Keenan, F.P., Aller, L.H., Exter, K.M., Hyung, S Pollacco, D.L. 20
cl3	all	Mendoza, C. 1982, in Planetary Nebulae, IAU Symp No. 103 ed b Holland), 143
cl4	cs	Galavis, M.E., Mendoza, C., & Zeippen, C.J. 1995, A&AS, 111, 34
cl5	cs	Saraph, H.E., & Storey, P.J., 1999, A&AS, 134, 369
cl9	as	Saraph, H.E. & Tully, J.A. 1994, A&AS, 107, 29
CMB	temp	Mather, J.C., Fixsen, D.J., Shafer, R.A., Mosier, C Wilkinson, D.T.

CO	chem	Terzieva, R., & Herbst, E. 1998, ApJ, 501, 207
CO	dissoc	Hollenbach, D.J., Takahashi, T., & Tielens, A. 1991, ApJ, 377, 192
CO	dissoc	Black, J.H., & van Dishoeck, E.F. 1988, ApJ, 334, 771
co11	as	Pelan, J., & Berrington, K.A. 1995, A&A Suppl, 110, 209
CO-H2	collision	de Jong, T., Chu, S-I., & Dalgarno, A. 1975, ApJ, 199, 69
CO-He	collision	McKee, C.F., Storey, J.W.V., Watson, D.M., & Green, S., 1982, ApJ, 259,
continuum	background	Haardt, Francesco, & Madau, Piero, 1996 ApJ, 461, 20
continuum	background	Haardt, Francesco, & Madau, Piero, 1996, ApJ, 461, 20
continuum	background	Haardt, Francesco, & Madau, Piero, 2005, in preparation
continuum	CrabNebula	Davidson, K., and Fesen, 1985, ARAA
continuum	RT	Lightman, A.P., & White, T.R. 1988, ApJ, 335, 57
continuum	synchrotron	Rybicki, G. B., & Lightman, A.P. 1979 Radiative Processes in Astrophy
cosmic	background	Ostriker and Ikeuchi ApJL 268, L63
cosmic	background	Ikeuchi, S.; Ostriker, J. P., 1986, ApJ 301, 522
cosmic ray	ionization rate	Tielens, A.G.G.M., & Hollenbach, D., 1985, ApJ, 291, 722
cosmic ray	ionization rate	Maloney, P.R., Hollenbach, D., & Tielens, A. G. G. M., 1998, ApJ, 466, 5
cosmic ray	ionization rate	McKee, C.M., 1999, astro-ph 9901370
cosmic ray	ionization rate	Tielens, A.G.G.M., & Hollenbach, D., 1998, ApJ, 291, 722
cosmic ray	ionization rate	McKee, C.M., 1999, astro-ph 9901370
cosmicray	ionization	Williams, J.P., Bergin, E.A., Caselli, P Myers, P.C., & Plume, R. 1998, A
cosmicray	ionization	Williams, J.P., Bergin, E.A., Caselli, P Myers, P.C., & Plume, R. 1998, A
cr	heating	Wolfire et al.1995, ApJ, 443, 152
cr	ion	Williams, J.P., Bergin, E.A., Caseli, P., Myers, P.C., & Plume, R. 1998, A
Cr16	cs	Saraph, H.E. & Tully, J.A. 1994, A&AS, 107, 29
Cr8	cs	Pelan, J., & Berrington, K.A. 1995, A&A Suppl, 110, 209
cs	gbar	Fisher et al. (1996
cs	gbar	Gaetz & Salpeter (1983, ApJS 52, 155) and
cs	gbar	Mewe (1972, A&A 20, 215
dr	guess	Kraemer, S.B., Ferland, G.J., & Gabel, J.R. 2004, ApJ in press
ee	brems	Stepney and Guilbert, MNRAS 204, 1269 (1983
esc	prob	Bonilha et al. Ap.J. (1979) 233 649
f2	as	Buttler, K., & Zeippen, C.J., 1994, A&AS 108, 1
f2	cs	Galavis, M.E., et al. 1997, A&AS 123, 159
f4	cs	Lennon, D.J. Burke, V.M. 1994, A&AS, 103, 273
Fe	abund	Holweger, H., 2001, Joint SOHO/ACE workshop "Solar and Galactic C Robert F. Wimmer-Schweingruber. Publisher American Institute of Ph proceedings vol. 598 location: Bern Switzerland, March 6 - 9, 2001., p.2
Fe	CT	Tielens, A.G.G.M., & Hollenbach, D., 1985a, ApJ, 294, 722-746
Fe	CT	Prasad, S.S., & Huntress, W.T., 1980, ApJS, 43, 1-35
Fe	CT	Pequignot, D., & Aldrovandi, S.M.V., 1986, A&A, 161, 169-176
Fe	inner shell	Behar, E., Sako, M, Kahn, S.M 2001, ApJ, 563, 497-504
Fe	inner shell	Behar, E., & Netzer, H., 2002, ApJ, 570, 165-170
Fe	inner shell	Behar, E., Sako, M, Kahn, S.M 2001, ApJ, 563, 497-504
Fe	inner shell	Behar, E., & Netzer, H., 2002, ApJ, 570, 165-170
fe	rec	Arnaud, M. & Raymond, J 1992, ApJ, 398, 394
Fe1	As	Grevesse, N., Nussbaumer, H., & Swings, J.P. 1971, MNRAS, 151, 239-

Fe1	cs	Hollenbach & McKee 89
fe10	As	Aggarwal, K.M. & Keenan, F.P. 2004, A&A, 427, 763
fe10	as	Aggarwal, K.M. & Keenan, F.P. 2004, A&A, 427, 763
fe10	cs	Tayal, S.S., 2000, ApJ, 544, 575-580
fe10	cs	Aggarwal, K.M. & Keenan, F.P. 2005, A&A, 439, 1215
fe11	as	Mason, H. 1975, MNRAS 170, 651
fe11	as	Mendoza, C., & Zeippen, C.J. 1983, MNRAS, 202, 981
fe11	as	Fritzsche, S., Dong, C.Z., & Traebert, E., 2000, MNRAS, 318, 263
Fe11	as	Mendoza C. & Zeippen, C. J. 1983, MNRAS, 202, 981
fe11	as	Fritzsche, S., Dong, C.Z., & Traebert, E., 2000, MNRAS, 318, 263
Fe11	cs	Aggarwal, K.M., & Keenan, F.P. 2003, MNRAS, 338, 412
fe11	cs	Kafatos, M., & Lynch, J.P. 1980, ApJS, 42, 611
fe11	cs	Tayal, S.S., 2000, ApJ, 544, 575-580
fe11	energy	Fritzsche, S., Dong, C.Z., & Traebert, E., 2000, MNRAS, 318, 263
fe12	as	Tayal, S.S., & Henry, R.J.W. 1986, ApJ, 302, 200
fe12	cs	Tayal, S.S., Henry, R.J.W., Pradhan, A.K. 1987, ApJ, 319, 951
fe13	as	Shirai, T., Sugar, J., Musgrove, A., & Wiese, W.L., 2000 J Phys Ch
Fe13	as	Huang, K.-N. 1985, At. Data Nucl. Data Tables 32, 503
fe13	cs	Tayal, S.S., 2000, ApJ, 544, 575-580
Fe14	as	Trabert, E. 2004, A&A, 415, L39
Fe14	cs	Storey, P.J., Mason, H.E., Saraph, H.E., 1996, A&A, 309, 677
fe14	cs	Storey, P.J., Mason, H.E., Saraph, H.E., 1996, A&A, 309, 677
Fe17-23	recom	Arnaud & Raymond, 1992, ApJ, 398, 394
fe18	cs	Saraph, H.E. & Tully, J.A. 1994, A&AS, 107, 29
fe19	cs	Butler, K., & Zeippen, C.J., 2001, A&A, 372, 1083
fe2	as	Nahar, S., 1995, A&A 293, 967
fe2	as	Quinet, P., LeDourneuf, M., & Zeipppen C.J., 1996, A&AS, 120, 3
fe2	as	Furh, J.R., Martin, G.A., & Wiese, W.L., 1988; J Phys Chem Ref D
fe2	as	Giridhar, S., & Arellano Ferro, A., 1995; Ref Mexicana Astron As
fe2	as	Kurucz, R.L., 1995, SAO CD ROM 23
Fe2	As	Rasssen data from ftp://ftp.wins.uva.nl/pub/orth/iron
Fe2	As	Quinet, LeDourneuf, & Zeipppen (1996; A&AS 120, 361
Fe2	As	Furh, Martin, & Wiese (1988; J Phys Chem Ref Data 17, Suppl 4
Fe2	As	Giridhar & Arellano Ferro (1995; Ref Mexicana Astron Astrofis 3
Fe2	As	Kurucz (1995; SAO CD ROM 23
fe2	cs	Zhang, H.L., & Pradhan, A.K., 1995, A&A 293, 953
fe2	cs	Bautista, M., (private communication
fe2	cs	Mewe, R., 1972, A&AS 20, 215 (the g-bar approximation
fe2	cs	Zhang, H.L., & Pradhan, A., 1995, A&A, 293, 953
fe2	energy	Johansson, S., Brage, T., Leckrone, D.S., Nave, G Wahlgren, G.M.
fe2	model	Wills, B.J., Wills, D., Netzer, H. 1985, ApJ, 288, 143
fe2	pump rate	Netzer, H., Elitzur, M., & Ferland, G.J., 1985, ApJ, 299, 752-762
fe20	as	Merkelis, G., Martinson, I., Kisielius, R., & Vilkas, M.J., 1999 Phys
fe20	as	Merkelis, G., Martinson, I., Kisielius, R., & Vilkas, M.J., 1999 Phys
fe20	cs	Butler, K., & Zeippen, C.J., 2001, A&A, 372, 1078
fe20	cs	Butler, K., & Zeippen, C.J., 2001, A&A, 372, 1078

Fe21	cs	Aggarwall, K.M., 1991, ApJS 77, 677
fe22	as	Dankwort, W., & Trefftz, E., 1978, A&A 65, 93-98
fe22	as	Froese Fischer, C. 1983, J.Phys. B, 16, 157
fe22	as	Dankwort, W., & Trefftz, E., 1978, A&A 65, 93-98
fe22	as	Froese Fischer, C. 1983, J.Phys. B, 16, 157
fe22	cs	Zhang, H.L., Graziani, M., & Pradhan, A.K., 1994, A&A 283, 319
fe22	cs	Zhang, H.L., Graziani, M., & Pradhan, A.K., 1994, A&A 283, 319
Fe22	energy	Feldman, U., Curdt, W., Landi, E., Wilhelm, K., 2000, ApJ, 544, 508
fe23	cs	Bhatia, A.K., & Mason, H.E. 1986, A&A, 155, 413
fe24	cs	Cochrane, D.M., & McWhirter, R.W.P. 1983, PhyS, 28, 25
fe26	cs	Aggarwal, K.M., & Kingston, A.E. 1993, ApJS, 85, 187
fe3	as	Garstang, R.H., Robb, W.D., Rountree, S.P. 1978, ApJ, 222, 384
fe3	as	Garstang, R.H., 1957, Vistas in Astronomy, 1, 268
Fe3	as	Quinet, P., 1996, A&AS, 116, 573
Fe3	cs	Zhang, H. 1996, 119, 523
Fe3	energies	version 3 NIST Atomic Spectra Database
fe6	as	Garstang, R.H., Robb, W.D., Rountree, S.P. 1978, ApJ, 222, 384
Fe7	As	Berrington, K.A., Nakazaki, S., & Norrington, P.H. 2000, A&AS, 142, 3
Fe7	As	Berrington, K.A., Nakazaki, S., & Norrington, P.H. 2000, A&AS, 142, 3
Fe7	cs	Berrington, K.A., Nakazaki, S., & Norrington, P.H. 2000, A&AS, 142, 3
fe9	all	Flower, D.R. 1976, A&A, 56, 451
free-free	gaunts	Sutherland, R.S., 1998, MNRAS, 300, 321-330
gbar	cs	Van Regemorter, H., 1962, ApJ 136, 906
gbar	cs	Mewe,R., 1972, A&A 20, 215
grain	H2 heat	Takahashi & Uehara, ApJ, 561, 843
grain	H2 heat	Takahashi & Uehara, ApJ, 561, 843
grain	phys	Hollenbach, D.J., & McKee, C.F., 1979, ApJS, 41, 555
grain	phys	Hollenbach, D.J., & McKee, C.F., 1979, ApJS, 41, 555
grain	phys	Hollenbach, D.J., & McKee, C.F., 1979, ApJS, 41, 555
grain	physics	Bakes & Tielens, 1994, ApJ, 427, 822
grain	physics	Bakes & Tielens, 1994, ApJ, 427, 822
grain	physics	Weingartner & Draine, 2001, ApJS, 134, 263
grain	physics	van Hoof P.A.M., Weingartner J.C., et al., 2004, MNRAS, 350, 1330
grain	physics	Dwek E. & Smith R.K., 1996, ApJ, 459, 686
grain	physics	Draine & Sutin, 1987, ApJ, 320, 803
grain	physics	Weingartner & Draine, ApJS, 2001, 134, 263
grain	physics	Bakes & Tielens, 1994, ApJ, 427, 822
grain	physics	Weingartner & Draine, 2000
grain	physics	Spitzer, 1948, ApJ, 107, 6
grain	physics	Draine & Sutin, 1987, ApJ, 320, 803), PvH
grain	physics	Takahashi J., Uehara H., 2001, ApJ, 561, 843
grain	physics	Baldwin, Ferland, Martin et al., 1991, ApJ 374, 580
grain	physics	Baldwin, Ferland, Martin et al., 1991, ApJ 374, 580
grain	physics	Takahashi J., Uehara H., 2001, ApJ, 561, 843
grain	physics	Draine and Salpeter 79 Ap.J. 231, 77 (1979
grain	physics	Hansen, J. E., Travis, L. D. 1974, Space Sci. Rev., 16, 527

grain	physics	Desert, F.-X., Boulanger, F., Puget, J. L. 1990, A&A, 237, 215
grain	physics	Schutte, Tielens, and Allamandola (1993) ApJ, 415, 397
grain	physics	Weingartner & Draine, 2000, ApJ
grain	physics	Voshchinnikov N.V., Mathis J.S., 1999, ApJ, 526, 257
grain	physics	Farafonov V.G., 2000, Optics & Spectroscopy, 88, 441
grain	physics	Stognienko R., Henning Th., Ossenkopf V., 1995, A&A, 296, 797
grain	physics	Bruggeman D.A.G., 1935, Ann. Phys. (5th series), 24, 636
grain	physics	Stognienko R., Henning Th., Ossenkopf V., 1995, A&A, 296, 797
grain	physics	Bruggeman D.A.G., 1935, Ann. Phys. (5th series), 24, 636
grain	physics	Guhathakurta & Draine, 1989, ApJ, 345, 230
grain	physics	Guhathakurtha & Draine, 1989, ApJ, 345, 230
grain	physics	Guhathakurta & Draine, 1989, ApJ, 345, 230
grain	physics	Draine B.T., and Li A., 2001, ApJ, 551, 807
grain	physics	Guhathakurta & Draine, 1989, ApJ, 345, 230
grain	physics	Draine B.T., and Li A., 2001, ApJ, 551, 807
grain	physics	Dwek E., Arendt R.G., Fixsen D.J. et al., 1997, ApJ, 475, 565
grain	physics	Draine B.T., and Li A., 2001, ApJ, 551, 807
grain	physics	Takahashi, Junko, 2001, ApJ, 561, 254-263
grain	physics	van Hoof et al., 2001, ASP Conf. Series 247, p. 353 (astroph/0107
H	case C	Ferland, G.J. 1999, PASP, 111, 1524
H	CT	Kingdon, J, B., & Ferland, G.J. 1996, ApJS, 106, 205
H	ionization	Van Blerkom, D., & Hummer, D. G. 1967, MNRAS, 137, 353
H	rec cooling	LaMothe, J., & Ferland, G.J., 2001, PASP, 113, 165
H	rec cooling	LaMothe, J., & Ferland, G.J., 2001, PASP, 113, 165
H	recom cool	LaMothe, J., & Ferland, G.J., 2001, PASP, in press
H-	k	Paolo Lenzuni, David F. Chernoff, Edwin E. Salpeter, 1991, ApJS
H-	k	Paolo Lenzuni, David F. Chernoff, Edwin E. Salpeter, 1991, ApJS
H-	k	Stancil, P.C, & Lepp, S, & Dalgarno, A. 1998,ApJ, 509, 1-10
H-	k	Paolo Lenzuni, David F. Chernoff, Edwin E. Salpeter, 1991, ApJS
H-	k	Stancil, P.C., Lepp, S., Dalgarno, A.1998, ApJ,509,1-10
H-	mutual neut	Lepp, S., Stancil, P.C. & Dalgarno, A. 2002, J. Phys. B, 35, R57
H-	test	Ferland, G. J., & Persson, S. E. 1989, ApJ, 347, 656
H0	collisions	Lambert, D.L
H1	21cm	Liszt, H., 2001, A&A, 371, 698
H1	A	Gould, ApJ 423, 522
H1	As	Johnson L.C., 1972 ApJ 174 227
H1	collision	Vriens, L., & Smeets, A.H.M. 1980, Phys Rev A 22, 940
H1	collision	Vriens, L., & Smeets, A.H.M. 1980, Phys Rev A 22, 940
H1	cs	Smith, F.J., 1966, Planet. Space Sci 14, 929
H1	cs	Allison, A.C., & Dalgarno A., 1969, ApJ 158, 423
H1	cs	Zygelman, B. 2005, ApJ preprint doi:10.1086/'427682
H1	cs	Anderson, H., Ballance, C.P., Badnell, N.R., & Summers, H.P 200 2002
h1	cs	Callaway, J. 1983, Phys Let A, 96, 83
h1	cs	Zygelman, B., & Dalgarno, A. 1987, Phys Rev A, 35, 4085
h1	cs	Callaway, J. 1994, At. Data Nucl. Data Tables, 57, 9

H1	cs	Allison, A.C. & Dalgarno, A., 1969, ApJ 158, 423
H1	cs	Smith, F.J., 1966, Planet. Space Sci 14, 929
H2	As	Abgrall, H., Roueff, E., & Drira, I. 2000, A&AS, 141, 297-300
H2	As	Wolnievicz, L., Simbotin, I., and Dalgarno, A 1998, ApJS, 115, 293-313
H2	chemistry	Galli,D., & Palla, F. 1998, A&A, 335, 403-420
H2	chemistry	Palla, F., Salpeter, E.E., & Stahler, S.W., 1983, ApJ,271, 632-641
H2	coll Hp	Gerlich, D., 1990, J. Chem. Phys., 92, 2377-2388
H2	coll Hp	Gerlich, D., 1990, J. Chem. Phys., 92, 2377-2388
H2	collision	Sun, Y., & Dalgarno, A., 1994, ApJ, 427, 1053-1056
H2	collision	Le Bourlot, J., Pineau des Forets, G., & Flower, D.R. 1999, MNRAS, 305
H2	collisional dissociation	Dove, J.E., and Mandy, M. E., 1986, ApJ, 311, L93
H2	collisional dissociation	Dove, J.E., and Mandy, M. E., 1986, ApJ, 311, L93
h2	cool	Lepp, S., & Shull, J.M. 1983, ApJ, 270, 578
H2	cr excit	Tine, S., Lepp, S., Gredel, R., & Dalgarno, A. 1997, ApJ, 481, 282
H2	cr excit	Dalgarno, A., Yan, Min, & Liu, Weihong 1999, ApJS, 125, 237
H2	destruction	Draine, B.T., & Bertoldi, F., 1996, ApJ, 468, 269-289
H2	dissoc	Allison, A.C. & Dalgarno, A. 1969, Atomic Data, 1, 91
H2	dissoc	Tielens, A.G.G.M., & Hollenbach, D., 1985, ApJ, 291, 722
H2	dissoc	Bertoldi, F., & Draine, B.T., 1996, 458, 222
H2	dissoc	Elwert et al., in preparation
H2	energies	Abgrall
H2	energies	Sharp, T. E., 1971, Atomic Data, 2, 119
H2	energies	Abgrall
h2	fits	Tielens, A.G.G.M., & Hollenbach, D., 1985a, ApJ 291, 722
H2	form	Cazaux, S., & Tielens, A.G.G.M., 2002, ApJ, 575, L29
H2	form	Cazaux, S., & Tielens, A.G.G.M., 2002, ApJ, 575, L29
H2	form	Cazaux, S., & Tielens, A.G.G.M., 2002, ApJ, 575, L29
H2	form	Sternberg, A. & Neufeld, D.A. 1999, ApJ, 516, 371
H2	form	Karpas, Z., Anicich, V., & Huntress, W.T. 1979, J Chem Phys, 70, 2877 ph/0404288
H2	form	Launay, J.R., Le Dourneuf, M., & Zeippen, C.J 1991, A&A, 252, 842-852
H2	form	Cazaux, S., & Tielens, A.G.G.M., 2002, ApJ, 575, L29
H2	form	Launay, J.M., Le Dourneuf, M., & Zeippen, 1991, A&A, 252, 842-852
H2	formation	Takahashi, J., & Uehara, H., 2001, ApJ, 561, 843-857
H2	formation	Le Bourlot, J, 1991, A&A, 242, 235
H2	formation	Le Bourlot, J, 1991, A&A, 242, 235
H2	formation destribution	Draine, B.T., & Bertoldi, F., 1996, ApJ, 468, 269-289
H2	grain formation	Hollenback, D., & McKee, C.F., 1979, ApJS, 41, 555 eq 3.4 3.8
H2	grain physics	Jura, M., 1974, ApJ, 197, 581
H2	grain physics	Jura, M., 1974, ApJ, 197, 581
H2	grain physics	Jura, M., 1975, ApJ, 197, 575
H2	H2_stat wght	Shull, J.M., & Beckwith, S., 1982, ARAA, 20, 163-188
H2	k	Millar, T.J. et.al, 1997,A&AS, 121, 139

H2	l	Maloney et.al, 1996,ApJ, 466, 561
H2	photo cs	Allison, A.C. & Dalgarno, A. 1969, Atomic Data, 1, 91
H2	photo cs	Yan, M., Sadeghpour, H.R., & Dalgarno, A., 1998, ApJ, 496, 1044
H2	photo cs	Yan, M., Sadeghpour, H.R., & Dalgarno, A., 1998, ApJ, 496, 1044
H2	photo cs	Yan, M.; Sadeghpour, H. R.; Dalgarno, A. 1998, ApJ, 496, 1044
H2	population	Krstic, P.S., preprint
H2	rates	Lenzuni et al. apj sup 76, 759
H2	rates	Janev et al
H2	rates	Latter, W.B., & Black, J.H., 1991, Ap.J. 372, 161
H2	rates	Lenzuni et al. apj sup 76, 759, quoted from Janev et al
H2	rot	Lepp, S., & Shull, J.M., 1983, ApJ, 270, 578-582
H2	temperature law	Sternberg, A., & Neufeld, D.A. 1999, ApJ, 516, 371-380
H2	temperature law	Draine, B.T., & Bertoldi, Frank, 1996, ApJ, 468, 269-289
H2	temperature law	Sternberg, A., & Neufeld, D.A. 1999, ApJ, 516, 371-380
H2*	k	Tielens, A.G.G.M., & Hollenbach, D., 1985, ApJ, 291, 722
H2*	k	Tielens, A.G.G.M., & Hollenbach, D., 1985, ApJ, 291, 722-746
H2*	k	Tielens, A.G.G.M., & Hollenbach, D., 1985, ApJ, 291, 722-746
H2+	chemistry	Dalgarno, A., & Lepp, S., 1987, in Astrochemistry, eds M.S. Vard Dordrecht, p 109
H2+	chemistry	Stancil, P.C., 1994, ApJ, 430, 360
H2+	k	Stancil, P.C, & Lepp, S, & Dalgarno, A. 1998,ApJ, 509, 1-10
H2+	k	Stancil, P.C, & Lepp, S, & Dalgarno, A. 1998,ApJ, 509, 1-10
H2+	photodissoc	Buckingham, R.A., Reid, S., & Spence, R. 1952, MNRAS 112, 382,
H3+	DR	McCall, B.J., et al. 2003, Nature, in press (astro-ph 0302106
H3+	DR	McCall, B.J., et al. 2003, Nature, in press (astro-ph 0302106
H3+	k	Maloney et.al, 1996,ApJ, 466, 561
H3+	k	Stancil, P. C., Lepp, S., and Dalgarno, A 509, 1-10; Table 1, reactio
HD	cooling	Puy, D., Grenacher, L, & Jetzer, P., 1999, A&A, 345, 723
He	As	Drake, G.W.F., Atomic, Molecular, and Optical Physics Handboo
He	As	Hummer, D. G. \& Storey, P. J. 1998, MNRAS 297, 1073
He	As	Drake, G.W.F, Atomic, Molecular, and Optical Physics Handboo
He	CS	Seaton, M. J. 1962, Proc. Phys. Soc. 79, 1105
He	CS	Vrinceanu, D. \& Flannery, M. R. 2001, PhysRevA 63, 032701
He	cs	Pengelly, R.M., & Seaton, M.J., 1964, MNRAS, 127, 165
He	CS	Seaton, M. J. 1962, Proc. Phys. Soc. 79, 1105
He	CS	Vrinceanu, D. \& Flannery, M. R. 2001, PhysRevA 63, 032701
He	cs	Pengelly, R.M., & Seaton, M.J., 1964, MNRAS, 127, 165
He	CT	Zygelman, B., Dalgarno, A., Kimura, M., & Lane, N.F 1989, Phys
He	CT	Stancil, P.C., Lepp, S., & Dalgarno, A. 1998, ApJ, 509, 1
He	Diel Recom	Gu, M. F. private communication, 2003
He	DR	Aldrovandi, S.M.V., & Pequignot, D. 1973, A&A 25, 137
He	FSM	Drake, G. W. F. 1996, in Atomic, Molecular, \& Optical Physics H (New York: AIP Press
He	FSM	Bauman, R. P., Porter, R. L., Ferland, G. J., \& MacAdam, K. B. 2
He	l-mixing	Seaton, M.J., 1962, Proc. Phys. Soc
He	l-mixing	Pengelly, R.M., & Seaton, M.J., 1964, MNRAS, 127, 165

He	l-mixing	Vrinceanu, D. & Flannery, M. R. 2001, PhysRevA 63, 032701
He	l-mixing	Hezel, T. P., Burkhardt, C. E., Ciocca, M., He, L-W Leventhal, J. J. 1992
He	PCS	Peach, G. 1967 MmRAS 71, 13
He	PCS	Hummer, D.G., & Storey, P.J. 1998, MNRAS 297, 1073
He	pcs	Verner, D. A., Verner, E. M., \& Ferland , G. J. 1996 Atomic Data and N p.1
He 1	cs	Bray, I., Burgess, A., Fursa, D.V., & Tully, J.A 2000, A&AS, 146, 481-49
He 1	cs	Sawey, P.M.J., & Berrington, K.A. 1993, ADNDT 55, 81
He	CS	Vriens, L., & Smeets, A.H.M. 1980, Phys Rev A 22, 940
He	l-mixing	Kazansky, A. K. & Ostrovsky, V. N. 1996, JPhysB: At. Mol. Opt. Phys.
He triplets		Robbins, R.R. 1968, ApJ 151, 497R
He1	coll	KingdonJ., & Ferland, G.J. 1995, ApJ, 442, 714-725
he1	cs	Seaton, M.S. 1964, Plan Sp Sci 12, 55
he1	cs	Berrington, Keith, 2001, private communication - email follows
He1	cs	Bray, I., Burgess, A., Fursa, D.V., & Tully, J.A., 2000, A&AS, 146, 481-4
he2	cs	Aggarwal, K.M., Callaway, J., Kingston, A.E., Unnikrishnan, K 1992, A
HeH+	k	Galli, D., & Palla, F. 1998, A&A,335,403-420
heh+	rate	Zygelman, B., and Dalgarno, A. 1990, ApJ 365, 239
HeI	2nu	Johnson,W. 2002, private communication
HeI	As	Lach, G, & Pachucki, K, 2001, Phys. Rev. A 64, 042510
HeI	icf by	Ballantyne,D.R., Ferland, G.J., & Martin, P.G., 2000, ApJ 536, 773-777
Helike	2pho	Derevianko, A., & Johnson, W.R. 1997, Phys. Rev. A 56, 1288
Helike	As	Lin, C.D., Johnson, W.R., and Dalgarno, A. 1977 Phys. Rev. A 15, 1, 010
Helike	CS	Zhang, Honglin, & Sampson, Douglas H. 1987, ApJS 63, 487
Helike	defects	Drake, G.W.F., editor. Atomic, Molecular & Optical Physics Handboo Precision Calculations for Helium", G.W.F. Drake AIP Press: Woodbu
Helike	FSM	Bauman, R., MacAdams, K., and Ferland, G. (2003
Helike	PCS	Verner, D.A., Ferland, G.J., Korista, K.T., & Yakovlev, D.G 1996a, ApJ
He-like	As	Johnson, W.R., Savukov, I.M., Safronova, U.I Dalgarno, A., 2002, ApJS
He-like	As	Savukov, I.M., Johnson, W.R., & Safronova, U.I astro-ph 0205163
He-like	As	Johnson, W.R., Savukov, I.M., Safronova, U.I Dalgarno, A., 2002, ApJS astro.ph. 0201454
He-like	As	Johnson, W.R., Savukov, I.M., Safronova, U.I Dalgarno, A., 2002, ApJS astro.ph. 0201454
He-like	Energies	Landi et al., 2005; ApJSS, in press
He-like	Energies	Dere, K. P. et al. 1997 Astronomy and Astrophysics Suppl. Ser., Vol. 1
He-like	PCS	Fernley, J. A., Taylor, K. T., & Seaton, M. J. 1987 J. Phys. B: At. Mol. Ph
He-like	PCS	Cunto, W., Mendoza, C., Ochsenbein, F., & Zeippen, C.J. 1993 A{\&}A
He-like	RR	Seaton, M.J. 1959, MNRAS 119, 81S
HI	2nu	Spitzer, L., & Greenstein, J., 1951, ApJ, 114, 407
HI	abs	Tielens & Hollenbach 1985 ApJ 291, 722
HI	cs	Allen 1973, Astro. Quan. for low Te
HI	cs	Sampson and Zhang 1988, ApJ, 335, 516 for High Te
Hlike	cs	Sampson and Zhang 1988, ApJ, 335, 516
H-like	A	Lipesles, M., Novick, R., & Told, N., 1966 Phys Rev Let, 15, 690
Hydro	2nu	Goldman,S.P. & Drake,G.W.F. 1981 Phys. Rev. A 24, 183

ion	DR	Ali, B., Blum, R. D., Bumgardner, T. E., Cranmer, S. R Ferland, G 1991, PASP, 103, 1182
iron	uta	R. Kisielius, A. Hibbert, G.J. Ferland M.E. Foord, S.J. Rose, P. van MNRAS 344, 696-706
ism	field	Draine, B.T. & Bertoldi, F. 1996, ApJ, 468, 269
K0	CT	Watanabe, Dutta, C.M., Nordlander, P., Kimura, M., & Dalgarno
k11	cs	Saraph, H.E. & Tully, J.A. 1994, A&AS, 107, 29
k3	cs	Pelan, J., & Berrington, K.A. 1995, A&A Suppl, 110, 209
k4	cs	Galavis, M.E., Mendoza, C., & Zeippen, C.J. 1995, A&AS, 111, 34
k6	cs	Galavis, M.E., Mendoza, C., & Zeippen, C.J. 1995, A&AS, 111, 34
k7	cs	Saraph, H.E., & Storey, P.J. A&AS, 115, 151
Klein-Nishina	cs	Rybicki and Lightman
la	esc	Hummer and Kunasz 1980 Ap.J. 236,609
La	escp	Hummer, D.G., & Kunasz, P.B., 1980, ApJ, 236, 609
Li	CT	Stancil, P.C., & Zygelman, B., 1996, ApJ, 472, 102
Li0	CT	ORNL data base for charge transfer
line	desp	Netzer, H., Elitzur, M., & Ferland, G. J. 1985, ApJ, 299, 752
line	escp	Hummer, D.G., xxxx, JQRST, 26, 187
line	shielding	Federman, S.R., Glassgold, A.E Kwan, J. 1979, ApJ, 227, 466
liner	model	Ferland, G. J., & Netzer, H. 1983, ApJ, 264, 105
l-mix	all	Vrinceanu, D. & Flannery, M. R. 2001, PhysRevA 63, 032701
Ly	scattering	Gavrila, M., 1967, Physical Review 163, 147
many	recom	Landini & Monsignori Fossi, 1991, A&AS, 91, 183
mco	rot	Emerson, D., 1996, Interpreting Astronomical Spectgra, p289
Mg+3	CT	Butler, S.E., & Dalgarno, A., 1980b, ApJ, 241, 838
Mg+4	CT	Butler, S.E., & Dalgarno, A., 1980b, ApJ, 241, 838
Mg0	CT	ORNL data base for charge transfer
mg1	as	Mendoza, C. 1982, in Planetary Nebulae, IAU Symp No. 103 ed b Holland), 143
mg1	cs	Leep, D., & Gallagher, A. 1976, Phys Rev A, 13, 148
mg10	cs	Cochrane, D.M., & McWhirter, R.W.P. 1983, PhyS, 28, 25
mg2	cs	Sigut, A., & Pradhan, A.K., 1994, J Phys B sub
mg4	cs	Saraph, H.E. & Tully, J.A. 1994, A&AS, 107, 29
mg5	as	Mendoza, C., & Zeippen, C.J. 1987, MNRAS, 224, 7p
mg5	cs	Butler, K., & Zeippen, C.J. 1994, A&AS, 108, 1
mg5	cs	Butler, K., & Zeippen, C.J. 1994, A&AS, 108, 1
mg6	all	Kafatos, M., & Lynch, J.P. 1980, ApJS, 42, 611
mg6	as	Becker, Butler, Zeippen, 1989, A&A 221, 375
mg6	cs	Ramsbottom & Bell 1997, A&AS 125, 543
mg7	cs	Lennon, D.J. Burke, V.M. 1994, A&AS, 103, 273
mg8	as	Chandra, S. 1982, SoPh, 75, 133
mg8	cs	Zhang, H.L., Graziani, M., Pradhan, A.K. 1994, A&A, 283, 319
mg9	as	Muhlethaler, H.P., & Nussbaumer, H. 1976, A&A 48, 109
mg9	as	Fleming, J., Bell, K.L, Hibbert, A., Vaeck, N., Godefroid, M.R 199
mg9	cs	Keenan, F.P. Berrington, K.A., Burke, P.G., Dufton, P.L Kingston

Mn	CT	Pequignot, D., & Aldrovandi, S.M.V., 1986, A&A, 161, 169-176
mn17	cs	Saraph, H.E. & Tully, J.A. 1994, A&AS, 107, 29
mn9	cs	Pelan, J., & Berrington, K.A. 1995, A&A Suppl, 110, 209
model	DQHER	Ferland et al. 1984 Ap.J. 281, 194
model	pdr	Le Petit, F., Roueff, E., & Herbst, E. 2004 A&A, 417, 993
N	abund	Holweger, H., 2001, Joint SOHO/ACE workshop "Solar and Galactic C Robert F. Wimmer-Schweingruber. Publisher American Institute of Ph proceedings vol. 598 location: Bern Switzerland, March 6 - 9, 2001., p.2
N+1	CT	Butler, S.E., & Dalgarno, A., 1980b, ApJ, 241, 838
N+2	CT	Sun, Sadeghpour, Kirby, Dalgarno, and Lafyatis, cfa preprint 4208
N+2	CT	Fand&Kwong, ApJ 474, 529
N+3	CT	Butler, S.E., & Dalgarno, A., 1980b, ApJ, 241, 838
N+4	CT	Feickert, Blint, Surratt, and Watson, (preprint Sep 84). Ap.J. in press
N+4	CT	Rittby et al J Phys B 17, L677, 1984
n1	as	Butler, K., & Zeippen, C.J. 1984, A&A, 141, 274
n1	cs	Tayal, S.S., 2000, ADNDT, 76, 191
n1	photo	Henry, R., ApJ 161, 1153
n2	as	Nussbaumer, H., & Rusca, C. 1979, A&A, 72, 129
n2	as	Brage, T., Hibbert, A., Leckrone, D.S. 1997, ApJ, 478, 423
n2	cs	Lennon, D.J., & Burke, V.M., 1994, A&AS, 103, 273-277
n2	cs	Hudson, C.E. & Bell, K.L. 2004, MNRAS, 348, 1275 and A&A, 430, 725
n2	cs	Stafford, R.P., Bell, K.L, Hibbert, A. & Wijesundera, W.P. 1994
n2	cs	Lennon, D.J., & Burke, V.M., 1994, A&AS, 103, 273-277
n2	CT	Sun Sadeghpour, Kirby Dalgarno and Lafyatis, cfa preprint 4208
n2	rec	Liu, X.W., Storey, P.J., Barlow, M.J., Danziger, I.J., Cohen, M & Bryce, I
n3	as	Froese Fischer, C. 1983, J.Phys. B, 16, 157
n3	as	Stafford, R.P., Hibbert, A., Bell, K.L. 1993, MNRAS, 260, L11
n3	as	Nussbaumer, H., & Storey, P.J., 1979, A&A, 71, L5
n3	cs	Blum, R.D., & Pradhan, A.K., 1992, ApJS 80, 425
n4	as	Flemming, J., Brage, T., Bell, K.L., Vaeck, N., Hibbert, A Godefroid, M. ApJ, 455, 758
n4	cs	Ramsbottom, C.A., Berrington, K.A., Hibbert, A., Bell, K.L. 1994 Physi
n4	cs	Ramsbottom, C.A., Berrington, K.A., Hibbert, A., Bell, K.L. 1994 Physi
n5	cs	Cochrane, D.M., & McWhirter, R.W.P. 1983, PhyS, 28, 25
Na, Al	recom	Landini & Monsignori Fossi, 1990, A&AS, 82, 229
Na0	CT	Dutta, C.M., Nordlander, P., Kimura, M., & Dalgarno, A., 2001, Phys R
Na0	CT	Watanabe, Dutta, C.M., Nordlander, P., Kimura, M., & Dalgarno, A., 2
na3	cs	Saraph, H.E. & Tully, J.A. 1994, A&AS, 107, 29
na4	cs	Butler, K., & Zeippen, C.J. 1994, A&AS, 108, 1
na5	as	Kaufman, V., & Sugar, J. 1986, J Phys Chem Ref Dat, 15, 321
na5	cs	Mendoza, C. 1982, in Planetary Nebulae, IAU Symp No. 103 ed by D.R Holland), 143
na7	cs	Lennon, D.J. Burke, V.M. 1994, A&AS, 103, 273
Ne	abund	Holweger, H., 2001, Joint SOHO/ACE workshop "Solar and Galactic C Robert F. Wimmer-Schweingruber. Publisher American Institute of Ph proceedings vol. 598 location: Bern Switzerland, March 6 - 9, 2001., p.2

Ne+2	CT	Butler, S.E., & Dalgarno, A., 1980b, ApJ, 241, 838
Ne+3	CT	Butler, S.E., & Dalgarno, A., 1980b, ApJ, 241, 838
Ne+4	CT	Butler, S.E., & Dalgarno, A., 1980b, ApJ, 241, 838
ne10	cs	Aggarwal, K.M., & Kingston, A.E. 1991, PhyS, 44, 517
ne2	cs	Saraph, H.E. & Tully, J.A. 1994, A&AS, 107, 29
ne3	as	Mendoza, C. 1982, in Planetary Nebulae, IAU Symp No. 103 ed b Holland), 143
ne3	cs	Butler, K., & Zeippen, C.J. 1994, A&AS, 108, 1
ne3	cs	Butler, K., & Zeippen, C.J. 1994, A&AS, 108, 1
ne4	as	Zeippen, C.J. 1982, MNRAS 198 111
ne4	cs	Giles, K. 1981, MNRAS, 195, 63
ne4	cs	Ramsbottom, C.A., Bell, K.L., & Keenan, F.P. 1998, MNRAS, 293,
ne5	as	Baluja, K.L. 1985, J.Phys. B, 18, L413
ne5	as	Baluja, K.L. 1985, J.Phys. B, 18, L413
ne5	cs	Lennon, D.J. & Burke, V.M. 1991, MNRAS 251, 628
ne5	cs	Lennon, D.J. Burke, V.M. 1994, A&AS, 103, 273
ne5	cs	Mendoza, C. 1982, in Planetary Nebulae, IAU Symp No. 103 ed b Holland), 143
ne6	as	Froese Fischer, C. 1983, J.Phys. B, 16, 157
ne6	cs	Zhang, H.L., Graziani, M., Pradhan, A.K. 1994, A&A, 283, 319
ne7	as	Fleming, J., Bell, K.L, Hibbert, A., Vaeck, N., Godefroid, M.R 199
ne7	cs	Berrington, K.A., Burke, P.G., Dufton, P.L., Kingston, A.E. 1985 A
ne7	cs	Dufton, P.L., Doyle, J.G., Kingston, A.E. 1979, A&A, 78, 318
ne7	cs	Ramsbottom, C.A., Berrington, K.A., Bell, K.L. 1995 At. Data Nuc
ne8	??	Cochrane, D.M., & McWhirter, R.W.P. 1983, PhyS, 28, 25
Ni	CT	Pequignot, D., & Aldrovandi, S.M.V., 1986, A&A, 161, 169-176
Ni1	cs	Hollenbach, D. & McKee, C.F. 1989, ApJ, 342, 306
ni12	cs	Pelan, J., & Berrington, K.A. 1995, A&A Suppl, 110, 209
ni12	cs	Mathews, A., Ramsbottom, C.A., Bell, K.L., & Keenan, F.P., 1998
nlr_liner	model	Ferland, G. J., & Netzer, H. 1983, ApJ, 264, 105
O	abund	Allende Prieto, C Lambert, D.L., & Asplund, M., 2001, ApJ, 556,
O	abundance	Meyers, D.M., Jura, M., & Cardelli, J.A., 1998, ApJ, 493, 222-229
O	CT	Stancil et al. 1999, A&AS, 140, 225-234
O+2	CT	Butler, S.E., & Dalgarno, A., 1980b, ApJ, 241, 838
O+3	CT	Butler, S.E., & Dalgarno, A., 1980b, ApJ, 241, 838
O+4	CT	Butler, S.E., & Dalgarno, A., 1980b, ApJ, 241, 838
o1	as	Berrington, K.A. 1988, J.Phys. B, 21, 1083
o1	cs	Berrington, K.A. 1988, J.Phys.B, 21, 1083 for Te > 3000K
o1	cs	Bell, Berrington & Thomas 1998, MNRAS 293, L83 for 50K <= Te
o1	cs	Launay & Roueff 1977, AA 56, 289
o1	cs	Berrington, K.A. 1988, J.Phys.B, 21, 1083 for Te > 3000K
o1	cs	Bell, Berrington & Thomas 1998, MNRAS 293, L83 for 50K <= Te
o2	as	Wiese, W.L., Fuhr, J.R., Deters, T.M. 1996, J Phys Chem Ref Data
o2	cs	McLaughlin, B.M., & Bell, K.L. 1993, ApJ, 408, 753
o2	cs	McLaughlin, B.M., & Bell, K.L. 1998, J Phys B 31, 4317
o2	cs	McLaughlin, B.M., & Bell, K.L. 1993, ApJ, 408, 753

o3	as	Storey, P.J., & Zeippen, C.J., 2000, MNRAS, 312, 813-816
o3	as	Storey, P.J., & Zeippen, C.J., 2000, 312, 813-816
o3	as	Nussbaumer, H., & Storey, P., 1981, A&A, 99, 177
o3	as	Mathis, J.S., & Liu, X.-W., 1999, ApJ, 521, 212-216
o3	as	Galavis, M.E., Mendoza, C., & Zeippen, C.J., 1997, A&AS, 123, 159-171
o3	cs	Lennon, D.J. Burke, V.M. 1994, A&AS, 103, 273
o3	cs	Lennon, D.J. Burke, V.M. 1994, A&AS, 103, 273
o3	cs	Burke, V.M., Lennon, D.J., & Seaton, M.J. 1989, MNRAS, 236, 353
o3	cs	Lennon, D.J. Burke, V.M. 1994, A&AS, 103, 273
o3	cs	Aggarwal, K.M., 1985 A&A 146, 149
O3	CT	Dalgarno+Sternberg ApJ Let 257, L87
O3	CT	Gargaud et al AA 208, 251, (1989
o4	as	Brage, T., Judge, P.G., & Brekke, P. 1996, ApJ. 464, 1030
o4	as	Brage, T., Judge, P.G., & Brekke, P. 1996, ApJ. 464, 1030
o4	cs	Zhang, H.L., Graziani, M., Pradhan, A.K. 1994, A&A, 283, 319
o4	cs	Blum, R.D., & Pradhan, A.K. 1992, ApJS 80, 425
o4	cs	Blum, R.D., & Pradhan, A.K., 1992, ApJS 80, 425
o4	cs	Zhang, H.L., Graziani, M., Pradhan, A.K. 1994, A&A, 283, 319
o4	cs	Berrington, K.A., Burke, P.G., Dufton, P.L., Kingston, A.E. 1985 At. Da
o4	cs	Blum, R.D., & Pradhan, A.K., 1992, ApJS 80, 425
o4	cs	Zhang, H.L., Graziani, M., & Pradhan, A.K., 1994, A&A 283, 319
o5	cs	Berrington, K.A., Burke, P.G., Dufton, P.L., Kingston, A.E. 1985 At. Da
o5	cs	Fleming, J., Bell, K.L, Hibbert, A., Vaeck, N., Godefroid, M.R 1996, MN
o6	vs	Cochrane, D.M., & McWhirter, R.W.P. 1983, PhyS, 28, 25
oi	cs	Federman, S.R., & Shipsey, E.J. 1983, ApJ, 269, 791
oi	cs	Tielens, A.G.G., & Hollenbach, D. 1985, ApJ, 291, 722
oi	cs	Monteiro & Flower 1987, MNRAS 228, 101
oi	cs	Jaquet et al. 1992, J.Phys.B 25, 285
oi	cs	Pequignot, D. 1990, A&A 231, 499
oi	cs	Chambaud et al., 1980, J.Phys.B, 13, 4205 (upto 5000K
oi	cs	Roueff, private communication (10,000K and 20,000K
OI	photoexcitation	Storzer, H., & Hollenbach, D. 2000, ApJ, 539, 751-759
P	CT	Pequignot, D., & Aldrovandi, S.M.V., 1986, A&A, 161, 169-176
p2	as	Mendoza, C., & Zeippen, C.J., 1982, MNRAS 199, 1025
p2	as	Mendoza, C., & Zeippen, C.J., 1982, MNRAS 199, 1025
p2	cs	Krueger, T.K., and Czyzak, S.J., 1970, Proc Roy Soc London A 318, 531
p3	as	Kaufman, V., & Sugar, J., 1986, J Phys Chem Ref Data 15, 321
p3	cs	Krueger, T.K., and Czyzak, S.J., 1970, Proc Roy Soc London A 318, 531
p4	cs	Saraph, H.E. & Tully, J.A. 1994, A&AS, 107, 29
PAH	heating	Bakes, E.L.O., & Tielens, A.G.G.M. 1994, ApJ, 427, 822
PAH	heating	Bakes, E.L.O., & Tielens, A.G.G.M. 1994, ApJ, 427, 822
PAH	opacities	Desert, F.-X., Boulanger, F., Puget, J. L. 1990, A&A, 237, 215
PAH	opacities	Schutte, W.A., Tielens, A.G.G.M., Allamandolla, L.J., 1993, ApJ, 415, 39
PAH	opacities	Bregman, J.D., Allamandola, L.J., Witteborn, F.C., Tielens, A.G.G.M Ge 791
phys	const	Mohr P.J. & Taylor B.N., 1998 Codata, see Reviews of Modern Physics

		http://www.physics.nist.gov/constants
PN	abundances	Aller+Czyzak, ApJ Sup 51, 211
RT	continuum shielding	Federman, S.R., Glassgold, A.E Kwan, J. 1979, ApJ, 227, 466
rt	esc proc	Ferland, G.J., 1999, ApJ, 512, 247
RT	wind	Castor, J.I., Abbott, D.C., & Klein, R.I., 1975, ApJ, 195, 157
S+1	CT	Butler, S.E., & Dalgarno, A., 1980b, ApJ, 241, 838
S+2	CT	Butler, S.E., & Dalgarno, A., 1980b, ApJ, 241, 838
S+3	CT	Butler, S.E., & Dalgarno, A., 1980b, ApJ, 241, 838
S+4	CT	Butler, S.E., & Dalgarno, A., 1980b, ApJ, 241, 838
S0	CT	ORNL data base for charge transfer
S1	cs	Hollenbach, D. & McKee, C.F. 1989, ApJ, 342, 306
s12	all	Saha, H.P., & Trefftz, E. 1983, SoPh, 87, 233
s12	as	Froese Fischer, C. 1983, J.Phys. B, 16, 157
s12	as	Saha, H.P., & Trefftz, E. 1983, SoPh, 87, 233
s12	cs	Oliva, E., Pasquali, A., & Reconditi, M. 1996, A&A, 305, 210
s14	cs	Cochrane, D.M., & McWhirter, R.W.P. 1983, PhyS, 28, 25
s2	as	trans Mendoza, C., & Zeippen, C.J., 1982, MNRAS, 198, 127
s2	cs	Ramsbottom, C.A., Bell, K.L., Stafford, R.P. 1996 At. Data Nucl. D
s2	cs	Tayal, S., 1997, ApJS, 111, 459
s2	cs	Ramsbottom, C.A., Bell, K.L., Stafford, R.P. 1996, ADNDT, 63, 57
s3	as	Mendoza, C. 1982, in Planetary Nebulae, IAU Symp No. 103 ed b Holland), 143
s3	as	Mendoza, C., & Zeippen, C.J. 1982, MNRAS, 199, 1025
s3	cs	Galavis, M.E., Mendoza, C., & Zeippen, C.J. 1995, A&AS, 111, 34
s3	cs	Tayal, S.S., and Gupta, G.P. 1999 ApJ 526, 544
s3	cs	Galavis, M.E., Mendoza, C., & Zeippen, C.J. 1995, A&AS, 111, 34
s3	cs	Tayal, S.S., and Gupta, G.P. 1999 ApJ 526, 544
s3	cs	Ho, Y.K., & Henry,R.J.W. 1984, ApJ, 282, 816
s3	cs	Tayal, S.S. 1997, ApJ 481, 550
s3	cs	Hayes, M.A., 1986, J Phys B 19, 1853
s3	cs	Tayal, S.S. 1997, ApJ 481, 550
S4	As	Hibbert, A., Brage, T., Fleming, J. 2002, MNRAS 333, 885
s4	as	Johnson, C.T., Kingston, A.E., Dufton, P.L. 1986, 220, 155
s4	as	Dufton, P.L., Hibbert, A., Kingston, A.E. & Doschek, G.A. 1982 A
s4	as	Hibbert, A., Brage, T., & Fleming, J., 2002, MNRAS, 333, 885
s4	cs	Tayal, S.S., 2000, ApJ 530, 1091
s4	cs	Tayal, S.S., 2000, ApJ 530, 1091
s4	energy	Martin, W.C, Zalubas, R., & Musgrove, A., 1990, J Phys Chem Re
s5	as	Mendoza, C. 1982, in Planetary Nebulae, IAU Symp No. 103 ed b Holland), 143
s5	as	Dufton, P.L., Hibbert, A., Keenan, F.P, Kingston, A.E Doschek, G
s5	cs	Dufton, P.L., & Kingston, A.E. 1984, J.Phys. B, 17, 3321
s5	cs	Dufton, P.L., & Kingston, A.E. 1984, J.Phys. B, 17, 3321
s6	as	Mendoza, C. 1982, in Planetary Nebulae, IAU Symp No. 103 ed b Holland), 143

s6	cs	Dufton, P.L., & Kingston, A.E. 1987, J.Phys. B, 20, 3899
s8	cs	Saraph, H.E. & Tully, J.A. 1994, A&AS, 107, 29
s9	all	Kafatos, M., & Lynch, J.P. 1980, ApJS, 42, 611
s9	cs	Butler, K., & Zeippen, C.J. 1994, A&AS, 108, 1
sc13	cs	Saraph, H.E. & Tully, J.A. 1994, A&AS, 107, 29
sc5	cs	Pelan, J., & Berrington, K.A. 1995, A&A Suppl, 110, 209
sec	ioniz	Xu and McCray 1991, Ap.J. 375, 190
Si	abund	Holweger, H., 2001, Joint SOHO/ACE workshop "Solar and Galactic C Robert F. Wimmer-Schweingruber. Publisher American Institute of Ph proceedings vol. 598 location: Bern Switzerland, March 6 - 9, 2001., p.2
Si I	cs	Hollenbach, D. & McKee, C.F. 1989, ApJ, 342, 306
Si+1	CT	Butler, S.E., & Dalgarno, A., 1980b, ApJ, 241, 838
Si+2	CT	Gargaud, M., McCarroll, R., & Valiron, P. 1982, A&ASup, 45, 603
Si+3	CT	Butler, S.E., & Dalgarno, A., 1980b, ApJ, 241, 838
Si+3	CT	Fang, Z., & Kwong, H.S. 1997 ApJ 483, 527
Si+4	CT	Opradolce et al., 1985, A&A, 148, 229
Si0	CT	ORNL data base for charge transfer
Si0	CT	Prasad, S.S., & Huntress, W.T., 1980, ApJS, 43, 1-35
si10	as	Chandra, S. 1982, SoPh, 75, 133
si10	cs	Saha, H.P., & Trefftz, E. 1982, A&A, 116, 224
si10	cs	Zhang, H.L., Graziani, M., Pradhan, A.K. 1994, A&A, 283, 319
si10	cs	Bell, K.L., & Ramsbottom, C.A., 2000, ADNDT, 76, 176-190
si11	as	Muhlethaler, H.P., & Nussbaumer, H. 1976, A&A 48, 109
si11	cs	Berrington, K.A., Burke, P.G., Dufton, P.L., Kingston, A.E 1985, At. Da
si11	cs	Lennon, D.J. Burke, V.M. 1994, A&AS, 103, 273
si11	cs	Kafatos, M., & Lynch, J.P. 1980, ApJS, 42, 611
si12	cs	Cochrane, D.M., & McWhirter, R.W.P. 1983, PhyS, 28, 25
si2	as	Dufton, P.L., Keenan, F.P., Hibbert, A
si2	as	morton et al 88 (apj sup
si2	cs	Barinovs, G., van Hemert, M., Krems, R. & Dalgarno, A. 2005, ApJ, 620
si2	cs	Dufton, P.L., Keenan, F.P., Hibbert, A
si3	as	Callegari, F., & Trigueiros, A.G., 1998, ApJS, 119, 181
si3	cs	Callaway, J. 1994, At. Data Nucl. Data Tables, 57, 9
si3	cs	Dufton, P.L., & Kingston, A.E. 1989, MNRAS, 241, 209
si3	cs	Dufton, P.L., & Kingston, A.E. 1994, ADNDT, 57, 273
si4	as	Mendoza, C. 1982, in Planetary Nebulae, IAU Symp No. 103 ed by D.K Holland), 143
si4	cs	Dufton, P.L., & Kingston, A.E. 1987, J.Phys. B, 20, 3899
si6	cs	Saraph, H.E. & Tully, J.A. 1994, A&AS, 107, 29
Si7	As	Galavis, M.E., Mendoza, C., * Zeippen, C.J. 1997, A&AS, 123, 159
si7	cs	Kafatos, M., & Lynch, J.P. 1980, ApJS, 42, 611
si7	cs	Butler, K., & Zeippen, C.J. 1994, A&AS, 108, 1
Si7	data	Bhatia, A.K., & Landi, E. 2003, ApJ, 585, 587-597
si8	cs	Kafatos, M., & Lynch, J.P. 1980, ApJS, 42, 611
si9	as	Baluja, K.L. 1985, J.Phys. B, 18, L413
si9	cs	Aggarwal, K.M. 1983, J.Phys. B, 16, L59

si9	cs	Lennon, D.J. Burke, V.M. 1994, A&AS, 103, 273
si9	cs	Aggarwal, K.M. 1984, ApJS, 54, 1
solar	abund	Grevesse, N., & Sauval, A.J., 2001, Space Science Review, 85, 161-
Ti	CT	Pequignot, D., & Aldrovandi, S.M.V., 1986, A&A, 161, 169-176
ti14	cs	Saraph, H.E. & Tully, J.A. 1994, A&AS, 107, 29
ti6	cs	Pelan, J., & Berrington, K.A. 1995, A&A Suppl, 110, 209
Tspin	21 cm	Abel, N.P., Brogan, C.L., Ferland, G.J., O'Dell, C.R Shaw, G. & Tr
tsuite	blr	Kwan, H., & Krolik, J. 1981, Ap.J. 250, 478
tsuite	blr	Netzer, H., & Ferland, G.J. 1984, PASP 96, 593 Table 1
v15	cs	Saraph, H.E. & Tully, J.A. 1994, A&AS, 107, 29
v7	cs	Pelan, J., & Berrington, K.A. 1995, A&A Suppl, 110, 209
XUV	extinction	Cruddace et al. 1974 ApJ 187, 497
Zn 4	wl	Dinerstein, H.L., Gaballe, T.R> 2001, ApJ, 562, 515-520
Zn04	energy	van Kleef, Th. A. M., Joshi, Y.N., Barakat, M.N. 1984, Phys. Script
Zn04	wl	Dinerstein, H.L., & Gaballe, T.R. 2001, ApJ, 562, 515-520

12. REFERENCES

Abbott, D. C. 1982, ApJ, 259, 282
Abel, N. P., Brogan, C. L., Ferland, G. J., O'Dell, C. R., Shaw, G., & Troland, T. H. 2004, ApJ, 609, 247-260 (astro-ph/0404399)
Abel, N.P., Ferland, G.J., Shaw, G. & van Hoof, P.A.M. 2005, ApJS, 161, 65 (astro-ph/0506514)
Adams, T. 1972, ApJ, 174, 439
Aldrovandi, S., & Péquignot, D. 1972, A&A, 17, 88
Aldrovandi, S., & Péquignot, D. 1974, Revista Brasileira de Fisica, 4, 491
Ali, B., Blum, R. D., Bumgardner, T. E., Cranmer, S. R., Ferland, G. J., Haefner, R. I., & Tiede, G. P. 1991, PASP, 103, 1182
Allen, C. W. 1976, *Astrophysical Quantities*, Third Edition (London: Athlone Press)
Allende Prieto, C., Lambert, D.L., & Asplund, M., 2001, ApJ, 556, L63
Allende Prieto, C., Lambert, D.L., & Asplund, M., 2002, ApJ, 573, L137
Aller, L. H. 1984, in *Physics of Thermal Gaseous Nebulae*, (Dordrecht: Reidel)
Aller, L. H., & Czyzak, S. J. 1983, ApJS, 51, 211.
Anders, E., & Grevesse, N. 1989, Geochim. Cosmochim. Acta, 53, 210
Anderson, H., Ballance, C.P., Badnell, N.R., & Summers, H.P., 2000, J Phys B, 33, 1255Arimoto, N., & Yoshii, Y. 1987, A&A, 173, 23
Antonucci, Robert, 1993, ARA&A, 31, 473
Aviv, N., Barlow, T.A., Laor, A., Sargent, W.L.W., & Blandford, R.D. 1998, MNRAS 297, 990
Armour, Mary-Helen, Ballantyne, D.R., Ferland, G.J., Karr, J., & Martin, P.G., 1999, PASP 111, 1251-1257
Arnaud, M., & Raymond, J. 1992, ApJ, 398, 394
Arnaud, M., & Rothenflug, R. 1985, A&AS, 60, 425
Asplund, M., Grevesse, N., & Sauval, A.J. 2005, in *Cosmic Abundances as Records of Stellar Evolution and Nucleosynthesis*, ASP Conf Ser, F.N. Bash & T.G. Barnes, editors (astro-ph 0410214)
Avni, Y., & Tananbaum, H. 1986, ApJ, 305, 83
Avni, Y., Worrall, D. M., & Morgan, W. A. ApJ, 1995, 454, 673
Avrett, E. H., & Loeser, R. 1988, ApJ, 331, 211
Bahcall, J.H., & Kozlovsky, B.-Z. 1969, ApJ, 155, 1077
Bajtlik, S., Duncan, R. C., & Ostriker, J. P. 1988, ApJ, 327, 570
Bakes, E.L.O. & Tielens, A.G.G.M. 1994, ApJ, 427, 822 (BT94)
Balbus, S. A., & McKee, C. F. 1982, ApJ, 252, 529
Baldwin J. A., Ferland, G. J., Korista, K. T., Carswell, R., Hamann, F., Phillips, M., Verner, D., Wilkes, B., & Williams, R. E. 1996, ApJ, 461, 683
Baldwin, J. A., Ferland, G. J., Korista K. T., & Verner, D. 1995, ApJ, 455, L119
Baldwin, J.A., Ferland, G.J., Korista, K.T., Hamann, F., & Dietrich, M. 2003, ApJ, 582, 590
Baldwin, J., Ferland, G. J., Martin, P. G., Corbin, M., Cota, S., Peterson, B. M., & Slettebak, A. 1991, ApJ, 374, 580 (BFM)
Baldwin, J.A., Verner, E.M., Verner, D.A., Ferland, G.J., Martin, P.G., Korista, K.T., & Rubin, R. H., 2000, ApJS, 129, 229-246
Baldwin, J., Wampler, J., & Gaskell, C. M. 1989, ApJ, 338, 630
Balick, B., Gammon, R. H., & Hjellming, R. 1974 PASP, 86, 616
Ballantyne, D.R., Ferland, G.J., & Martin, P.G., 2000, ApJ 536, 773-777

Bässgen, G., Bässgen, M., & Grewing, M. 1988, A&A, 200, 51
Bates, D. R., Kingston, A. E., & McWhirter, R. W. P. 1962, Proc R Soc, A267, 297
Bauman, R.P., Porter, R.L., Ferland, G.J., & MacAdam, K. B. 2005, ApJ, 628, 541 (astro-ph/0504083)
Bechtold, J., Weymann, R. J., Lin, Z., & Malkan, M. A. 1987, ApJ, 315, 180
Behar, E., Sako, M, Kahn, S.M., 2001, ApJ, 563, 497-504
Behar, E., & Netzer, H., 2002, ApJ, 570, 165-170
Bell, K. L., Kingston, A. E., & McIlveen, W. A. 1975, J. Phys. B 8, 358
Benjamin, Robert A., Skillman, Evan D., & Smits, Derek P., 1999, ApJ, 514, 307
Bergin, E.A., Langer, W.D., & Goldsmith, P. F. 1995, ApJ, 441, 222
Berger, M. J., & Seltzer, S. M. 1965, NASA SP-3012
Bergeron, J., & Collin-Souffrin, S. 1971, A&A, 14, 167
Bergman, J.D., Allamandola, L. J., Witteborn, F. C., Tielens, A. G. G. M. & Geballe, T. R. 1989, ApJ, 344, 791
Berrington, K. A., & Pelan, A. 1995, A&AS, 114, 367
Berrington, K.A., Nakazaki, S., & Norrington, P.H. 2000, A&AS, 142, 313
Bertoldi, F., & Draine, B. T. 1996, ApJ, 458, 222
Bethe, H. 1930, Ann. Phys. 5, 325
Bica, E. 1988, A&A, 195, 76
Bieniek, R. J., & Dalgarno, A. 1979, ApJ, 228, 635
Binette, L., Prieto, A., Szuszkiewicz, E., & Zheng, W. 1989, ApJ, 343, 135
Black, J. H. 1978, ApJ, 222, 125
Black, J. H. 1987, in *Interstellar Processes*, ed. D.J. Hollenbach & H.A. Thronson, (Dordrecht: Reidel), p 731
Black, J.H. & van Dishoeck, E.F. 1987, ApJ, 322, 412
Bohm, D., & Aller, L. H. 1947, ApJ, 105, 131
Bonihala, J. R. M., Ferch, R., Salpeter, E. E., Slater, G., & Noerdlinger, P. 1979, ApJ, 233, 649
Borkowski, K. J., & Harrington, J. P. 1991, ApJ, 379, 168
Bottorff, M.C., Baldwin, J.A., Ferland, G.J., Ferguson, J.W., & Korista, K.T. 2002, ApJ, 581 932
Bottorff, M. C., Ferland, & Gary J., 2000, MNRAS 316, 103-106
Bottorff, M.C. & Ferland, G.J. 2001a, ApJ, 549, 118-132
Bottorff, M. C., Ferland, & Gary J., 2002, ApJ 568, 581-591
Bottorff, Mark, Ferland, Gary, Baldwin, Jack, & Korista, Kirk, 2000, ApJ, 542, 644-654
Bottorff, Mark C.; Baldwin, Jack A.; Ferland, Gary J.; Ferguson, Jason W.; Korista, Kirk T. 2002, ApJ, 581, 932
Bottorff, M., Lamothe, J., Momjian E., Verner, E., Vinkovic, D. & Ferland, G. 1998 PASP, 110, 1040
Boyd, R., & Ferland, G.J. 1987, ApJ, 318, L21
Bowen, I. S. 1960, ApJ, 132, 1
Bray, I., Burgess, A., Fursa, D.V., & Tully, J.A., 2000, A&AS, 146, 481
Bregman, J. D., Allamandola, L. J., Tielens, A. G. G. M., Geballe, T. R., & Witteborn, F. C. 1989, ApJ, 344, 791
Broad, J. T., & Reinhardt, W. P. 1976, Phys Rev A 14, 2159
Brocklehurst, M., 1970, MNRAS, 148, 417
Brocklehurst, M., 1972, MNRAS, 157, 211
Brooks, Frederick P., 1995, *The Mythical Man-Month, Essays on Software Engineering*, (Reading: Addison-Wesley)
Brown, R. L., & Mathews, W. G. 1970, ApJ, 160, 939

Burgess, A. 1965, ApJ, 141, 1588
Burgess, A., & Summers, H. P. 1969, ApJ, 157, 1007
Burgess, A., & Summers, H. P. 1976, MNRAS, 174, 345
Burgess, A., & Tully, J. A. 1992, A&A, 254, 436
Butler, S. E., Bender, C. F., & Dalgarno, A. 1979, ApJ, 230, L59
Butler, S. E., & Dalgarno, A. 1979, ApJ, 234, 765
Butler, S. E., Heil, T. G., & Dalgarno, A. 1980, ApJ, 241, 442
Butler, S. E., & Dalgarno, A. 1980, ApJ, 241, 838
Callaway, J. 1994, At Dat Nuc Dat Tab 57, 9
Cameron, A.G.W. 1982, in *Essays in Nuclear Astrophysics*, ed CA Barnes, DD Clayton, & DN Schramm, (Cambridge: Cambridge University Press)
Canfield, R. C., & Puetter, R. C. 1980, ApJ, 236, L7
Cardelli, J. A. 1994, Science 264, 209
Cardelli, J. A., et al. 1991, ApJ, 377, L57
Castor, J.I., Abbott, D.C., & Klein, R.I., 1975, ApJ, 195, 157-174
Carswell R. F. & Ferland, G. J. 1988, MNRAS, 235, 1121
Castor, J. I. 1970, MNRAS, 149, 111
Cazaux, S., & Tielens, A.G.G.M., 2002, ApJ, 575, L29-L32
Chaffee, F. H., & White, R. E. 1982, ApJS, 50, 169
Chamerlain, J.W., 1956, ApJ, 124, 390
Chan, E. S., Avrett, E. H., & Loeser, R. 1991, A&A, 247, 580
Chapman, R. D., & Henry, R. J. W. 1971, ApJ, 168, 169
Chidichimo, M. C. 1981, J. Phys. B., 14, 4149
Clavel, J., & Santos-Lleo, M. 1990, A&A, 230, 3
Clegg, R. E. S. 1987, MNRAS, 229, 31p
Clegg, R. E. S., & Harrington, J. P. 1989, MNRAS, 239, 869
Clegg, R.E.S., Storey, P.J., Walsh, J.R., & Neale, L. 1997, MNRAS, 284, 348
Cohen, E. R., & Taylor, B. N. 1987, Rev Mod Phys 57, 1121
Cota, S. A. 1987, Ph.D. Thesis, OSU
Cota, S. A., & Ferland, G. J. 1988, ApJ, 326, 889
Cowie, L. L., & Songaila, A. 1986, ARA&A 24, 499
Cowling, T.G., 1976, Magnetohydrodynamics, (Hilger; Bristol)
Craig, I.J.D., & Brown, J.C., 1986, *Inverse Problems in Astronomy* (Adam Hilger: Bristol)
CrinkLaw, G., Federman, S. R., & Joseph, C. L. 1994, ApJ, 424, 748
Crosas, M., & Weisheit, J.C. 1993, MNRAS, 262, 359
Cruddace, R., Paresce, F., Bowyer, S., & Lampton, M. 1974, ApJ, 187, 497
Cunto, W., Mendoza, C., Ochsenbein, F., Zeippen, C. J. 1993, A&A 275, L5
Dalgarno, A., & Kingston, A. E. 1963, Observatory, 83, 39
Dalgarno, A., & McCray, R. A. 1972, ARA&A, 10, 375
Dalgarno, A., & McCray, R. A. 1973, ApJ, 181, 95
Dalgarno, A., & Roberge, W. G. 1979, ApJ, 233, L25
Dalgarno, A., Yan, Min, & Liu, Weihong 1999, ApJS, 125, 237
Davidson, K. 1972, ApJ, 171, 213
Davidson, K. 1975, ApJ, 195, 285
Davidson, K. 1977, ApJ, 218, 20
Davidson, K., & Netzer, H. 1979, Rep. Prog. in Physics 51, 715

Davidson, K., & Fesen, R.A. 1985, ARA&A, 23, 119
de Jong, T., Chu, S-I., & Dalgarno, A. 1975, ApJ, 199, 69
Deguchi, S., & Watson, W.D. 1985, ApJ, 290, 578-586
Desert, F.-X., Boulanger, F., & Puget, J. L. 1990, A&A, 237, 215
Dove, J. E., Rush, A., Cribb, P., & Martin, P. G. 1987, ApJ, 318, 379
Dove, J. E., & Mandy, M. E. 1986, ApJ, 311, L93
Draine, B. T. 1978, ApJS, 36, 595
Draine, B.T., & Bertoldi, Frank, 1996, ApJ, 468, 269-289
Draine, B. T., & Lee, H. M. 1984, ApJ, 285, 89
Draine, B. T., & Salpeter, E. E. 1979, ApJ, 231, 77
Draine, B. T., & Sultin, B. 1987, ApJ, 320, 803
Drake, G., 1993, Chapt 3 in *Long Range Casimir Forces, theory and recent experiments on atomic systems*, edited by Levin & Mihca, Plenum Press
Drake, G. W. F. 1996, in *Atomic, Molecular, and Optical Physics Handbook*, ed. G. W. F. Drake (Woodbury: AIP), 154
Drake, S. A., & Ulrich, R.K. 1980, ApJS, 42, 351
Drawin, H.W. 1969, Z. Physic 225, 483
Dyson, J.E., & Williams, D.A. 1997, *The Physics of the Interstellar Medium* (Bristol; Institute of Physics Publishing)
Elitzur, M. 1982, Rev. Mod. Phys 54, 1125
Elitzur, M. 1984, ApJ, 280, 653
Elitzur, M, 1992, *Astronomical Masers*, (Dordrecht: Kluwer)
Elitzur, M., Ferland, G. J., Mathews, W. G., & Shields, G. 1983, ApJ, 272, L55
Elitzur, M., & Ferland, G. J. 1986, ApJ, 305, 35
Elvis, M. et al. 1994, ApJS, 95, 1
Elwert, T., et al. 2006, in preparation
Emerson, D. 1996, *Interpreting Astronomical Spectra*, (Chichester: John Wiley & Sons)
Fabian, A. C., Pringle, J. E., & Rees M. J. 1976, MNRAS, 175, 43
Federman, S. R., Glassgold, A.E., & Kwan, J. 1979, ApJ, 227, 466
Federman, S. R., et al. 1993, ApJ, 413, L51
Federman, S. R. & 2003,
Fenley, J.A., Taylor, K.T., & Seaton, M.J. 1987, J. Phys. B. 20, 6457-6476
Ferguson, J. W., Ferland, G. J., & A. K. Pradhan, 1995, ApJ, 438, L55
Ferguson, J. W., & Ferland, G.J. 1997, ApJ, 479, 363
Ferguson, J. W., Korista, K. T., Baldwin, J. A., & Ferland, G. J. 1997, ApJ, 487, 122
Ferguson, J W., Korista, Kirk. T., and Ferland, Gary J., 1997, ApJS 110, 287-297
Ferguson, J W., Korista, Kirk. T., Verner, D.A., & Ferland, Gary J., 2001, ASP Conference Series, Vol 247, *Spectroscopic Challenges of Photoionized Plasmas*, G Ferland & D Savin, editors.
Ferland, G. J. 1977, ApJ, 212, L21
Ferland, G. J. 1979, MNRAS, 188, 669
Ferland, G. J. 1980a, MNRAS, 191, 243
Ferland, G. J. 1980b, BAAS, 12, 853
Ferland, G. J. 1980c, PASP, 92, 596
Ferland, G. J. 1986, PASP, 98, 549
Ferland, G. J. 1986, ApJ, 310, L67
Ferland, G. J. 1992, ApJ, 389, L63 NIII

Ferland, G. J. 1993, ApJS, 88, 49
Ferland, G. J. 1999, PASP, 111, 1524
Ferland, G. J. 1999a, in *Quasars and Cosmology*, ASP 162, p 147 ed G Ferland & J Baldwin (astro-ph/0307450)
Ferland, G. J., 1999b, ApJ 512 247-249
Ferland, G.J., 2000, RMxAC, 9, 153
Ferland, G.J., 2001a, PASP, 113, 41
Ferland, G.J., 2001b, ASP Conference Series, Vol 247, *Spectroscopic Challenges of Photoionized Plasmas*, G Ferland & D Savin, editors (astro-ph/0210161)
Ferland, G.J., 2003a, in *Star formation through time*, 2003, by Gary J. Ferland, ASP Conf 297, E. Pérez, R.M. González Delgado, & G. Tenorio-Tagle, eds, p 69
Ferland, G.J., 2003b, ARA&A, 41, 517
Ferland, G. J., Baldwin J. A., Korista, K. T., Hamann, F., Carswell, R., Phillips, M., Wilkes, B., & Williams, R. E. 1996, ApJ, 461, 683
Ferland, G., Binette, L., Contini, M., Harrington, J., Kallman, T., Netzer, H., Péquignot, D., Raymond, J., Rubin, R., Shields, G., Sutherland, R., & Viegas, S. 1995, in *The Analysis of Emission Lines*, Space Telescope Science institute Symposium Series, R. Williams & M. Livio, editors (Cambridge: Cambridge University Press)
Ferland, G. J., & Elitzur, M. 1984, ApJ, 285, L11
Ferland, G. J., Fabian, A. C., & Johnstone, R.M. 1994, MNRAS, 266, 399
Ferland, G. J., Fabian, A. C., & Johnstone, R.M. 2002, MNRAS, 333, 876
Ferland, G. J., Henney, W. J., Williams, R. J. R., Arthur, S. J. 2002, RMxAC, 12, 43
Ferland, G. J., Korista, K.T. & Peterson, B.M. 1990, ApJ, 363, L21
Ferland, G. J., Korista, K.T., Verner, D. A., & Dalgarno, A. 1997, ApJ, 481, L115
Ferland, G. J. Korista, K.T. Verner, D.A. Ferguson, J.W. Kingdon, J.B. Verner, & E.M. 1998, PASP, 110, 761
Ferland, G. J., Lambert, D. L., Netzer, H., Hall, D. N. B., & Ridgway, S. T. 1979a, ApJ, 227, 489
Ferland, G. J., Lambert, D. L., Slovak, M., Shields, G. A., & McCall, M. 1982, ApJ, 260, 794
Ferland, G. J., & Mushotzky, R. F. 1982, ApJ, 262, 564
Ferland, G. J., & Mushotzky, R. F. 1984, ApJ, 286, 42
Ferland, G. J., & Netzer, H. 1979, ApJ, 229, 274
Ferland, G. J., & Netzer, H. 1983, ApJ, 264, 105
Ferland, G. J., Netzer, H., & Shields, G. A. 1979, ApJ, 232, 382
Ferland, G. J., Peterson, B. M., Horne, K., Welsh, W. F., & Nahar, S. N. 1992, ApJ, 387, 95
Ferland, G. J., & Persson, S. E. 1989, ApJ, 347, 656
Ferland, G. J., & Rees, M. J. 1988, ApJ, 332, 141
Ferland, Gary & Savin, Daniel Wolf, 2001, *Spectroscopic Challenges of Photoionized Plasmas*, ASP Conference Series Vol. 247, (San Francisco: Astronomical Society of the Pacific)
Ferland, G. J., & Shields, G. A. 1978, ApJ, 226, 172
Ferland, G. J., & Shields, G. A. 1985, in *Astrophysics of Active Galaxies & Quasi-stellar Objects*, J.S. Miller, Ed.
Ferland, G. J., & Truran, J. W. 1981, ApJ, 244, 1022
Ferland, G. J., Williams, R. E., Lambert, D. L., Shields, G. A., Slovak, M., Gondhalekar, P. M., & Truran, J. W. 1984, ApJ, 281, 194
Field, G. B. 1965, ApJ, 142, 431
Francis, P. J. 1993, ApJ, 407, 519

Friedrich, H. 1998, Theoretical Atomic Physics, (Berlin: Springer)
Fuhr, J. R., Martin, G. A., & Wiese, W. L. 1988, J. Phys. Chem. Ref. Data, 17, Suppl. 4
Gaetz, T. J., & Salpeter, E. E. 1983, ApJS, 52, 155
Garstang, R.H. 1958, MNRAS, 118, 57
Gavrila, M. 1967, Phys Rev 163, 147, also JILA Report #86, Sept 19, 1966
Ginzburg, V. I., & Syrovatskii, S. I. 1964, *The Origin of Cosmic Rays*, (Oxford: Pergamon)
Gould, R. S. 1978, ApJ, 219, 250
Grandi, S.A., 1975, ApJ, 196, 465
Grandi, S.A., 1975, ApJ, 199, 43
Grandi, S.A., 1976, ApJ, 206, 658
Gredel, R., Lepp, S., & Dalgarno, A. 1987, ApJ, 323, L137
Gredel, R., Lepp, S., Dalgarno, A., & Herbst, E. 1989, ApJ, 347, 289
Greenhouse, M., et al. 1993, ApJS, 88, 23
Grevesse, N., & Anders, E. 1989, *Cosmic Abundances of Matter*, AIP Conference Proceedings 183, p. 1, Ed. C. J. Waddington, (New York: AIP)
Grevesse, N. & Noels, A. 1993 in *Origin & Evolution of the Elements*, ed. N. Prantzos, E. Vangioni-Flam, & M. Casse p. 15 (Cambridge: Cambridge Univ. Press)
Grevesse, N., & Sauval, A.J., 1998, Space Science Review, 85, 161-174
Guhathakurta, P., & Draine, B. T. 1989, ApJ, 345, 230
Guilbert, P. W. 1986, MNRAS, 218, 171
Guilbert, P., & Rees, M. J. 1988, MNRAS, 233, 475
Haardt, Francesco, & Madau, Piero, 1996, ApJ, 461, 20
Habing, H. J. 1968, Bull. Astr. Inst. Netherlands 19, 421
Habart, E. Boulanger, F. Verstraete, L. Walmsley, C.M., & Pineau des Forets G., 2004, A&A 414, 531, astro-ph/ 0311040
Halpern, J. P., & Grindlay, J. E. 1980, ApJ, 242, 1041
Hamann, F., & Ferland, G. J. 1992, ApJ, 391, L53
Hamann, F., & Ferland, G. J. 1993, ApJ, 418, 11
Hamann, F., & Ferland, G. J. 1999, ARAA, 37, 487
Harrington, J. P. 1969, ApJ, 156, 903
Harrington, J. P. 1973, MNRAS, 162, 43
Hasegawa, T. I. & Herbst, E. 1993, MNRAS, 261, 83
Hasegawa, T. I., Herbst, E., & Leung, C.M. 1992 ApJS, 82, 167
Hauschildt, P.H., & Baron, E., 1999, J. Comp. Appl. Math, 109, 41-63
Heiles, C. & Crutcher, R. 2005, *Magnetic Fields in Diffuse H I and Molecular Clouds*, Chapter in Cosmic Magnetic Fields, astro-ph/0501550
Heiles, C. & Troland, T.H. 2005, ApJ, 624, 773
Heitler, W. 1954, *The Quantum Theory of Radiation* (Oxford: Oxford University Press)
Henney, W. J. Arthur, S. J. Williams, R. J. R. & Ferland, G. J. 2005, ApJ, 621, 328 (astro-ph 0501034)
Hilborn, Robert C., 1982, American Journal of Physics, 50, 982-986, erratum, 51 471
Hjellming, R. M. 1966, ApJ, 143, 420
Hogg, D.W. 1999, astro-ph/9905116
Hollenbach, D., & McKee, C. F. 1979, ApJS, 41, 555
Hollenbach, D., & McKee, C. F. 1989, ApJ, 342, 306
Hollenbach, D.J., Takahashi, T., & Tielens, A.G.G.M., 1991, ApJ, 377, 192-209
Hollenbach, D.J., & Tielens, A. G. G. M. 1997, ARA&A, 35, 179

Hollenbach, D.J., & Tielens, A.G.G.M. 1999, Rev Mod Phys 71, 173
Holweger, H., 2001, Joint SOHO/ACE workshop "Solar and Galactic Composition". Edited by Robert F. Wimmer-Schweingruber. Publisher: American Institute of Physics Conference proceedings vol. 598 location: Bern, Switzerland, March 6 - 9, 2001, p.23
Hubbard, E. N., & Puetter, R. C. 1985, ApJ, 290, 394
Hubeny, I. 2001, Hubeny 2001 Spectroscopic Challenges of Photoionized Plasmas, ASP Conference Series Vol. 247. Edited by Gary Ferland and Daniel Wolf Savin. San Francisco: Astronomical Society of the Pacific, p.197
Hummer, D. G. 1962, MNRAS, 125, 21
Hummer, D. G. 1968, MNRAS, 138, 73
Hummer, D. G. 1988, ApJ, 327, 477
Hummer, D. G, Berrington, K. A., Eissner, W., Pradhan, A. K., Saraph H. E., Tully, J. A. 1993, A&A, 279, 298
Hummer, D. G., & Kunasz, P.B. 1980, ApJ, 236, 609
Hummer, D. G., & Seaton, M. J. 1963, MNRAS, 125, 437
Hummer, D. G., & Storey, P. J. 1987, MNRAS, 224, 801
Hummer, D. G., & Storey, P. J. 1992, MNRAS, 254, 277
Hutchings, J.B. 1976, ApJ, 205, 103
Ikeuchi, S., & Ostriker, J. P. 1986, ApJ, 301, 522
Jackson, J. D. 1975, *Classical Electrodynamics* (New York: Wiley)
Kaler, J., & Jacoby, G. 1991, ApJ, 372, 215
Janev, R. K., Langer, W. D., Post, D. E., & Evans, K. 1987, *Elementary Processes in Hydrogen–Helium Plasmas* (Berlin: Springer--Verlag)
Jenkins, E. B. 1987, in *Interstellar Processes*, D. Hollenbach & H. Thronson, Eds, (Dordrecht: Reidel), p.533
Johnson, L. C. 1972, ApJ, 174, 227
Johnstone, R. M., Fabian, A. C., Edge, A. C., & Thomas, P. A. 1992, MNRAS, 255, 431
Jones, A.P., Tielens, A. G. G. M., & Hollenbach, D.J. 1996, 469, 740-764
Jura, M., 1974, ApJ, 191, 375-379
Jura, M., 1975, ApJ, 197, 575-580
Kaler, J., 1978, ApJ, 220, 887
Kallman, T. R., & McCray, R. 1982, ApJS, 50, 263
Karzas, W. J., & Latter, R. 1961, ApJS, 6, 167
Kaastra, J. S., & Mewe, R. 1993, A&AS, 97, 443
Kato, T. 1976, ApJS, 30, 397
Kellerman, K. I. 1966, ApJ, 146, 621
Khromov, G. S. 1989, Space Science Reviews 51, 339
Kingdon, J. B., & Ferland, G. J. 1991, PASP, 103, 752
Kingdon, J. B., & Ferland, G. J. 1993, ApJ, 403, 211
Kingdon, J. B., & Ferland, G. J. 1995, ApJ, 450, 691
Kingdon, J. B., & Ferland, G. J. 1996, ApJS, 106, 205
Kingdon, J. B., Ferland, G. J., & Feibelman, W.A. 1995, ApJ, 439, 793
Kingdon J.B., & Ferland, G.J., 1998, ApJ 506, 323-328
Kingdon, J. B., & Ferland, G. J. 1998, ApJ, 516, L107-109
Korista, K. T., Baldwin, J. A., & Ferland, G. J. 1998, ApJ, 507, 24
Korista, K. T., & Ferland, G. J. 1989, ApJ, 343, 678

Korista, K. T., & Ferland, G. J. 1998, ApJ, 495, 672
Korista, K. T., Ferland, G. J., & Baldwin, J. 1997, ApJ, 487, 555
Kraemer, S.B., Ferland, G.J., & Gabel, J.R. 2004, ApJ, 604, 556
Krolik, J., McKee, C. M., & Tarter, C.B. 1981, ApJ, 249, 422
Kurucz, R. L. 1970, SAO Special Reports 309
Kurucz, R. L. 1979, ApJS, 40, 1
Kurucz, R. L. 1991, in *Proceedings of the Workshop on Precision Photometry: Astrophysics of the Galaxy*, ed. A. C. Davis Philip, A. R. Upgren, & K. A. James, (Schenectady: Davis), 27
Kwan, J., & Krolik, J. 1981, ApJ, 250, 478
Lambert, D. L., & Pagel, B. E. J. 1968, MNRAS, 141, 299
La Franca, Franceshini, A., Cristiani, S., & Vio, R. 1995, A&A, 299, 19
Lambert, D.L. 1993, Phys Scrip T47, 186
Lame N. J., & Ferland, G. J. 1991, ApJ, 367, 208
LaMothe, J., & Ferland, G.J., 2001, PASP, 113, 165
Landini, M., & Monsignori Fossi, B. 1990, A&AS, 82, 229
Landini, M., & Monsignori Fossi, B. 1991, A&AS, 91, 183
Lanzafame, A., Tully, J. A., Berrington, K. A., Dufton, P. L., Byrne, P. B., & Burgess, A. 1993, MNRAS, 264, 402
Laor, A., & Draine, B. T. 1993, ApJ, 402, 441
Latter, W. B., & Black, J. H. 1991, ApJ, 372, 161
Lea, S., & Holman, G. 1978, ApJ, 222, 29
Le Bourlot, J., 2000, A&A, 360, 656-662
Le Bourlot, J., Pineau des Forets, G., & Flower, D.R. 1999, MNRAS, 305, 802
Leitherer, Claus; Schaerer, Daniel; Goldader, Jeffrey D.; Delgado, Rosa M. González; Robert, Carmelle; Kune, Denis Foo; de Mello, Duília F.; Devost, Daniel; Heckman, Timothy M. 1999, ApJS, 123, 3
Lennon, D. J., & Burke, V. M. 1991, MNRAS, 251, 628
Lenzuni, P., Chernoff, D. F., & Salpeter, E. E. 1991, ApJS, 76, 759
Levich, E. V., & Sunyaev, R.A. 1970, Astrophysical Letters 7, 69
Lepp, S., & Shull, J. M. 1983, ApJ, 270, 578
Li, Aigen, & Draine, B.T. 2001, ApJ, 554, 778L
Lightman, A. P., & White, T.R. 1988, ApJ, 335, 57
Liske, J., 2000, MNRAS, 319, 557-561
Lites, B. W., & Mihalas, D. 1984, Solar Physics 93, 23
Liu, X.-W., Storey, P. J., Barlow, M. J., & Clegg, R. E. S. 1995, MNRAS, 272, 369
Longair, M. S. 1981, *High Energy Astrophysics*, (Cambridge: Cambridge University Press)
Lotz, W. 1967, ApJS, 14, 207
Launay, J.R., Le Dourneuf, M., & Zeippen, C.J., 1991, A&A, 252, 842-852
MacAlpine, G. M. 1971, ApJ, 175, 11
Maguire, S. 1993, *Writing Solid Code*, (Redmond: Microsoft Press)
Maguire, S. 1994, *Debugging the Development Process*, (Redmond: Microsoft Press)
Mallik, D. C. V., & Peimbert, M. 1988, Rev Mexicana 16, 111
Maloney, P.R., Hollenbach, D.J., & Tielens, A. G. G. M., 1996, ApJ, 466, 561
Martin, P. G. 1979, *Cosmic Dust* (Oxford: Clarendon Press)
Martin, P. G. 1988, ApJS, 66, 125
Martin, P. G., & Ferland, G. J. 1980, ApJ, 235, L125

Martin, P.G., & Rouleau, F., 1991, in Malina R.F., Bowyer S., eds, Extreme Ultraviolet Astronomy, Pergamon Press, Oxford, p. 341
Martin, P. G., & Whittet, D. C. B. 1990, ApJ, 357, 113
Masters, A. R., Pringle, J. E., Fabian, A. C., & Rees, M. J. 1977, MNRAS, 178, 501
Mather, J.C., Fixsen, D.J., Shafer, R.A., Mosier, C., & Wilkinson, D.T. 1999, ApJ, 512, 511
Mathews, W. G., Blumenthal, G. R., & Grandi, S. A. 1980, ApJ, 235, 971
Mathews, W. G., & Ferland, G. J. 1987, ApJ, 323, 456
Mathis, J. S. 1982, ApJ, 261, 195
Mathis, J. S. 1985, ApJ, 291, 247
Mathis, J. S., Rumpl, W., & Nordsieck, K. H. 1977, ApJ, 217, 425
Mathis, J. S., & Wallenhorst, S. G. 1981, ApJ, 244, 483
Matteucci, F., & Tornambe, A. 1987, A&A, 185, 51
Matteucci, F., & Greggio, A. 1986, A&A, 154, 279
Mazzotta, P., Mazzitelli, G., Colafrancesco, C., & Vittorio, 1998, A&AS 133, 403-409
McCall, B.J., et al. 2003, Nature, 422, 500
McKee, C. F. 1999, preprint, Astro-ph 9901370
Mendoza, C. 1983, in *Planetary Nebulae*, IAU Sym 103, D. R. Flower, Ed., p 143, (Dordrecht: Reidel)
Meyer, D.M., Jura, M., & Cardelli, J.A. 1998, ApJ, 493, 222-229
Mewe, R. 1972, A&A, 20, 215
Mihalas, D. 1972, *Non-LTE Model Atmospheres for B & O Stars*, NCAR-TN/STR-76
Mihalas, D. 1978, *Stellar Atmospheres*, 2nd Edition (San Francisco: W.H. Freeman)
Mihalszki, J. S., & Ferland, G. J. 1983, PASP, 95, 284
Mohr P.J. & Taylor B.N., 1998 Codata, see Reviews of Modern Physics, Vol. 72, No. 2, 2000
Morrison, R., & McCammon, D. 1983, ApJ, 270, 119
Morton, D. C., York, D. G., & Jenkins, E. B. 1988, ApJS, 68, 449
Nahar, S. N., & Pradhan, A. K. 1992, ApJ, 397, 729
Netzer, H. 2004, ApJ, 604, 551
Netzer, H. 1990, in *Active Galactic Nuclei, Saas-Fee Advanced Course 20*, Courvorsier, T.J.-L., & Mayor, M., (Springer-Verlag; Berlin)
Netzer, H., Elitzur, M., & Ferland, G. J. 1985, ApJ, 299, 752
Netzer, H., & Ferland, G. J. 1984, PASP, 96, 593
Neufeld, D. A. 1989, Harvard Research Exam
Neufeld, D.A., 1990, ApJ, 350, 216
Neufeld, D. A., & Dalgarno, A. 1989, Phys Rev A, 35, 3142
Novotny, Eva, 1973, *Introduction to Stellar Atmospheres*, (New York; Oxford University Press)
Nussbaumer, H., & Storey, P. J. 1983, A&A, 126, 75
Nussbaumer, H., & Storey, P. J. 1984, A&AS, 56, 293
Nussbaumer, H., & Storey, P. J. 1986, A&AS, 64, 545
Nussbaumer, H., & Storey, P. J. 1987, A&AS, 69, 123
O'Dell, C.R., 2001, ARAA, 39, 99
Oliveira, S., & Maciel, W. J. 1986, Ap&SS, 126, 211
Oliva, E., Pasquali, A., & Reconditi, M. 1996, A&A, 305, 210
Olive, K.A., Steigman, G., & Walker, T.P., 2000, Physics Reports, 333-334, 389-407
Osterbrock, D. E. 1951, ApJ, 114, 469
Osterbrock, D. E., & Ferland, G.J. 2006, *Astrophysics of Gaseous Nebulae & Active Galactic Nuclei*, 2nd edition, (Mill Valley; University Science Press) (AGN3)

Osterbrock, D. E., & Flather, E. 1959, ApJ, 129, 26
Osterbrock, D. E., Tran, H. D., & Veilleux, S. 1992, ApJ, 389, 305
Ostriker, J. P., & Ikeuchi, S. 1983, ApJ, 268, L63
Pacholczyk, A. G. 1970, *Radio Astrophysics* (San Francisco: Freeman)
Pagel, B. E. J. 1997, *Nucleosynthesis and Chemical Evolution of Galaxies*, (Cambridge: Cambridge University Press)
Palla, F., Salpeter, E. E., & Stahler, S. W. 1983, ApJ, 271, 632
Peebles, P. J. E. 1971, *Physical Cosmology*, (Princeton: Princeton U. Press)
Peimbert, M. 1967, ApJ, 150, 825
Pengelly, R. M. 1964, MNRAS, 127, 145
Pengelly, R.M., & Seaton, M.J., 1964, MNRAS, 127, 165
Péquignot, D. 1986, *Wordshop on Model Nebulae*, (Paris: l'Observatoire de Paris) p363
Péquignot, D., & Aldrovandi, S.M.V. 1986, A&A, 161, 169
Péquignot, D., Ferland, G.J., et al., 2001, in ASP Conference Series, Vol 247, *Spectroscopic Challenges of Photoionized Plasmas*, G Ferland & D Savin, editors
Péquignot, D., Petitjean, P., & Boisson, C. 1991, A&A, 251, 680
Péquignot, D., Stasinska, G., & Aldrovandi, S. M. V. 1978, A&A, 63, 313
Percival, I.C., & Richards, D., 1978, MNRAS, 183, 329
Peterson, B.M. 1993, PASP, 105, 247
Peterson, J. R., Aberth, W., Moseley, J., & Sheridan, J. 1971, Phys Rev A, 3, 1651
Pettini, M., & Bowen, D.V., 2001, ApJ, 560, 41
Poglitsch, A., Krabbe, A., Madden, S.C., Nikola, T., Geis, N., Johansson, L., Stacey, G. & Sternberg, A. 1995, ApJ, 454, 293
Porquet, D., & Dubau, J. 2000, A&AS, 143, 495
Porter, R.L., Bauman, R.P., Ferland, G.J., & MacAdam, K. B. 2005, ApJ, 622, 73L (astro-ph/0502224)
Prasad, S.S., & Huntress, W.T., 1980, ApJS, 43, 1-35
Press W. H., Teukolsky, S.A., Vetterling, W. T., & Flannery, B. P. 1992, *Numerical Recipes*, (Cambridge; Cambridge University Press)
Puetter, R. C. 1981, ApJ, 251, 446
Puy, D., Alecian, G., Le Bourlot, J., Leorat, J., & Pineau des Forets, G. 1993, A&A, 267, 337
Puy, D., Grenacher, L, & Jetzer, P., 1999, A&A, 345, 723
Rauch, T. 1997 A&A, 320, 237
Rauch, T. 2002, H-Ni grid, available at http://astro.uni-tuebingen.de/~rauch
Raymond, J. C., Cox, D. P., & Smith, B. W. 1976, ApJ, 204, 290
Rees, M. J., Netzer, H., & Ferland, G. J. 1989, ApJ, 347, 640
van Regemorter, H. 1962, ApJ, 136, 906
Rephaeli, Y. 1987, MNRAS, 225, 851
Reilman, R. F., & Manson, S. T. 1979, ApJS, 40, 815, errata 46, 115; 62, 939
Roberge, W. G., Jones, D., Lepp, S., & Dalgarno, A. 1991, ApJS, 77, 287
Röllig, M., et al., 2006, Leiden PDR comparison, A&A in press
Rossi, B. 1952, *High-Energy Particles* (New York; Prentice-Hall)
Rouleau, F., & Martin, P.G. 1991, ApJ, 377, 526
Rowan, T. 1990, *Functional Stability Analysis of Numerical Algorithms*, Ph.D. Thesis, Department of Computer Sciences, University of Texas at Austin
Rubin, R. H. 1968, ApJ, 153, 671
Rubin, R. H. 1983, ApJ, 274, 671

Rubin, R. H. Martin, P. G. Dufour, R. J. Ferland, G. J Baldwin, J. A. Hester, J. J. & Walter, D. K. 1998, ApJ, 495, 891
Rubin, R. H., Simpson, J. R., Haas, M. R., & Erickson, E. F. 1991, ApJ, 374, 564
Rutten, Rob, 2002, Radiative transfer in stellar atmospheres, at http://www.fys.ruu.nl/~rutten/node20.html
Rybicki, G. B., & Hummer, D. G. 1991, A&A, 245, 171
Rybicki, G. B., & Hummer, D. G. 1992, A&A, 262, 209
Rybicki, G. B., & Hummer, D. G. 1994, A&A, 290, 553
Rybicki, G. B., & Lightman, A.P. 1979, *Radiative Processes in Astrophysics* (New York: Wiley)
Sanders, D. B., et al. 1989, ApJ, 347, 29
Saraph, H. E. 1970, J.Phys.B., 3, 952
Savage, B. D., & Jenkins, E.B. 1972, 172, 491
Savage, B. D., & Sembach, K. R. 1996, ARA&A, 34, 279
Savin, Daniel Wolf, 2000, ApJ, 533, 106
Savin, D. W.; Kahn, S. M.; Linkemann, J.; Saghiri, A. A.; Schmitt, M.; Grieser, M.; Repnow, R.; Schwalm, D.; Wolf, A.; Bartsch, T.; Brandau, C.; Hoffknecht, A.; Müller, A.; Schippers, S.; Chen, M. H.; Badnell, N. R., 1999, ApJS, 123, 687
Sciortino, S., et al. 1990, ApJ, 361, 621
Scott, J. S., Holman, G. D., Ionson, J. A., & Papadopoulos, K. 1980, ApJ, 239, 769
Schaerer D., de Koter, A., Schmutz, W., & Maeder, A. 1996ab, A&A, 310, 837, & A&A, 312, 475
Schaerer D., & de Koter A. 1997, A&A, 322, 592
Schuster, A. 1905, ApJ, 21, 1
Schutte, W. A., Tielens, A. G. G. M., & Allamandola, L. J. 1993, ApJ, 415, 397
Schwarzschild, M. 1965, *Structure & Evolution of the Stars*, (New York: Dover)
Seaton, M. J. 1959, MNRAS, 119, 81
Seaton, M. J. 1959, MNRAS, 119, 90
Seaton, M. J. 1987, J.Phys. B, 20, 6363
Sellgren, K., Tokunaga, A. T., & Nakada, Y. 1990, ApJ, 349, 120-125
Sellmaier, F. H., Yamamoto, T., Pauldrach, A. W. A., & Rubin, R. H. 1996, A&A, 305, L37
Shaw, G. Ferland, G.J. Abel, N.P. Stancil, P.C. &van Hoof, P.A.M. 2005, ApJ, 624, 794, (astro-ph/0501485)
Shields, G. A. 1976, ApJ, 204, 330
Shine, R. A., & Linsky, J. L. 1974, Solar Physics 39, 49
Shull, J. M. 1979, ApJ, 234, 761
Shull, J.M., & Beckwith, S. 1982, ARA&A, 20, 163
Shull, J. M., & Van Steenberg, M. E. 1982, ApJS, 48, 95
Shull, J. M., & Van Steenberg, M. E. 1985, ApJ, 298, 268
Sellgren, K., Tokunaga, A. T., & Nakada, Y. 1990, ApJ, 349, 120
Sellmaier, F.H., Yamamoto, T., Pauldrach, A.W.A., Rubin, R.H 1996, A&A, 305, 37
Sikora, M., Begelman, M. C., & Rudak, B. 1989, ApJ, 341, L33
Simonyi, C. 1977, *Meta-Programming: A Software Production Method*, Thesis, Stanford University
Simpson, J. P. 1975, A&A, 39, 43
Smits, D.P., 1996, MNRAS, 278, 683
Snow, T. P., & Dodger, S. L. 1980, ApJ, 237, 708
Snow, T. P., & York, D. G. 1981, ApJ, 247, L39
Snow, T. P., & Witt, A. 1996, ApJ, 468, L65

Spitzer, L. 1948, ApJ, 107, 6
Spitzer, L. 1962, *Physics of Fully Ionized Gasses*, (New York: Interscience)
Spitzer, L. 1978, *Physical Processes in the Interstellar Medium*, (New York: Wiley)
Spitzer, L. 1985, ApJ, 290, L21
Spitzer, L., & Tomasko, M. G. 1968, ApJ, 152, 971
Stasinska, G. & Szczerba, R 1999, A&A, 352, 297
Stecher, T. P., & Williams, D. A. 1967, ApJ, 149, 29
Steenbock, W. & Holweger, H. 1984, A&A, 130, 319
Sternberg, A., & Dalgarno, A. 1989, ApJ, 338, 197
Sternberg, A., & Neufeld, D.A. 1999, ApJ, 516, 371-380
Stoy, R. H. 1933, MNRAS, 93, 588
Storey, P. J. 1981, MNRAS, 195, 27p
Storey, P. J. 1994, A&A, 282, 999
Storey, P. J., & Hummer, D. G. 1991, Comput. Phys. Commun. 66, 129
Storey, P. J., & Hummer, D. G. 1995, MNRAS, 272, 41 (on the web at http://adc.gsfc.nasa.gov/adc-cgi/cat.pl?/catalogs/6/6064/)
Suchkov, A., Allen, R.J., & Heckman, T. M. 1993, ApJ, 413, 542-547
Swings, P., & Struve, O. 1940, ApJ, 91, 546
Takahashi, Junko, 2001, ApJ, 561, 254-263
Tarter, C. B. 1967, Ph. D. Thesis, Cornell University
Tarter, C. B., & McKee, C. F. 1973, ApJ, 186, L63
Tarter, C. B., Tucker, W.H., & Salpeter, E.E., 1969, ApJ, 156, 943
Telfer, R.C., Zheng, W., Kriss, G.A., & Davidsen, A.F. 2002, ApJ, 565, 773
Tielens, A.G.G.M. 2005, *The Physics and Chemistry of the Interstellar Medium*, (Cambridge: Cambridge University Press)
Tielens, A. G. G. M., & Hollenbach, D. 1985a, ApJ, 291, 722
Tielens, A. G. G. M., & Hollenbach, D. 1985b, ApJ, 291, 746
Tinsley, B. 1979, ApJ, 229, 1046
Tout, C. A., Pols, O. R., Eggleton, P. P. & Han, Z. 1996, MNRAS, 281, 257
Turner, J., & Pounds, K. 1989, MNRAS, 240, 833
Van Blerkom, D., & Hummer, D. G. 1967, MNRAS, 137, 353
Veigele, WM. J. 1973, Atomic Data Tables, 5, 51
van Dishoeck, E.F., & Black, J.H., 1988, ApJ, 334, 771
van Hoof, P. A. M. 1997, PhD Thesis, University of Groningen
van Hoof, P.A.M., Beintema, D.A., Verner D.A., & Ferland, G.J., 2000a, A&A 354, L41-L44
van Hoof, P.A.M., Van de Steene, G.C., Beintema, D.A., Martin, P.G., Pottasch, S.R., Ferland, G. J., 2000b, ApJ 532, 384-399
van Hoof, P.A.M., Weingartner, J.C., Martin, P.G., Volk, K., & Ferland, G.J., 2001, in *Challenges of Photoionized Plasmas*, (G Ferland & D. Savin, eds) ASP Conf Ser 247, 363-378 (astro-ph/0107183)
van Hoof, P.A.M., Weingartner, J.C., Martin, P.G., Volk, K., & Ferland, G.J., 2004, MNRAS, 350, 1330 (astro-ph/0402381)
van Regemorter, H. 1962, ApJ, 136, 906
Vedel, H., Hellsten, U., & Sommer-Larsen, J. 1994, MNRAS, 271, 743
Vernazza, J. E., Avrett, E. H., & Loeser, C. B. 1981, ApJS, 45, 635
Verner, D. A., Yakovlev, D. G., Band, I. M., & Trzhaskovshaya, M. B. 1993, ADNDT, 55, 233
Verner, D. A., & Yakovlev, 1995, A&AS, 109, 125

Verner, D. A., & Ferland, G. J. 1996, ApJS, 103, 467
Verner, D. A., Ferland, G. J., Korista, K., & Yakovlev D. G. 1996, ApJ, 465, 487
Verner, D. A., Verner, K., & Ferland, G. J. 1996, ADNDT, 64, 1
Verner, E.M. Verner, D.A. Korista, K.T. Ferguson , J.W. Hamann, F. & Ferland, G.J. 1999, ApJS 120, 101
Voronov, G. S. 1997, ADNDT, 65, 1
Voit, G. M. 1991, ApJ, 377, 1158
Volk, K., and Kwok, S. 1988, ApJ, 331, 435
Vriens, L., & Smeets, A. H. M. 1980, Phys Rev A, 22, 940
Vrinceanu, D. & Flannery, M. R. 2001, PhysRevA 63, 032701
Watson, W. D. 1972, ApJ, 176, 103
Weingartner, J.C., & Draine, B.T., 2001a, ApJS, 134, 263
Weingartner, J.C., & Draine, B.T., 2001b, ApJ, 548, 296
Weingartner, J.C., & Draine, B.T., 2001c, ApJ, 563, 842
Weisheit, J. C. 1974, ApJ, 190, 735
Weisheit, J. C., & Collins, L. A. 1976, ApJ, 210, 299
Weisheit, J. C., & Dalgarno, A. 1972, Astrophysical Letters, 12, 103
Weisheit, J., Shields, G. A., & Tarter, C. B. 1981, ApJ, 245, 406
Wen, Z., & O'Dell, C.R. 1995, ApJ, 438, 784-793
Werner, K., & Heber, U. 1991, in *Stellar Atmospheres: Beyond Classical Models*, p 341, NATO ASI Series C, eds. L. Crivellari, I. Hubney, & D. G. Hummer, (Dordrect: Kluwer)
White, R. E. 1986, ApJ, 307, 777
Wiese, W.L., Fuhr, J.R., & Deters, T.M., 1996, J Phys Chem Ref Data, Monograph 7
Wiese, W. L., Smith, M. W., & Glennon, B. M. 1966, NSRDS-NBS 4
Wilkes, B. J., Ferland, G. J., Truran, J., & Hanes, D. 1981, MNRAS, 197, 1
Wilkes, et al 1994, ApJS, 92, 53
Wilkinson, D. T. 1987, in *13th Texas Symposium on Relativistic Astrophysics*, M. P. Ulmer, ed., (Singapore: World Scientific), p209
Williams, J.P., Bergin, E.A., Caselli, P., Myers, P.C., & Plume, R. 1998, ApJ, 503, 689
Williams, R. E. 1967, ApJ, 147, 556
Williams, R. E. 1992, ApJ, 392, 99
Wills, B., Netzer, H., & Wills, D. 1985, ApJ, 288, 94
Wilson, T. L., & Rood, R. T. 1994, ARA&A, 32, 191
Wing, W.H., & MacAdam, K.B., 1978, in *Progress in Atomic Spectroscopy*, Part A, W. Hanle & H. Kleinpopper, eds
Winslow, A. M. 1975, Lawrence Livermore Lab. report UCID-16854
Wishart, A. W. 1979, MNRAS, 187, 59p
Wolfire, M. G., Tielens, A., & Hollenbach, D. 1990, ApJ, 358, 116
Worral et al. 1987, ApJ, 313, 596
Wyse, A. B. 1941, PASP, 53, 184
York, D. G., Meneguzzi, M., & Snow, T. 1982, ApJ, 255, 524
Xu, Y., & McCray, R. 1991, ApJ, 375, 190
Zamorani, G., et al. 1981, ApJ, 245, 357
Zheng, W., Kriss, G.A., Telfer, R.C., Grimes, JP. & Davidsen, A.F. 1997, ApJ, 475, 469
Zsargó, J. & Federman, S. R. 2003, ApJ, 589, 319
Zuckerman, B. 1973, ApJ, 183, 863
Zycki, P. T., Krolik, J. H., Zdziarski, A. A., & Kallman, T. R. 1994, 437, 597

Zygelman, B., & Dalgarno, A. 1990, ApJ, 365, 239

13. INDEX